

THE EFFECT OF METAL CHLORIDE ADDITIONS UPON THE EXTRACTION OF NICKEL  
FROM LATERITIC ORES BY HYDROCHLORIC ACID

by

Carlos Enrique Jimenez-Novoa

A thesis presented to the University of Leeds in fulfilment of the  
requirements for the award of the degree of

Doctor of Philosophy

Department of Mining and Mineral Sciences

February 1980

## ABSTRACT

Although lateritic nickel ores are efficiently leached by pure dilute hydrochloric acid at atmospheric pressure and temperature between ambient and 90°C, the degree of extraction of nickel, as well as iron and magnesium is considerably decreased in the presence of moderate concentrations of the respective cations in the leach liquor. In the case of nickel itself extraction falls to zero at concentrations of Ni<sup>2+</sup> of about 20 g/l for most laterite ores. Increase in free acid concentration or temperature does not improve the extraction.

It has been shown that the poor extraction is not due to cessation of the reaction between the acid and the ore but to the formation of a layer of insoluble reaction product which prevents further dissolution of the cations.

The problem may be solved by the application of washing with pure dilute HCl. The washing parameters have been studied and a leach-washing flowsheet is proposed that would permit leach liquor containing at least 20 g/l nickel to be produced with 92-95% extraction from the ore.

The leaching of the cations Ni, Mg and Fe was found to obey a kinetic model of the form

$$1 - \frac{2}{3} R - (1 - R)^{2/3} = kt,$$

where R is the fraction of cation extracted, up to a certain fraction of extraction after which a change to another mechanism of leaching occurred. This fraction depended on both the cation involved and the

temperature. The kinetics were chemically controlled up to 50-60°C and diffusion controlled at higher temperatures.

## CONTENTS

	Page
ABSTRACT	
CHAPTER 1 INTRODUCTION	1
CHAPTER 2 GENERAL REVIEW OF THE EXTRACTIVE METALLURGY OF NICKELIFEROUS LATERITES	3
2.1 Introduction	3
2.2 Mineralogical aspects	3
2.3 Pyrometallurgy	7
2.4 Hydrometallurgy	9
CHAPTER 3 EXPERIMENTAL	24
3.1 Outline	24
3.2 Leaching studies	25
3.2.1. Leaching techniques	25
3.2.2. Atomic absorption analysis	27
3.2.3. Electron probe microanalysis	29
3.2.3.1. Procedure	32
3.3 Washing studies	33
3.3.1. Washing technique	33
CHAPTER 4 LEACHING OF LATERITIC NICKEL ORES IN HYDROCHLORIC ACID WITH METAL CHLORIDES ADDITION	39
4.1 Introduction	39
4.2 General characteristics of selected nickeliferous laterites.	39



	Page
4.3 Leaching testwork	41
4.3.1. Leaching of laterites with nickel chloride addition	42
4.3.2. Leaching of laterites with magnesium chloride addition	54
4.3.3. Leaching of laterites with ferric chloride addition	59
4.3.4. Maximization of nickel extraction during the leaching stage by optimi- zation of leaching variables	64
4.3.4.1. Temperature	64
4.3.4.2. Acid concentration	67
4.3.4.3. Contact time	70
4.3.5. Effect of pulp density upon cation extraction from a silicate ore leached in HCl containing different nickel concentrations	73
4.3.6. Lump leaching	75
CHAPTER 5 KINETICS OF ACID DISSOLUTION OF A LATERITIC NICKEL ORE	83
5.1 Experimental	83
5.2 Effect of temperature	84
5.3 Effect of acid concentration	84
5.4 Effect of particle size	85
5.5 Cation dissolution	107
5.6 Reaction mechanism	148

	Page
CHAPTER 6      WASHING	155
6.1    Introduction	155
6.2    Single batch washing	155
6.2.1.    Effect of leaching variables upon the cation extraction during the washing of leaching residues	155
6.2.1.1    Temperature, acid concen- tration and particle size	156
6.2.1.2.    Pulp density	159
6.2.2    Effect of washing variables upon cation extraction during the washing of leach residues	163
6.2.2.1    Acid concentration, tempera- ture and agitation.	164
6.2.2.2    Contact time and solid/liquid ratio	170
6.3    Multistage batch cross-current washing	177
6.3.1    Washing of residues in a 4-stage cross-current system	180
6.4    Multistage batch counter-current washing	195
6.4.1    Washing system	195
6.4.2    Preliminary counter-current washing tests	201
6.4.3    Maximization of nickel concentration in the product solution from the washing	208

	Page
CHAPTER 7      PROPOSED INTEGRATED FLOWSHEET FOR HYDRO- CHLORIC ACID LEACHING OF NICKELIFEROUS LATERITES	225
CHAPTER 8      CONCLUSION	232
ACKNOWLEDGEMENTS	
REFERENCES	
APPENDIX I	
APPENDIX II	

## CHAPTER 1

### INTRODUCTION

The importance of lateritic nickel ore deposits as a potential source of nickel has in recent years prompted detailed studies of such deposits, and of methods of extracting nickel. Although relatively low in nickel, 1% on average, the enormous tonnage available makes them a viable proposition. Today, about 40% of the world's nickel is derived from lateritic oxidized ores found mostly in tropical countries. The balance is likely to shift further in this direction since these ores account for over 80% of land-based world nickel reserve. Thus, with more and more nickel being derived from lateritic ores, significant efforts are being devoted to methods of extraction, whether they be pyrometallurgical or hydrometallurgical, with much development work devoted to the latter.

Many of the hydrometallurgical processes patented for selective extraction of nickel and cobalt from lateritic ores include: (a) a pretreatment stage, usually reduction roasting, and/or (b) a high temperature pressure leaching stage. A typical example of route (a) is the Sherritt-Gordon's ammonia leach process in the Philippines<sup>(1,2)</sup> and of route (b) acid leaching at Moa Bay<sup>(3,4)</sup>. The ease of regeneration and low cost of the leaching reagents have, in the past, outweighed the cost of elaborate process plant equipment. However, with higher fuel costs (considering the ores as 1% nickel and 99% gangue) and increasingly stringent effluent control regulations, the incentive has been towards the development of low temperature-pressure leaching systems within a

closed cycle extraction process. Reviews by Meddings and Evans<sup>(5)</sup> and Derry<sup>(6)</sup> deal with the applications of low and high pressure hydrometallurgy.

The application of direct aqueous hydrochloric acid leaching (low pressure-temperature) to nickeliferous laterites has been investigated in the past by Strong and Rice<sup>(7,8)</sup>. Although leaching is not selective, the use of hydrochloric acid has certain advantages stemming from its good reactivity the ease with which mixed chloride solutions can be separated by solvent extraction and the ease of regenerating hydrochloric acid from metal chloride. The build up of magnesium chloride can be utilised to the advantage of the process, and the excellent regeneration efficiencies by spray roasting mean that all chloride liquors can be processed and acid recycled to the leaching stage.

Prompted by the encouraging results reported by Strong and Rice, this research is an attempt to study further the aqueous hydrochloric acid leaching of nickeliferous laterites at low pressure - temperature.

## CHAPTER 2

### GENERAL REVIEW OF THE EXTRACTIVE METALLURGY OF NICKELIFEROUS LATERITES

#### 2.1. Introduction

The recovery of nickel from nickeliferous laterites is difficult because of their complex mineralogy and the limited applicability of established technology<sup>(9)</sup>. The orebodies are usually inhomogeneous and contain little or no sulphur. Preliminary beneficiation, apart from selective open pit stripping, is impossible and treatment depends on the type of deposit<sup>(10)</sup>.

The complexity of the ores has led to the development of a variety of possible extractive techniques. Four of these, namely matte smelting, ferronickel smelting, sulphuric acid leaching at elevated pressures, and reduction followed by ammonia leaching, are in commercial operation<sup>(9)</sup>. The basic principles of these processes have been described in considerable detail by Boldt<sup>(11)</sup>, and no attempt will be made here to review these data. A review by Canterford<sup>(12)</sup> has dealt with the recent improvements in these processes as well as new innovations for the treatment of lateritic nickel ores. In view of the detailed reviews by Canterford<sup>(12)</sup> and Strong<sup>(13)</sup> only the more recent aspects of the subject are discussed in this chapter.

#### 2.2. Mineralogical Aspects

The low grade and complexity of nickeliferous laterites is a result of their mode of formation<sup>(14)</sup> and despite many attempts to physically upgrade the ore<sup>(15,16)</sup>, in general the whole orebody

must be treated.

The process of laterization is extremely complex and because of variations in geological and geochemical factors, there are vast differences in lateritic ores, both within one deposit, and between deposits. The general concept of a laterite deposit is that it consists of three zones<sup>(14)</sup>: (a) an upper, highly ferruginous zone in which the nickel is associated with hydrated iron oxide (limonite ore); (b) an intermediate zone consisting of limonitic and silicate ore (transition ore); (c) a lower zone which is enriched in clay minerals derived from the original ultrabasic bedrock (silicate ore). The complete separation of Fe and Ni into distinct zones however, is never realized. Thus, if Ni is retained in the upper zone with the iron through prevailing weathering factors, while the Mg and Si are removed, such a deposit is termed a limonitic ore, or a nickeliferous iron ore, or a ferruginous nickel ore. If the Ni is partially separated from the Fe, and is associated at greater depth with the Mg and Si, the ore is termed a nickel silicate or serpentine ore. The term "garnierite" is often used to describe nickel-containing silicate minerals, but in fact "garnierite" is not a distinct well defined mineral species<sup>(18)</sup>. "Garnierite" is usually high magnesia, high silica ore, while limonite is a high iron ore, predominantly goethite.

The typical composition of limonitic and silicate laterites falls within the ranges shown in Table 2.1<sup>(17)</sup>, while the average composition of several deposits are given in Table 2.2<sup>(17)</sup>. These tables indicate that each deposit is different, but a more important point is that there are large variations within each deposit.

Table 2.1. Chemical composition ranges (%) for nickel laterites<sup>(17)</sup>

	Limonic	Silicate
Ni	0.10 - 3.0	1.0 - 4.0
Co	0.05 - 0.25	0.05 - 0.08
Fe	35.0 - 60.0	8.0 - 18.0
Cr	1.0 - 3.0	0.8 - 2.0
MgO	0.2 - 1.0	25.0 - 38.0
Al <sub>2</sub> O <sub>3</sub>	4.0 - 18.0	1.0 - 3.0
SiO <sub>2</sub>	1.3 - 6.0	40.0 - 55.0
CuO	0.6 - 1.0	1.0 - 2.0
MnO	0.3 - 2.5	0.5 - 1.0

Table 2.2. Average composition (%) of several laterite deposits<sup>(17)</sup>

	Limonic laterite			Silicate laterite	
	Cuban	Philippine	New Caledonia	Philippine	New Caledonia
Ni	1.24	1.20	1.40	1.48	2.27
Co	0.12	0.12	0.26	0.03	0.16
Fe	41.9	48.0	45.0	12.4	26.8
Mg	1.6	0.3	0.3	17.5	7.4
Cr	1.6	2.3	2.2	0.9	1.4
Mn	0.5	0.8	1.1	0.2	0.4
Al	1.8	3.5	2.2	1.3	0.9
SiO <sub>2</sub>	10.6	2.0	9.2	32.4	21.4



Since the metallurgical behaviour of an ore is directly dependent upon the mineralogical characteristics of that ore, and because of the complex nature of laterites, nearly all commercial and laboratory metallurgical processes are optimized on the basis of a constant feed material. Canterford<sup>(14)</sup> however, has demonstrated that even when using a feed of constant composition, there are significant variations in processing behaviour within and between different feed lots. Thus, it has now been recognized that variations in recovery, consumption of reagents, product quality, etc. for a given process are related to the variation in mineralogy between the constant chemical composition feed lots.

A procedure to aid the selection of appropriate process to extract nickel from lateritic ores was proposed by Limerick<sup>(18)</sup> in his Ph.D. dissertation. The procedure involves experimentally determining those mineralogical features of nickeliferous laterites which can be correlated with the efficiency of two extractive processes. These were; direct hydrochloric acid leaching at low pressure and temperature, and gaseous reduction and subsequent aqueous chlorination - conditions as described by Queneau<sup>(19)</sup>. The usefulness of the proposal relies on the inherent assumption that; (a) the mineralogical components of an ore can be defined and identified; (b) the proportion of the various components in any sample can be readily determined; (c) the mineralogical features which affect process efficiency can be identified and measured; (d) correlation can be established; and (e) there are no significant interaction between components. The validity of these assumptions and its impact on the practicability of the scheme as a whole were evaluated in the laboratory, but remain to

be tested on a large scale.

### 2.3. Pyrometallurgy

Two new important projects on the extraction of nickel from lateritic ores using the pyrometallurgical route have been reported at Soroako<sup>(20)</sup> in Indonesia and at Lake Izabel<sup>(21)</sup> in Eastern Guatemala. At Soroako, kiln-dried ore is reduced in a 100 m kiln, sulphidized with liquid elemental sulphur at the kiln-discharge, with the product then being melted in what is understood to be the world's largest circular electric furnace, 6 m high x 18 m diam. and rated at 45 MVA<sup>(22)</sup>. The 25% Ni matte product is transferred to a top blown rotary furnace and up-graded to a 75% Ni, 25% S Bessemer matte with the iron being slagged with silica flux. The completed project is expected to have three such identical processing streams with a total annual production of about 45,000 mt of nickel. The same route is to be used by Exmibal (Lake Izabel), where a similarly sized furnace is employed with conventional Peirce-Smith converters instead of the top blown units to upgrade the matte to 75% Ni, 22% S. and less than 1% Fe. The electric furnace is planned to operate at about 1,540°C, with a 0.5m metal layer and 1.2 m of magnesia-silicate slag<sup>(21)</sup>.

Currently in New Caledonia, electric smelting is used to produce a crude ferronickel, some of which is either refined directly or sulphidized using a new sulphur-shrouded tuyere injection process in Peirce-Smith converters<sup>(23)</sup>. Many of the existing pyrometallurgical lateritic processes produce ferronickel metal 25-50% Ni. Moussoulos<sup>(24)</sup> has reported an interesting application of the top blown rotary

converter to upgrade such ferronickel alloys to 90% Ni which would then be suitable for further refining by electrolytic process if required by the market. The basis of the process is the converting of the iron and the utilization of the heat released for the simultaneous smelting of a large amount of lateritic ore. In this way, the temperature of the process can be controlled and appreciable amounts of additional nickel and oxygen are introduced, affecting favourably the process economics<sup>(25)</sup>. The operation is carried out advantageously in a top-blown converter with pure oxygen. The ore, crushed to 6 mm is fed at a controlled rate through a jacketed pipe, which passes through the hood. It falls on the molten metal surface and is immediately entrained in the turbulence produced by the oxygen jet, introduced at the center of the converter, through a lance. Under these conditions, the heat transfer is accelerated and the smelting of the ore is very rapid. The vigorous agitation of the melt favour reactions among the different compounds present, which include higher iron oxides, nickel oxide cobalt oxide, silica and other compounds introduced by the added ore, as well as the blast of pure oxygen.

The following main reactions represent the chemistry of the process:

- 1)  $2 [\text{Fe}]^* + \text{O}_2 = 2(\text{FeO})^* \quad \Delta H_{1500^\circ\text{C}} = -111 \text{ Kcal}$
- 2)  $(\text{Fe}_2\text{O}_3) + [\text{Fe}] = 3(\text{FeO}) \quad \Delta H_{1500^\circ\text{C}} = 25.1 \text{ Kcal}$
- 3)  $(\text{NiO}) + [\text{Fe}] = [\text{Ni}] + (\text{FeO}) \quad \Delta H_{1500^\circ\text{C}} = 4.2 \text{ Kcal}$
- 4)  $(\text{CoO}) + [\text{Fe}] = [\text{Co}] + (\text{FeO}) \quad \Delta H_{1500^\circ\text{C}} = 4.6 \text{ Kcal}$
- 5)  $2(\text{FeO}) + (\text{SiO}_2) = (2\text{FeO}.\text{SiO}_2) \quad \Delta H_{1500^\circ\text{C}} = 16.0 \text{ Kcal}$

\* [ ] into the metallic bath, ( ) into the liquid slag.

With the exception of reaction (1), which releases a considerable amount of heat, all the others are endothermic at 1500°C<sup>(26)</sup>.

Reaction (1), whose enthalpy amounts to -55.5 Kcal per mole of FeO, is overwhelmingly predominant during converting. This reaction consumes the greater amount of iron and is the source of the energy required for the smelting of the added ore. Therefore, reaction (1) determines the mass of ore which is smelted and hence, it influences directly all the remaining reactions, and in particular, the extraction of more nickel and cobalt from the ore by reactions (3) and (4). Thus, the heat released by the oxidation of the iron is of basic importance to the process. If the oxidation is carried out rapidly in a converter blown with pure oxygen, heat losses are limited considerably and a large amount of ore can be smelted per unit of iron converted. This favourably affects the economics of the process.

Production of nickel from lateritic ores is characterised by very high energy requirements. More than half Exmibal's operating costs are reportedly for fuel<sup>(21)</sup>. The energy requirement for nickel via lateritic smelting is reported<sup>(22)</sup> to be  $396 \times 10^6$  Btu/ton ( $4.6 \times 10^8$  KJ/tonne) of ferronickel as compared with  $144 \times 10^6$  Btu/ton ( $1.95 \times 10^8$  KJ/tonne) for electrolytic nickel for production via sulphide ores. Energy requirement in lateritic processing are certainly an important issue facing this future source of nickel. It remains to be seen whether the hydrometallurgical or pyrometallurgical route has a clear advantage in this respect. A study of energy consumption in nickel production as was conducted for copper<sup>(27)</sup> would be most welcome.

#### 2.4. Hydrometallurgy

A major problem in hydrometallurgical approaches to the treatment of nickeliferous laterites is the well-known difficulty in achieving selective nickel dissolution, leaving the major impurity elements -

iron and/or magnesium - in the leach residues. The Moa Bay process is the only example of a system in which the ore is leached directly to give selective extraction of nickel. In this case, a high temperature sulphuric acid leach under autoclave conditions results in iron hydrolysis. The process however, has been shown to be unsuitable for laterite ores with a high magnesium content. The relatively high content of magnesia means that sulphuric acid leaching of a silicate laterite will result in a large acid consumption and a high dissolved magnesium level. One approach to this difficulty has been proposed by Kay<sup>(28)</sup>. This involves a leach to dissolve nickel and magnesium followed by two stages of neutralization with magnesium oxide for iron removal and nickel recovery as hydroxide. The inversed solubility of magnesium sulphate with increasing temperature allows magnesium sulphate to be recovered by crystallization at about 230°C, followed by decomposition to give magnesium oxide and sulphur dioxide for the manufacture of recycled sulphur acid.

Published information on the sulphuric acid pressure leaching of limonite is scarce. Work performed in support of the large scale operation at Moa Bay in Cuba was first detailed by Carlson and Simons<sup>(4)</sup>, then extended by Sobol<sup>(29-31)</sup> and Chavez<sup>(32)</sup>. Carlson and Simons reported on the kinetics and mechanism of this pressure leach, demonstrating the importance of the acid-ore ratio and temperature; kinetics of nickel extraction were explained by three nickel-bearing species, but no proof was given. Perhaps the most remarkable feature of this work was the shape of the nickel extraction curves. Most of the leaching was complete in the first few minutes, with little extraction occurring during the remaining hour. Recently, Chou,

Queneau and Rickard<sup>(33)</sup> have presented laboratory results on the sulphuric acid pressure leaching of nickeliferous limonite from southern New Caledonia. This investigation extends that of Carlson and Simons. Particular attention was given to the first portion of the leaching period; the effect of temperature (225°C to 300°C), acid-to-ore ratio (0.21 to 0.30), % solids (10 to 45), particle size (-20 to -270 mesh), and agitation (50 to 600 rpm) on nickel extraction and selectivity were discussed. In general the authors established that increasing temperature increases the initial rate of nickel extraction; increasing acid/ore ratio increases total nickel extraction and nickel extraction rate; and decreasing the % solids increases leaching selectivity and acid utilization (i.e. less sulphur is lost to the leach residues). The temperature dependence of the nickel extraction rate between 250° and 275°C is pronounced during the first 10 min. of leaching, but becomes almost temperature independent after 15 mins. Also, the 225°C and 300°C reaction temperatures results in significantly lower nickel extraction than does the 250 to 275°C intermediate range. Low temperature apparently does not provide the driving force needed for rapid nickel extraction, and very high temperature apparently results in coprecipitation of nickel with the solid hydrolysis products. Nickel extraction is insensitive to agitation after 30 sec of leaching, showing that during most of the reaction period the diffusion of a reacting species through a liquid boundary layer was not limiting. The fact that nickel extraction is independent of agitation after a brief initial mixing period, verify one of Sobol's concepts: to attain high leaching rates and complete conversion, rapid and perfect mixing of the ore

and acid is required<sup>(29)</sup>. However, Sobol also stated that "intensive agitation is required during the time the sludge remains in the reactor to attain complete conversion"<sup>(30)</sup>. This statement is quite contrary to the results obtained in this study.

Concerning overall improvement of the leach response, the authors concluded that laterite leaching is best conducted at temperatures higher than 250°C and at solids less than 30%. The acid/ore ratio level should be that required to attain reasonable nickel extraction at an acceptable rate.

Other established and proposed process in which the aim is to leach only nickel (and cobalt) involve a pretreatment step, which is most commonly a reduction roast. Under controlled conditions, high-temperature reduction allows most of the nickel and small fractions of the iron to be reduced to an iron-nickel alloy. This alloy must be leached from a matrix of, essentially, iron oxides and magnesium olivine. Several leachants are effective in extracting nickel from the reduction-roast product with varying degrees of selectivity. The most familiar example is presented by the commercially applied ammonia leach process<sup>(34)</sup> (Caron process) in which iron from the alloy dissolves and reprecipitates as hydroxide, while magnesium is not extracted. Power and Geiger<sup>(17)</sup> deal with the application of the reduction roast ammoniacal ammonium carbonate leach to nickel laterites.

Other leaching systems reported include aerated dilute sulphuric acid<sup>(35-37)</sup> and aqueous solutions of sulphur dioxide<sup>(38,39)</sup>. Although metallic iron and iron oxides are attacked in acidic systems, hydrolysis allows the dissolved iron to be reduced to a low level. Some magnesium also dissolves, although the extent of magnesium dissolution can be

restricted by taking advantage of its relatively slow dissolution rate. The use of chlorination to leach nickel from reduction roasted laterite (limonite) also has been studied<sup>(40)</sup>. If the solution contains substantially no free acid, magnesium dissolution is minimized, while extraction of iron may be limited to the iron content of the alloy. A recent paper presented by Roorda<sup>(41)</sup> deals with the advantages of chlorination.

In an interesting paper presented by Distin<sup>(42)</sup> it has been suggested that under certain conditions, copper sulphate solution might be an effective leachant for metallic nickel from reduction-roasted laterite. According to Distin, the use of this reagent would result in metallic nickel and iron dissolution only through the cementation reaction:



Attack of iron oxides and magnesium silicates would be minimized by operating with an effectively acid-free solution. In brief, the work outlined in the paper describes attempts to evaluate the technical feasibility of a process based on copper sulphate leaching under non-autoclave conditions, as shown in Fig. 2.1. After copper sulphate leaching of the reduced laterite, solid/liquid separation would provide a weakly acidic solution of nickel and iron sulphates, and a leach residue containing metallic copper. Copper recovery by flotation is envisaged followed by oxidation of the concentrate and redissolution of copper oxide in slightly greater than the stoichiometric amount of acid. The claimed advantages of this system are that rapid extraction of metallic nickel may be obtained under non-autoclave conditions in only a weakly corrosive environment, while gas transfer into the solution is not required. The effluent would, essentially,



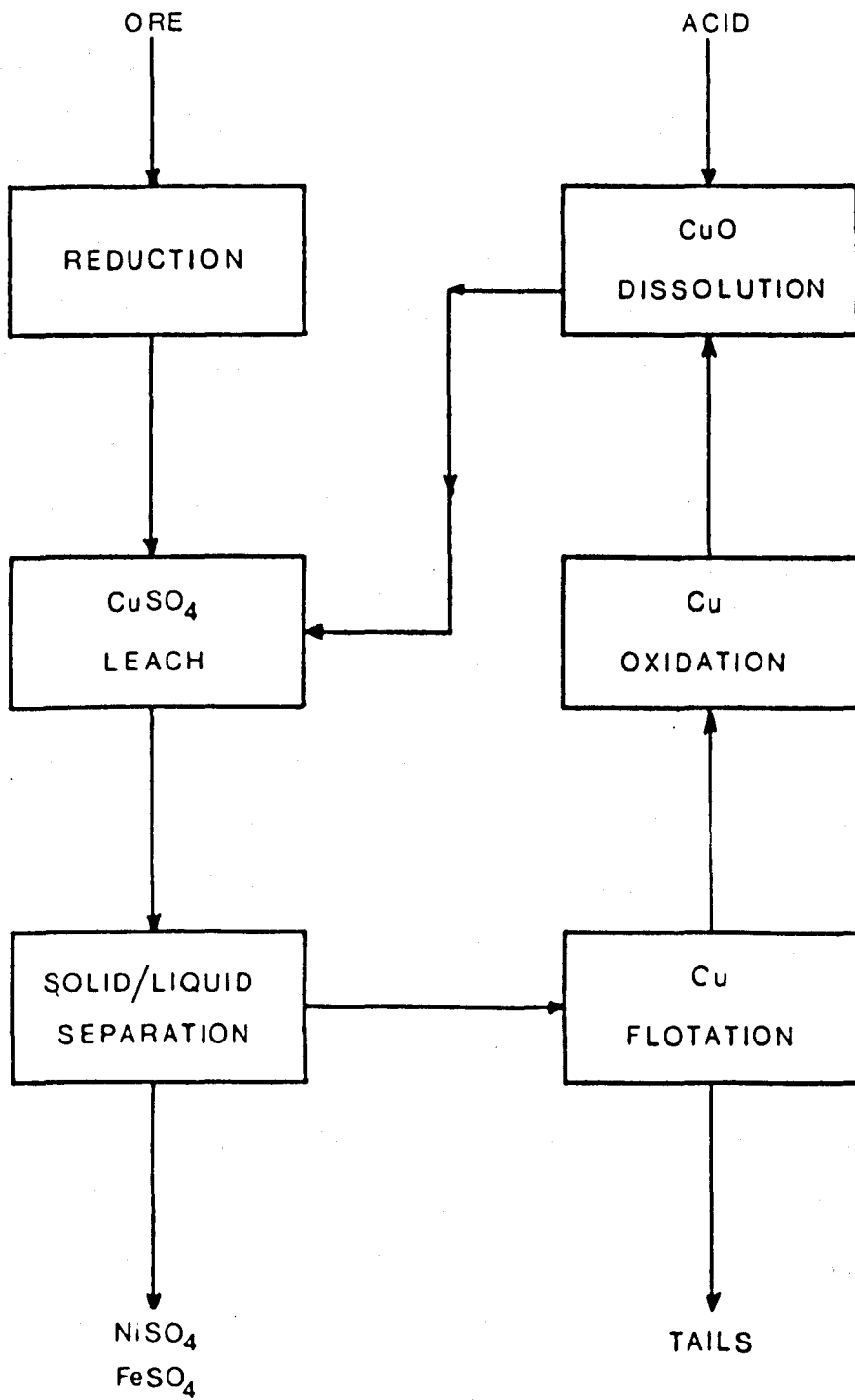


Fig 2.1 Conceptual flowsheet for copper sulphate leaching of reduced laterite. (42)

contain dissolved iron only, which could be precipitated by neutralization with lime. Distin however, made it clear that the advantages must be balanced against the necessity for flotation, concentrate oxidation, and copper oxide dissolution.

Another interesting two part paper recently presented by De Graff<sup>(43)</sup> (investigating why recovery of nickel from silicates is lower than from limonites) deals with the leaching of reduced laterites using the Caron liquor;  $4.4 \text{ mol dm}^{-3} \text{ NH}_3 + 1.0 \text{ mol dm}^{-3} \text{ CO}_2$  (Part I), and the use of EDTA (ethylenediamine tetra acetic acid) as a non-selective leach liquor, as well as a sodium citrate liquor buffered with  $\text{NaHCO}_3$  and containing sodium dithionite as a reductant for Fe(III). The use of ferric chloride, hydrochloric acid and  $\text{HCl} + \text{HF}$  are also reported (Part II). The results are compared with those obtained with the standard Caron liquor. Detailed studies on oxygen consumption during ammonia leach and precipitation of  $\text{Fe}(\text{OH})_3$  were reported.

Certainly, there are many other processes which have been proposed to achieve selectivity, but most of them have certain aspects in common. These are: (a) a pretreatment stage, commonly reduction roasting, and/or (b) a high temperature-pressure leaching stage. The choice between these two routes is perhaps influenced by many variables other than chemistry, such as energy, reagent costs, and materials of construction.

The ability to obtain selective nickel dissolution without a pre-roast or high pressure conditions would be an attractive feature of an overall process for nickel recovery from laterites. One such approach which, in principle, is applicable to laterite, is that of Bauer and Lindstrom<sup>(44)</sup>. These authors showed that copper could be extracted rapidly from low grade carbonate ores containing large amounts of

calcium by leaching with alkaline solutions of ethylenediaminetetraacetate (EDTA) at temperatures up to 80°C.

The stabilities of the copper and nickel E.D.T.A. complexes are similar. With regard to laterites with a high magnesium content, nickel is much more strongly complexed by E.D.T.A. than magnesium. For high iron limonites, operation in a basic solution would limit ferric dissolution while retaining any dissolved nickel, despite the higher stability of the ferric-E.D.T.A. complex than that of nickel.

Bryson and Distin<sup>(45)</sup> have evaluated the technical feasibility of such a process based on the leaching of a serpentine (1.65% Ni, 6.1% Fe, 20.2% Mg) and a limonitic (1.51% Ni, 49.7% Fe, 0.66% Mg) ores into E.D.T.A. solutions at atmospheric pressure at temperatures between 25°C and 90°C, followed by reduction with hydrogen (400 p.s.i. - 120°C or 140°C) to produce metallic nickel and regenerated leachant. In brief, Bryson and Distin concluded that nickel may be leached selectively from the raw serpentine and limonite components of a laterite using E.D.T.A. solutions at PH between 11 and 13 and at about 90°C. The leaching process is slow, especially for limonite if the major contained mineral is  $2\text{Fe}_2\text{O}_3 \cdot 3\text{H}_2\text{O}$ . (After 48 hours leach at 90°C and PH13 with 1.5 moles E.D.T.A. per mole of nickel in the ore, nickel extraction from the serpentine and limonite were 87% and 27% respectively). However partial decomposition of the mineral structures by calcination gives substantial increases in reaction rates. Reduction from a leach solution at PH13 with 800 p.s.i. hydrogen at 140°C for 3 hours gave 91% nickel recovery and a solution that can be used effectively as recycle leachant.

According to the experimental results presented in this paper any practical application based on an E.D.T.A. leach should exclude limonitic material due to the extremely slow leach kinetics and as the authors have stated, data for a wide range of materials would be needed before the potential of any process based on an E.D.T.A leach could be judged with certainty. Perhaps the most interesting feature of Bryson and Distin's work is the strong influence of pre-calcination (providing partial decomposition of the mineral structures) on dissolution rates, which indicates that the leaching response is highly sensitive to laterite mineralogy.

Obviously there is much scope when dealing with lateritic ores for the development of a process which requires no pretreatment stages and utilises leaching under low temperature and pressure conditions. Strong<sup>(13)</sup> has studied the use of hydrochloric acid for the non-selective leaching of unreduced lateritic nickel ores of both types, high iron content "limonites" and low iron content "serpentine". In this, it was demonstrated that silicates and limonites (classified on the basis of physical measurements; infra-red; differential thermal and X-ray diffraction analysis) react differently in acid solution and that the mineralogy of the nickel bearing phase plays an important part in determining the overall reactivity of the laterite towards acid extraction. Final extraction values are uniquely related to the solubility of the laterite, which is increased with the severity of the leaching conditions. (The effect of surface area, reaction time, temperature and acid concentrations were studied to optimize extraction conditions for both types of ore).

Barber and Wilson<sup>(46)</sup> have reported electrolytic leaching of a lateritic nickel ore in hydrochloric acid. Lupton and Perry<sup>(47)</sup>

have also reported the use of hydrochloric acid to leach an Egyptian Copper ore (2% Cu, 0.5% Ni) with the nickel in a chamosite gangue similar to laterite. The latter have shown that in order to have a feasible acid regeneration from the chloride solution a high metal concentration for both copper and nickel was necessary. These workers also showed what has become the basis for the present research; that is the decrease of nickel extraction when increasing the nickel concentration in the leach liquor, but did not offer any explanation.

Although hydrochloric acid provides a non-selective leaching, the use of this leaching reagent might be used for direct leaching at low temperature-pressure, as both metal oxides and recycled acid can be recovered by pyrohydrolysis of acid leach solutions<sup>(48,49)</sup> and the removal of impurities such as iron and copper is easier from chloride media<sup>(50)</sup>. The only industrial application of hydrochloric acid in nickel hydrometallurgy is the Falconbridge Matte leach process<sup>(51,52)</sup>. A detailed look at this process is perhaps informative as it embodies all the advantages of acid extraction and solvent extraction from chloride media<sup>(52)</sup> albeit from a nickel matte. Fig. 2.2. illustrates the unit operations involved. The basic principles are:

- 1) Selective dissolution of nickel from a finely ground matte with strong acid leach (7.5N). Copper and platinum metals are left as an insoluble sulphide residue.
- 2) Separation, by solvent extraction, of any anionic complexes formed during leaching.
- 3) Recovery of nickel utilizing the fact that increasing acid strength decreases nickel chloride solubility.

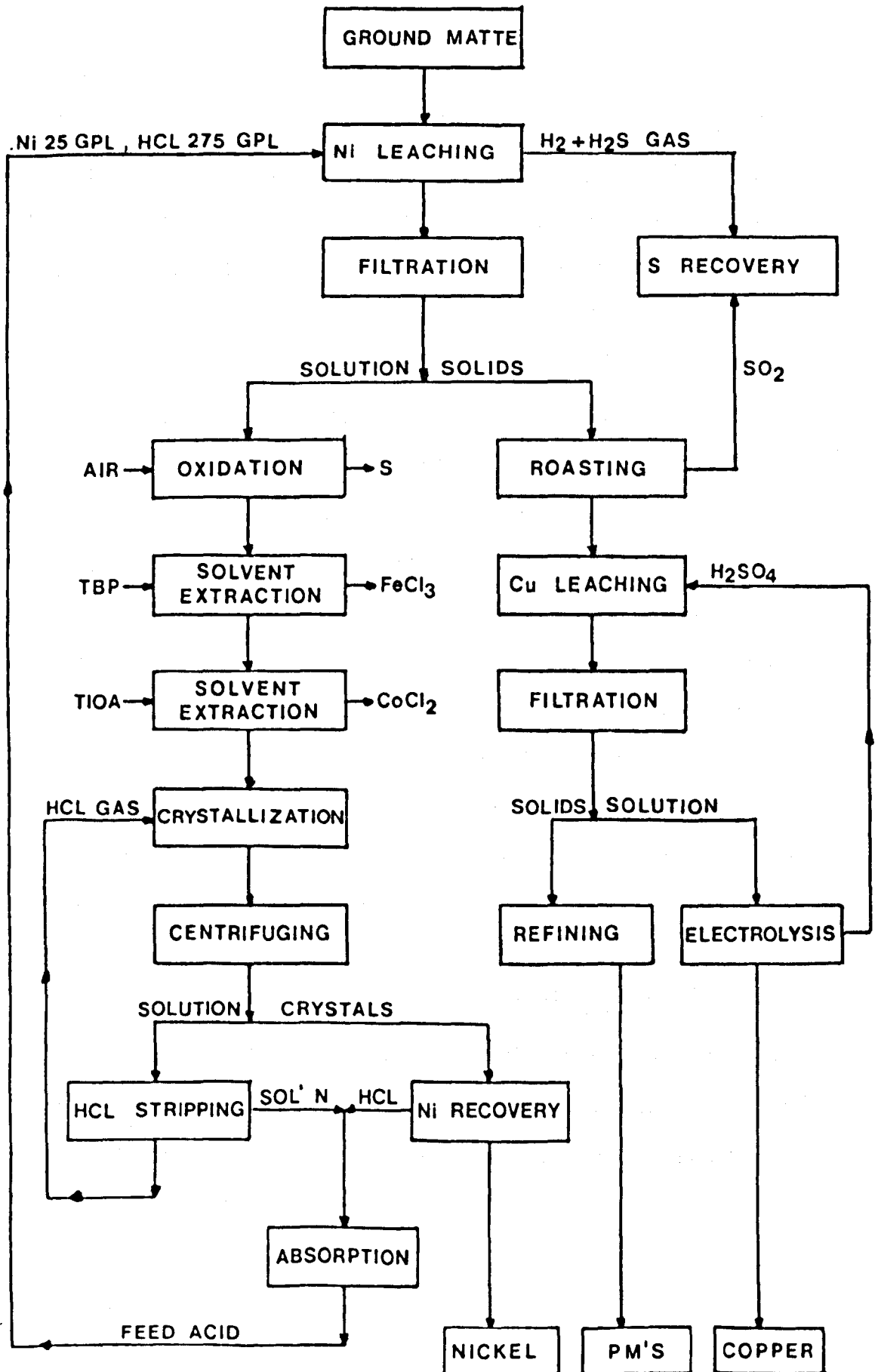
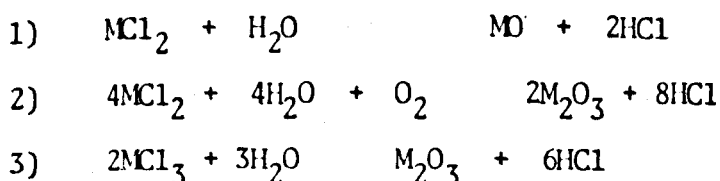


Fig. 2.2 Falconbridge Matte Leach Process

The process conditions (7.5 N acid, 70°C) enable the use of ordinary rubber-lined acid-proof equipment for gas, liquid and solid handling, overcoming the major problem of plant corrosion. Nickel chloride is recovered by crystallization and converted to oxide and hydrogen chloride gas in a fluidized-bed reactor<sup>(53,54)</sup>. "Nickel 98" is the final product after reduction.

Certainly, chloride processes involving gaseous reactants have good selectivity and because of their high volatility are easily recovered by distillation and adsorption (for details see references 55 to 61). However, although numerous processes exist the wider application of aqueous chloride technology is limited by reagent cost and the problem of regeneration of the leaching medium. Probably the most prohibitive feature of chloride routes is the excessive corrosion of plant equipment. The use of hydrochloric acid in hydrometallurgical processes has been restricted due to these factors and perhaps because further metal separation steps are necessary due to lack of selectivity. However, the high efficiency of recovering acid from chloride leach liquor by high temperature hydrolysis with steam at 650°-800°C (both the Amon reactor<sup>(62,63)</sup> and Woodall-Duckham<sup>(49)</sup> spray roaster are designed for this purpose), may perhaps make the use of hydrochloric acid feasible. The chemistry of metal chloride hydrolysis can be represented very simply by the following reaction types:



where M is (1)  $\text{Ni}^{2+}$ ,  $\text{Mg}^{2+}$   
 (2)  $\text{Fe}^{2+}$ ,  $\text{Mn}^{2+}$ ,  $\text{Co}^{2+}$   
 (3)  $\text{Fe}^{3+}$ ,  $\text{Al}^{3+}$ ,  $\text{Cr}^{3+}$

This offers the possibility of closed circuit operations with no waste products. The Woodall-Duckham process<sup>(49)</sup> has been applied commercially to many different applications, which fall largely into three categories:

- 1) Steel pickling - where the acid is regenerated to reduce acid costs and eliminate pollution; the iron oxide recovered is a secondary, although valuable, by-product.
- 2) Mineral upgrading - where a low grade mineral, such as ilmenite or silica sand, can be upgraded by leaching out unwanted contaminants.
- 3) Metal oxide production - where the feed material may be a natural metal chloride (e.g. magnesium chloride) and the regeneration process is used to produce a high-quality metal oxide (magnesia), with HCl as the by-product.

Obviously, in all these applications, the optimum use of HCl regeneration is only obtained by considering the combined process as an integrated facility. A paper presented by Connors<sup>(64)</sup> deals with the optimum use of regeneration in all these processes. The application of hydrochloric acid to metal extraction from ores are few, the most notable of these being the Peace River Iron Process<sup>(65,66)</sup> which was actually applied to scrap and failed due to market problems, lateritic iron ores in India<sup>(67)</sup> and more recently, manganese nodules<sup>(68)</sup> have been investigated with a view to acid extraction.



The recovery of nickel from acidic chloride solution by pressure reduction of nickel hydroxide (Derry process<sup>(69,70)</sup>) is certainly an interesting proposition for the leaching of nickeliferous laterites (especially serpentines) in hydrochloric acid. Derry and Whittemore<sup>(69)</sup> have reported the use of magnesia as an alkali to precipitate nickel hydroxide from acidic chloride solution. The authors showed that magnesia is an ideal alkali because even when used in an excess, the rise in pH is not sufficient to remove all the nickel ions from solution (reduction proceeds via reduction of a small residual concentration of nickel ions in solution). In addition magnesia has the advantage that for chloride solutions that magnesia and hydrochloric acid can be readily recovered from the magnesium chloride reduction end solutions.

Strong and Rice<sup>(7)</sup> have proposed in a general way the type of flow sheet that could be envisaged for the leaching of lateritic nickel ores (serpentine) in hydrochloric acid, involving the Derry process as a means of recovering nickel from chloride solution using MgO (recycled from spray roasting) as an alkali to precipitate nickel hydroxide. Strong and Rice suggested that excess of MgO could be sold as a by-product, as could the high grade Fe<sub>2</sub>O<sub>3</sub> produced. A similar flow-sheet is proposed in this research (see Fig. 7.3 in Chapter 7).

In general and as a summary it might be said that many patents and processes exist for the treatment of lateritic nickel ores. Most of those via hydrometallurgy involve a pretreatment stage and/or high pressure-temperature leaching stage in order to achieve selectivity.

Aqueous chloride routes make metal separation easier but lack the desired selectivity for nickel and cobalt over iron. However, it is possible that these disadvantages might be off set by a lowering of energy consumption as it would not be necessary to heat large amounts of inert material to a high temperature. Although metal and acid recovery can be achieved the corrosion aspect of acid processes still remains one of the major obstacles to metal extraction using hydrochloric acid as a leaching reagent. Many of the problems however, have been overcome in recent years.

## CHAPTER 3

### EXPERIMENTAL

#### 3.1. Outline

The experimental work of this research project involved the following aspects:

1. Leaching of nickeliferous laterites in hydrochloric acid with metal chlorides additions;

- Leaching of both silicate and limonite laterite ores in HCl solutions with addition of  $\text{NiCl}_2$ .
- Leaching of silicate laterite ores in HCl solutions with addition of  $\text{MgCl}_2$ .
- Leaching of limonite laterite ores in HCl solutions with addition of  $\text{FeCl}_3$ .
- Maximization of nickel extraction by optimization of leaching variables (temperature, acid concentration and contact time).
- Effect of pulp density upon cation extraction.
- Lump leaching.

2. Kinetics of acid dissolution of a lateriteic nickel ore .

- Effect of leaching variables upon cation extraction from a lateritic nickel ore leached in pure HCl and in HCl containing nickel in solution (temperature, acid concentration, particle size).

3. Washing of leach residues with pure dilute hydrochloric acid.

- Single-stage batch system.
- Multistage batch cross-current system
- Multistage batch counter-current system.

### 3.2. Leaching studies

All leaching tests were performed in 500 ml capacity cylindrical flanged quickfit glass vessels held by clamps into a water bath equipped with thermostat and circulating pump. The operating temperature of both the water bath and of the solution into the vessels was controlled to an accuracy of about  $\pm 0.1 - 0.2^{\circ}\text{C}$  (checked by thermometer). Each vessel was equipped with a reflux condenser and a stirrer driven by a variable speed electric motor. A photograph of the apparatus is given in Fig. 3.1.

#### 3.2.1. Leaching technique

Appropriate volumes of pure hydrochloric acid was added to the leaching vessels and whilst stirring, the operating temperature was raised. Depending on the experiment, known weights of  $\text{NiCl}_2$ ,  $\text{MgCl}_2$  or  $\text{FeCl}_3$  were added to the vessels. Weighed amounts of fresh ore were then added into the vessels and leached for the required time. At the completion of each run, samples of leach liquors (clear solution) were withdrawn and stored for atomic absorption analysis. The leach residues were then washed with an excess of pure  $\text{HCl}$  (diluted) whilst being filtered. Filtration was performed using a buchner funnel with double layer of 42 ashless whatman filter paper. After filtration, solid residues were dried at about  $110^{\circ}\text{C}$ , weighed (to determine the weight of laterite dissolved) and stored for atomic absorption analysis.

During the leaching tests for the kinetic studies, the procedure was similar, except that the samples of leach liquor were withdrawn (by pipette) at various times during the reaction.

Each leaching test was performed at least 3 times and the results given are an average of the three. The accuracy was about  $\pm 1\%$ .

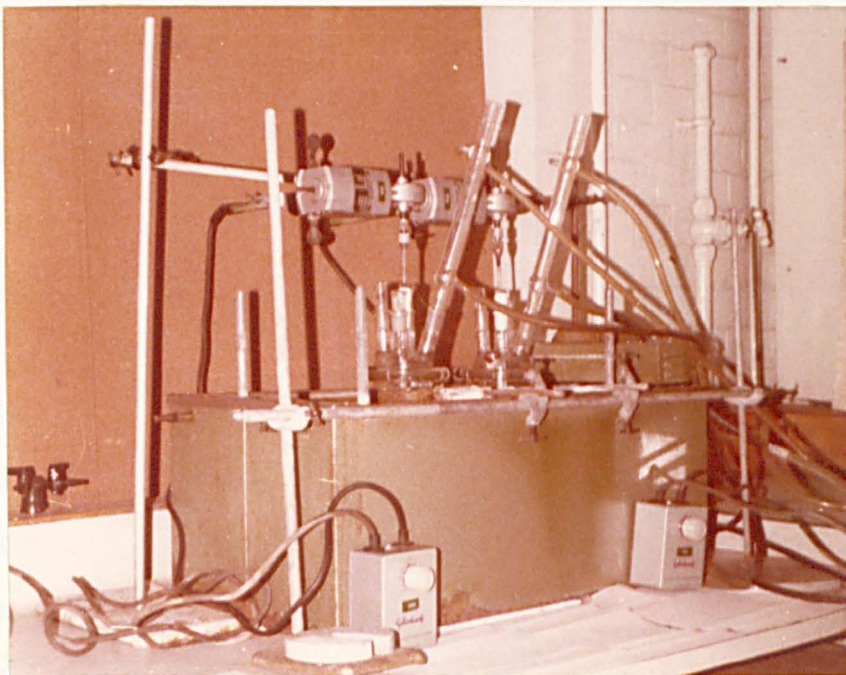


Fig. 3.1 Leaching Apparatus

### Digestion Technique

Either direct acid digestion, or fusion and subsequent dissolution are the most commonly applied methods of taking laterite samples into solution. General procedures for both methods are given by Young<sup>(75)</sup> and Pflum<sup>(76)</sup>. In direct acid dissolution, the incorporation of

### 3.2.2. Atomic Absorption Analysis

Considering the mineralogy and chemical composition of the laterites studied and the needs for analysis of both leach liquors and residues, the analytical method chosen should enable determination of the elements of interest over the full range of concentration and in the presence of large amounts of other substances. The capability of atomic absorption spectrophotometry (A.A.S.) to determine numerous elements in a large number of samples rapidly and simply makes this method particularly attractive for this research. Its principal advantages are:

- a) it shows high sensitivity for a wide range of metals and it is highly specific,
- b) any one metal can normally be determined in the presence of large amounts of other substances,
- c) it is rapid, simple and requires only small amounts of sample.

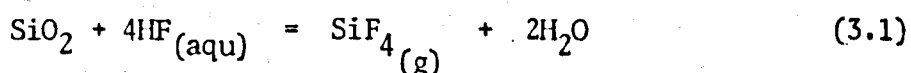
Thus, owing to the above mentioned advantages, it was decided to apply A.A.S. for the determination of nickel, iron and magnesium in each laterite subject to leaching and for the subsequent analysis of leach liquors and residues. The principles and instrumentation for this method of analysis are well documented in the literature<sup>(71-74)</sup> and will not be discussed here.

The analytical procedure involved a digestion technique and metal determination as below:

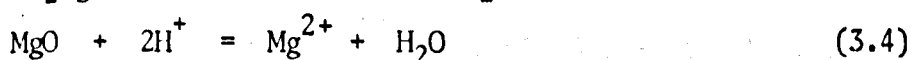
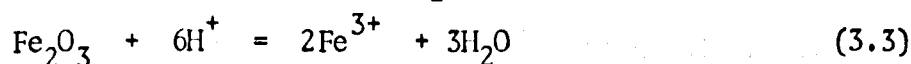
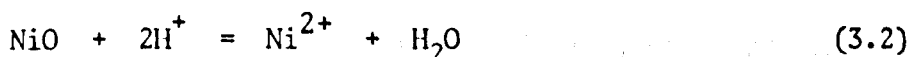
#### Digestion Technique

Either direct acid digestion, or fusion and subsequent dissolution are the most commonly applied methods of taking laterite samples into solution. General procedures for both methods are given by Young<sup>(75)</sup> and Easton<sup>(76)</sup>. In direct acid dissolution, the incorporation of

metal ions in silicate phases requires the use of hydrofluoric acid mixtures to attack the silicate. The silicon is lost from solution as silicon tetrafluoride gas:



and therefore cannot be determined by this method. However, the other elements of interest remain in solution:



The major anion present will depend on the other acid(s) used in combination with hydrofluoric acid - normally, hydrochloric, perchloric, sulphuric or nitric acid - since excess of HF is boiled off.

In this work, nickel, iron and magnesium were taken into solution by decomposition of the samples in a hydrofluoric, perchloric and nitric acid mixture. In this, a weighed amount of sample (0.1g) was transferred to a 25 ml conical flask, then 5 ml  $\text{HClO}_4$  (70% W/W), 2 ml  $\text{HNO}_3$  (70% W/W) and 1 ml HF (40% W/W) were added. This mixture was digested for 1 hour (using a funnel in the flask neck as an anti-splash device) and taken to dryness. The residue was then taken up in diluted hydrochloric acid to provide a 5% acid concentration in the final volume.

#### Metal determination

A Varian Techtron AA5 spectrophotometer instrument was employed, using hollow cathode lamps<sup>(77)</sup> and air-acetylene flame (for nickel and iron determination) and a nitrous oxide-acetylene flame (for magnesium determination). Two wavelengths were used for the

determination of each nickel, iron and magnesium, depending upon the sensitivity required. Nickel was analysed at either 232.0 nm (0-12  $\mu\text{g ml}^{-1}$ ) or 352.4 nm (15-60  $\mu\text{g ml}^{-1}$ ), iron at 248.3 nm (2-10  $\mu\text{g ml}^{-1}$ ) or 372.0 nm (25-100  $\mu\text{g ml}^{-1}$ ) and magnesium at 285.2 nm (0.1 - 0.4  $\mu\text{g ml}^{-1}$ ) or 202.5 nm (5-20  $\mu\text{g ml}^{-1}$ ). Standards for nickel were diluted from a 1000  $\mu\text{g ml}^{-1}$  solution (prepared by diluting pure nickel metal in hydrochloric acid) and made up to volume with the appropriate matrix solution. Similarly, standards for iron and magnesium were diluted from 1000  $\mu\text{g ml}^{-1}$  stock solutions.

Interference from iron<sup>(74,78)</sup> (see Table 3.1 - Effect of iron in the determination of nickel<sup>(13)</sup>), which enhances nickel absorption in the low temperature air-acetylene flame due to the formation of undissociated Fe-Ni oxides<sup>(13)</sup>, was overcome by adding similar amounts of solution of a given iron concentration to the standards, providing a comparable matrix solution for nickel determination. Interference from aluminium, which suppresses magnesium absorption in low-temperature air-acetylene flame because of the formation of stable aluminate, was avoided by using the high-temperature nitrous oxide acetylene flame<sup>(77)</sup>. Potassium chloride solution (1000 ppm) was added in identical volumes to both standards and samples, to compensate for the increase in ionization<sup>(13)</sup>.

No interference was observed during determination of iron.

### 3.2.3. Electron Probe Microanalysis

Electron probe microanalysis provides a means of determining the chemical composition of very small volumes at the surface of



Table 3.1. Effect of iron in the determination of nickel <sup>(13)</sup>

System		Iron Content (ppm)					
		0	100	200	300	400	500
A* 1.00	B*	1.0	1.02	1.05	1.17	1.18	1.23
	C*	0.0	1.70	4.94	17.74	18.77	22.86
A 2.00	B	2.0	2.04	2.10	2.28	2.31	2.36
	C	0.0	2.20	4.60	13.93	15.64	18.03
A 4.00	B	4.0	4.01	4.02	4.44	4.51	4.52
	C	0.0	0.42	0.55	11.47	12.62	13.30
A 8.00	B	8.0	8.01	8.16	8.80	8.91	8.96
	C	0.0	0.37	2.05	9.92	10.21	12.19
A 10.00	B	10.0	10.04	10.06	10.98	11.10	11.28
	C	0.0	3.38	6.00	9.20	11.1	12.10

\* A - True concentration of nickel present (ppm)

\* B - Observed concentration of nickel

\* C - % enhancement of nickel value

polished thin sections of rocks or mineral mounts. The name derives from the essential feature of a fine electron beam which is directed at the point to be analysed. The x-ray generated by the impact of the beam are characteristic of the elements present, and their intensity is an approximately linear function of concentration.

In its simplest form the electron-probe microanalysis consists of an electron-optical system which focuses an electron beam into an area about 1  $\mu\text{m}$  diameter on the surface of the specimen, a stage on which the specimen and standards are mounted, a microscope which allows the area of interest to be selected and positioned in the electron beam, and one or more spectrometer which select and measure the intensity of the characteristic radiation of the elements to be determined. The basic measurement is a comparison of the net intensity of a particular x-ray line generated in the specimen with that generated in the standard of the same incident current. A detailed description of the instrumentation and principle of the electron-beam microanalyser is given by Long<sup>(79)</sup>.

The application of the electron probe analysis to mineralogical and metallurgical problems is well documented by the literature<sup>(80-84)</sup>. Its application to lateritic nickel ores both before and after leaching has been reported by Limerick<sup>(18)</sup>. In this, it is reported that due to the physical and chemical nature of the laterites a number of problems arise when applying the probe, of which the significance depends on the purpose of the probe investigation. For example, if the data is to be used simply as an indicator of relative levels of an element in different components, then a fairly large, random error can be tolerated so long as the levels of, say, nickel concentration are not too close

in the various components. However, if a modal analysis is required to indicate the proportion of total nickel content associated with each component, then absolute nickel concentrations are necessary. The physical and chemical nature of the sample will affect the levels of accuracy.

Nickel is present in laterites at concentrations of about 1%, at which level it is readily measured by the probe, but its determination in residues after 90% extraction may be a problem. Under favourable conditions the electron-probe is capable of detecting nickel at that level (0.1%), but it requires a polished specimen with the absolute minimum of surface relief<sup>(79)</sup>. However, since laterites may contain coarse-grained, hard material like quartz and chromite in close association with soft, fine-grained friable minerals<sup>(18)</sup>, it is extremely difficult to produce a polished section free of relief, plucking, scratches, etc. This makes analysis of elements at low concentration highly inaccurate.

In this research, microprobe analysis was used merely as an indicator of the relative concentrations of nickel, iron and magnesium in a reaction product layer in lump particles leached in pure HCl and in HCl solutions with additions of NiCl<sub>2</sub>, MgCl<sub>2</sub> and FeCl<sub>3</sub>.

#### 3.2.3.1. Procedure

Each specimen was mounted in a Metaserve press (at 140°C and 200 bar pressure), using black bakelite moulding powder as mounting material. Subsequently, the mounted specimens were submitted to a series of rotary polishers (metaserve) with the following polishing sequence:

- 1 - 400 grit standard water proof sand paper
- 2 - 600 grit standard water proof sand paper
- 3 - 6 micron diamond spray compound plus lubricant
- 4 - 1 micron diamond spray compound plus lubricant
- 5 - 0.05 micron linde gamma alumina plus water

The polished specimens were then carbon coated<sup>(79)</sup>, examined (using a Vickers M55 microscope) and photographed prior to examination in the electron probe microanalyser.

Finally, determination of the elements of interest (Ni, Fe and Mg) was performed using a JEOL JXA 50A electron probe microanalyser, where pure elements were used as standard. These analyses were performed by the Department of Earth Sciences, University of Leeds.

### 3.3. Washing studies

This work involved the systematic washing of leach residues (from a laterite nickel ore leached in HCl solution containing high nickel concentration) with pure HCl in a:

Single-stage batch system

Multistage batch cross-current system

Multistage batch counter-current system

#### 3.3.1. Washing technique

Single-stage batch system:-

At the completion of the leaching, the mixture was transferred to a washing unit (glass vessel) where it was allowed to settle until a clear solution was obtained, after which a known volume of leach liquor was withdrawn (this allowed the volume of leach liquor remaining associated with the solids to be known). A given volume of pure dilute

HCl was then added to the slurry, which was mixed and allowed to settle for 30 minutes (it was experimentally determined that a practical equilibrium was almost reached for 30 minutes contact time, see section 6.2.2.2. in Chapter 6). It should be noted, that in some experiments agitation was provided. In those cases, the mixture was stirred for a given period of time, after which it was allowed to settle as in the previous cases. At the completion of this operation, a known volume of clear wash solution was withdrawn (overflow) and sampled for atomic absorption analysis. The slurry residues (underflow) were then filtered, dried and weighed. Atomic absorption analysis was only performed for those solid residues from washing experiments where the nickel concentration in the washing solution (at practical equilibrium) was extremely low. The reason for this lies on the fact that a perfect solid/liquid separation could not be achieved, thus unless the solution associated with the solid residues contained no nickel (or the content was extremely low and could be considered negligible) and no further nickel can be extracted from the solid by the washing, the analysis of solid residues would provide inaccurate results. This is because, if solid residues associated with a solution containing high nickel concentration were to be submitted to atomic absorption analysis, and the solid/liquid separation has been imperfect (even when slightly imperfect), nickel in the solution which is entrained with the solids would alter the true nickel content in the solids. If an attempt was made to remove the nickel in solution by diluting it with further washing of the residues, the true content of the nickel in the solids would also be altered, because by contacting the solids with a solution with a lower nickel concentration,

extraction of nickel from the solids would occur, i.e. the lower the nickel concentration in the washing solution, the higher the nickel extraction from the solid residues, as will be seen later in Chapter 6.

Multistage batch cross-current system:-

This washing system is an extension of the single-stage washing system, where the leach residues are successively contacted in "n" stages with known equal volumes of pure HCl. In this, with the exception of the first stage the feed to any stage is the underflow slurry from the preceding stage. A single final underflow slurry results, and the overflow stream from each stage may be combined to provide a single final product washing solution.

The washing procedure used in this system was merely a repetition of that previously described for a single-stage system. In this procedure, at each washing stage an overflow stream (clear wash solution) and an underflow stream (slurry residues) were obtained after a given period of contact time in which a 'practical equilibrium' was assumed to be reached. Thus, on the assumption that each stage was at practical equilibrium (i.e. the wash solution associated with the solid residues in the underflow has the same solute (say nickel) concentration as that in the overflow), samples of wash solution for atomic absorption analysis were withdrawn from the overflow streams only. Analysis of the solid residues from the underflows were not performed, unless the nickel concentration in the solution associated with the solid residues was extremely low.

Multistage batch counter-current system:-

In this washing system, overflow and underflow streams flow from stage to stage countercurrently and provide two final products.

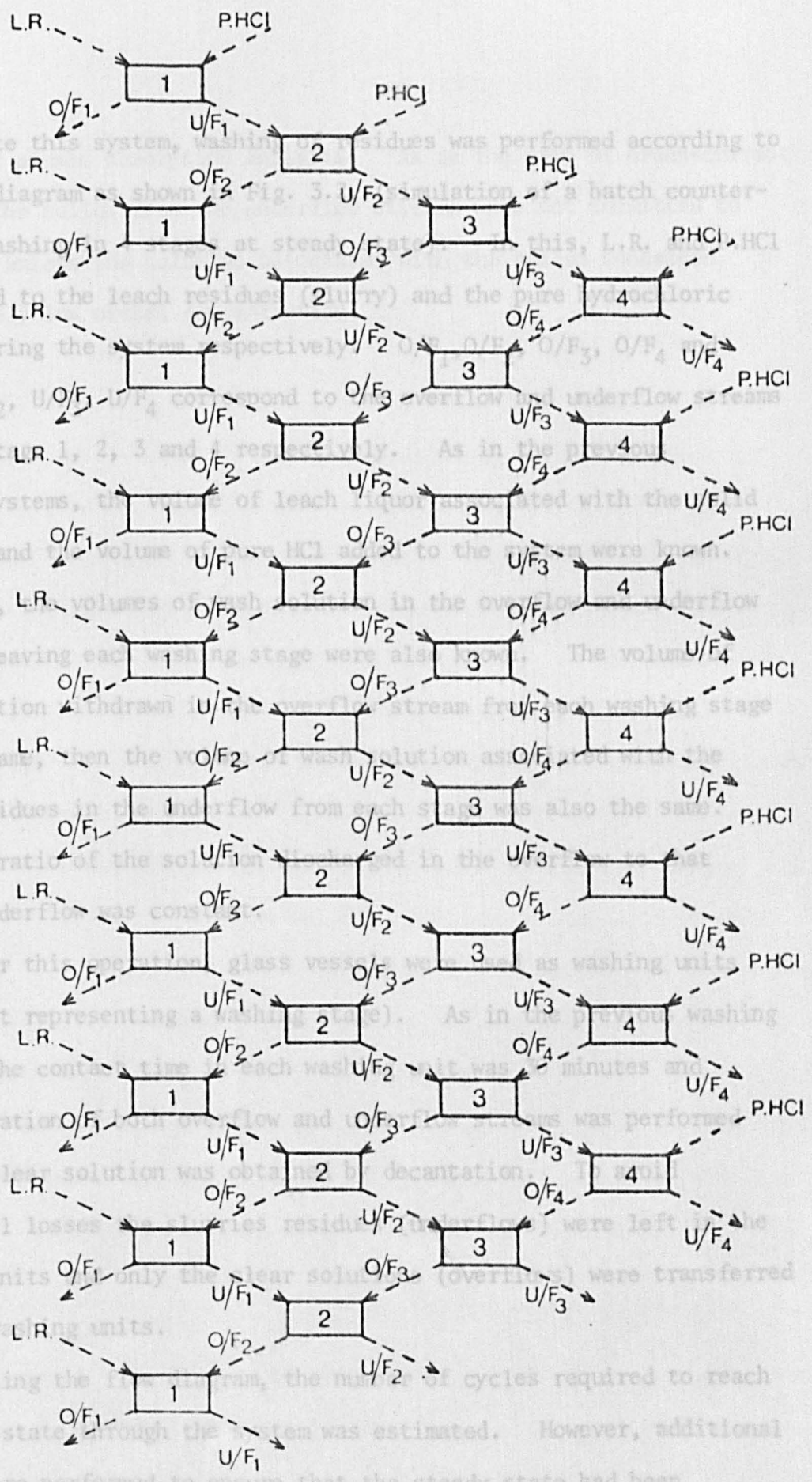


Fig 3.2 Simulation of a batch counter-current washing in 4 stages (at steady state).

To simulate this system, washing of residues was performed according to the flow diagram as shown in Fig. 3.2. (simulation of a batch counter-current washing in 4 stages at steady state). In this, L.R. and P.HCl correspond to the leach residues (slurry) and the pure hydrochloric acid entering the system respectively.  $O/F_1, O/F_2, O/F_3, O/F_4$  and  $U/F_1, U/F_2, U/F_3, U/F_4$  correspond to the overflow and underflow streams leaving stage 1, 2, 3 and 4 respectively. As in the previous washing systems, the volume of leach liquor associated with the solid residues and the volume of pure HCl added to the system were known. Similarly, the volumes of wash solution in the overflow and underflow streams leaving each washing stage were also known. The volume of wash solution withdrawn in the overflow stream from each washing stage was the same, then the volume of wash solution associated with the solid residues in the underflow from each stage was also the same. Thus the ratio of the solution discharged in the overflow to that in the underflow was constant.

For this operation, glass vessels were used as washing units (each unit representing a washing stage). As in the previous washing system, the contact time in each washing unit was 30 minutes and the separation of both overflow and underflow streams was performed after a clear solution was obtained by decantation. To avoid mechanical losses the slurries residues (underflows) were left in the washing units and only the clear solutions (overflows) were transferred between washing units.

Using the flow diagram, the number of cycles required to reach a steady state through the system was estimated. However, additional cycles were performed to ensure that the steady state had been reached. Samples of each overflow stream were taken from the latter



cycles for atomic absorption analysis. As in the case of cross-current washing, the solids from the underflow streams were not submitted to analysis, unless the solution associated with the solids contained an extremely low nickel concentration.

## CHAPTER 4

### LEACHING OF LATERITIC NICKEL ORES IN HYDROCHLORIC ACID WITH METAL

#### CHLORIDES ADDITION

##### 4.1 Introduction

Strong<sup>(13)</sup> reported that during leaching of a nickeliferous laterite (serpentine) with hydrochloric acid in a multiple contact system (that is the leach acid is repeatedly contacted with fresh ore), it was observed that as the number of contacts was increased (increasing the aqueous concentrations of  $\text{NiCl}_2$ ,  $\text{MgCl}_2$  and  $\text{FeCl}_3$  in the leach acid) the extraction of nickel, iron and magnesium gradually decreased. A similar effect on nickel extraction from a chamosite ore with 0.5% Ni was reported by Lupton and Perry<sup>(47)</sup>.

It was thought initially that the addition of other cations e.g.  $\text{Mg}^{2+}$  or  $\text{Fe}^{3+}$  to the leach solution might increase nickel recovery by displacing the nickel or iron that might have been adsorbed by the residues. This theory has subsequently been shown to be incorrect but the effects of such additions are of considerable interest.

The work involved in this chapter describes a study of the effect of the addition of metal chlorides,  $\text{NiCl}_2$ ,  $\text{MgCl}_2$  and  $\text{FeCl}_3$ , to the leach acid (HCl) upon the extraction of nickel, iron and magnesium.

##### 4.2 General characteristics of selected nickeliferous laterites.

Seven laterites from the same batch of samples as used by Strong<sup>(13)</sup> were selected and coded as shown in Table 4.1. Their places of origin and mineralogy are also indicated. A detailed chemical analysis<sup>(13)</sup>

Table 4.1. Origin and Mineralogy of selected laterite nickel ores <sup>(13)</sup>

LATERITE ORES		CONSTITUENTS		REMARKS
Code	Origin	Major	Minor	
A	Phillippines	Altered serpentine	Quartz, Fe oxides	Mottled silicate with brown iron staining, hard rock
B	New Caledonia	Serpentine	Quartz, magnetite	Brownish-green veined silicate, hard rock.
C	Oregon, U.S.A.	Garnierite	Quartz, talc	Brilliant green fragments in a highly silicified matrix
D	Australia	Garnierite, goethite	Magnetite, Chromite	Small green fragments in a soft, powdery brown matrix.
E	Philippines	Goethite	Magnetite	Friable, nodular concretions with a rotted texture, light ochre colour
F	New Caledonia	Goethite	Magnetite	Hard, dark brown nodules similar to ore-E
G	Cuba	Goethite	Quartz, chromite	Very friable, irregular lumps. Rotted texture breaks down into a soft brown powder

for each of these laterites is given in Appendix I. From this table and according to the chemical analyses, it is possible to classify these laterites into two groups. The first (ores A-C) is characterized by a high  $\text{SiO}_2$  and  $\text{MgO}$  and a low  $\text{Fe}_2\text{O}_3$  content, and the second (ores E-G) by a low  $\text{MgO}$  and  $\text{SiO}_2$  content and high  $\text{Fe}_2\text{O}_3$ . Ore D is a mixture of both groups. Thus, ores A to C can be classified as "silicates" <sup>(7)</sup>, while ores E to G as "Limonites", and ore D as a mixture of both. These ores were chosen to cover the whole range of lateritic compositions as the chemical analyses show. No discrete nickel minerals are present in these ores <sup>(13)</sup> but it is generally assumed that nickel isomorphically replaces magnesium in the brucite layer in serpentines <sup>(7)</sup> and is associated with goethite <sup>(13)</sup>, either in solid solution or as an intimate mixture, in the limonitic ores.

Because of Strong's detailed work <sup>(7,13)</sup> on the chemical composition and mineralogy of these laterites, it was considered that no further study was necessary on these aspects, and his work was taken as the basis for the present research. However, even though chemical composition data for the seven laterites were available, determination of nickel, iron and magnesium for these laterites were performed. The results of these analyses (see Appendix I) showed an excellent agreement with those given by Strong.

#### 4.3 Leaching testwork

The experimental apparatus, procedure and analytical method of analysis for the leach work have already been described in Chapter 3 (see sections 3.2 to 3.2.2 ).

Leaching conditions such as temperature, acid concentration, contact time and pulp density are specified for each test or set of experiments. Details of the particle size distribution (ores A to G) used for most of the leach work are given in Appendix I.

#### 4.3.1. Leaching of laterites with nickel chloride addition

To study the effect of the aqueous nickel chloride concentration, in the leaching acid (HCl), upon the extraction of nickel, iron and magnesium from the selected laterites, sets of 7 leaching tests with nickel chloride additions to give from 0 to 20 g/l Ni, were carried out for each of the silicate and limonitic nickel ores. The leaching conditions chosen for these experiments were:

Temperature	=	70°C
Acid concentration	=	4 mol/dm <sup>3</sup>
Contact time	=	1 hour
Pulp density	=	10% solid
Size distribution	=	as in Appendix I
Agitation	=	strong stirring

The results of these tests are presented in Tables 4.2 and 4.3, where cation extractions from each of the laterites are given both before and after the washing of the leach residues. The weight of ore dissolved (%) is also included. From these tables it is seen that those extraction data obtained before the washing of leach residues (as determined by analyses of the leach liquors) clearly show that nickel concentration in the leach acid has a marked effect on the cation extraction during the leaching of these laterites. This effect can be seen in Figs. 4.1 to 4.7, where plots of cation extraction (%) versus nickel concentration in the leach acid are illustrated for

Table 4.2 Cation extraction from laterite ores A to D leached in HCl solutions containing different nickel concentrations ( $4 \text{ mol/dm}^3 \text{ HCl}$ ,  $70^\circ\text{C}$ , 1 hour contact time 10% solid and size distribution as in appendix I)

Ore	Nickel concentration in leach acid (g/l)	Cation extraction %						O.D. %
		B.W.R.			A.W.R.			
		Ni	Fe	Mg	Ni	Fe	Mg	
A	0	97.2	92.8	93.4	97.8	92.9	93.7	63.4
	2	80.0	92.1	93.1	97.1	92.7	93.4	62.9
	4	63.3	91.6	92.5	98.4	94.0	93.0	63.3
	8	27.2	90.2	91.8	93.5	92.8	94.2	63.2
	12	11.2	88.7	90.3	96.1	91.8	93.2	61.2
	16	3.0	88.1	87.9	97.2	93.3	90.7	64.0
	20	0.0	87.5	87.4	97.7	92.6	93.2	62.8
B	0	91.6	94.9	94.4	98.0	97.5	98.1	57.5
	2	86.4	94.8	93.8	96.2	97.1	94.3	56.9
	4	78.3	94.6	93.6	98.4	98.0	96.6	57.0
	8	51.8	92.8	91.4	98.2	97.8	98.1	55.3
	12	12.4	92.0	88.3	97.1	95.9	98.4	53.9
	16	5.7	90.5	87.5	98.4	98.0	96.1	58.2
	20	0.0	89.9	87.2	97.8	98.3	97.7	56.8
C	0	44.6	70.1	68.4	45.3	72.0	68.6	17.6
	2	39.9	69.5	68.0	44.7	71.6	68.0	18.3
	4	34.8	68.6	66.7	42.9	69.9	67.2	20.2
	8	32.0	67.8	64.9	43.5	72.1	67.8	16.7
	12	20.5	67.3	67.2	45.0	74.2	71.1	18.5
	16	12.2	66.3	62.9	41.8	70.0	66.8	20.1
	20	0.0	64.9	61.2	44.2	73.0	68.4	17.9
D	0	75.4	68.2	81.2	75.5	69.4	83.0	44.2
	2	73.3	68.1	80.9	75.8	67.2	81.6	43.7
	4	69.6	67.4	79.4	76.1	70.2	81.8	44.3
	8	44.2	66.3	77.4	78.2	69.5	82.2	41.1
	12	8.6	65.7	75.6	71.5	66.3	79.5	43.2
	16	1.5	65.2	74.4	77.0	71.0	82.4	43.9
	20	0.0	64.7	72.6	75.8	70.2	82.1	45.7

B.W.R. = cation extraction determined before washing of leach residues

A.W.R. = cation extraction determined after washing of leach residues

O.D. = weight of ore dissolved.

Table 4.3 Cation extraction from laterite ores E to G leached in HCl solutions containing different nickel concentrations. (4 mol/dm<sup>3</sup> HCl, 70°C, 1 hour contact time 10% solid and size distribution as in appendix I)

Ore	Nickel concentration in leach acid (g/l)	Cation extraction %				O.D. %
		B.W.R.		A.W.R.		
		Ni	Fe	Ni	Fe	
E	0	80.3	98.3	82.0	98.5	78.6
	2	75.8	96.8	81.7	97.3	78.1
	4	72.2	94.1	82.4	98.0	79.0
	8	50.2	91.9	80.6	98.3	76.9
	12	10.6	88.6	78.9	96.1	75.4
	16	2.2	86.2	82.2	98.1	78.4
	20	0.0	84.9	81.5	98.2	77.8
F	0	81.4	99.3	81.5	99.3	75.2
	2	77.8	98.9	78.9	99.0	74.3
	4	74.9	96.7	80.2	99.3	77.1
	8	61.3	90.9	80.7	98.1	73.1
	12	8.8	87.1	84.2	99.5	75.5
	16	1.9	86.4	82.3	97.1	75.3
	20	0.0	86.1	79.9	93.7	73.6
G	0	69.0	78.2	74.0	83.8	68.2
	2	66.9	77.7	72.5	85.2	62.7
	4	55.7	77.2	74.1	79.4	64.1
	8	21.2	75.9	73.2	81.2	59.9
	12	7.3	75.3	69.8	78.6	64.8
	16	1.3	74.8	71.5	80.0	66.4
	20	0.0	74.1	69.5	83.2	62.4

B.W.R. = cation extraction determined before washing of leach residues

A.W.R. = cation extraction determined after washing of leach residues

O.D. = weight of ore dissolved.

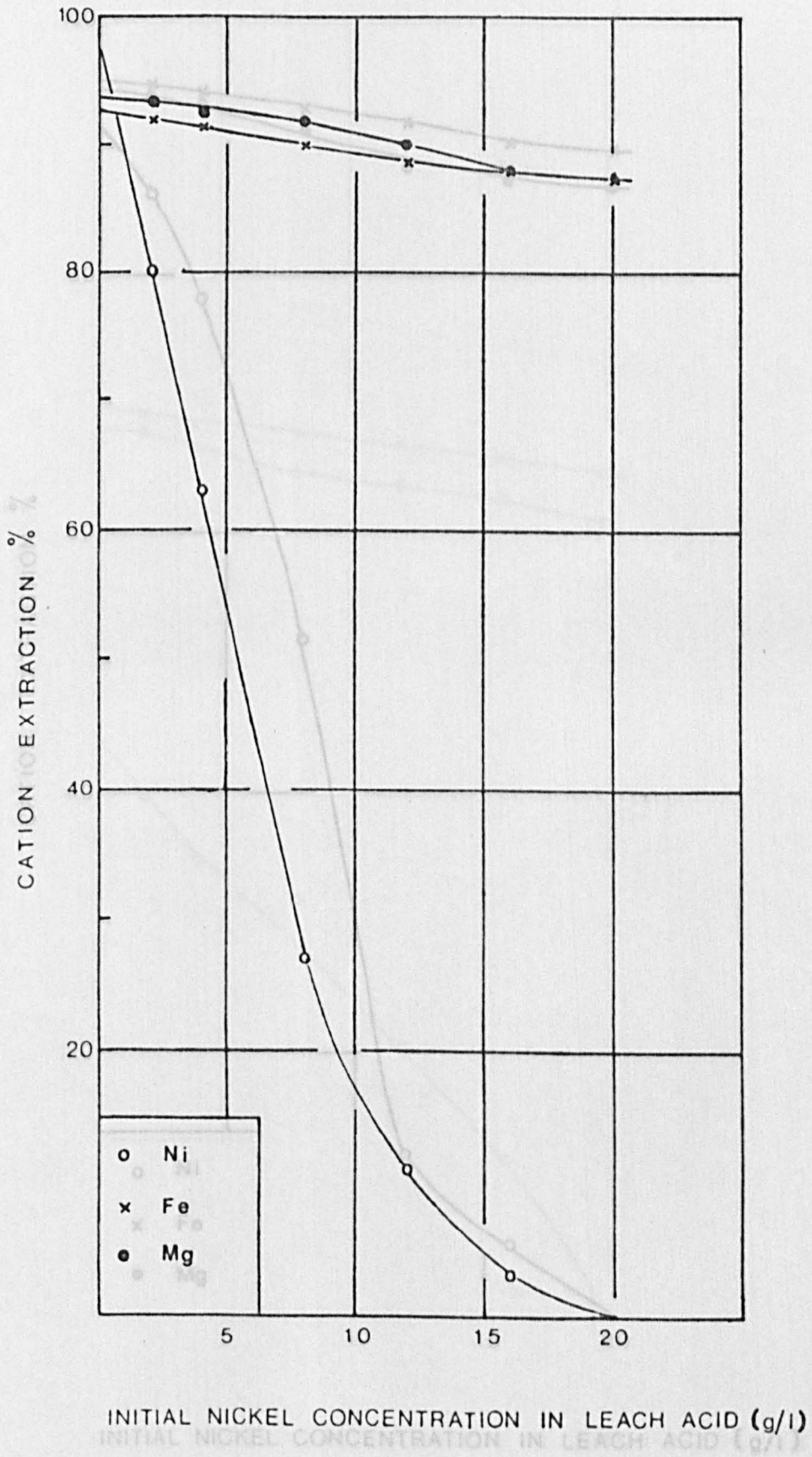


Fig. 41 Effect of nickel concentration in the leach acid on cation extraction from Ore-A (B.W.R.)



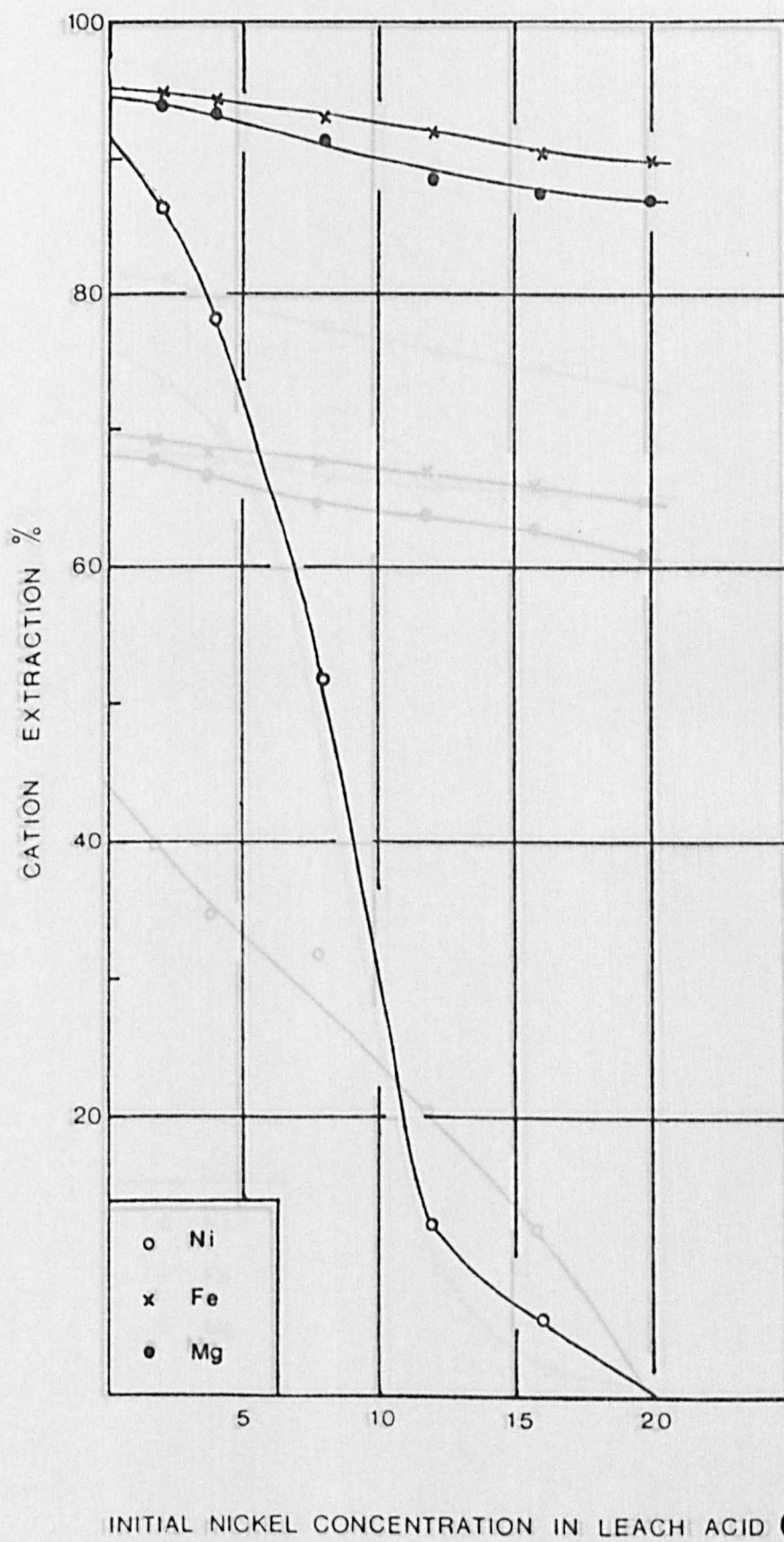


Fig. 4.2 Effect of nickel concentration in the leach acid on cation extraction from Ore-B (B.W.R.)

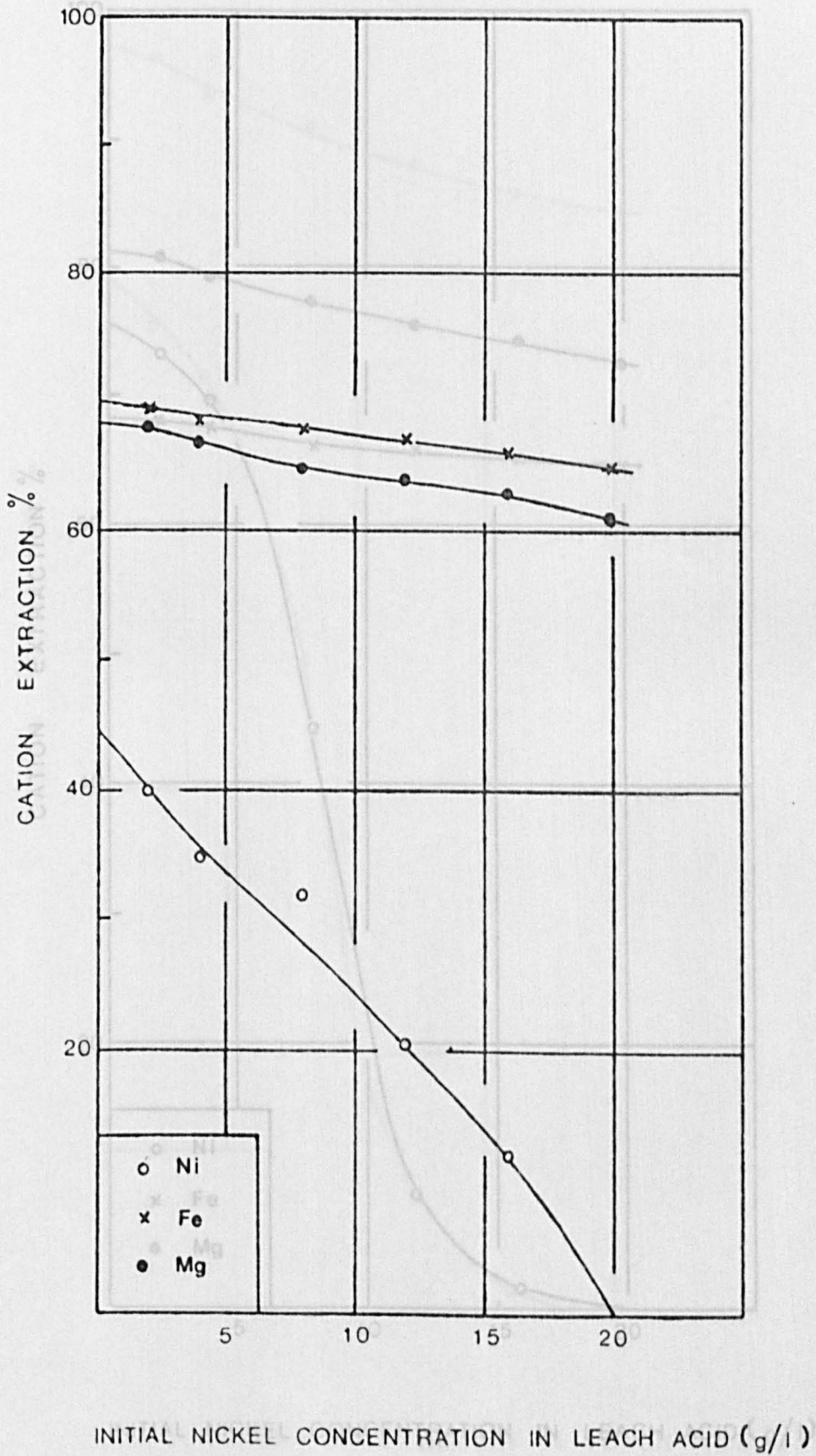


Fig 4.3 Effect of nickel concentration in the leach acid on cation extraction from Ore-C (B.W.R.)

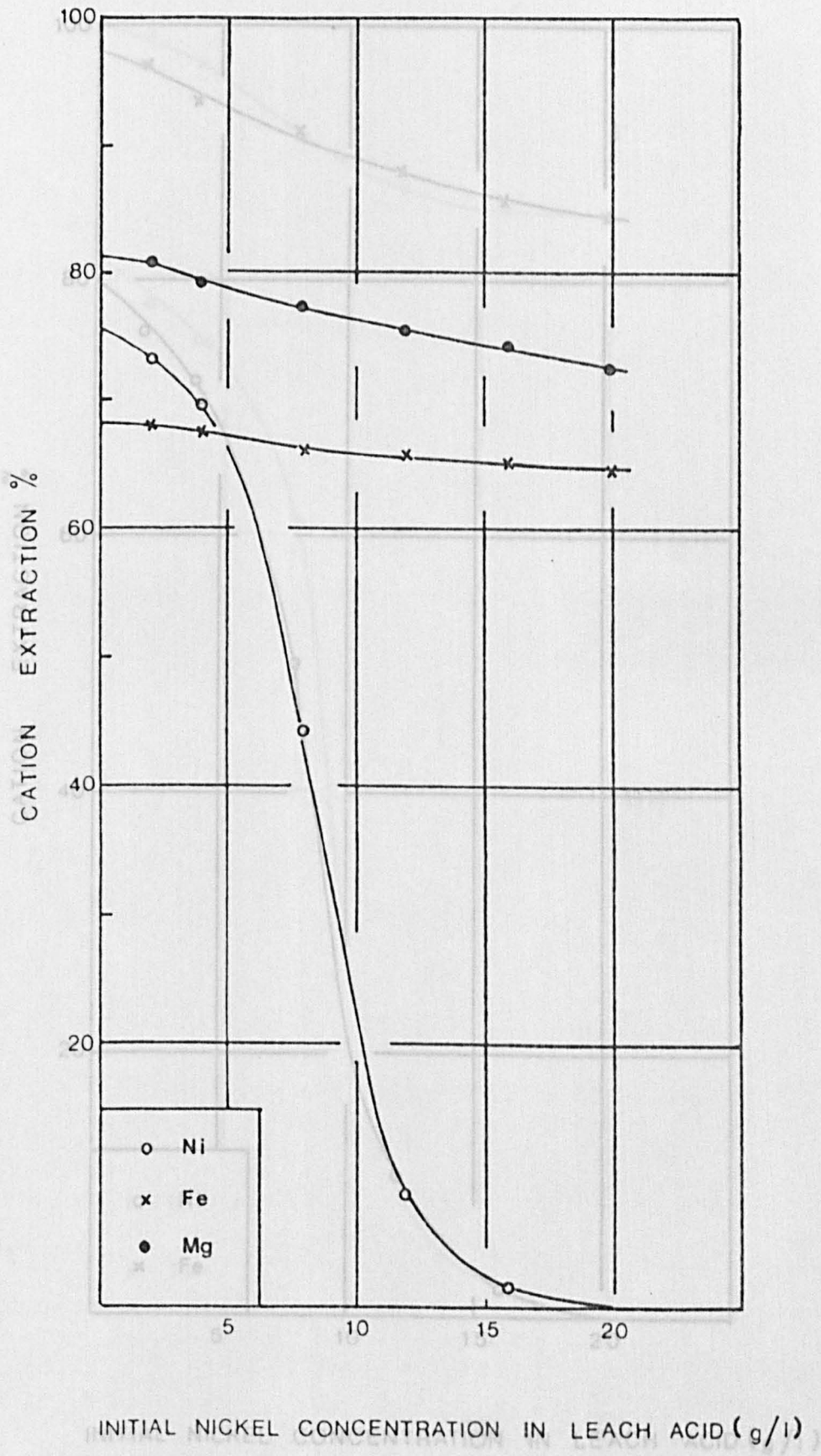


Fig. 4.4 Effect of nickel concentration in the leach acid on cation extraction from Ore-D (B.W.R.)



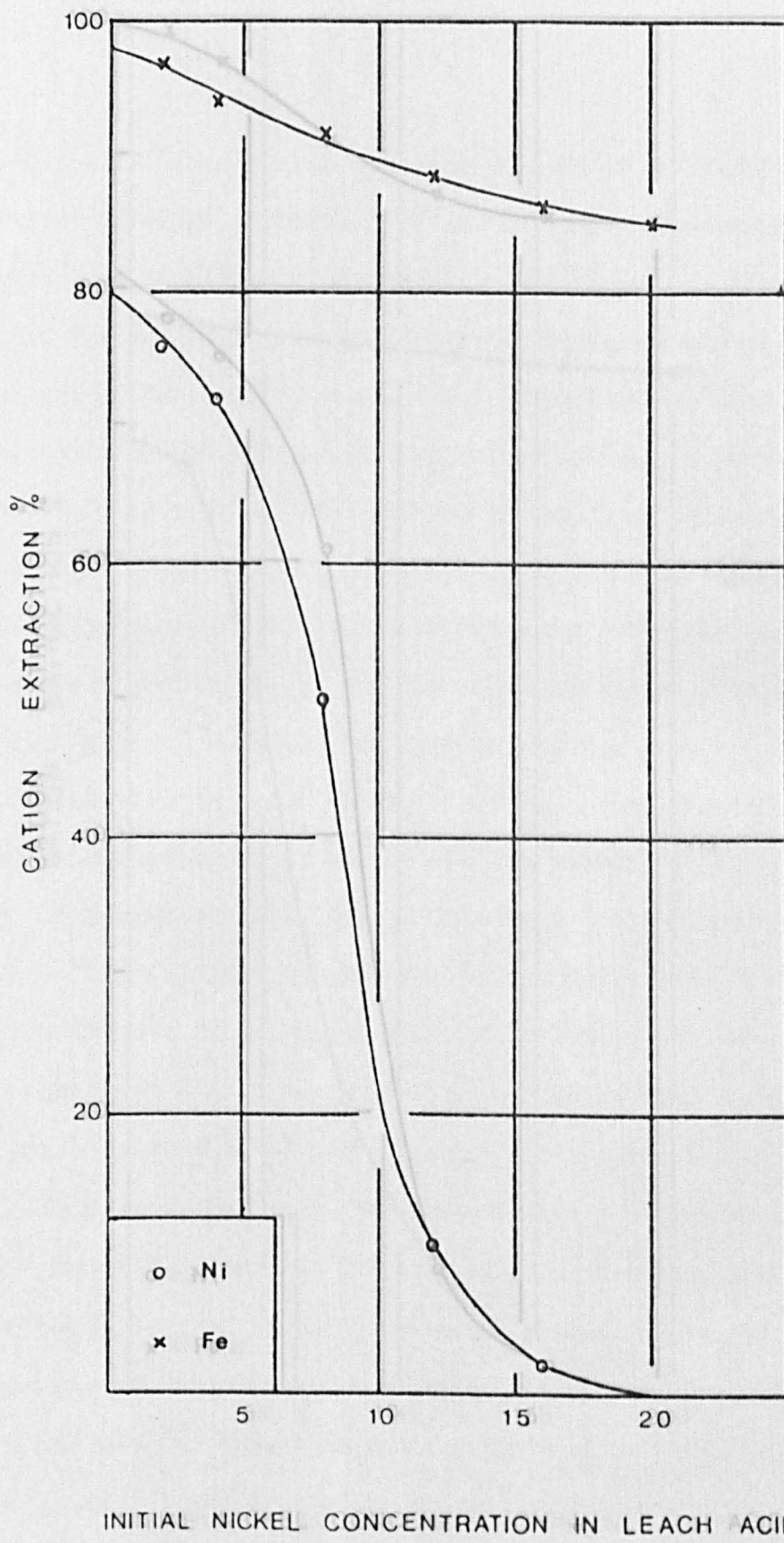


Fig 4.5 Effect of nickel concentration in the leach acid on cation extraction from Ore- E (B.W.R)

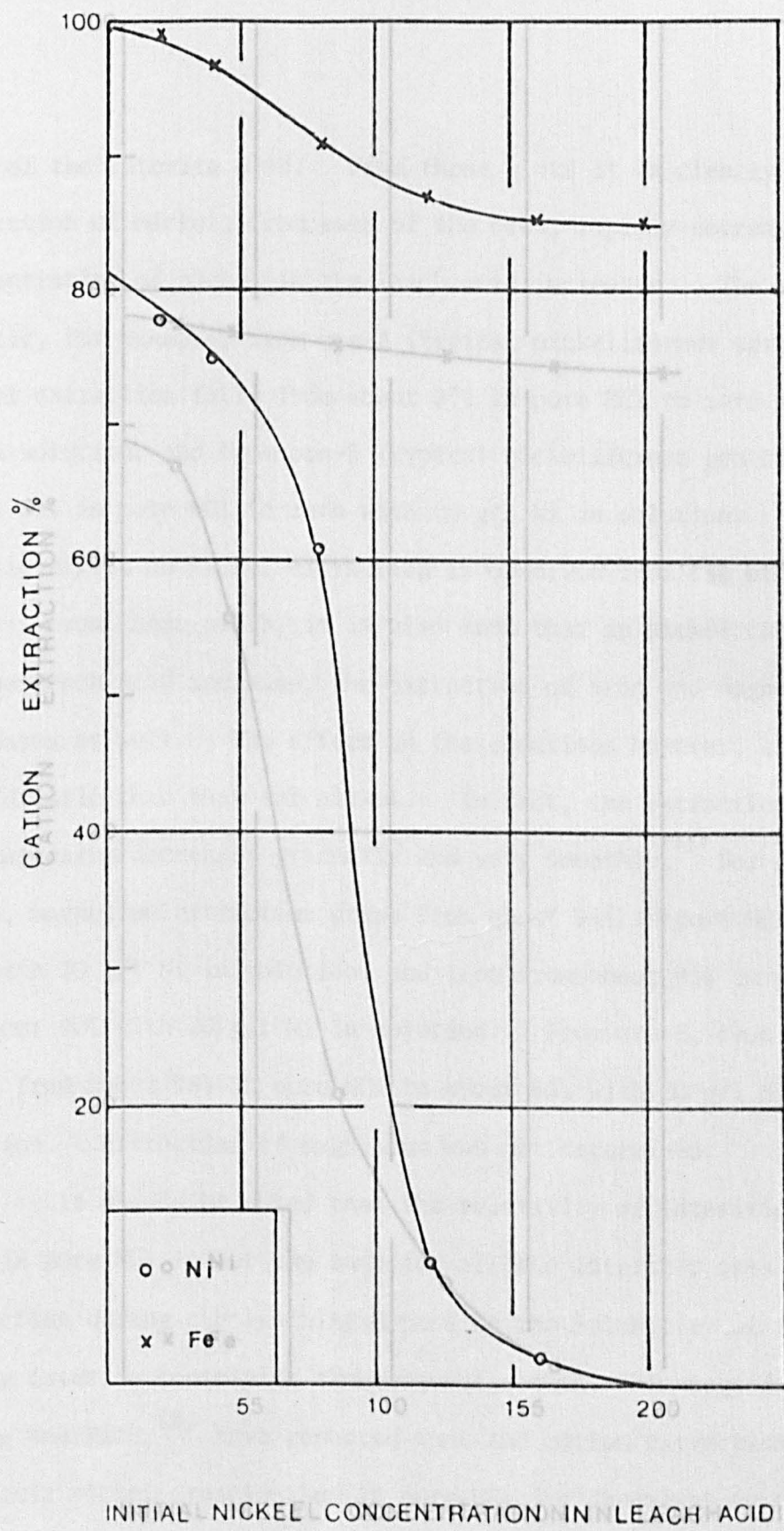


Fig. 4.6 Effect of nickel concentration in the leach acid on cation extraction from Ore-F (B.W.R.)

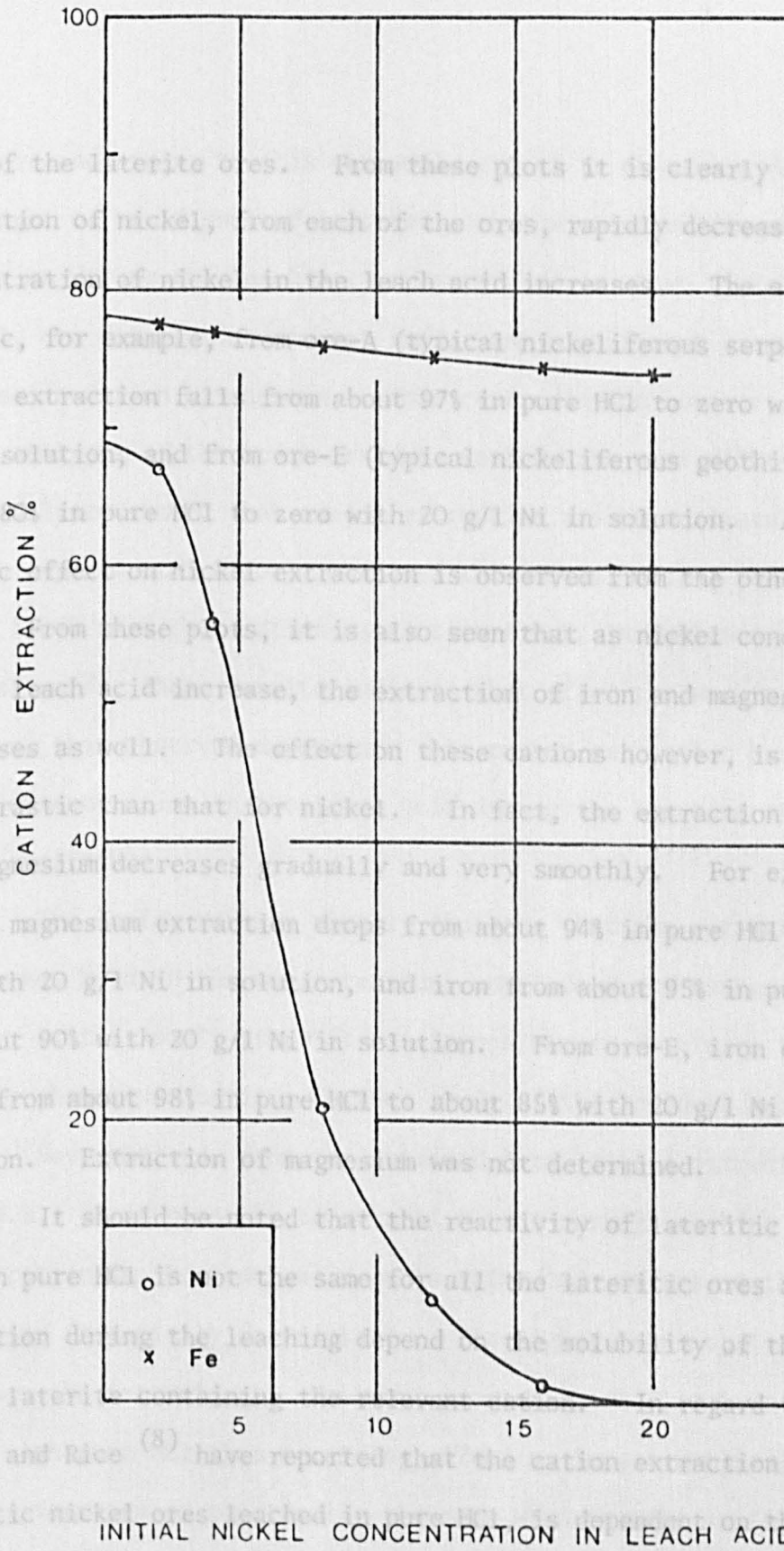


Fig. 4.7 Effect of nickel concentration in the leach acid on cation extraction related to the weight of laterite dissolved during the leaching from Ore-G (B.W.R.)

each of the laterite ores. From these plots it is clearly seen that extraction of nickel, from each of the ores, rapidly decreases as the concentration of nickel in the leach acid increases. The effect is drastic, for example, from ore-A (typical nickeliferous serpentine), nickel extraction falls from about 97% in pure HCl to zero with 20 g/l Ni in solution, and from ore-E (typical nickeliferous goethite) from about 80% in pure HCl to zero with 20 g/l Ni in solution. A similar drastic effect on nickel extraction is observed from the other laterite ores. From these plots, it is also seen that as nickel concentration in the leach acid increase, the extraction of iron and magnesium decreases as well. The effect on these cations however, is much less drastic than that for nickel. In fact, the extraction of iron and magnesium decreases gradually and very smoothly. For example, from ore-B, magnesium extraction drops from about 94% in pure HCl to about 87% with 20 g/l Ni in solution, and iron from about 95% in pure HCl to about 90% with 20 g/l Ni in solution. From ore-E, iron extraction drops from about 98% in pure HCl to about 85% with 20 g/l Ni in solution. Extraction of magnesium was not determined.

It should be noted that the reactivity of lateritic nickel ores in pure HCl is not the same for all the lateritic ores and cation extraction during the leaching depend on the solubility of the part of the laterite containing the relevant cation. In regard to this, Strong and Rice <sup>(8)</sup> have reported that the cation extraction from lateritic nickel ores leached in pure HCl, is dependent on the quantity of the octahedral layer (for silicate ores) and goethite (for limonite ores) dissolved in the acid solution. Thus, cation extraction can be related to the weight of laterite dissolved during the leaching <sup>(13)</sup>.

Therefore, according to this one would expect to observe a decrease in the weight of ore dissolved together with the observed decrease of cation extraction during the leaching. However, as is shown by Tables 4.2 and 4.3, ore dissolution did not suffer any significant change with the decrease in cation extraction. This contradiction however, was explained by the analyses of the leach residues washed with pure diluted HCl. These analyses showed that cation extraction was approximately the same (within experimental error), whatever the initial nickel concentration in the leach acid (see cation extraction A.W.R. in Tables 4.2 and 4.3). In other words, these results indicate that after the washing of leach residues, this observed dependence that cation extraction has on the nickel concentration in the leach acid during the leaching stage is no longer applicable.

The latter results clearly indicate that the extracted cations are somehow held in the solid residues until they are washed out, However, at this early stage it was impossible to determine the reason for this phenomenon until a further study of the residues had been undertaken. Nevertheless, from the obtained data (cation extraction B.W.R. and A.W.R.) it is possible to establish that during leaching nickel concentration in the leach acid has a retarding effect on the cation extraction (especially for nickel). The higher the nickel concentration, the lower the extraction. However, as soon as the leach residues are washed with pure HCl this retarding effect no longer applies, and the cation extraction is practically the same whatever the initial nickel concentration in the leach acid.



Perhaps it is worth mentioning that before the analyses of the washed leach residues, it was thought that the decrease of cation extraction with increasing nickel concentration in the leach acid was perhaps caused by some kind of adsorption phenomenon, where nickel in solution (i.e. that initially present in the solution or liberated during the leaching) was adsorbed by the surface of the solid or perhaps replaced nickel and magnesium ions already leached from the lattice. Thus, a set of experiments were performed leaching fresh ore with pure HCl, filtering the residues and washing them very well with pure HCl. Before they went dry, they were then treated with acid containing a high nickel concentration. The purpose of this was to determine if solid residues could reabsorb some nickel from the leach solution. The results however, were negative; no adsorption of nickel by the residues occurred. It was also observed that no standard adsorption isotherms (e.g. Freundlich, Langmuir or B.E.T. <sup>(85)</sup>) would fit the decrease in nickel extraction with rising nickel concentration observed in Figs. 4.1 to 4.7. The use of a radioactive tracer (cobalt 60) was also suggested to determine any possible adsorption, but it was considered unnecessary because of the new observations obtained after analysis of the washed leach residues.

#### 4.3.2. Leaching of Laterites with magnesium chloride addition

For leaching tests with magnesium chloride additions, ores A, B and C (silicates with a high MgO content) were selected. Sets of 5 tests with MgCl<sub>2</sub> additions to give 0-100 g/l Mg were performed for each of these laterites using the same leaching conditions previously described for NiCl<sub>2</sub> additions (i.e. 4 mol/dm<sup>3</sup> HCl, 70°C, 1 hour contact

Table 4.4 Cation extraction from laterite ores A to C leached in HCl solutions containing different magnesium concentrations (4 mol/dm<sup>3</sup> HCl, 70°C, 1 hour contact time, 10% solid and size distribution as in appendix I).

Ore	Magnesium concentration in leach acid (g/l)	Cation extraction %						O.D. %
		B.W.R.			A.W.R.			
		Ni	Fe	Mg	Ni	Fe	Mg	
A	0	97.3	92.6	93.0	97.5	92.8	94.3	63.0
	10	96.6	92.1	89.7	97.1	93.1	94.0	62.2
	25	95.4	90.8	86.1	98.0	93.6	92.8	63.6
	50	91.7	88.3	73.2	97.4	93.0	94.6	61.9
	100	87.2	87.0	48.4	97.0	93.0	92.8	62.0
B	0	90.8	95.3	93.7	98.0	95.8	94.3	56.5
	10	90.3	90.1	89.5	98.3	93.8	96.6	54.7
	25	89.5	88.6	87.5	97.6	97.4	93.1	57.3
	50	87.4	83.9	80.2	98.0	98.2	96.4	57.5
	100	76.2	78.9	55.3	97.8	92.5	96.1	56.8
C	0	45.2	71.0	68.5	45.2	71.7	68.5	16.6
	10	44.0	69.7	67.9	44.7	72.1	68.3	18.0
	25	43.8	67.3	64.3	45.6	72.8	69.0	16.9
	50	43.1	62.4	35.1	43.8	72.0	67.8	18.2
	100	42.2	59.3	24.6	44.6	74.2	69.1	20.1

B.W.R. = Cation extraction determined before washing of leach residues

A.W.R. = Cation extraction determined after washing of leach residues

O.D. = weight of ore dissolved.

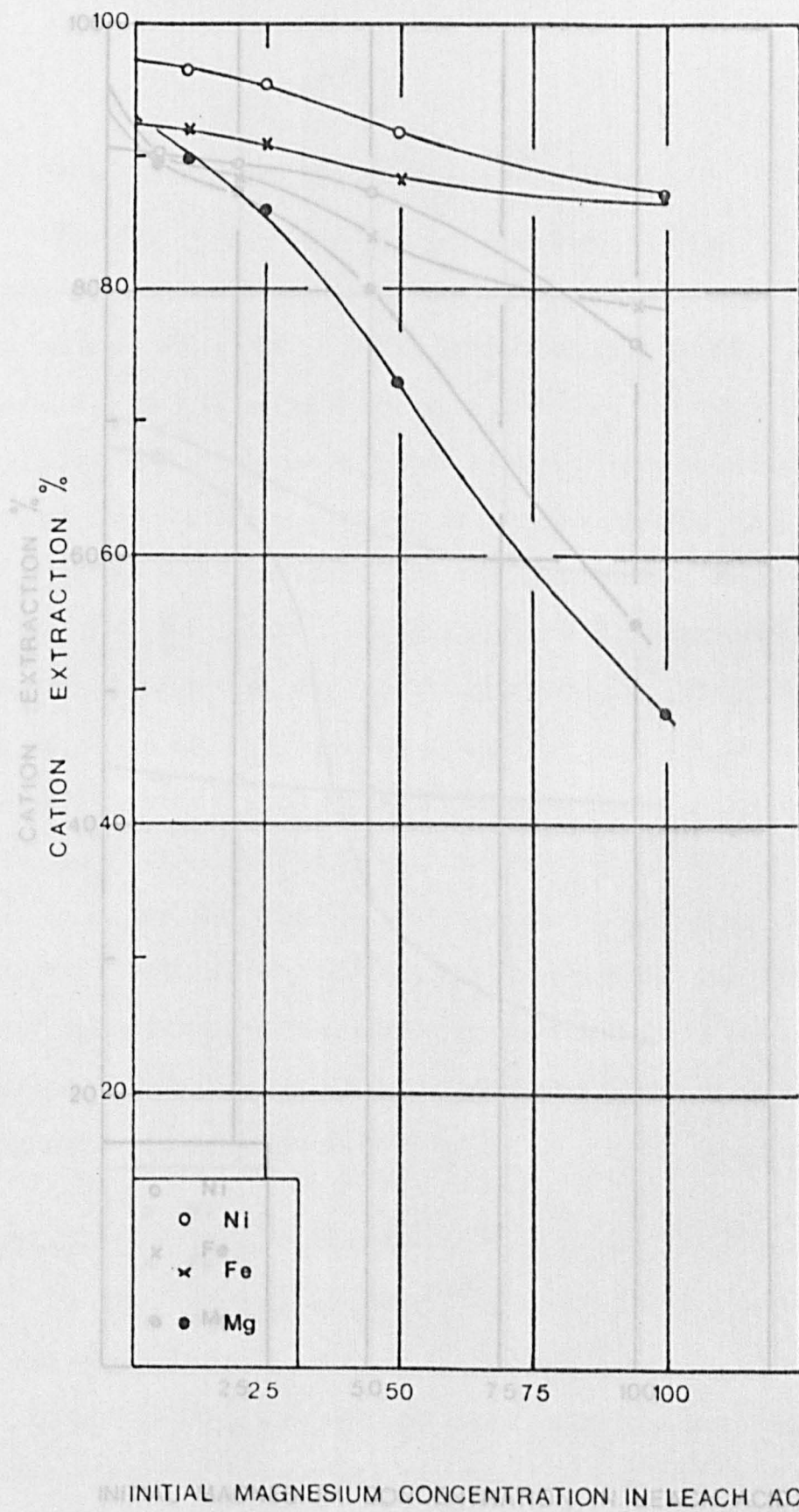


Fig. 4.8 Effect of magnesium concentration in the leach acid on cation extraction from Ore-A (B.W.R.)

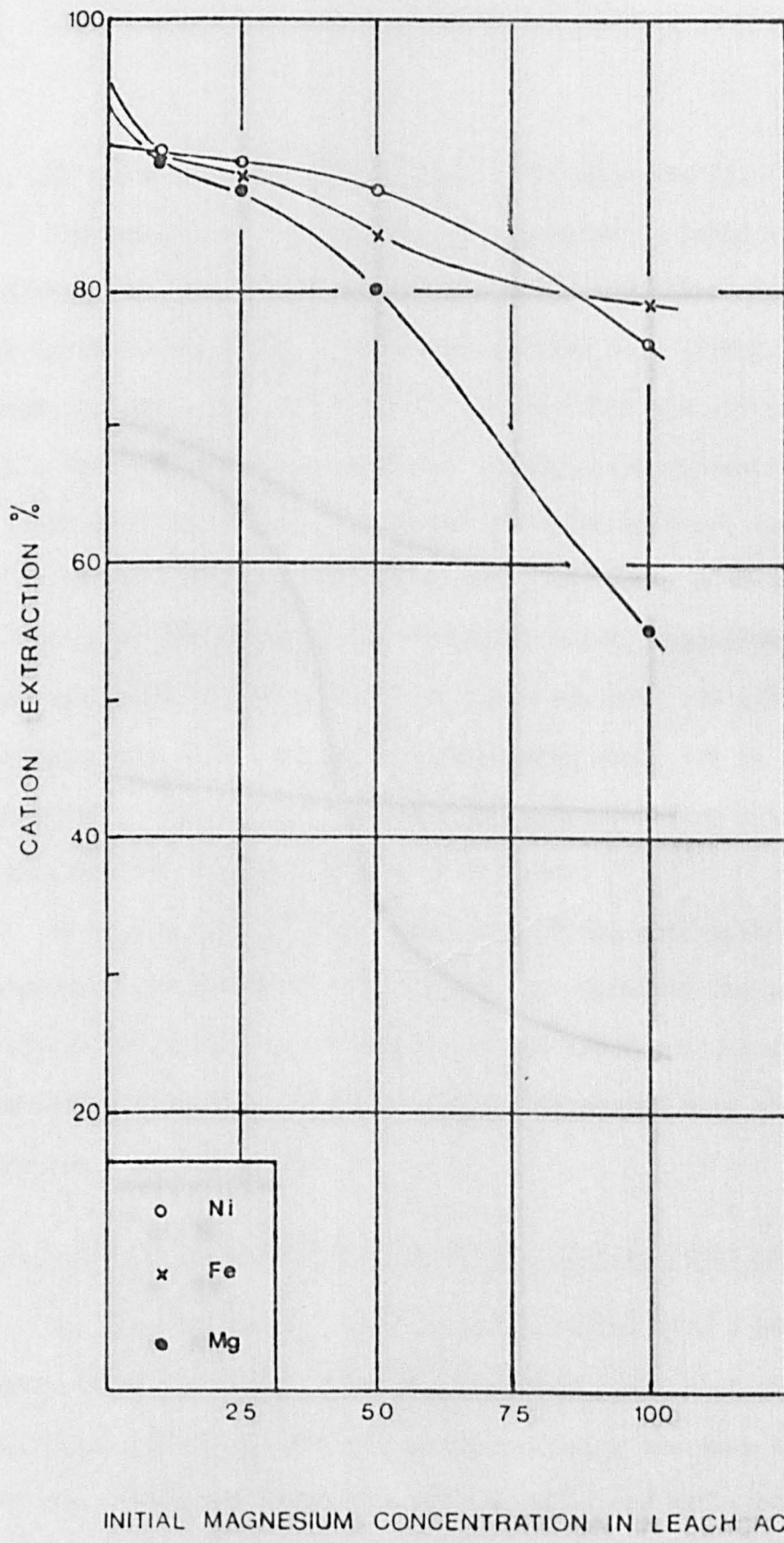
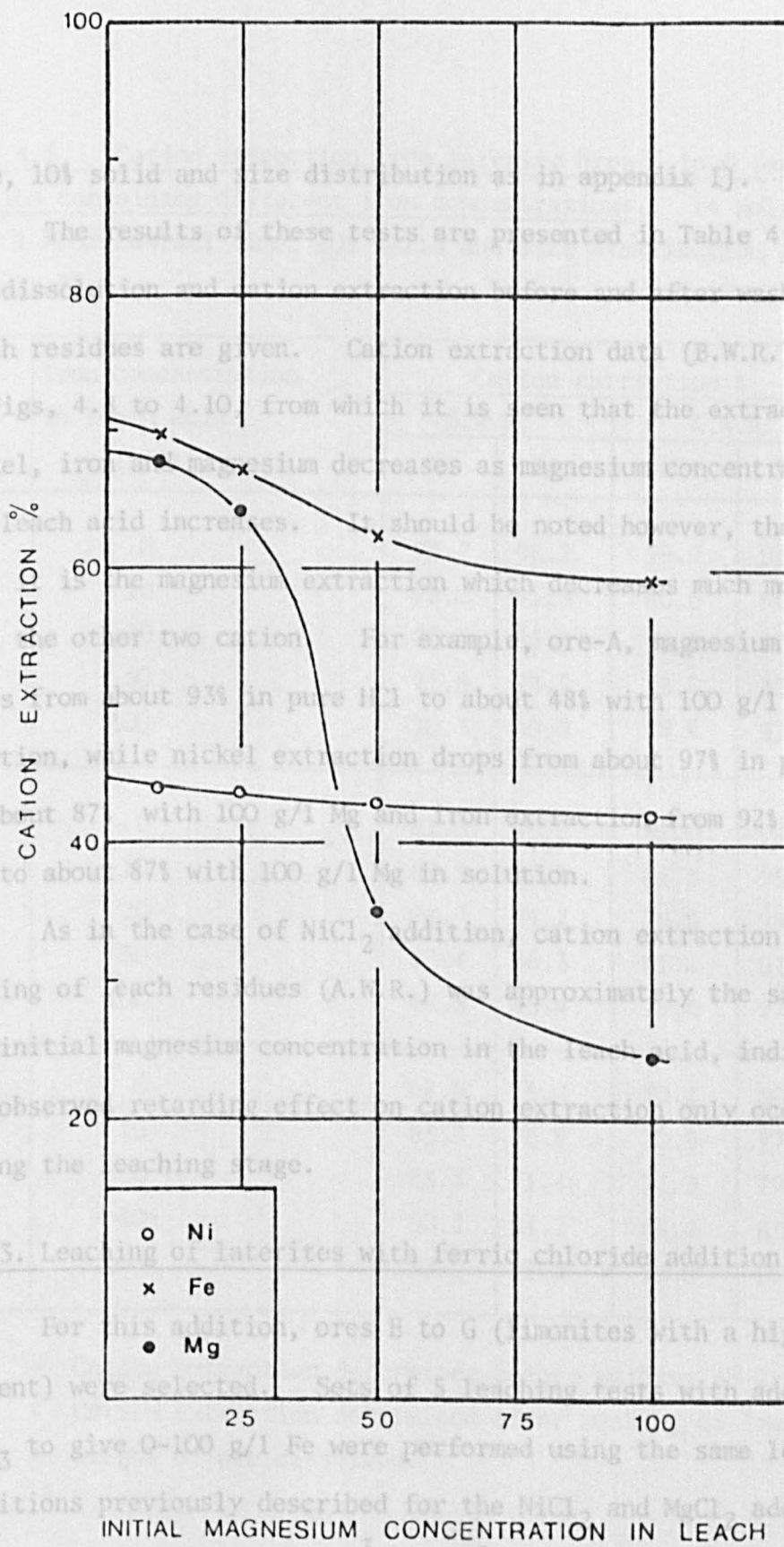


Fig 4.9 Effect of magnesium concentration in the leach acid on cation extraction from Ore-B ( B.W.R. )



INITIAL MAGNESIUM CONCENTRATION IN LEACH ACID (g/l)

Fig 4.10 Effect of magnesium concentration in the leach acid on cation extraction from Ore-C ( B. W.R.)

time, 10% solid and size distribution as in appendix I).

The results of these tests are presented in Table 4.4, where ore dissolution and cation extraction before and after washing of the leach residues are given. Cation extraction data (B.W.R.) are plotted in Figs, 4.8 to 4.10, from which it is seen that the extraction of nickel, iron and magnesium decreases as magnesium concentration in the leach acid increases. It should be noted however, that in this case it is the magnesium extraction which decreases much more rapidly than the other two cation. For example, ore-A, magnesium extraction drops from about 93% in pure HCl to about 48% with 100 g/l Mg in solution, while nickel extraction drops from about 97% in pure HCl to about 87% with 100 g/l Mg and iron extraction from 92% in pure HCl to about 87% with 100 g/l Mg in solution.

As in the case of  $\text{NiCl}_2$  addition, cation extraction after the washing of leach residues (A.W.R.) was approximately the same whatever the initial magnesium concentration in the leach acid, indicating that the observed retarding effect on cation extraction only occurred during the leaching stage.

#### 4.3.3. Leaching of laterites with ferric chloride addition

For this addition, ores E to G (limonites with a high  $\text{Fe}_2\text{O}_3$  content) were selected. Sets of 5 leaching tests with additions of  $\text{FeCl}_3$  to give 0-100 g/l Fe were performed using the same leaching conditions previously described for the  $\text{NiCl}_2$  and  $\text{MgCl}_2$  additions leaching tests (i.e. 4 mol/dm<sup>3</sup> HCl, 70°C, 1 hour contact time, 10% solid and size distribution as in appendix I).



Table 4.5. Cation extraction from laterite ores E to G leached in HCl solution containing different iron concentrations. (4 mol/dm<sup>3</sup> HCl, 70°C, 1 hour contact time, 10% solid and size distribution as in appendix I).

Ore	Iron concentration in leach acid (g/l)	Cation extraction %				O.D. %
		B.W.R.		A.W.R.		
		Ni	Fe	Ni	Fe	
E	0	79.7	98.2	79.7	98.5	78.1
	10	79.0	95.3	80.6	96.2	76.9
	20	73.6	86.9	76.8	96.9	75.8
	50	71.8	73.5	78.2	93.8	78.4
	100	70.3	59.9	79.4	97.7	78.6
F	0	81.3	99.2	82.0	99.2	74.3
	10	80.5	92.6	83.3	95.8	74.0
	20	78.7	84.2	79.8	98.1	75.5
	50	73.4	66.3	81.4	92.8	72.8
	100	68.8	45.4	79.6	97.5	73.1
G	0	68.9	78.2	70.2	80.4	63.7
	10	65.7	76.9	70.0	77.2	64.1
	20	63.4	71.4	71.3	79.5	66.5
	50	60.2	54.2	68.4	81.0	62.9
	100	57.9	41.8	72.0	80.5	60.4

B.W.R. = Cation extraction determined before washing of leach residues

A.W.R. = Cation extraction determined after washing of leach residues

O.D. = weight of ore dissolved.

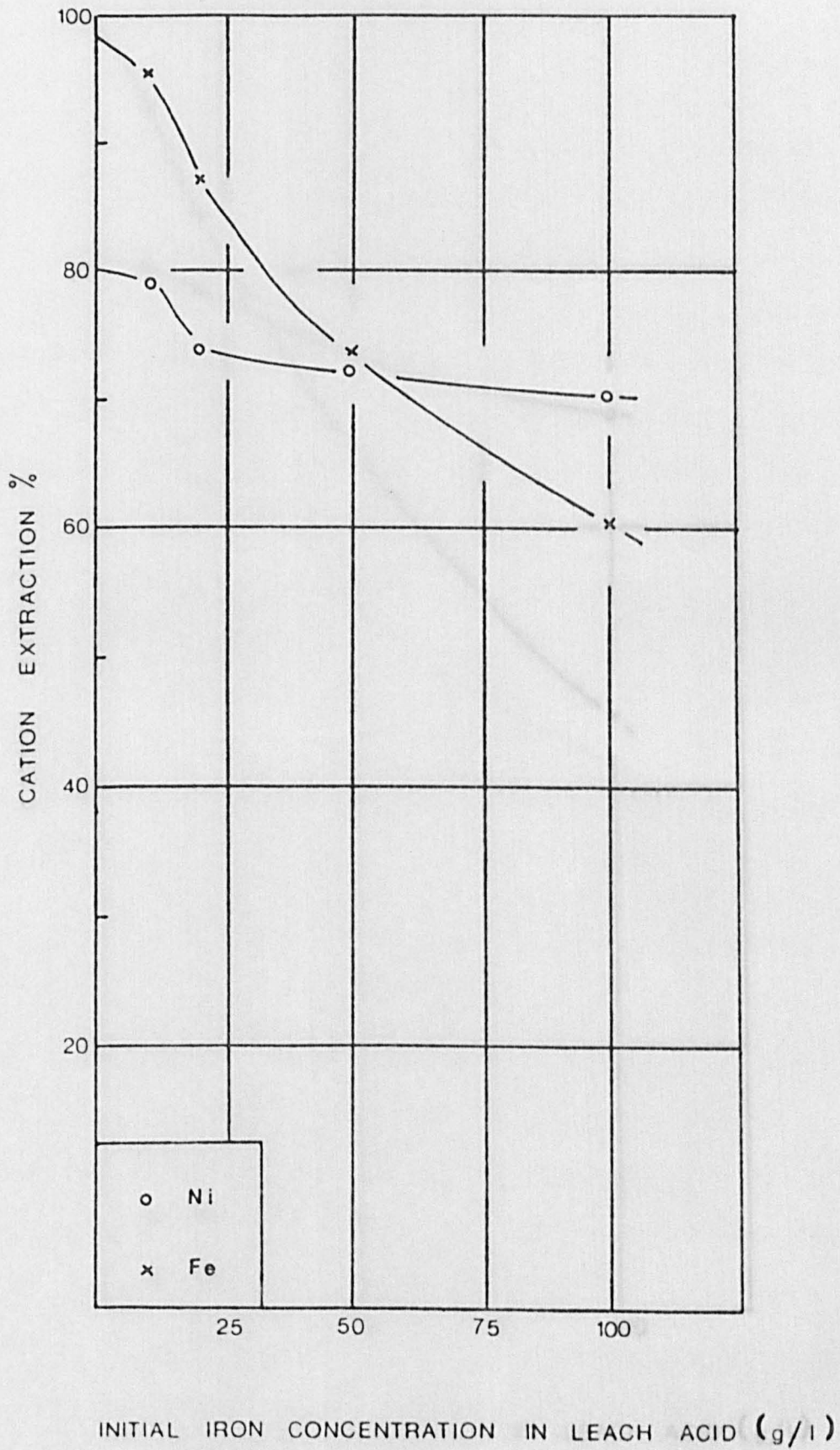


Fig. 4.11 Effect of iron concentration in the leach acid on cation extraction from Ore-E (B.W.R.)



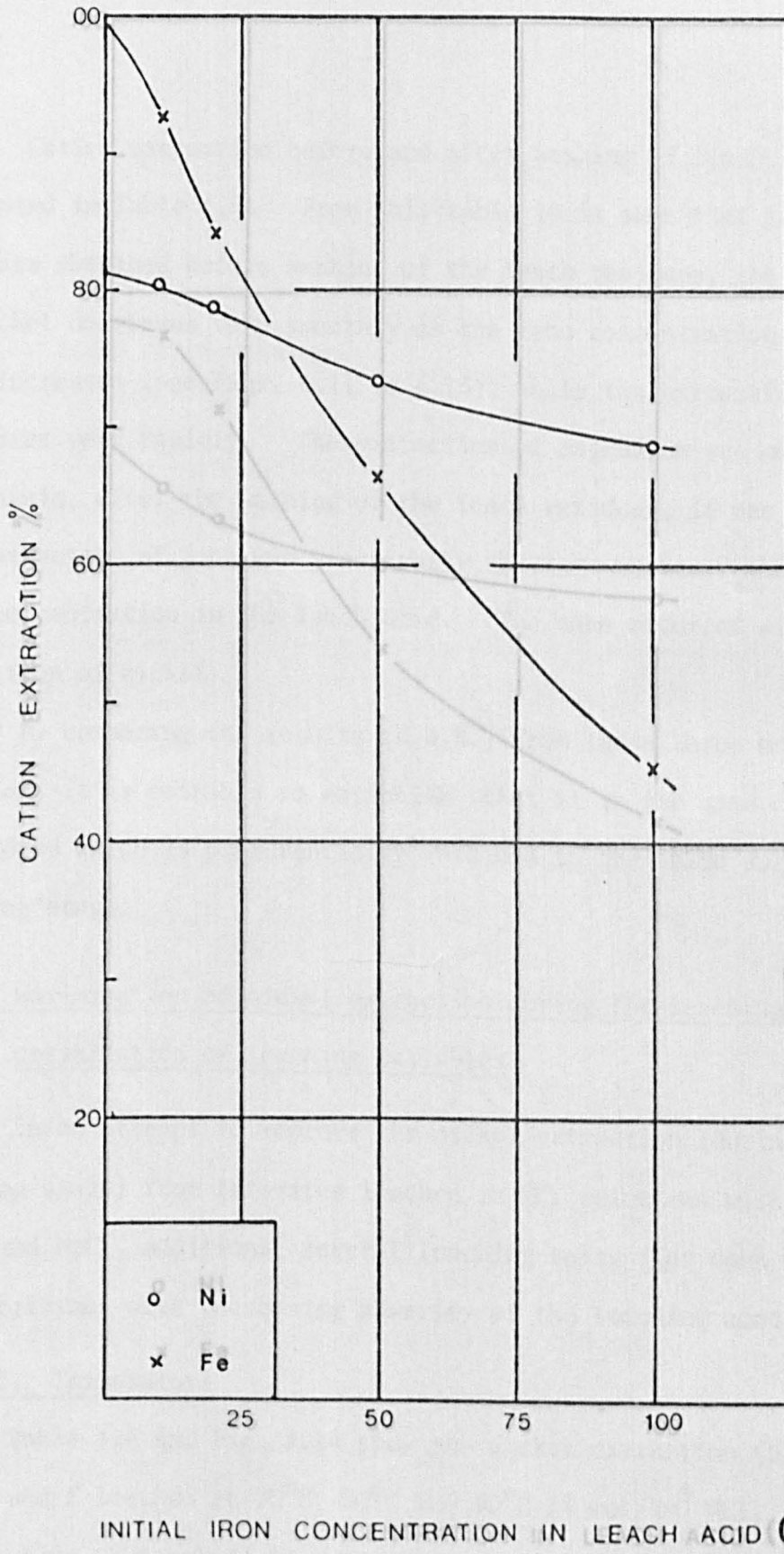


Fig 4.12 Effect of iron concentration in the leach acid on cation extraction from Ore-F (B.W.R.)

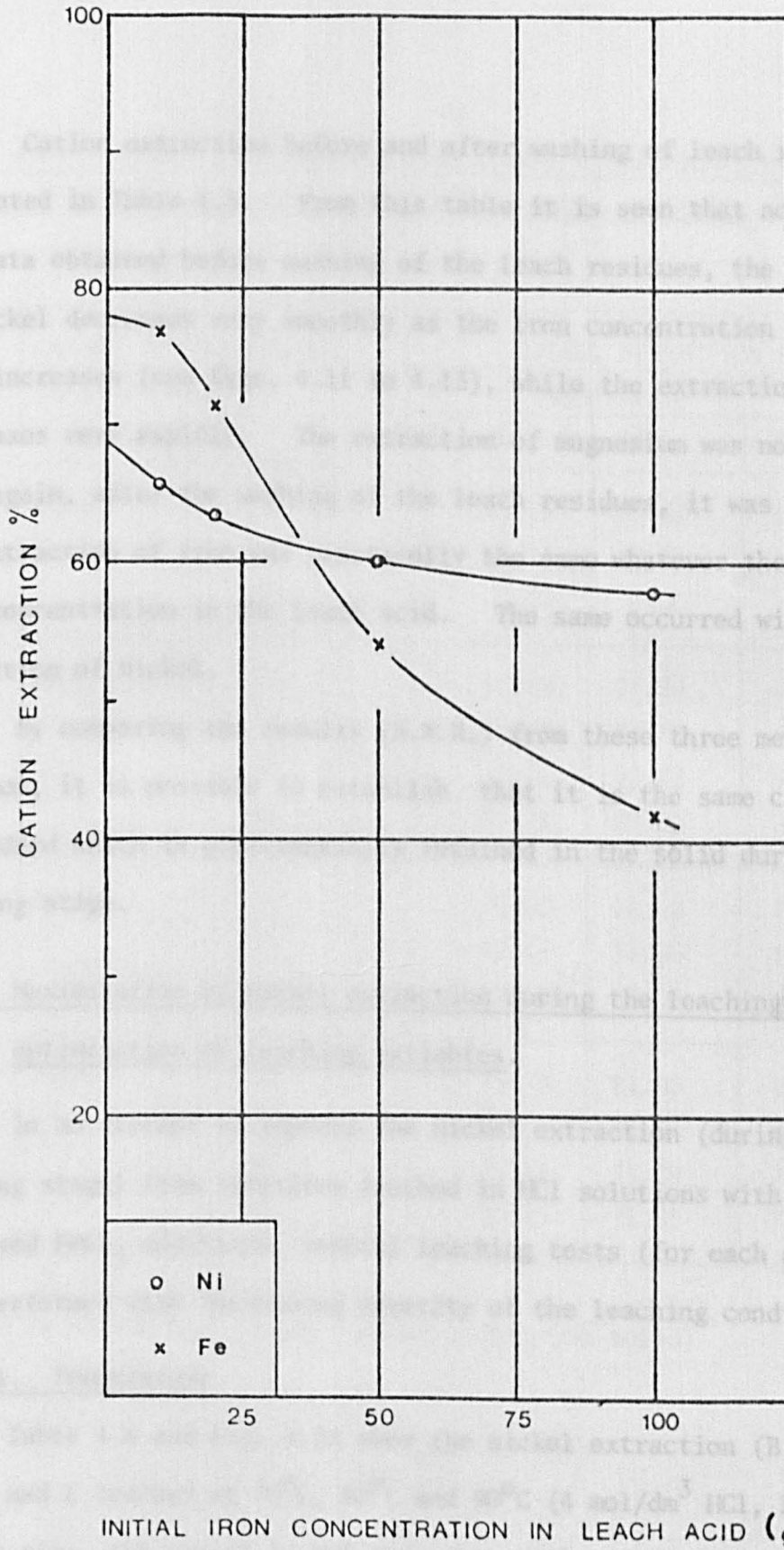


Fig. 4.13 Effect of iron concentration in the leach acid on cation extraction from Ore-G (B.W.R.)

Cation extraction before and after washing of leach residues are presented in Table 4.5. From this table it is seen that according to the data obtained before washing of the leach residues, the extraction of nickel decreases very smoothly as the iron concentration in the leach acid increases (see Figs. 4.11 to 4.13), while the extraction of iron decreases very rapidly. The extraction of magnesium was not determined. Once again, after the washing of the leach residues, it was found that the extraction of iron was practically the same whatever the initial iron concentration in the leach acid. The same occurred with the extraction of nickel.

By comparing the results (B.W.R.) from these three metal chloride addition, it is possible to establish that it is the same cation as that added which is preferentially retained in the solid during the leaching stage.

#### 4.3.4. Maximization of nickel extraction during the leaching stage by optimization of leaching variables.

In an attempt to improve the nickel extraction (during the leaching stage) from laterites leached in HCl solutions with  $\text{NiCl}_2$ ,  $\text{MgCl}_2$  and  $\text{FeCl}_3$  additions, several leaching tests (for each addition) were performed with increasing severity of the leaching conditions.

##### 4.3.4.1. Temperature

Table 4.6 and Fig. 4.14 show the nickel extraction (B.W.R.) from ores A and E leached at  $70^\circ\text{C}$ ,  $80^\circ\text{C}$  and  $90^\circ\text{C}$  ( $4 \text{ mol/dm}^3$  HCl, 1 hour contact time, 10% solid) in HCl solutions with addition of  $\text{NiCl}_2$  (to give 4, 12 and 20 g/l Ni),  $\text{MgCl}_2$  (to give 10, 25, 50 and 100 g/l Mg) and  $\text{FeCl}_3$  (to give 10, 20, 50 and 100 g/l Fe). From these results

Table 4.6. Effect of temperature on nickel extraction from ores A and E leached in HCl with additions of  $\text{NiCl}_2$ ,  $\text{MgCl}_2$  and  $\text{FeCl}_3$  (B.W.R.)

Ore	Cation concentration in leach acid (g/l)		NICKEL EXTRACTION %		
			Temperature °C		
			70	80	90
A	Nickel	4	63.25	65.69	67.12
		12	11.15	13.51	14.37
		20	0.00	0.00	0.00
	Magnesium	10	96.59	97.89	98.18
		25	95.48	96.13	96.35
		50	91.71	92.22	94.15
		100	87.71	89.36	90.82
E	Nickel	4	72.60	74.10	74.92
		12	12.17	14.39	16.25
		20	0.00	0.00	0.00
	Iron	10	79.75	81.80	83.57
		20	79.07	81.32	82.61
		50	72.19	75.79	76.00
		100	70.33	71.93	72.15

(4 mol/dm<sup>3</sup> HCl, 1 hour contact time, 10% solid)

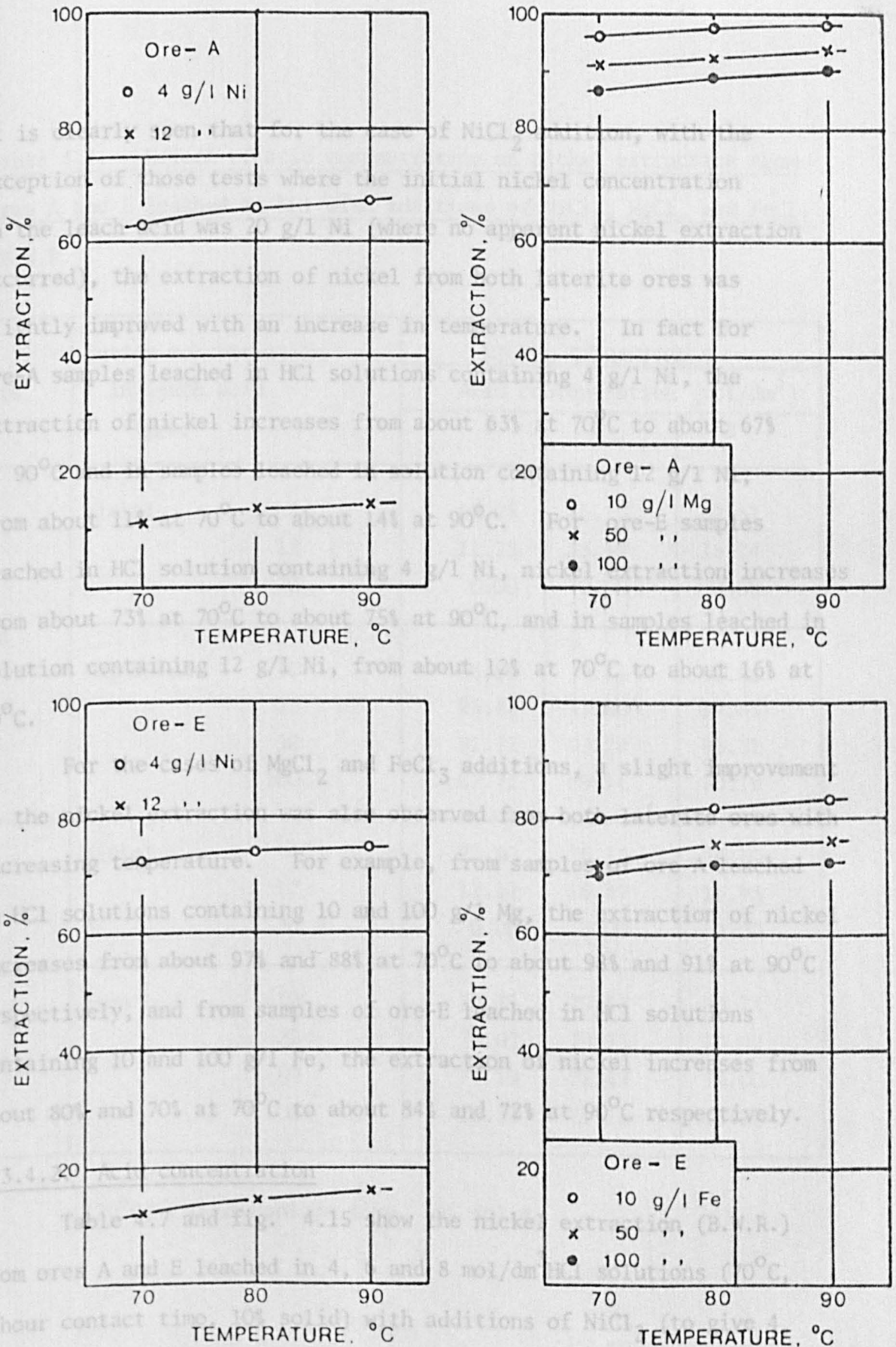


Fig. 4.14 Effect of temperature upon nickel extraction from Ore-A leached with additions of  $\text{NiCl}_2$  &  $\text{MgCl}_2$  and from Ore-E with  $\text{NiCl}_2$  &  $\text{FeCl}_3$ .



it is clearly seen that for the case of  $\text{NiCl}_2$  addition, with the exception of those tests where the initial nickel concentration on the leach acid was 20 g/l Ni (where no apparent nickel extraction occurred), the extraction of nickel from both laterite ores was slightly improved with an increase in temperature. In fact for ore-A samples leached in HCl solutions containing 4 g/l Ni, the extraction of nickel increases from about 63% at 70°C to about 67% at 90°C and in samples leached in solution containing 12 g/l Ni, from about 11% at 70°C to about 14% at 90°C. For ore-E samples leached in HCl solution containing 4 g/l Ni, nickel extraction increases from about 73% at 70°C to about 75% at 90°C, and in samples leached in solution containing 12 g/l Ni, from about 12% at 70°C to about 16% at 90°C.

For the cases of  $\text{MgCl}_2$  and  $\text{FeCl}_3$  additions, a slight improvement on the nickel extraction was also observed from both laterite ores with increasing temperature. For example, from samples of ore-A leached in HCl solutions containing 10 and 100 g/l Mg, the extraction of nickel increases from about 97% and 88% at 70°C to about 98% and 91% at 90°C respectively, and from samples of ore-E leached in HCl solutions containing 10 and 100 g/l Fe, the extraction of nickel increases from about 80% and 70% at 70°C to about 84% and 72% at 90°C respectively.

#### 4.3.4.2. Acid concentration

Table 4.7 and fig. 4.15 show the nickel extraction (B.W.R.) from ores A and E leached in 4, 6 and 8 mol/dm<sup>3</sup> HCl solutions (70°C, 1 hour contact time, 10% solid) with additions of  $\text{NiCl}_2$  (to give 4, 12 and 20 g/l Ni),  $\text{MgCl}_2$  (to give 10, 25, 50 and 100 g/l Mg) and  $\text{FeCl}_3$  (to give 10, 20, 50 and 100 g/l Fe). From these results, it is

Table 4.7. Effect of acid concentration on nickel extraction from ores A and E leached in HCl with additions of  $\text{NiCl}_2$ ,  $\text{MgCl}_2$  and  $\text{FeCl}_3$  (B.W.R.)

Ore	Cation concentration in leach acid (g/l)		NICKEL EXTRACTION %		
			Acid concentration ( $\text{mol/dm}^3$ )		
			4	6	8
A	Nickel	4	63.25	66.13	67.51
		12	11.15	13.17	15.24
		20	0.00	0.00	0.00
	Magnesium	10	96.59	97.45	97.82
		25	95.48	97.03	97.65
		50	91.71	93.24	93.31
		100	87.71	89.16	90.19
E	Nickel	4	72.60	76.55	78.10
		12	12.17	16.47	16.93
		20	0.00	0.00	0.00
	Iron	10	79.75	79.93	80.14
		20	79.07	79.75	79.92
		50	72.19	72.49	74.00
		100	70.33	71.15	71.86

(70°C, 1 hour contact time, 10% solid)

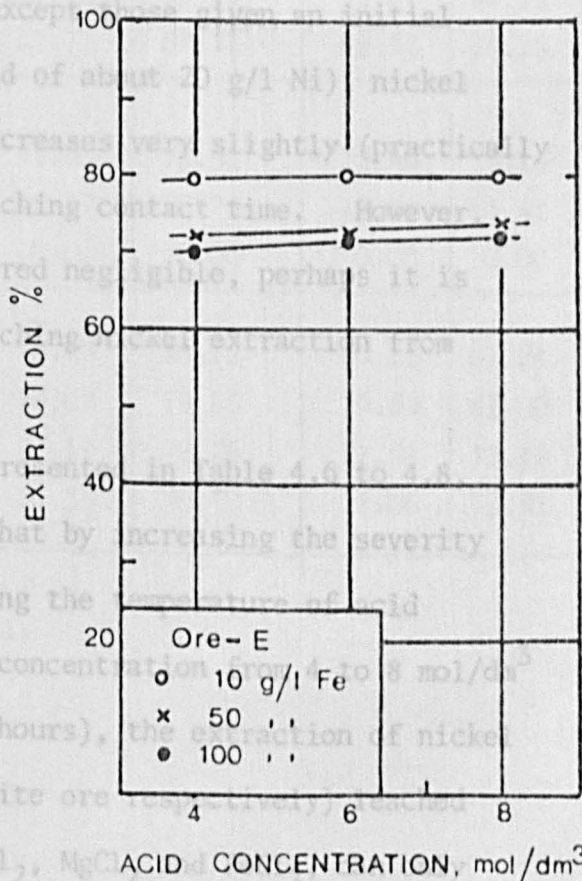
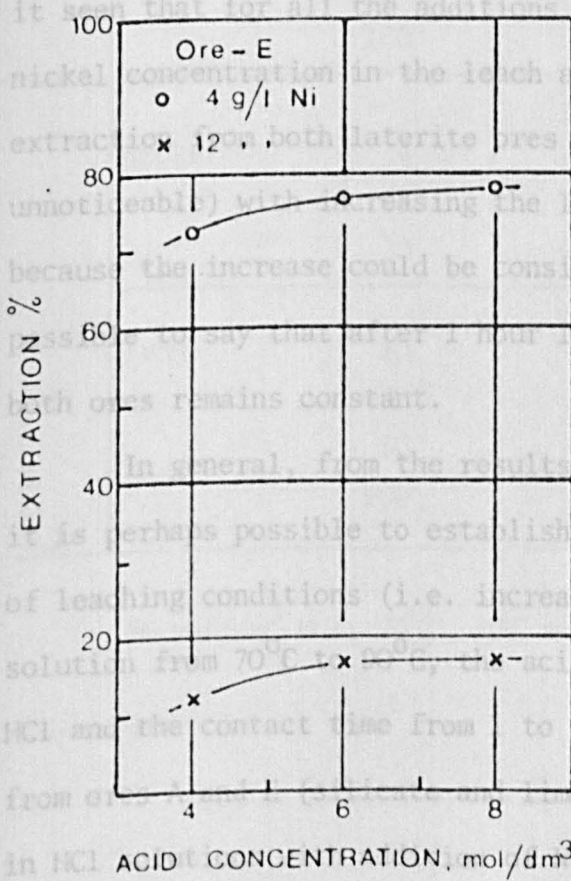
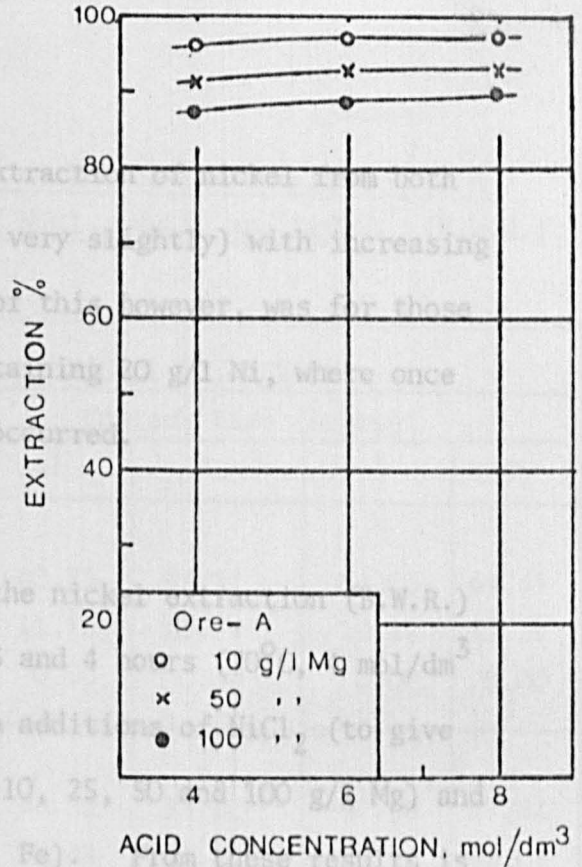
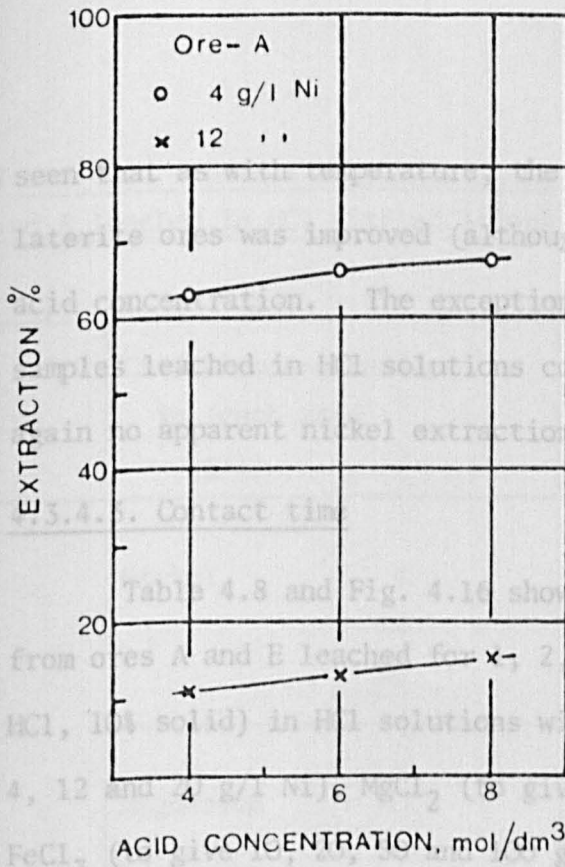


Fig. 4.15 Effect of acid concentration upon nickel extraction from Ore-A leached with additions of NiCl<sub>2</sub> & MgCl<sub>2</sub> and from Ore-E with NiCl<sub>2</sub> & FeCl<sub>3</sub>.



seen that as with temperature, the extraction of nickel from both laterite ores was improved (although very slightly) with increasing acid concentration. The exception of this however, was for those samples leached in HCl solutions containing 20 g/l Ni, where once again no apparent nickel extraction occurred.

#### 4.3.4.3. Contact time

Table 4.8 and Fig. 4.16 show the nickel extraction (B.W.R.) from ores A and E leached for 1, 2, 3 and 4 hours ( $70^{\circ}\text{C}$ ,  $4 \text{ mol/dm}^3$  HCl, 10% solid) in HCl solutions with additions of  $\text{NiCl}_2$  (to give 4, 12 and 20 g/l Ni),  $\text{MgCl}_2$  (to give 10, 25, 50 and 100 g/l Mg) and  $\text{FeCl}_3$  (to give 10, 20, 50 and 100 g/l Fe). From these results it is seen that for all the additions (except those given an initial nickel concentration in the leach acid of about 20 g/l Ni), nickel extraction from both laterite ores increases very slightly (practically unnoticeable) with increasing the leaching contact time. However, because the increase could be considered negligible, perhaps it is possible to say that after 1 hour leaching nickel extraction from both ores remains constant.

In general, from the results presented in Table 4.6 to 4.8, it is perhaps possible to establish that by increasing the severity of leaching conditions (i.e. increasing the temperature of acid solution from  $70^{\circ}\text{C}$  to  $90^{\circ}\text{C}$ , the acid concentration from 4 to  $8 \text{ mol/dm}^3$  HCl and the contact time from 1 to 4 hours), the extraction of nickel from ores A and E (silicate and limonite ore respectively) leached in HCl solutions with addition of  $\text{NiCl}_2$ ,  $\text{MgCl}_2$  and  $\text{FeCl}_3$ , can only be improved very slightly. Thus, in pure economic terms, to increase the severity of the leaching conditions would perhaps not

Table 4.8. Effect of contact time on nickel extraction from Ores A and E leached in HCl with additions of  $\text{NiCl}_2$ ,  $\text{MgCl}_2$  and  $\text{FeCl}_3$ . (B.W.R.)

Ore	Cation concentration in leach acid (g/l)		NICKEL EXTRACTION%			
			Contact time (hours)			
			1	2	3	4
A	Nickel	4	63.25	63.51	64.03	64.41
		12	11.15	11.79	12.22	12.39
		20	0.00	0.00	0.00	0.00
	Magnesium	10	96.59	97.21	97.59	97.84
		25	95.48	95.50	95.74	96.07
		50	91.71	92.14	92.81	94.25
		100	87.71	87.71	88.22	88.25
	E	Nickel	4	72.60	72.91	72.99
12			12.17	12.73	13.26	13.41
20			0.00	0.00	0.00	0.00
Iron		10	79.75	80.12	80.12	81.24
		20	79.07	79.15	79.63	81.00
		50	72.19	72.26	72.58	73.19
		100	70.33	70.79	71.06	72.31

(4 mol/dm<sup>3</sup> HCl, 70°C, 10% solid)

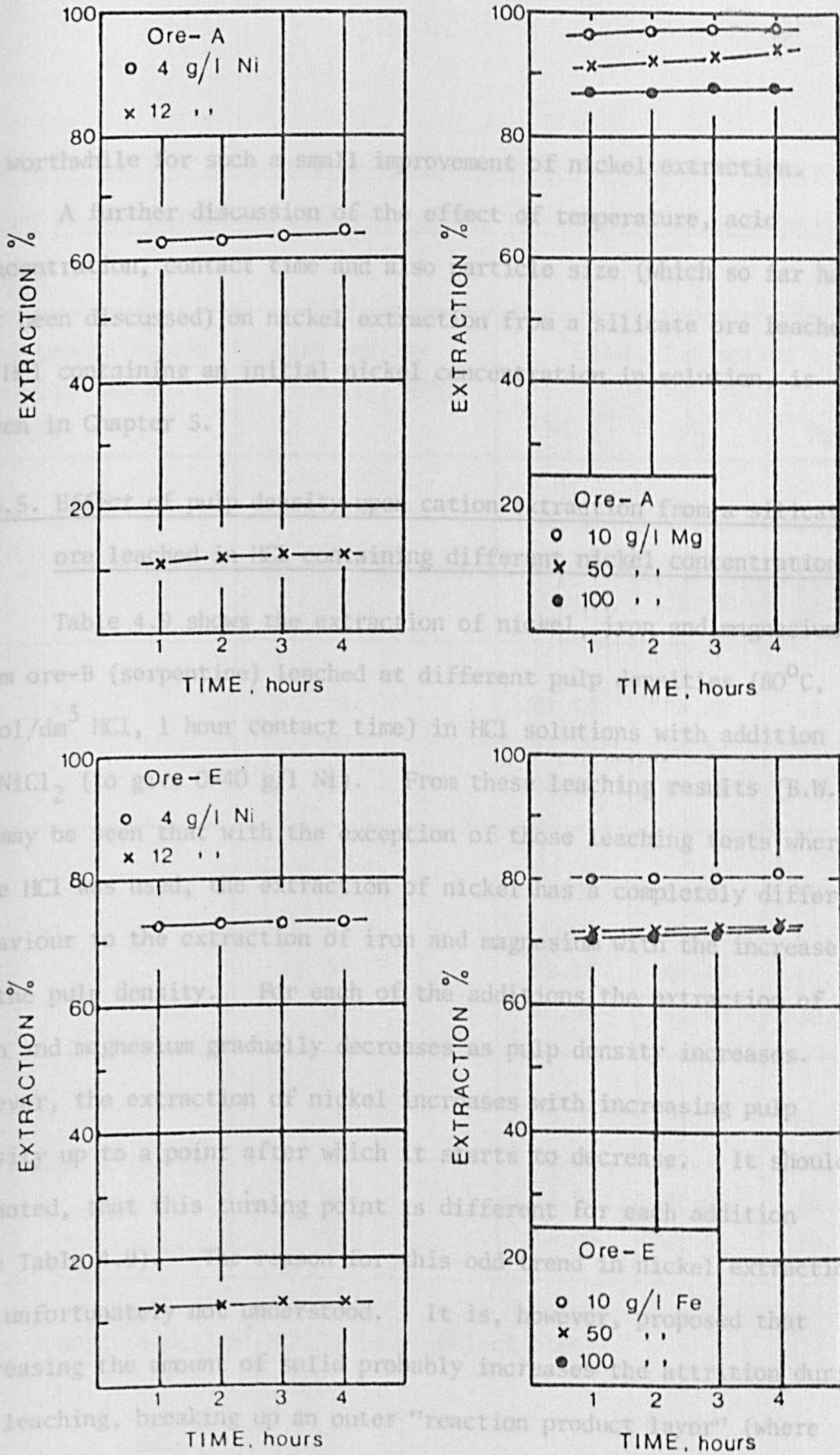


Fig. 4.16 Effect of contact time upon nickel extraction from Ore-A leached with additions of  $\text{NiCl}_2$  &  $\text{MgCl}_2$  and from Ore-E with  $\text{NiCl}_2$  &  $\text{FeCl}_3$ .

be worthwhile for such a small improvement of nickel extraction.

A further discussion of the effect of temperature, acid concentration, contact time and also particle size (which so far has not been discussed) on nickel extraction from a silicate ore leached in HCl containing an initial nickel concentration in solution, is given in Chapter 5.

#### 4.3.5. Effect of pulp density upon cation extraction from a silicate ore leached in HCl containing different nickel concentrations.

Table 4.9 shows the extraction of nickel, iron and magnesium from ore-B (serpentine) leached at different pulp densities (80°C, 6 mol/dm<sup>3</sup> HCl, 1 hour contact time) in HCl solutions with addition of NiCl<sub>2</sub> (to give 0-40 g/l Ni). From these leaching results (B.W.R.) it may be seen that with the exception of those leaching tests where pure HCl was used, the extraction of nickel has a completely different behaviour to the extraction of iron and magnesium with the increase in the pulp density. For each of the additions the extraction of iron and magnesium gradually decreases as pulp density increases. However, the extraction of nickel increases with increasing pulp density up to a point after which it starts to decrease. It should be noted, that this turning point is different for each addition (see Table 4.9). The reason for this odd trend in nickel extraction was unfortunately not understood. It is, however, proposed that increasing the amount of solid probably increases the attrition during the leaching, breaking up an outer "reaction product layer" (where perhaps nickel is retained in a crystallized or liquid form) allowing further removal of the nickel. The formation of this reaction

Table 4.9. Effect of pulp density upon cation extraction from Ore-B leached in HCl containing different nickel concentrations in solution (B.W.R.)

Nickel concentration in acid leach (g/l)	Pulp density (% solid, W/W)	Cation Extraction %		
		Ni	Fe	Mg
0	5	95.34	97.03	95.10
	10	89.83	94.70	94.39
	30	78.53	71.35	63.04
5	5	61.50	96.86	93.72
	10	78.26	94.62	93.54
	30	76.22	69.31	63.11
20	5	0.00	94.81	89.02
	10	0.00	90.73	87.25
	30	52.18	68.49	60.51
	40	46.36	41.63	30.14
40	5	0.00	93.41	86.45
	10	0.00	89.47	83.97
	30	17.32	66.05	56.69
	40	34.40	41.51	29.76

(80°C, 6 mol/dm<sup>3</sup> HCl, 1 hour contact time)

product layer is discussed in the following section.

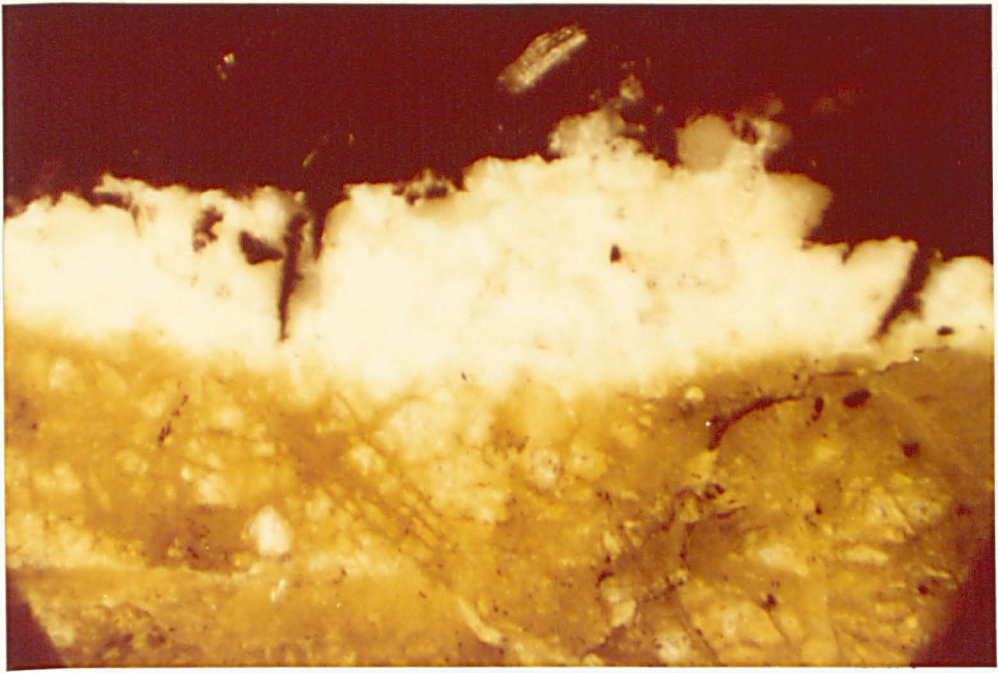
#### 4.3.6. Lump leaching

Lumps of about 1 cm diameter (ore-B) were leached in pure HCl and in HCl solutions containing  $\sim 65$  g/l Ni,  $\sim 100$  g/l Mg and  $\sim 100$  g/l Fe ( $80^{\circ}\text{C}$ ,  $6 \text{ mol/dm}^3$  HCl, 2 hour contact time). After leaching, each lump was sectioned and examined under a low power binocular microscope. This examination showed that:

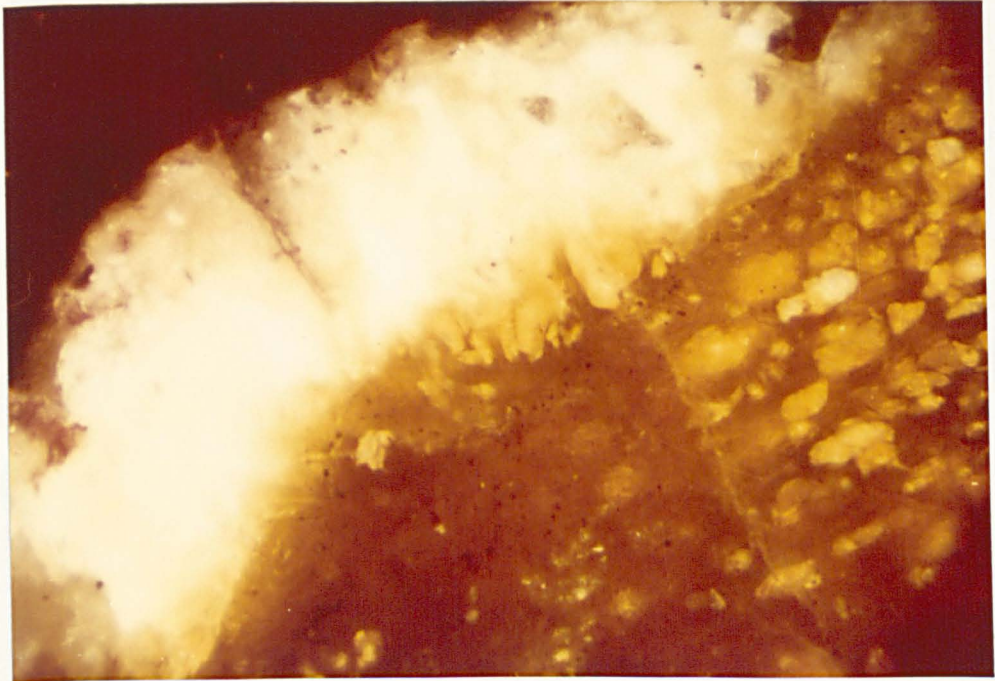
- a) each lump was surrounded by a visible layer of reacted material (also easily visible by the naked eye).
- b) this layer was irregular and friable
- c) for most of the lump samples, the layer appeared to have several cracks
- d) the colour of the layer was very distinct for each of the additions; yellowish-white for those lump samples leached in pure HCl, greenish-yellow for those leached with addition of  $\text{NiCl}_2$ , redish for those with  $\text{FeCl}_3$  and whitish-yellow for those with  $\text{MgCl}_2$ .

Selected lumps were mounted and polished for further microscopic (Vickers M55) observations and for microprobe analyses. Photographs showing the reaction product layer in each of these lumps were taken (see Figs.4.17 to 4.20). An unleached lump sample was also mounted, polished and photographed for comparison (see Fig. 4.21). From these, it may be seen that like the previous observations the layer was very irregular and contained many cracks. It should be noted however, that unlike the previous observations, the colour of the layer for most of the lumps was white-yellow. This was interpreted as perhaps being caused by the polishing.



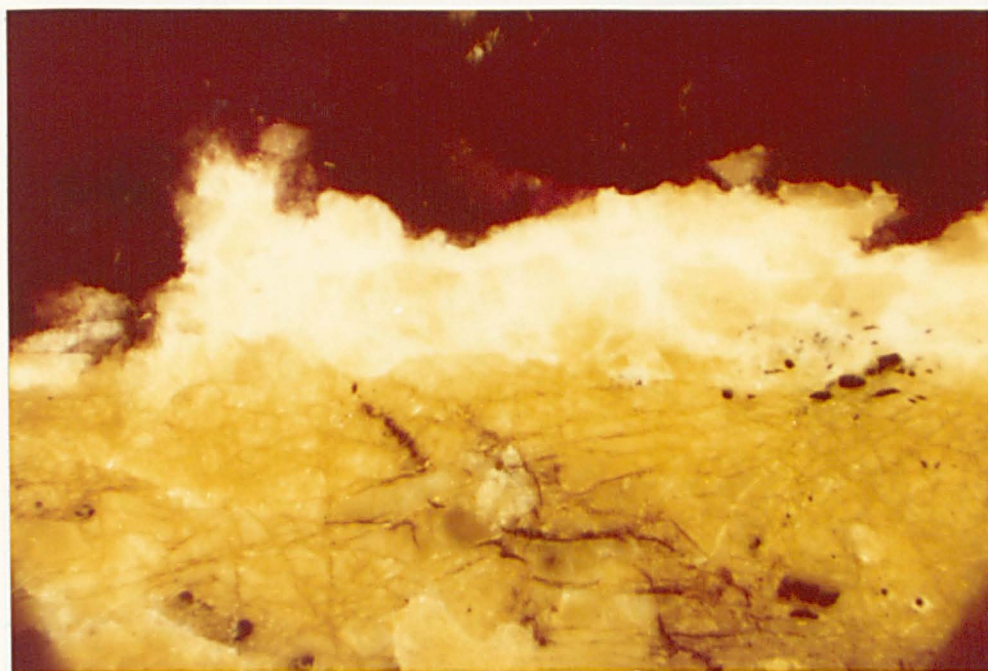


Mag. x 74

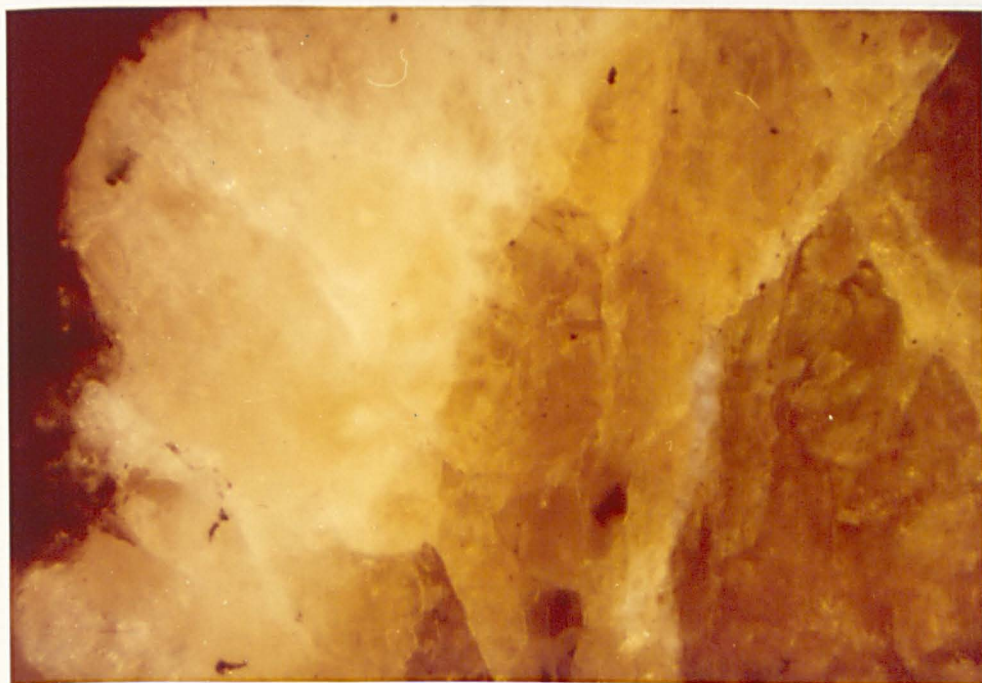


Mag. x 170

Fig. 4.17 Photographs of a lump particle leached in pure HCl showing the reaction product layer



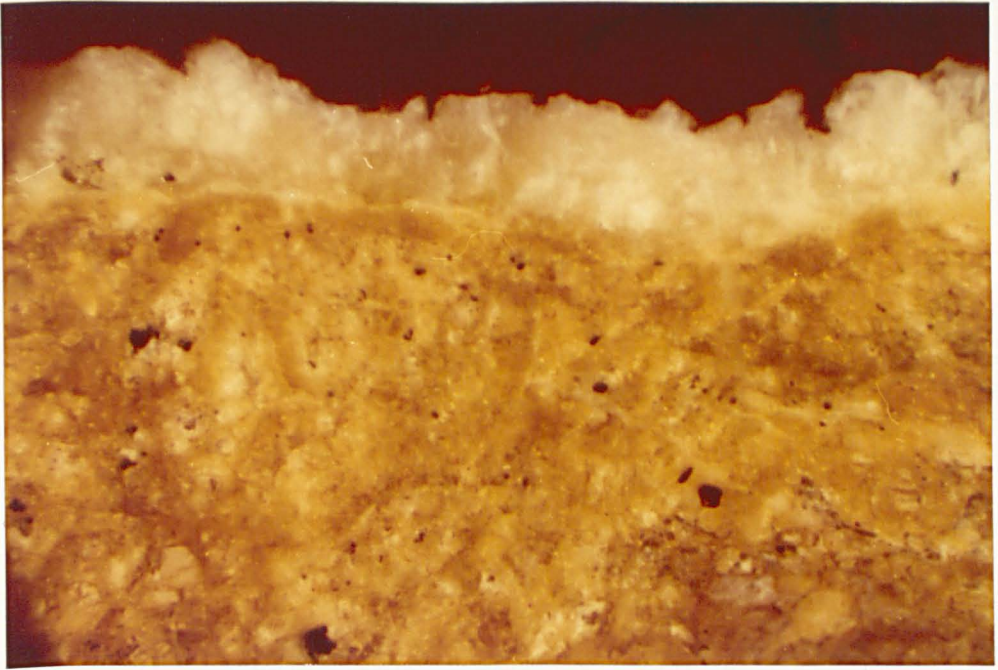
Mag. x 74



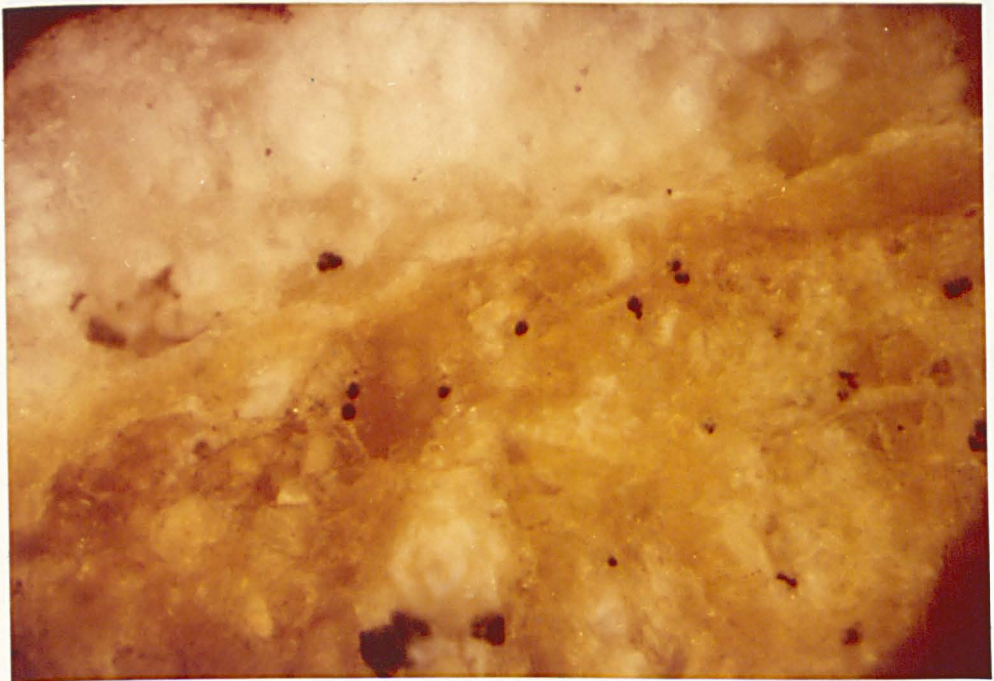
Mag. x 170

Fig. 4.18 Photographs of a lump particle leached in HCl containing Ni in solution showing the reaction product layer



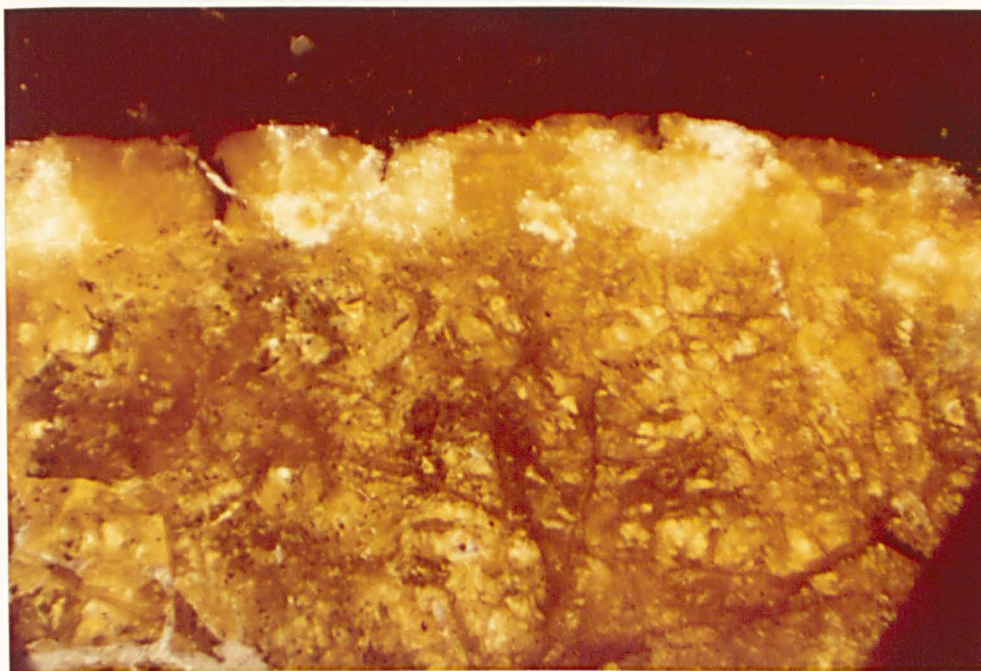


Mag. x 74

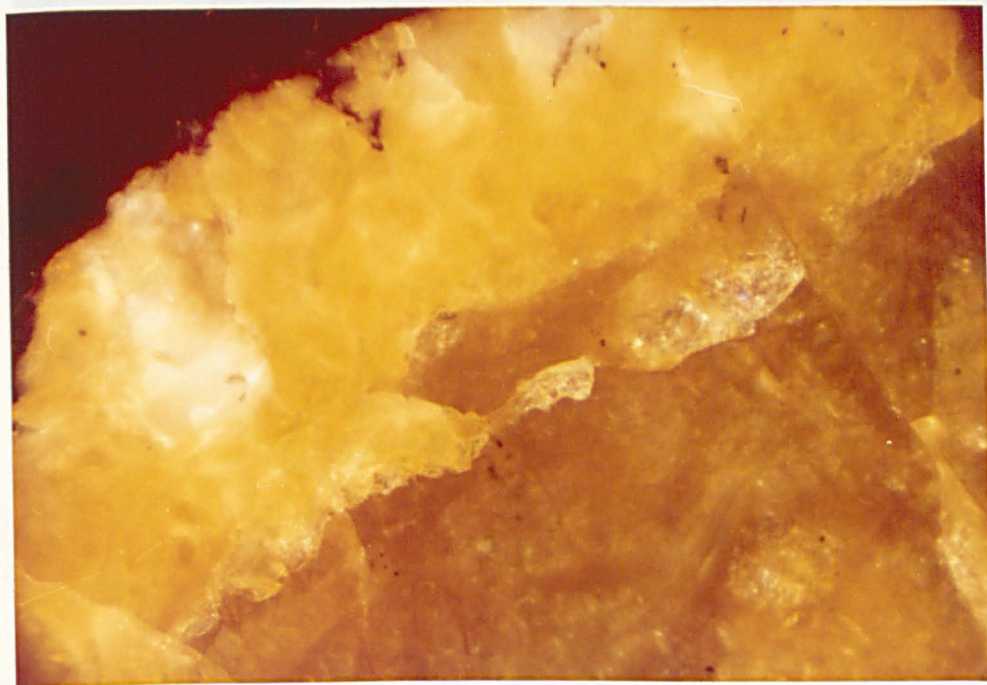


Mag. x 170

Fig. 4.19 Photographs of a lump particle leached in HCl containing Mg in solution showing the reaction product layer



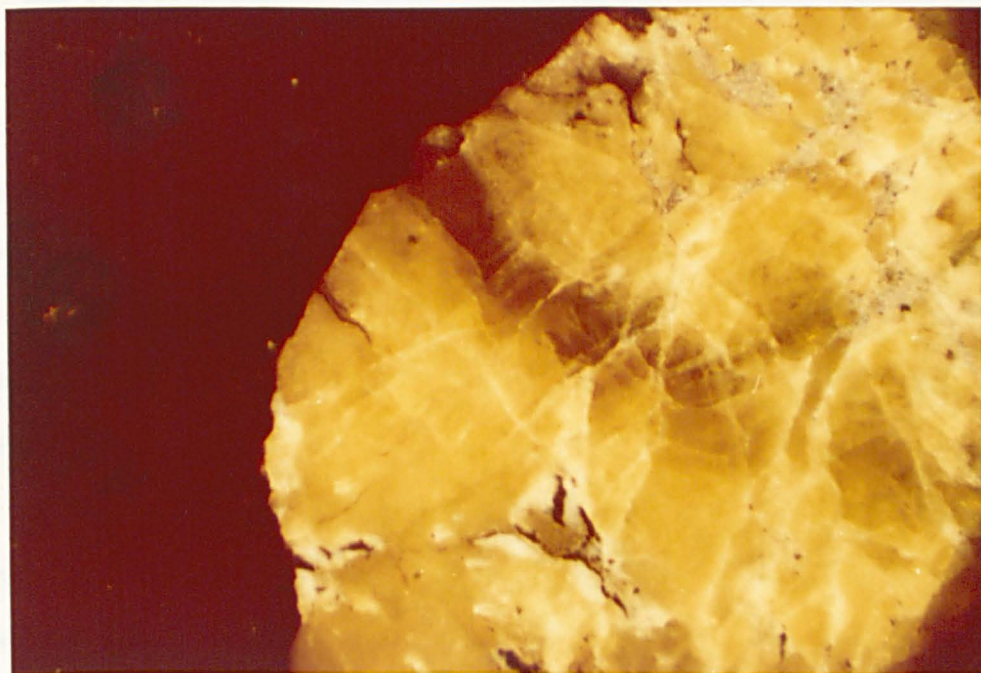
Mag. x 74



Mag. x 170

Fig. 4.20 Photographs of a lump particle leached in HCl containing Fe in solution showing the reaction product layer





Mag. x 74

Fig. 4.21 Photograph of an unleached lump particle

The microprobe analyses (which were intended to determine if the reaction product layer in those lumps leached with additions of  $\text{NiCl}_2$ ,  $\text{MgCl}_2$  and  $\text{FeCl}_3$ , contains a high concentration of nickel, magnesium and iron respectively) showed that the reaction product layer in all the lumps contains a very low (negligible) concentration of nickel, magnesium and iron. These results however, were considered incorrect because it was realised that during the polishing of the samples the cations dissolve out of the layer (i.e. by washing). Thus, no further stress was put on the microprobe work for the determination of an average nickel, magnesium and iron concentration in the layer.

Based on the evidence that a reaction product layer is formed during the leaching it is suggested that the decrease of nickel extraction with increasing nickel concentration in the leach acid could perhaps be attributed to crystallization of  $\text{NiCl}_2$  in the pores of the layer due to saturation of the solution in the pores caused by a faster chemical reaction (rapid rate of aqueous  $\text{NiCl}_2$  formation there) and a slow rate of diffusion (due to high nickel chloride concentration outside of the mineral; that is, in the bulk leaching solution). Certainly, another possibility for this saturation could be the diffusion of nickel into the layer from the bulk solution contributing to the overall rate of nickel concentration in the pores.

It should be noted that the idea that a solid crystallizes in the pores is supported to some extent by the slight increase in extraction with increasing severity of leaching, especially temperature. This theory clearly needs further study before it is established. However, this was not possible in the present work due to lack of time. Nevertheless, it is proposed that for future work, it would be worth-

while to determine the rate of nickel diffusion out of the pores of the layer and compare it with the rate at which nickel enters the pores due to chemical reaction. Then by estimating the volume of the pores, perhaps would be possible to determine the time that would take to saturate the solutions in the pores with  $\text{NiCl}_2 \cdot 2\text{H}_2\text{O}$  at a given set of leaching conditions and thus to stop the leaching reaction. This data should correlate with the % of nickel extraction v/s leaching time at high nickel concentrations. Similar calculations might be done for magnesium and iron.

Perhaps, it is worth mentioning that a similar explanation to a different but related problem in the dissolution of copper sulphide anodes have been reported by Peters<sup>(86)</sup> and Etienne<sup>(87)</sup>. The problem was why the potential v/s time curve shows a sharp rise at time  $>$  transition time  $\tau$ . This was attributed to crystallization of  $\text{CuSO}_4 \cdot 5\text{H}_2\text{O}$  at the bottom of the pores due to saturation of the solution in the pores caused by pressing and the volume change between digenite-covellite transitions.

CHAPTER 5

KINETICS OF ACID DISSOLUTION OF A LATERITIC NICKEL ORE

5.1 Experimental

Ore B, typical of the serpentine ores was selected to study the kinetics of dissolution of a lateritic nickel ore in hydrochloric acid. The mineral was ground to give a particle size distribution as shown in Table 5.1 and was leached at different temperatures (25°C, 40°C and 70°C), acid concentrations (1, 2 and 4 mol/dm<sup>3</sup>) and various periods of time (5, 10, 30, 60, 120 and 180 minutes). Leaching of different particle size fractions (-18+36, -72+150 and -150+300 B.S.M.) was also performed. A pulp density of 2% solid (W/V) was used for all experiments in order to maintain a large excess of leaching reagent.

All the leaching tests were performed in pure HCl solution, and in HCl solutions containing 5 g/l Ni. in order to study cation dissolution of both media.

Table 5.1 Particle size distribution of Ore-B.

Size Fraction B.S.M.	Weight Retained %
- 5 + 10	1.28
-10 + 18	13.59
-18 + 36	20.77
-36 + 72	11.28
-72 +150	11.67
-150 +300	13.59
-300	22.82

## 5.2 Effect of Temperature

Figs. 5.1 to 5.3 show the extraction of nickel, iron and magnesium with pure acid for different temperatures and contact times. From these, it is clear that increased temperature causes a significant increase in the <sup>rate of</sup> cation extraction. This may occur because increasing acid temperature increases the mobility and reactivity of the hydrogen ion, resulting in a more rapid attack on the silicate structure of the ore, removing the  $\text{OH}^-$  ions, and speeding up the destruction of the silicate lattice, which releases the cations from their position <sup>(8)</sup>.

Extraction of cations during leaching in HCl containing 5 g/l Ni. is presented in Figs. 5.4 and 5.5, where the extraction of iron and magnesium shows a similar behaviour to that in pure HCl, except that it is lower because of the presence of nickel in solution. As expected, nickel extraction was zero for each of the temperatures and contact times.

Again, from these results one can see that extraction of magnesium and iron is highly dependent on the temperature, as in the case of pure HCl. Details of the cation extractions at different temperatures in both acid media are given in Tables 5.2 and 5.3.

## 5.3 Effect of Acid Concentration

Figs 5.6 to 5.8 (Table 5.4) show how different concentrations of pure HCl (1, 2 and 4 mol/dm<sup>3</sup>) affect cation extraction at 25°C and 70°C. At both temperatures, increasing acid concentration increased the rate of extraction of nickel, iron and magnesium. This indicates that extraction of the three cations is dependent on the acid concentration

to a greater degree for some cations than for others. This is clearly shown in the named figures at 70°C, where iron is the most dependent on the acid concentration, followed by magnesium and nickel respectively. Results for nickel (Fig. 5.6), indicate that nickel extraction depends a great deal more on the temperature than it does on the acid concentration. Iron and magnesium extractions however (Figs. 5.7 and 5.8), are as highly dependent on the acid concentration as on the temperature.

Leaching of the ore in HCl containing 5 g/l Ni at different acid concentrations (1, 2 and 4 mol/dm<sup>3</sup>) also showed that cation extraction <sup>the rate of</sup> increased as the acid concentration increased (except for nickel, where extraction was zero). This can be seen in Figs. 5.9 and 5.10 (Table 5.5), where the extraction of iron and magnesium for each acid concentration at 25°C and 70°C is plotted against leaching time. Again, these results indicate that extraction of iron and magnesium are as highly dependent on temperature as on acid concentration.

#### 5.4 Effect of Particle Size

Figs. 5.11 to 5.15 show the cation extraction of both media at 70°C for different specific size fractions (-18+36, -72+150 and -150+300 B.S.M.) where the smaller the size, the higher the total extraction and the higher the rate of extraction, due to the larger surface area of the solid exposed to acid attack.

It will be seen later in the chapter how particle size and shape are very important parameters in the interpretation of cation dissolution kinetics.

Details of Figs. 5.11 to 5.15 are given in Tables 5.6 and 5.7.



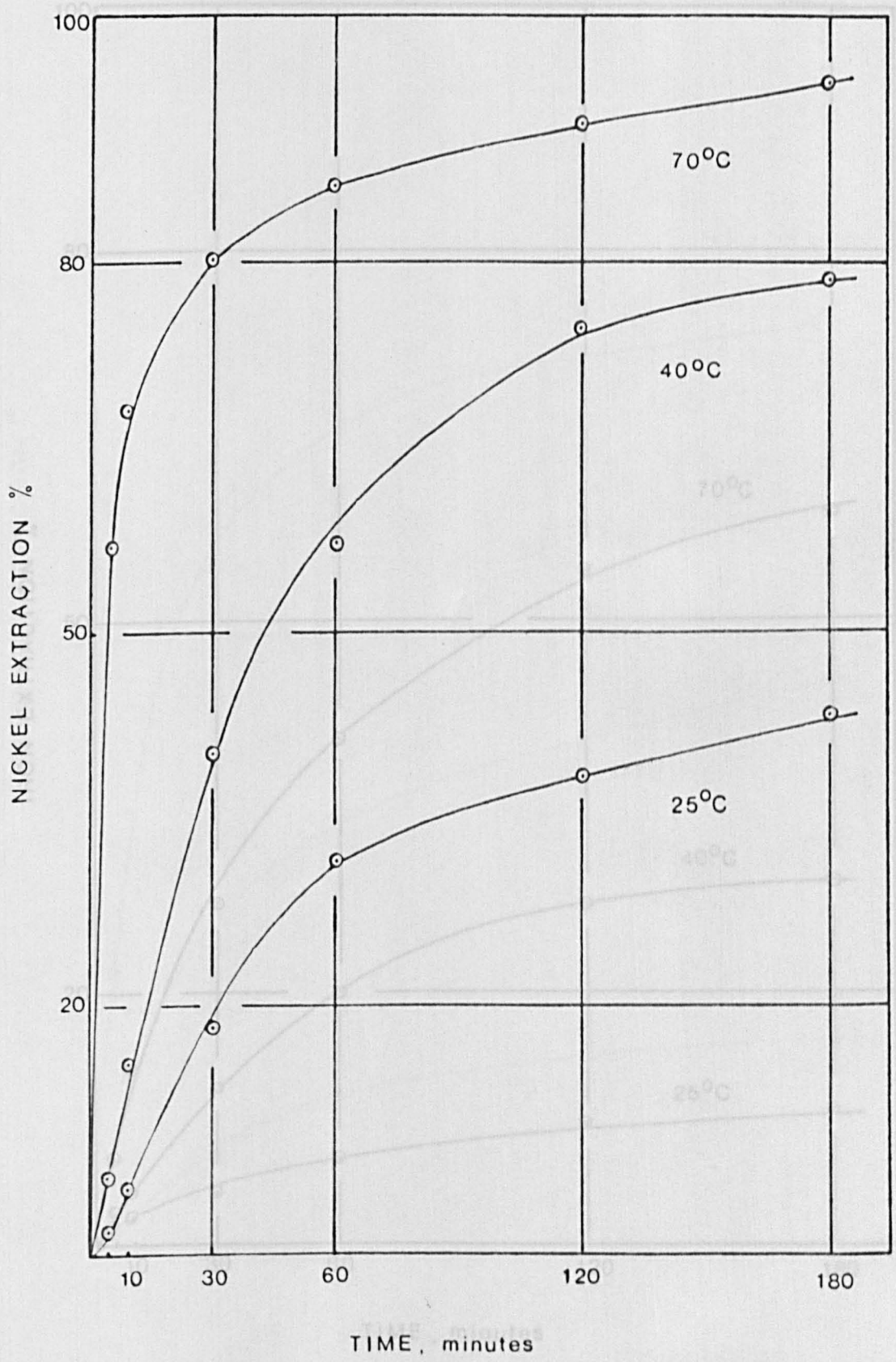


Fig. 5.1. Effect of temperature on nickel extraction kinetics (ore-B), pure HCl.

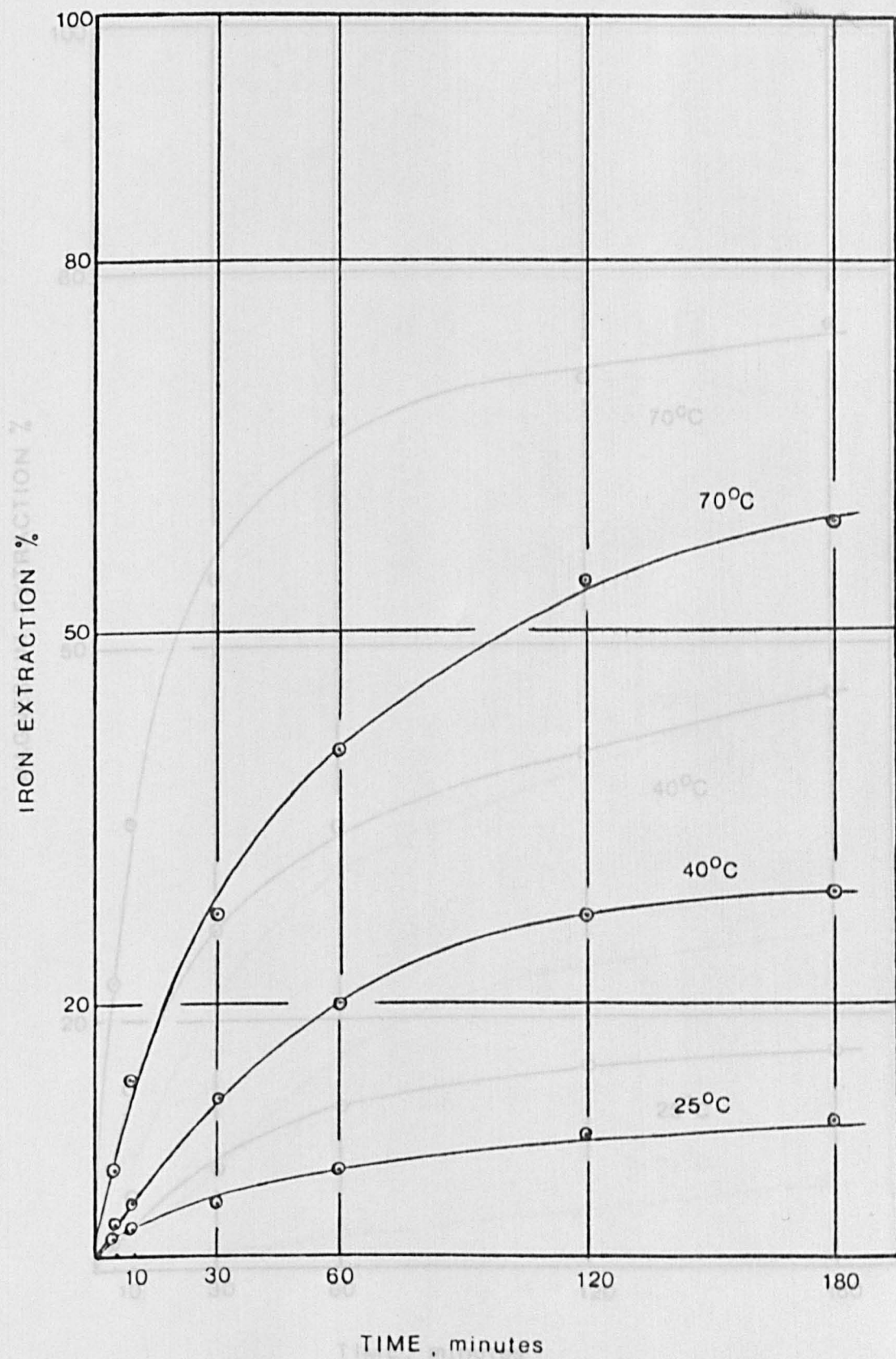


Fig. 5.2. Effect of temperature on iron extraction kinetics  
(ore-B), pure HCl.

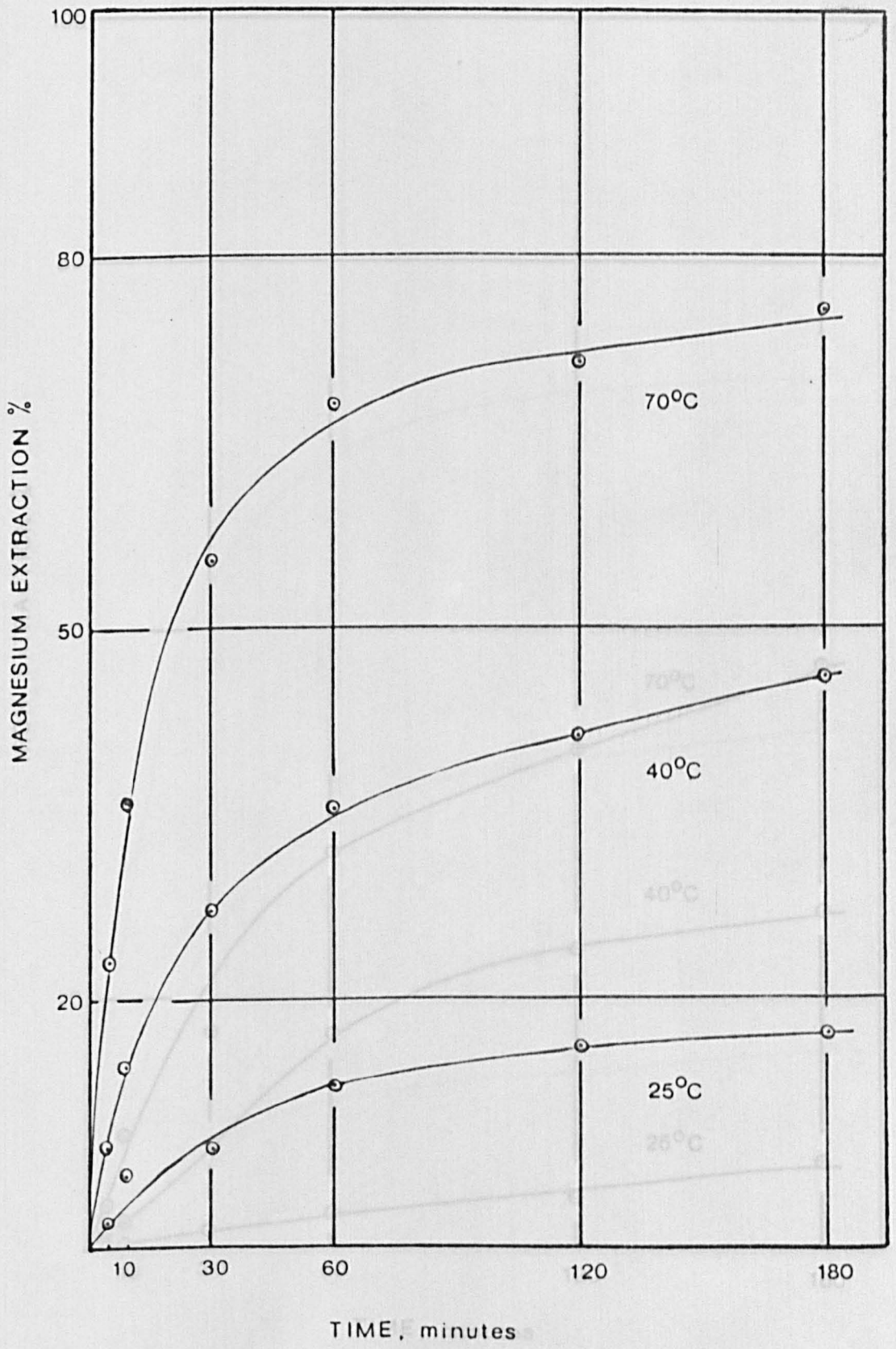


Fig. 5.3. Effect of temperature on magnesium extraction kinetics (ore - B), pure HCl.



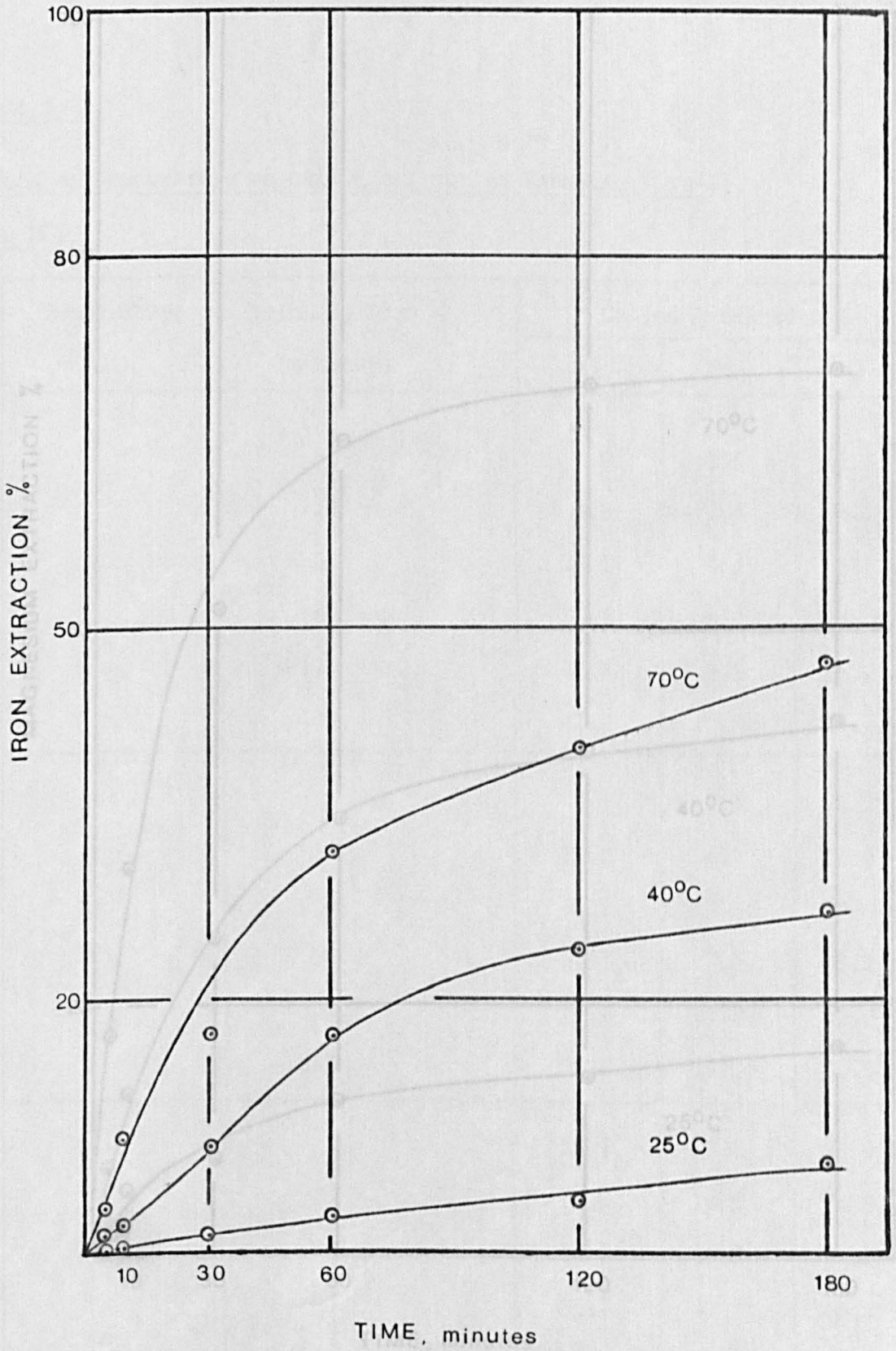


Fig. 5.4. Effect of temperature on iron extraction kinetics (ore-B), HCl containing 5 g/l Ni.

Table 5.2

Effect of temperature on cation extraction kinetics (Ore-B),

pure HCl

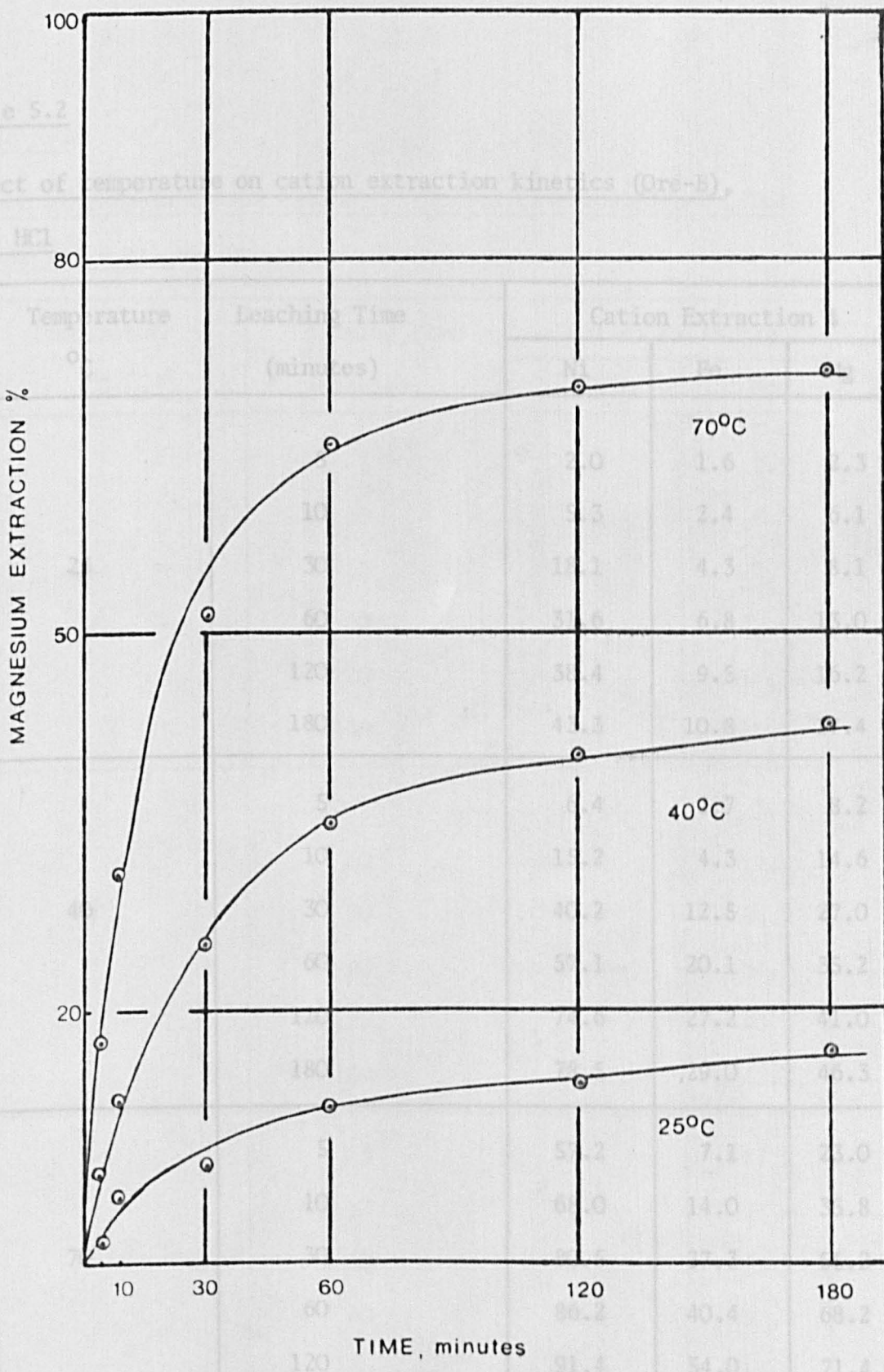


Fig. 5.5. Effect of temperature on magnesium extraction

kinetics (ore - B), HCl containing 5 g/l Ni.

Conditions: Pulp density 21 solid (W/V), 2 mol/dm<sup>3</sup> HCl

Table 5.2

Effect of temperature on cation extraction kinetics (Ore-B),  
 pure HCl

Temperature °C	Leaching Time (minutes)	Cation Extraction %		
		Ni	Fe	Mg
25	5	2.0	1.6	2.3
	10	5.3	2.4	6.1
	30	18.1	4.3	8.1
	60	31.6	6.8	13.0
	120	38.4	9.5	16.2
	180	43.3	10.8	17.4
40	5	6.4	2.7	8.2
	10	15.2	4.3	14.6
	30	40.2	12.5	27.0
	60	57.1	20.1	35.2
	120	74.6	27.2	41.0
	180	78.5	29.0	46.3
70	5	57.2	7.1	23.0
	10	68.0	14.0	35.8
	30	80.5	27.3	55.2
	60	86.2	40.4	68.2
	120	91.4	54.0	71.4
	180	94.8	58.6	75.5

Conditions: Pulp density 2% solid (W/V), 2 mol/dm<sup>3</sup> HCl

Table 5.3

Effect of temperature on cation extraction kinetics (Ore-B), HCl containing 5 g/l Ni.

Temperature °C	Leaching Time (minutes)	Cation Extraction	
		Fe	Mg
25	5	-	1.7
	10	-	5.4
	30	1.5	7.7
	60	2.8	12.4
	120	4.1	14.3
	180	7.0	16.8
40	5	1.3	7.3
	10	2.2	12.9
	30	8.6	25.2
	60	17.3	34.9
	120	24.0	40.3
	180	27.1	42.7
70	5	3.6	17.5
	10	9.1	30.6
	30	17.3	51.9
	60	31.8	65.3
	120	40.0	69.8
	180	47.2	71.0

Conditions: Pulp density 2% solid (W/V), 2 mol/dm<sup>3</sup> HCl



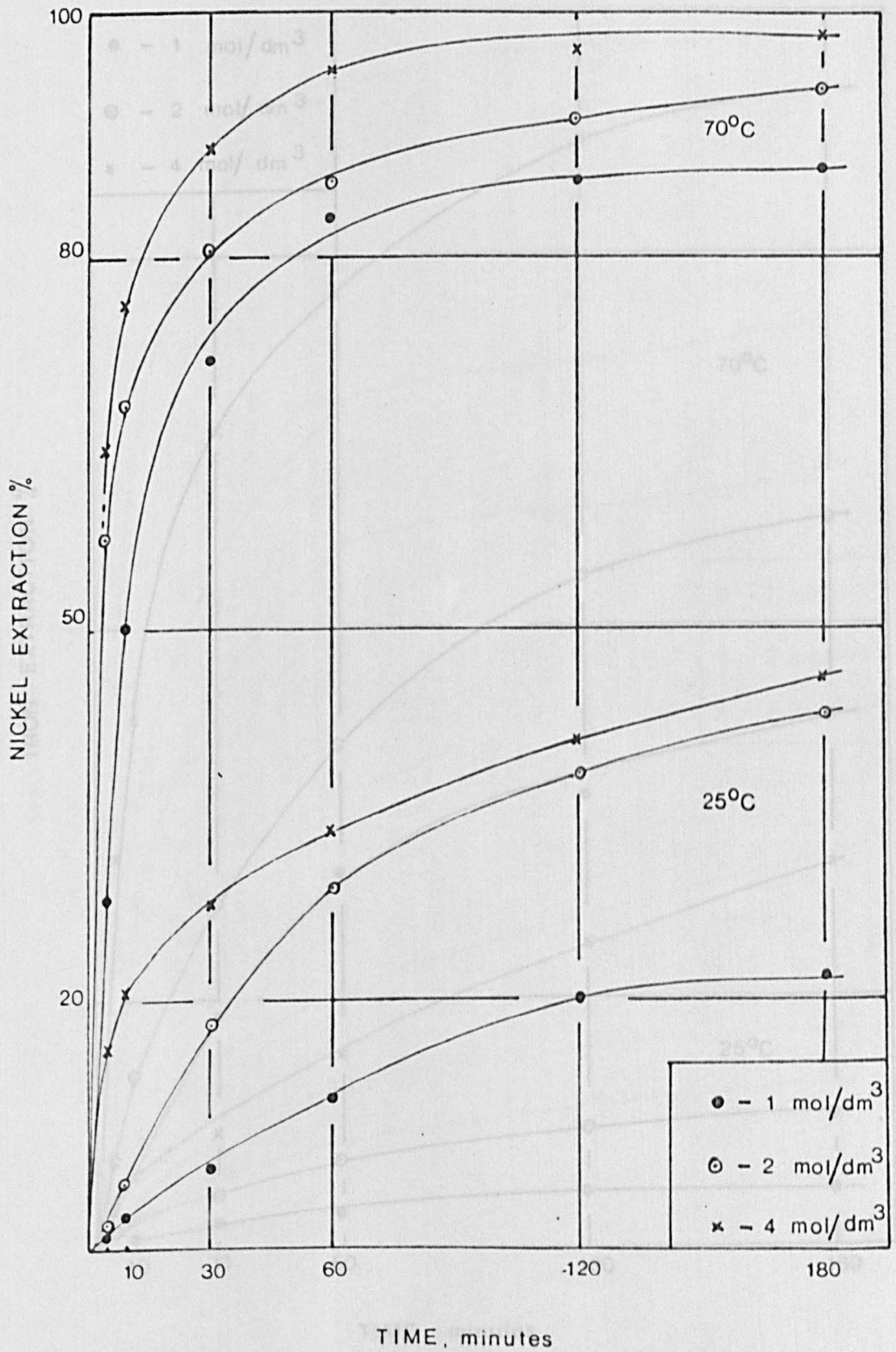


Fig 5.6. Effect of acid concentration and temperature on nickel extraction kinetics (ore-B), pure HCl.



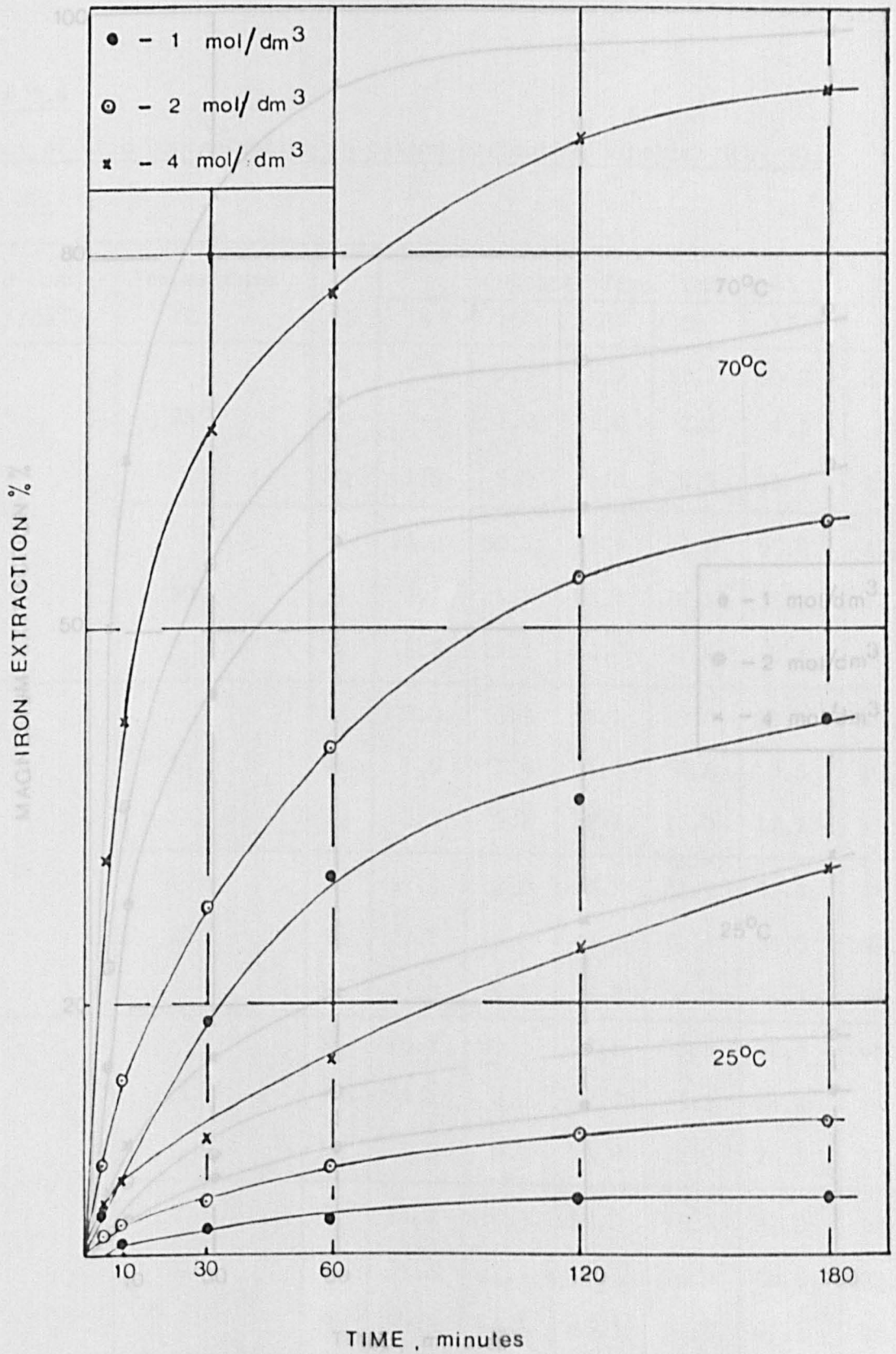


Fig. 5.7. Effect of acid concentration and temperature on iron extraction kinetics (ore - B), pure HCl.

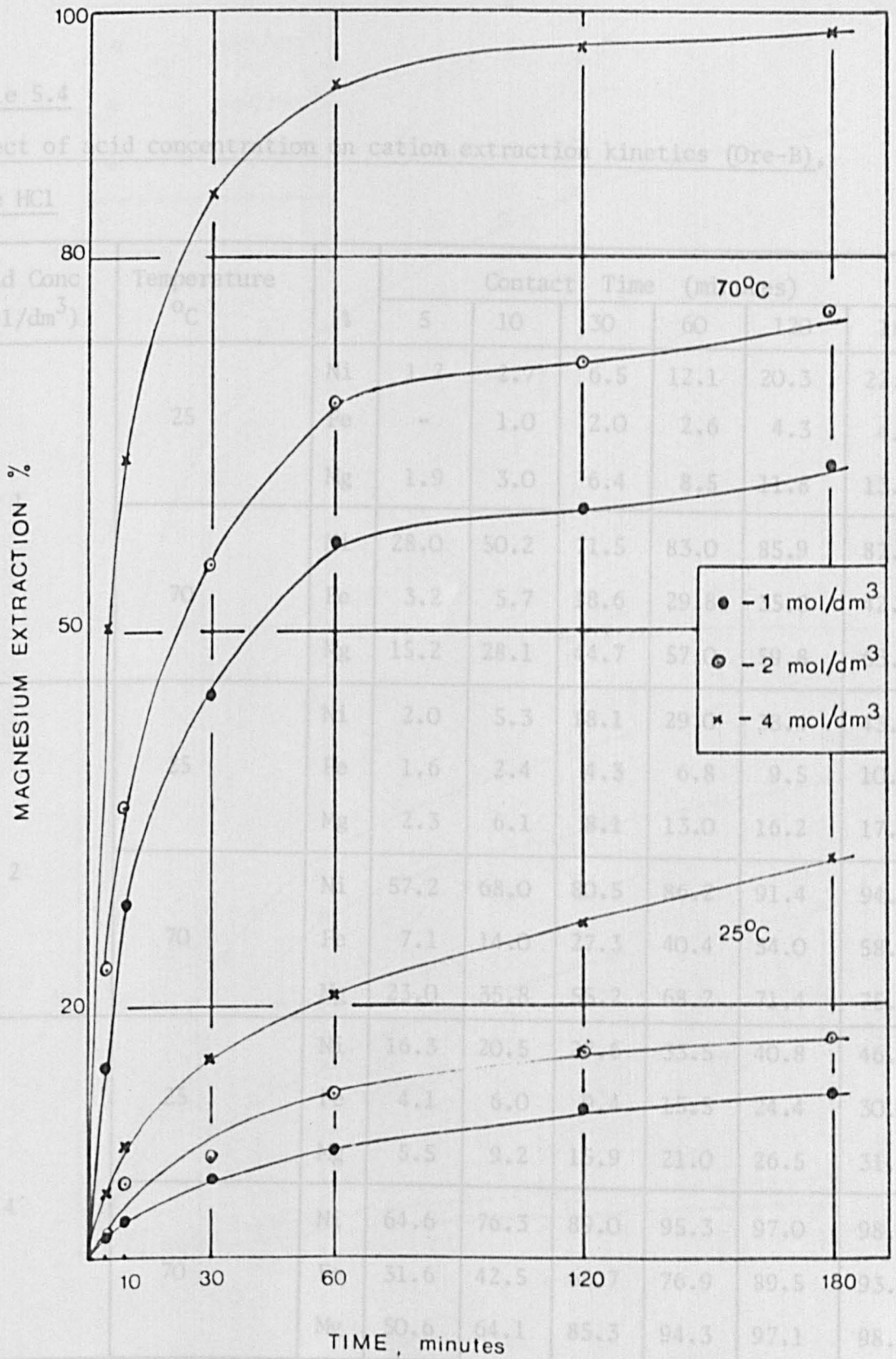


Fig 5.8. Effect of acid concentration and temperature on magnesium extraction kinetics (ore-B), pure HCl.

Table 5.4

Effect of acid concentration on cation extraction kinetics (Ore-B),  
pure HCl

Acid Conc (mol/dm <sup>3</sup> )	Temperature °C	%	Contact Time (minutes)					
			5	10	30	60	120	180
1	25	Ni	1.2	2.7	6.5	12.1	20.3	22.3
		Fe	-	1.0	2.0	2.6	4.3	4.5
		Mg	1.9	3.0	6.4	8.5	11.8	13.0
	70	Ni	28.0	50.2	71.5	83.0	85.9	87.4
		Fe	3.2	5.7	18.6	29.8	35.8	42.5
		Mg	15.2	28.1	44.7	57.0	59.8	63.2
2	25	Ni	2.0	5.3	18.1	29.0	38.4	43.3
		Fe	1.6	2.4	4.3	6.8	9.5	10.8
		Mg	2.3	6.1	8.1	13.0	16.2	17.4
	70	Ni	57.2	68.0	80.5	86.2	91.4	94.0
		Fe	7.1	14.0	27.3	40.4	54.0	58.6
		Mg	23.0	35.8	55.2	68.2	71.4	75.5
4	25	Ni	16.3	20.5	27.6	33.5	40.8	46.0
		Fe	4.1	6.0	9.4	15.5	24.4	30.8
		Mg	5.5	9.2	15.9	21.0	26.5	31.8
	70	Ni	64.6	76.3	89.0	95.3	97.0	98.3
		Fe	31.6	42.5	65.7	76.9	89.5	93.6
		Mg	50.6	64.1	85.3	94.3	97.1	98.5

Conditions: Pulp density 2% solid (W/V)

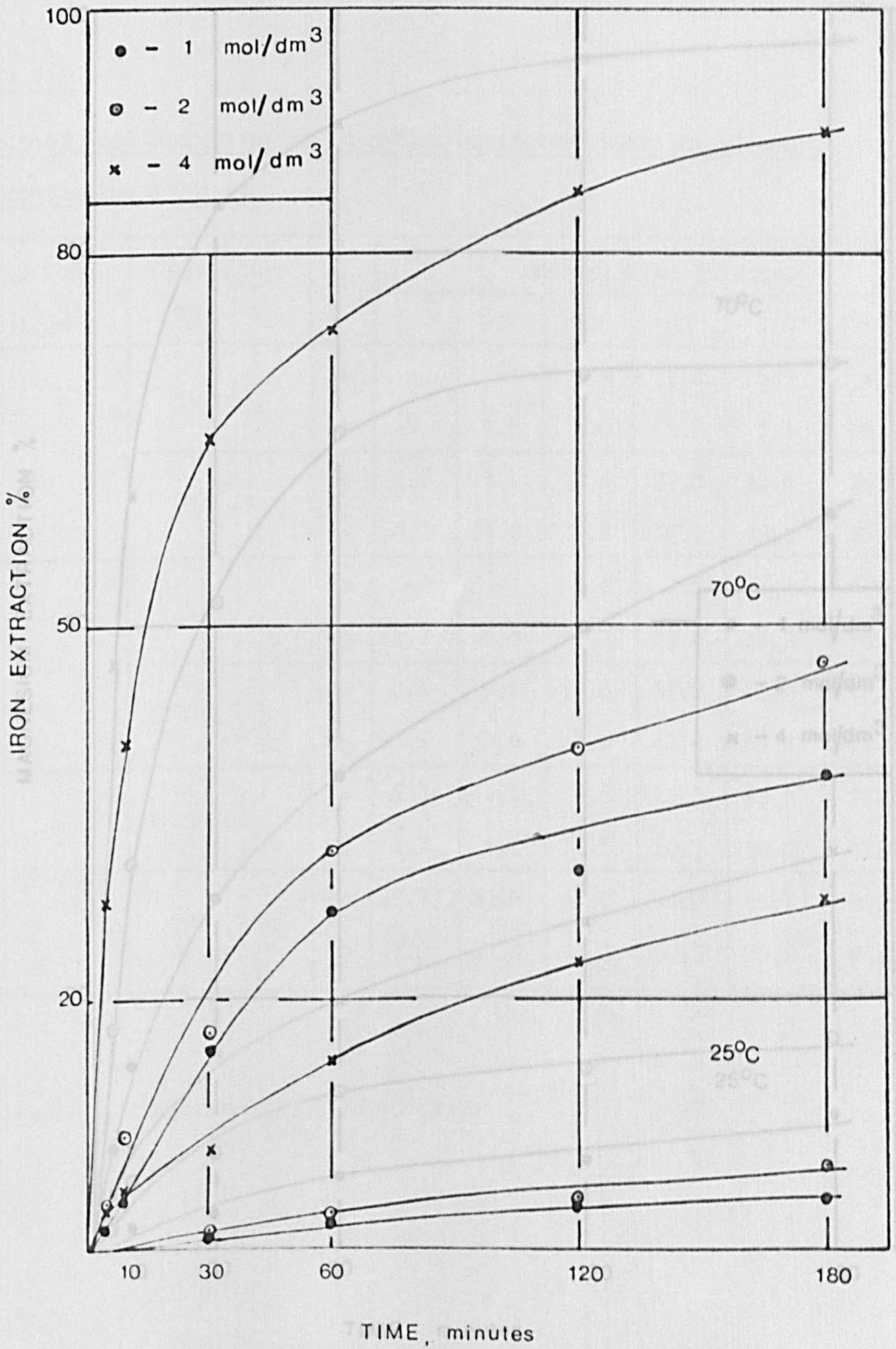


Fig. 5.9. Effect of acid concentration and temperature on iron extraction kinetics (ore-B), HCl containing 5 g/l Ni.



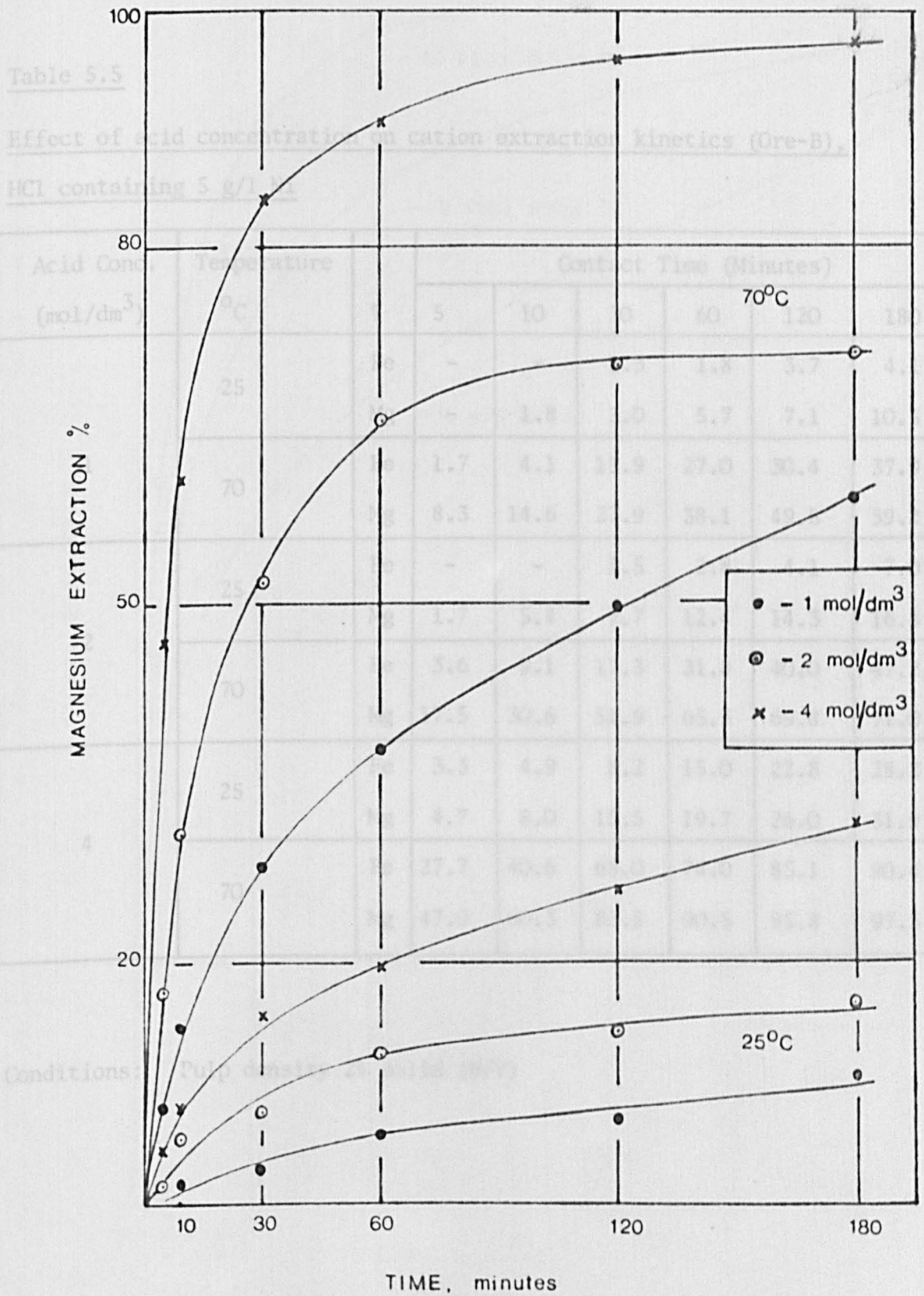


Fig. 5.10. Effect of acid concentration and temperature on magnesium extraction kinetics (ore-B), HCl containing 5 g/l Ni.

Table 5.5

Effect of acid concentration on cation extraction kinetics (Ore-B),

HCl containing 5 g/l Ni

Acid Conc. (mol/dm <sup>3</sup> )	Temperature °C	%	Contact Time (Minutes)					
			5	10	30	60	120	180
1	25	Fe	-	-	1.3	1.8	3.7	4.1
		Mg	-	1.8	3.0	5.7	7.1	10.5
	70	Fe	1.7	4.1	15.9	27.0	30.4	37.9
		Mg	8.3	14.6	27.9	38.1	49.8	59.2
2	25	Fe	-	-	1.5	2.8	4.1	7.0
		Mg	1.7	5.4	7.7	12.4	14.3	16.8
	70	Fe	3.6	9.1	17.3	31.8	40.0	47.2
		Mg	17.5	30.6	51.9	65.3	69.8	71.0
4	25	Fe	3.3	4.9	8.2	15.0	22.8	28.2
		Mg	4.7	8.0	15.5	19.7	26.0	31.9
	70	Fe	27.7	40.6	65.0	74.0	85.1	90.4
		Mg	47.0	60.3	83.8	90.5	95.8	97.5

Conditions: Pulp density 2% solid (W/V)

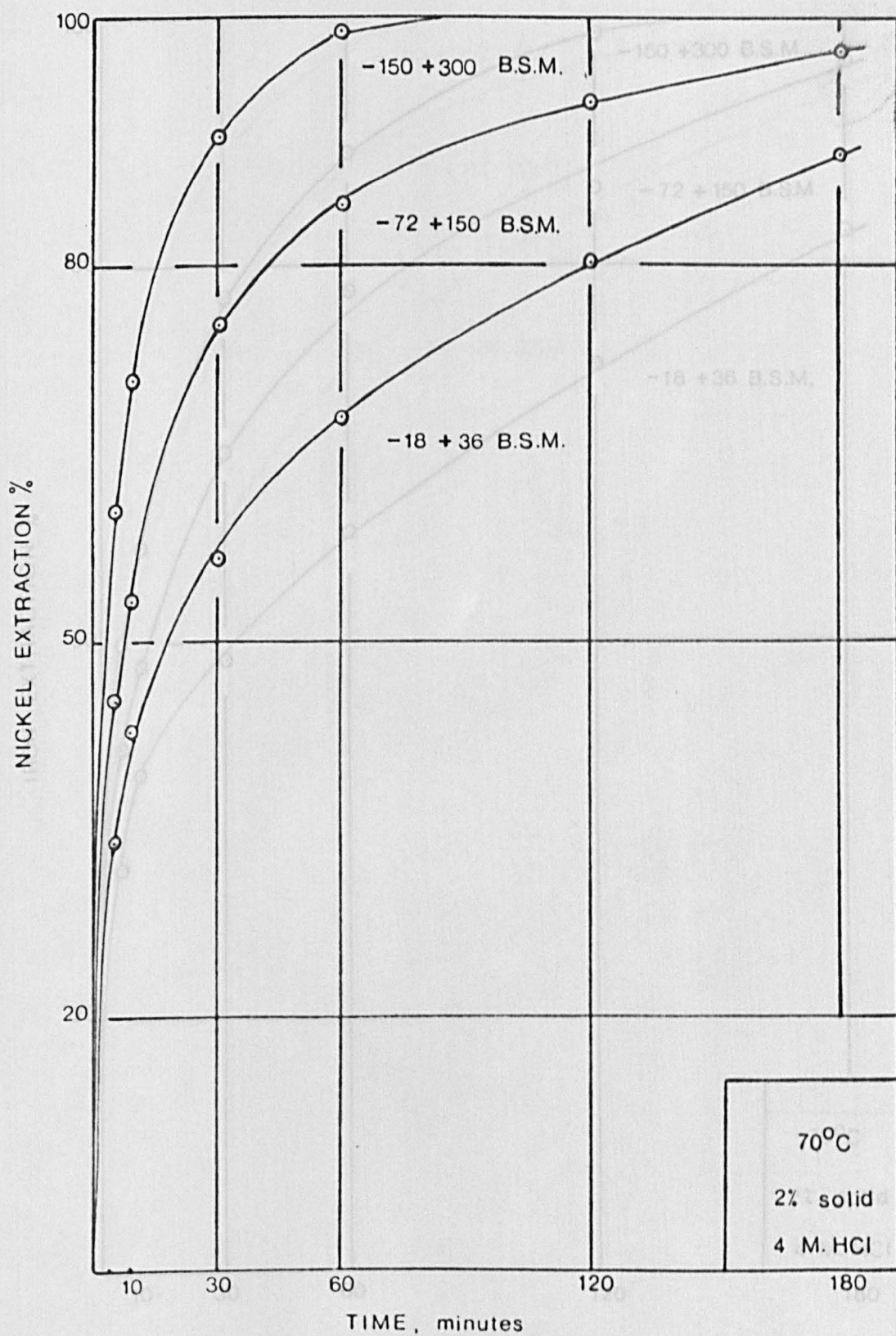


Fig. 5. 11. Effect of particle size on nickel extraction kinetics

Fig. 5. 12. Effect of particle size on iron extraction

(ore - B), pure HCl.

kinetics (ore - B), pure HCl.

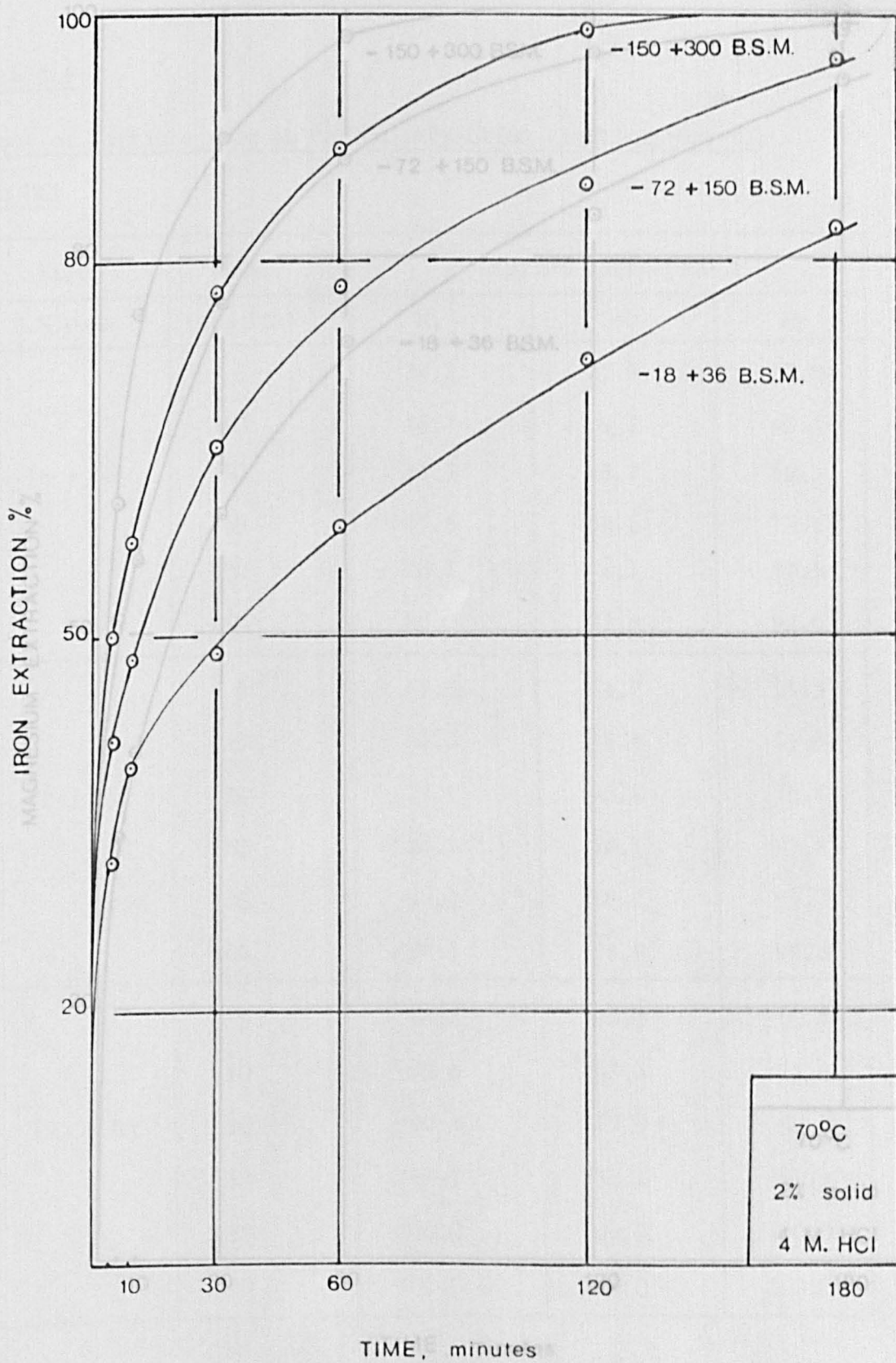


Fig. 5.12. Effect of particle size on iron extraction kinetics (ore - B), pure HCl.



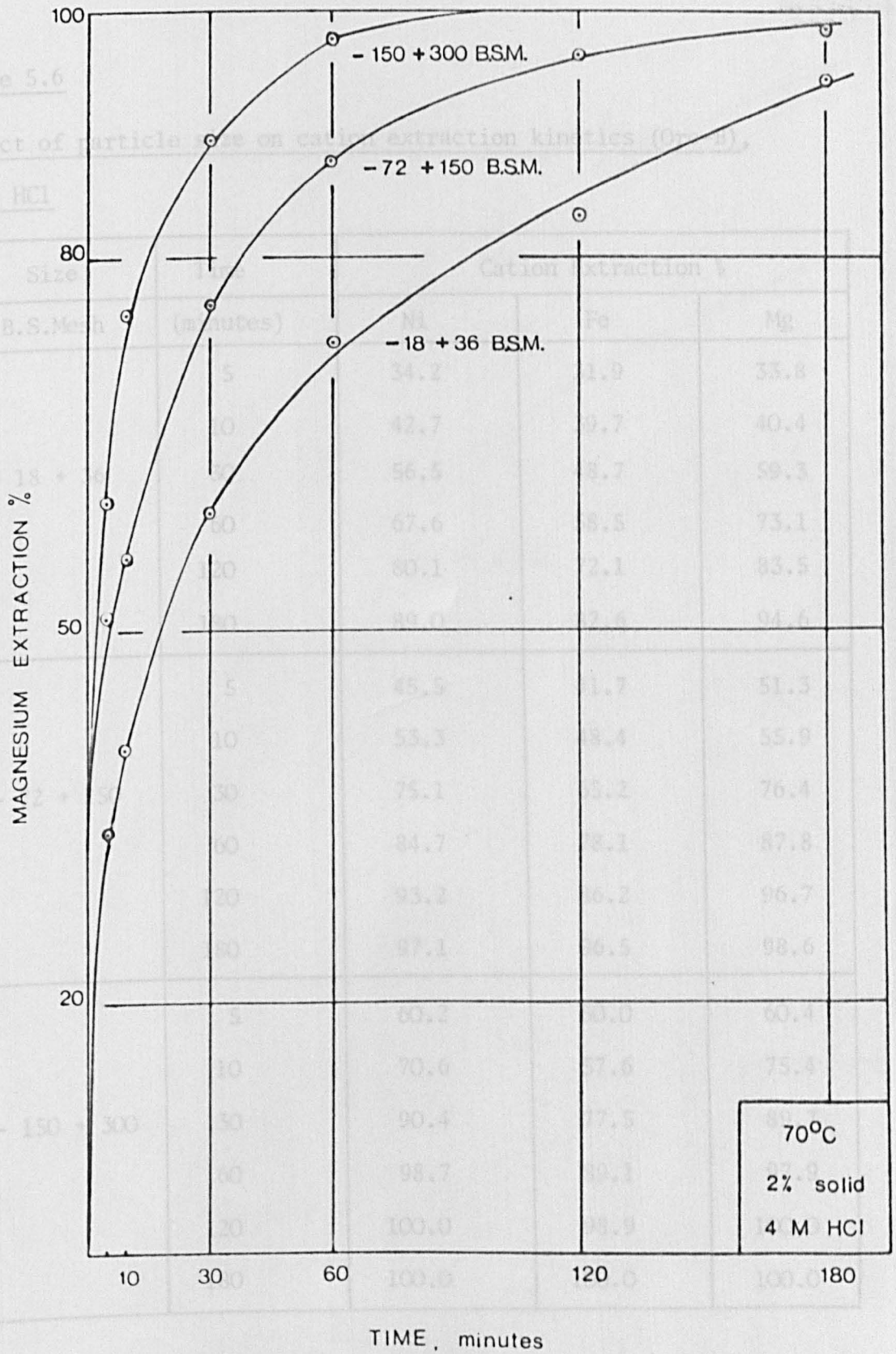


Fig. 5.13. Effect of particle size on magnesium extraction kinetics (ore - B), pure HCl.

Table 5.6

Effect of particle size on cation extraction kinetics (Ore-B),  
pure HCl

Size	Time	Cation Extraction %		
B.S.Mesh	(minutes)	Ni	Fe	Mg
- 18 + 36	5	34.2	31.9	33.8
	10	42.7	39.7	40.4
	30	56.5	48.7	59.3
	60	67.6	58.5	73.1
	120	80.1	72.1	83.5
	180	89.0	82.6	94.6
- 72 + 150	5	45.5	41.7	51.3
	10	53.3	48.4	55.9
	30	75.1	65.2	76.4
	60	84.7	78.1	87.8
	120	93.2	86.2	96.7
	180	97.1	96.5	98.6
- 150 + 300	5	60.2	50.0	60.4
	10	70.6	57.6	75.4
	30	90.4	77.5	89.7
	60	98.7	89.1	97.9
	120	100.0	98.9	100.0
	180	100.0	100.0	100.0

Conditions: 2% solid, 70°C, 4 mol/dm<sup>3</sup> HCl

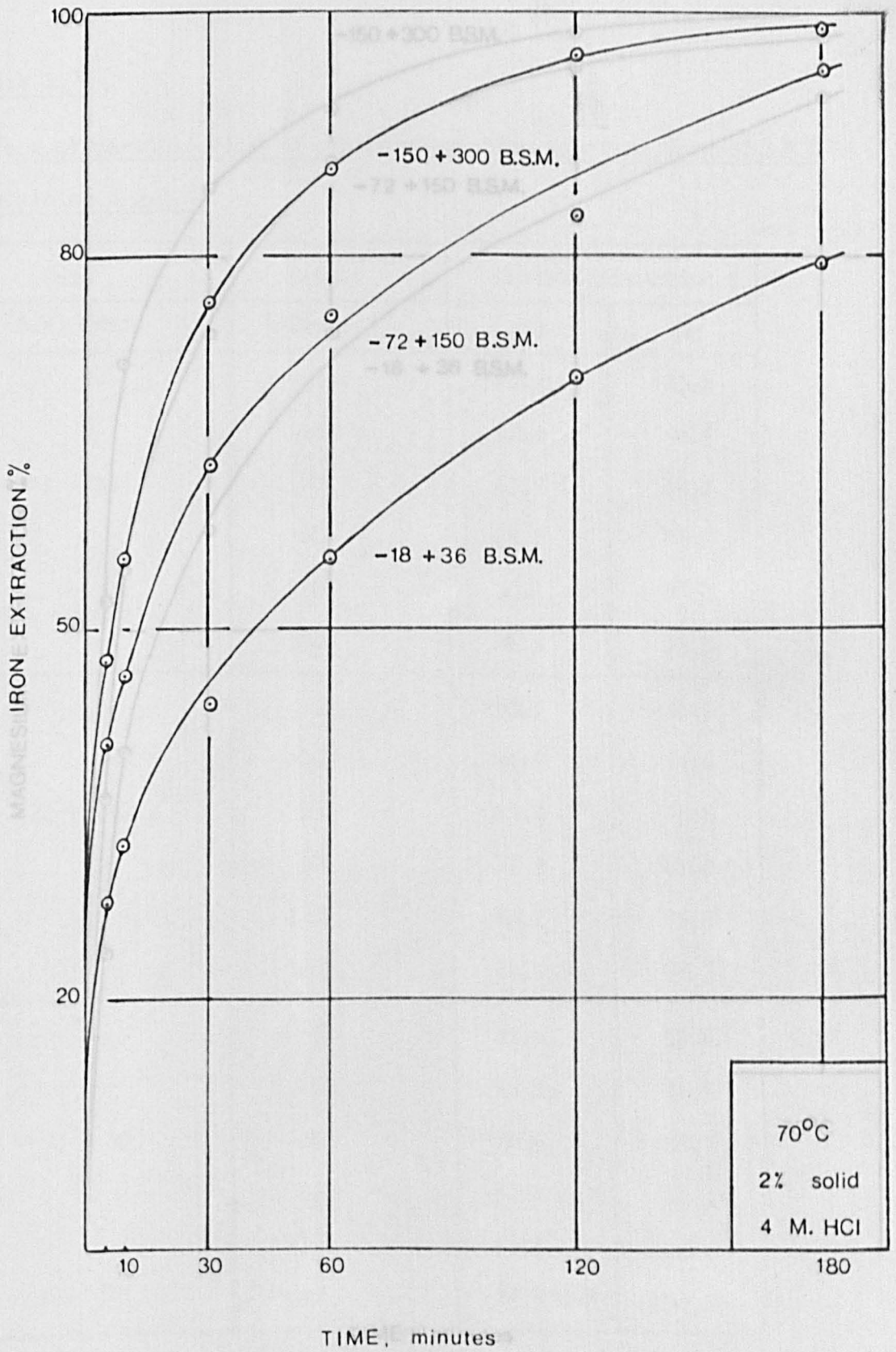


Fig. 5.14. Effect of particle size on iron extraction kinetics

Fig. 5.15. Effect of particle size on magnesium extraction (ore -B), HCl containing 5 g/l Ni.

kinetics (ore -B), HCl containing 5 g/l Ni.

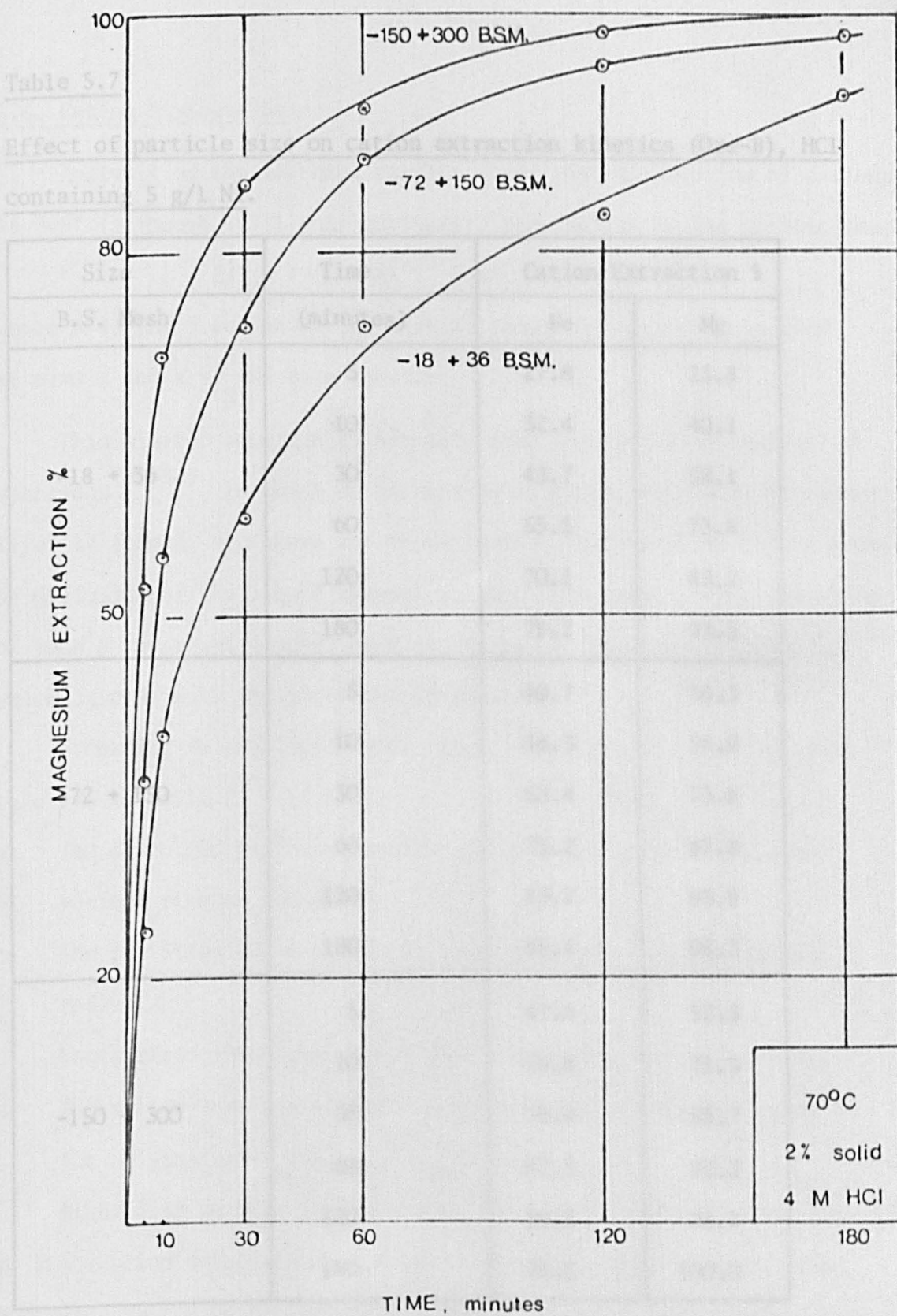


Fig. 5.15. Effect of particle size on magnesium extraction kinetics (ore -B), HCl containing 5 g/l Ni.

Table 5.7

Effect of particle size on cation extraction kinetics (Ore-B), HCl containing 5 g/l Ni.

Size	Time	Cation Extraction %	
B.S. Mesh	(minutes)	Fe	Mg
-18 + 36	5	27.8	23.8
	10	32.4	40.1
	30	43.7	58.1
	60	55.5	73.8
	120	70.1	83.2
	180	79.2	93.5
-72 + 150	5	40.7	36.3
	10	46.3	54.9
	30	63.4	73.8
	60	75.2	87.8
	120	83.2	95.9
	180	95.4	98.3
-150 + 300	5	47.6	52.5
	10	55.6	71.5
	30	76.4	85.7
	60	87.3	92.2
	120	96.5	98.4
	180	98.5	100.0

Conditions: 2% solid, 70°C, 4 mol/dm<sup>3</sup> HCl

### 5.5. Cation Dissolution

Analysis of the leaching results shows that dissolution of cations is best (although still only partially) represented by the kinetic law;

$$1 - \sqrt[3]{R} - (1 - R)^{2/3} = kt \quad \dots\dots (5.1)$$

where R is the fraction of the initial amount of cations dissolved at time t and k is the rate constant.

This kinetic equation is normally used for diffusion-controlled reactions<sup>(88-92)</sup>, in which an increasing thickness of reaction product layer is formed, and where the reaction rate is controlled by the rate of diffusion of the liquid reagent through this layer. The formation of such a layer was demonstrated in chapter 4 (see lump leaching), which agrees with the above interpretation.

According to the theory from which this model was derived, this rate law is valid<sup>(92)</sup> if:

- a) The dissolved reactant concentration at the unleached mineral surface remains constant.
- b) The particles are essentially spherical with the same initial radius.
- c) The surface roughness factor does not change during leaching.
- d) The silica reaction product occupies the same volume as that of the original silicate.

Figs. 5.16 to 5.20 show plots of the leaching results from Figs. 5.1 to 5.5 (cation dissolution in both media at different temperatures) according to the model (equation 5.1), which for convenience has been represented by  $\bar{R} \sqrt[3]{v/s t}$ . From these plots, one can see that nickel dissolution data in pure HCl (Fig. 5.16) at 25°C obeyed the equation



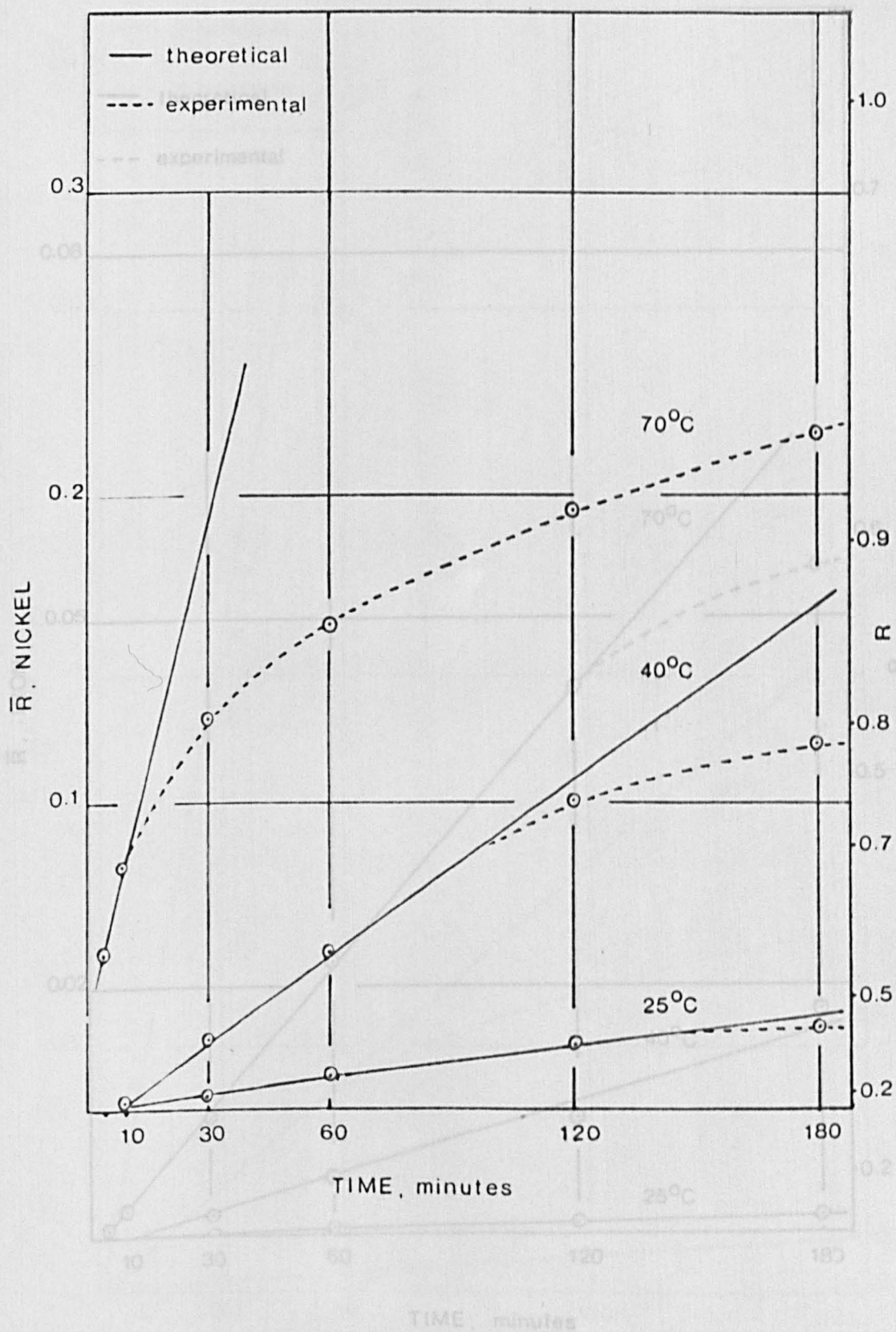


Fig. 5.16. Plot of  $\bar{R}$  v/s  $T$  for Nickel dissolved at different

temperatures  $\bar{R}$  (2 mol/dm<sup>3</sup> pure HCl).

temperatures (2 mol/dm<sup>3</sup> pure HCl).

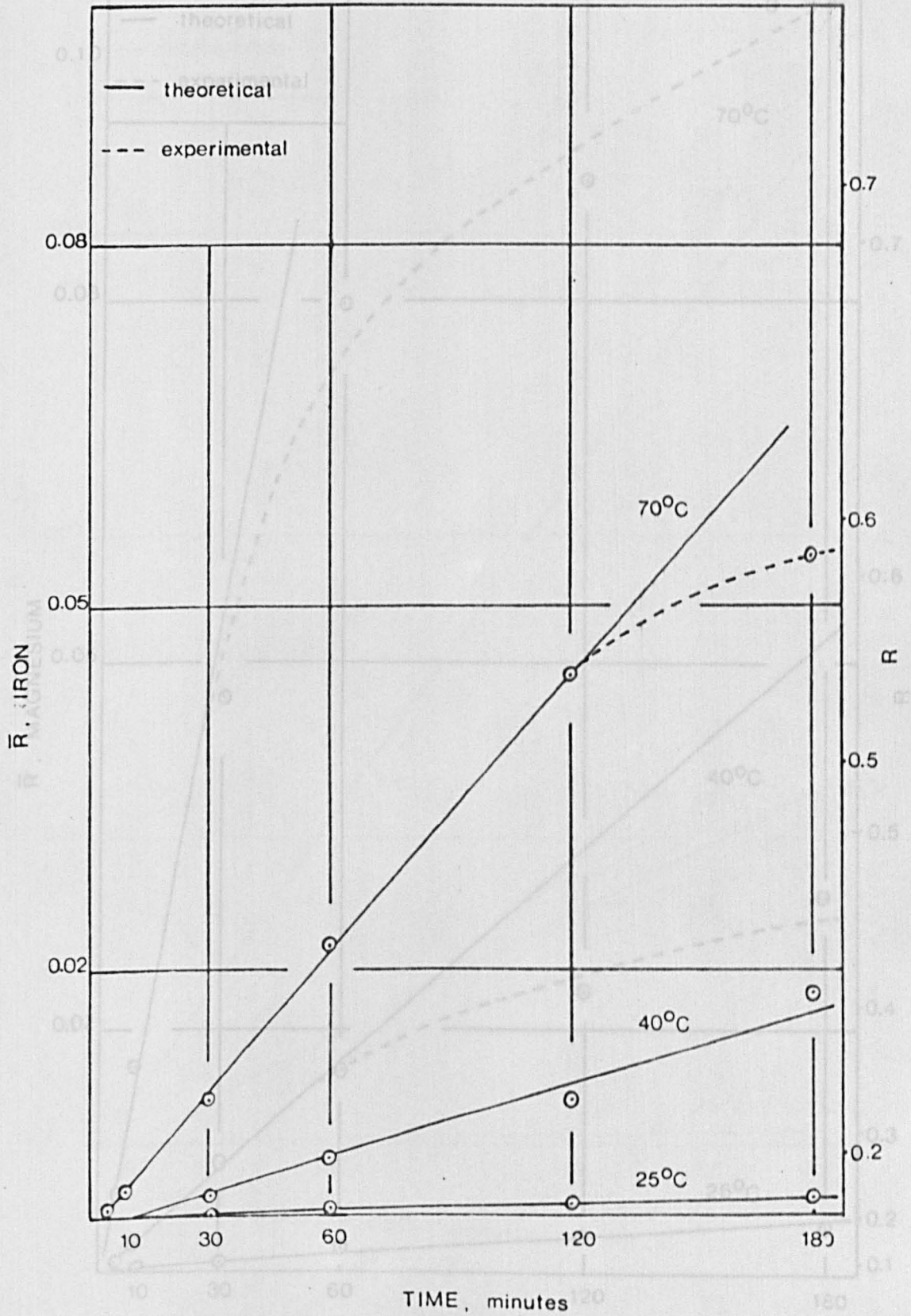


Fig. 5. 17. Plot of  $\bar{R}$  v/s T for iron dissolved at different temperatures ( 2 mol/dm<sup>3</sup> pure HCl ).



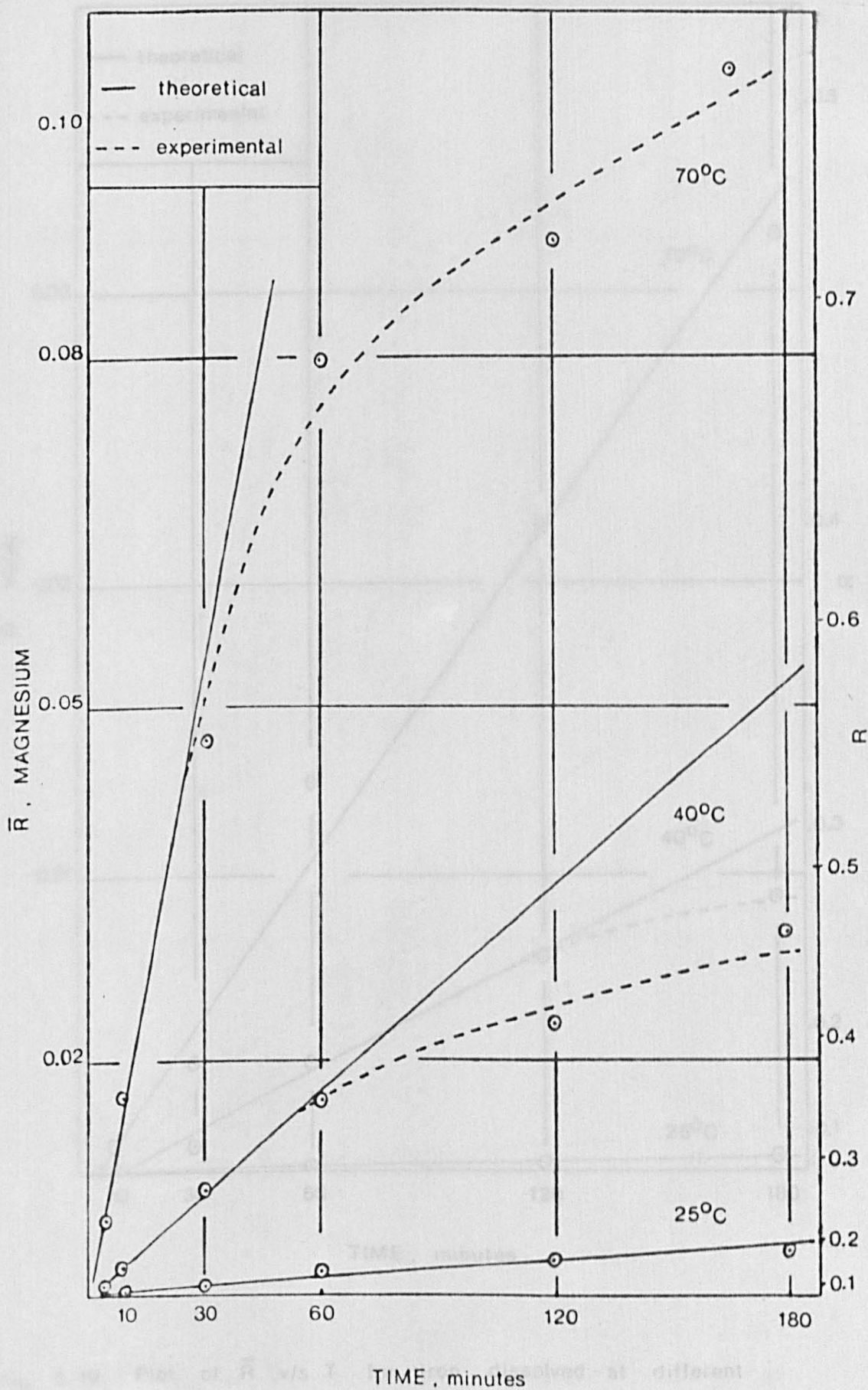


Fig. 5. 18. Plot of  $\bar{R}$  v/s T for magnesium dissolved at different temperatures (2 mol/dm<sup>3</sup> pure HCl).

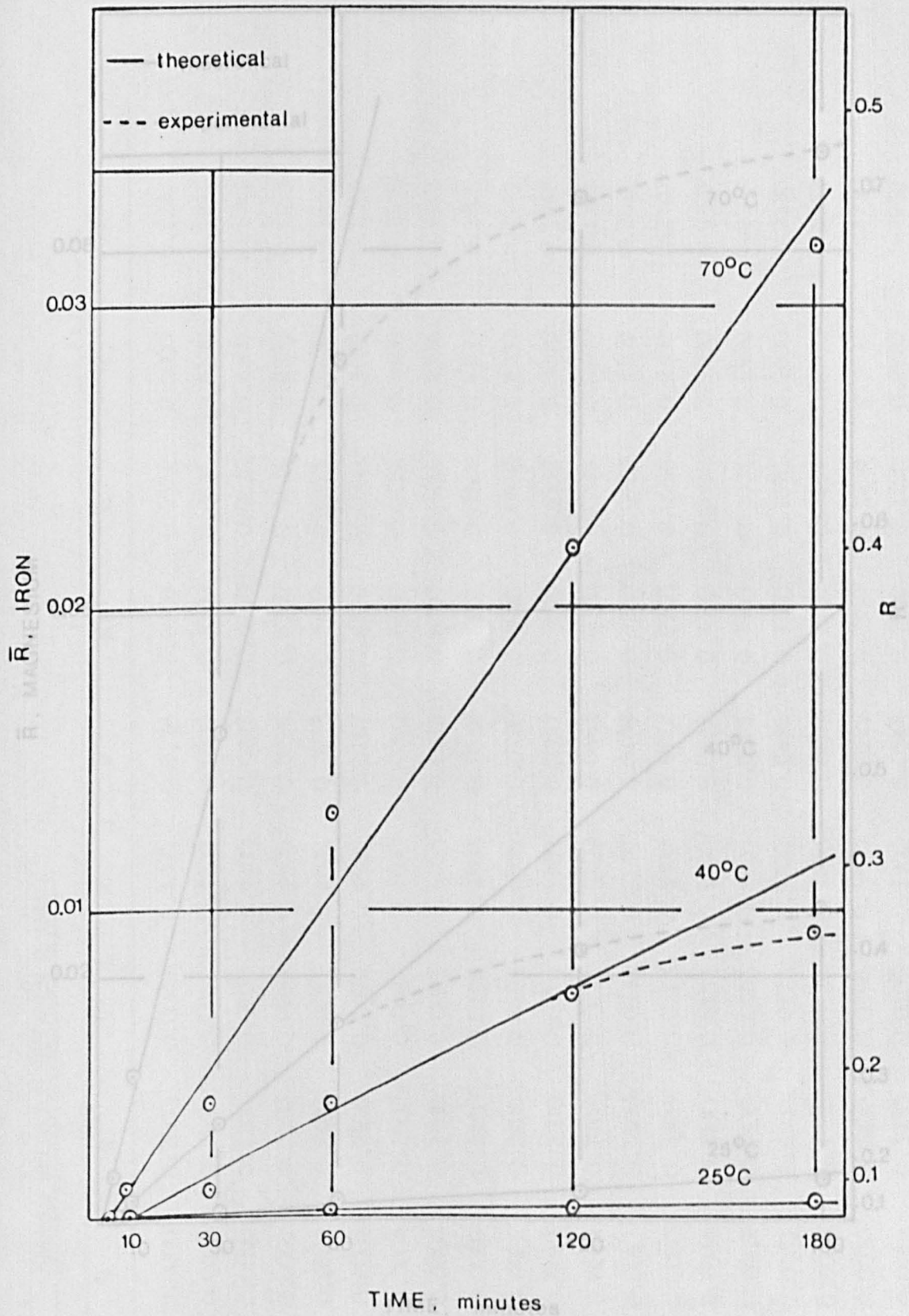


Fig. 5.19. Plot of  $\bar{R}$  vs  $T$  for iron dissolved at different temperatures ( $2 \text{ mol/dm}^3 \text{ HCl}$  containing  $5 \text{ g/l Ni}$ ).

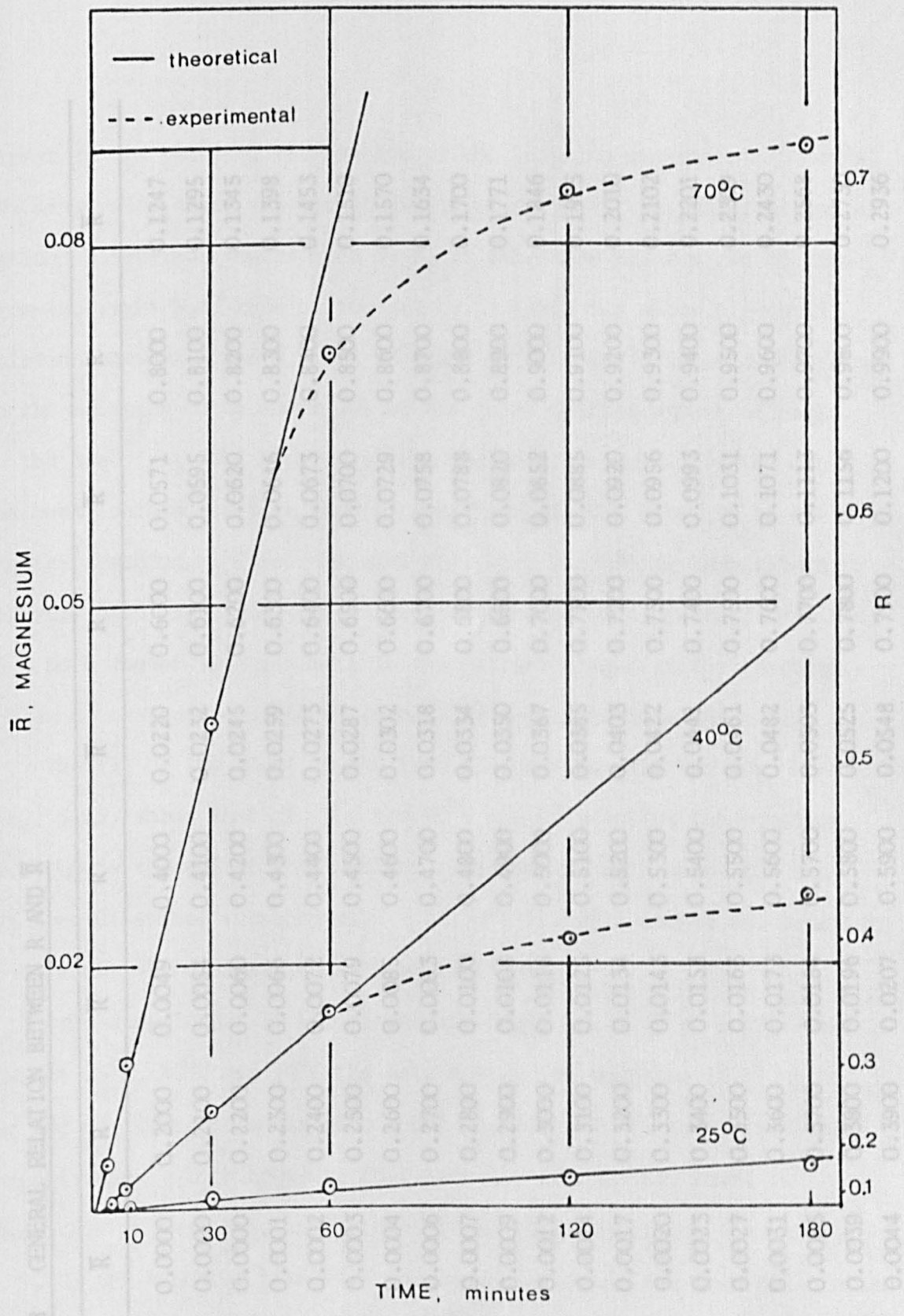


Fig. 5.20. Plot of  $\bar{R}$  v/s T for magnesium dissolved at different temperatures ( 2 mol/dm<sup>3</sup> HCl containing 5 g/l Ni),

TABLE 5.8 GENERAL RELATION BETWEEN R AND  $\bar{R}$

R	$\bar{R}$	R	$\bar{R}$	R	$\bar{R}$	R	$\bar{R}$	R	$\bar{R}$
0.0000	0.0000	0.2000	0.0049	0.4000	0.0220	0.6000	0.0571	0.8000	0.1247
0.0100	0.0000	0.2100	0.0054	0.4100	0.0232	0.6100	0.0595	0.8100	0.1295
0.0200	0.0000	0.2200	0.0060	0.4200	0.0245	0.6200	0.0620	0.8200	0.1345
0.0300	0.0001	0.2300	0.0066	0.4300	0.0259	0.6300	0.0646	0.8300	0.1398
0.0400	0.0002	0.2400	0.0072	0.4400	0.0273	0.6400	0.0673	0.8400	0.1453
0.0500	0.0003	0.2500	0.0079	0.4500	0.0287	0.6500	0.0700	0.8500	0.1510
0.0600	0.0004	0.2600	0.0085	0.4600	0.0302	0.6600	0.0729	0.8600	0.1570
0.0700	0.0006	0.2700	0.0093	0.4700	0.0318	0.6700	0.0758	0.8700	0.1634
0.0800	0.0007	0.2800	0.0100	0.4800	0.0334	0.6800	0.0788	0.8800	0.1700
0.0900	0.0009	0.2900	0.0108	0.4900	0.0350	0.6900	0.0820	0.8900	0.1771
0.1000	0.0012	0.3000	0.0116	0.5000	0.0367	0.7000	0.0852	0.9000	0.1846
0.1100	0.0014	0.3100	0.0125	0.5100	0.0385	0.7100	0.0885	0.9100	0.1925
0.1200	0.0017	0.3200	0.0134	0.5200	0.0403	0.7200	0.0920	0.9200	0.2010
0.1300	0.0020	0.3300	0.0143	0.5300	0.0422	0.7300	0.0956	0.9300	0.2102
0.1400	0.0023	0.3400	0.0153	0.5400	0.0441	0.7400	0.0993	0.9400	0.2201
0.1500	0.0027	0.3500	0.0163	0.5500	0.0461	0.7500	0.1031	0.9500	0.2309
0.1600	0.0031	0.3600	0.0173	0.5600	0.0482	0.7600	0.1071	0.9600	0.2430
0.1700	0.0035	0.3700	0.0184	0.5700	0.0503	0.7700	0.1113	0.9700	0.2568
0.1800	0.0039	0.3800	0.0196	0.5800	0.0525	0.7800	0.1156	0.9800	0.2730
0.1900	0.0044	0.3900	0.0207	0.5900	0.0548	0.7900	0.1200	0.9900	0.2936

almost to the point of termination of the leaching experiment (3 hours leaching) with about 40% nickel dissolved. (Note that the fraction of cations dissolved, represented by  $R$ , in all these figures can be read from the right hand side of the graph). Table 5.8 shows a general relation between  $R$  and  $\bar{R}$ . At 40°C and 70°C nickel dissolved according to the equation up to about 70% of the total initial amount of nickel in the ore. At 40°C departure from the model occurs after the ore has been leached for more than 1½ hours and at 70°C after 10 to 12 minutes leaching. This indicates that with increasing temperature, the rate acid attack on the silicate lattice becomes greater, resulting in a much higher reaction rate in the earlier stages of the reaction and as a consequence of this, an earlier departure from the model.

The fit of the model to the iron dissolution data for pure HCl (Fig. 5.17) shows that at 25°C and 40°C the data follow the equation (5.1) up to the end of the leaching experiments, with about 10% and 28% iron dissolved respectively. At 70°C the data obeyed the equation up to about 55% dissolution (2 hour leaching).

Iron dissolution in HCl containing 5 g/l Ni. (Fig. 5.19) shows that at 25°C, 40°C and 70°C the data mostly fit equation (5.1) up to the end of the experiments with about 7%, 27% and 47% iron dissolved respectively. Note however, that here the dissolution level is lower than in pure HCl, and perhaps if in the case of the leaching at 70°C, the leaching time were increased, allowing the iron dissolution to be increased up to about 60%, departure from the model would occur somewhere about 55%, as in the case of pure HCl.

The fit of the magnesium dissolution data to the model is very similar for both media (Fig. 5.18 and Fig. 5.20). At 25°C, the data



obeyed the equation up to the end of the experiment with about 17% magnesium dissolved (both media); at 40°C the model fits up to about 36% (pure HCl) and 35% (HCl containing 5 g/l Ni) after about 1 hour leaching in both cases; at 70°C the model fit up to 53% to 54% (pure HCl) and about 62% (HCl containing 5 g/l Ni) after 20-30 minutes leaching and 30 minutes leaching respectively.

In fact as illustrated by these plots (Figs. 5.16 to 5.20), for nickel (Fig. 5.16) the fit holds up to about  $R=0.7$ ; for iron (Figs. 5.17 and 5.19) perhaps up to  $R = 0.55$ ; and for magnesium (Figs. 5.18 and 5.20) to  $R = 0.4$ , or perhaps a little higher. The fit holds good for leaching times of up to 3 hours at 25°C, because dissolution is still very incomplete under these conditions.

These departures from the model can most probably be interpreted (13) as being caused mainly by the large range of particle sizes involved in each of these leaching experiments (see Table 5.1). This is because in samples such as these, where the smaller particles require a shorter leaching time for complete reaction, it is obvious that when increasing the temperature, the reaction rate is much faster in the earlier stages of the reaction than in the later stages, and, as a consequence of this, there is an earlier departure from the model. In the earlier stages of the reaction, most of the smaller particles are completely reacted, whilst the larger particles are only partially reacted, and clearly in the later stages of the reaction, the reaction rate slows down because there are only the larger particles still reacting.

From this, one can see that as with temperature, particle size should also have a marked effect on the rate of cation dissolution. To evaluate this effect, samples of ore were leached at specific size fractions (-18 + 36, -72 + 150 and -150 + 300 B.S.M.) in 4 mol/dm<sup>3</sup> acid concentration (both acid media) at 70°C. Plots of these leaching results according to the model are given in Figs. 5.21 to 5.25, where it is clearly shown that the smaller the particle size of the fraction, the faster the rate of cation dissolution. As illustrated by Figs. 5.21 to 5.23 (pure HCl) chemical dissolution data obeyed the model perhaps up to about 92%, 84% and 79% of the total initial amount of nickel, iron and magnesium respectively, and in Figs. 5.24 and 5.25 (HCl containing 5 g/l Ni) perhaps up to about 79% and 77% for iron and magnesium respectively. Note that in all these graphs, extrapolation of the linear rate plots to zero time, shows positive intercepts with the ordinate axes. This has also been generally observed in acid dissolution studies of phyllosilicate<sup>(93)</sup> where it was explained in terms of ultra rapid removal of broken-bond cations and of the rapid dissolution of small particles. Similar results were also obtained by G.J. Ross (1967) during the study of acid dissolution of an orthochlorite mineral<sup>(94)</sup>. From these graphs, one can see that these chemical dissolution data fit the model much better than the data from the leaching with a particle size distribution as shown in Table 5.1. This is because the rate of dissolution is more homogenous, corresponding to a relatively discrete size distribution. However, despite this improved fit, departure from the model still occurs when the percentages of cation dissolved are above 92% nickel, 84% iron and



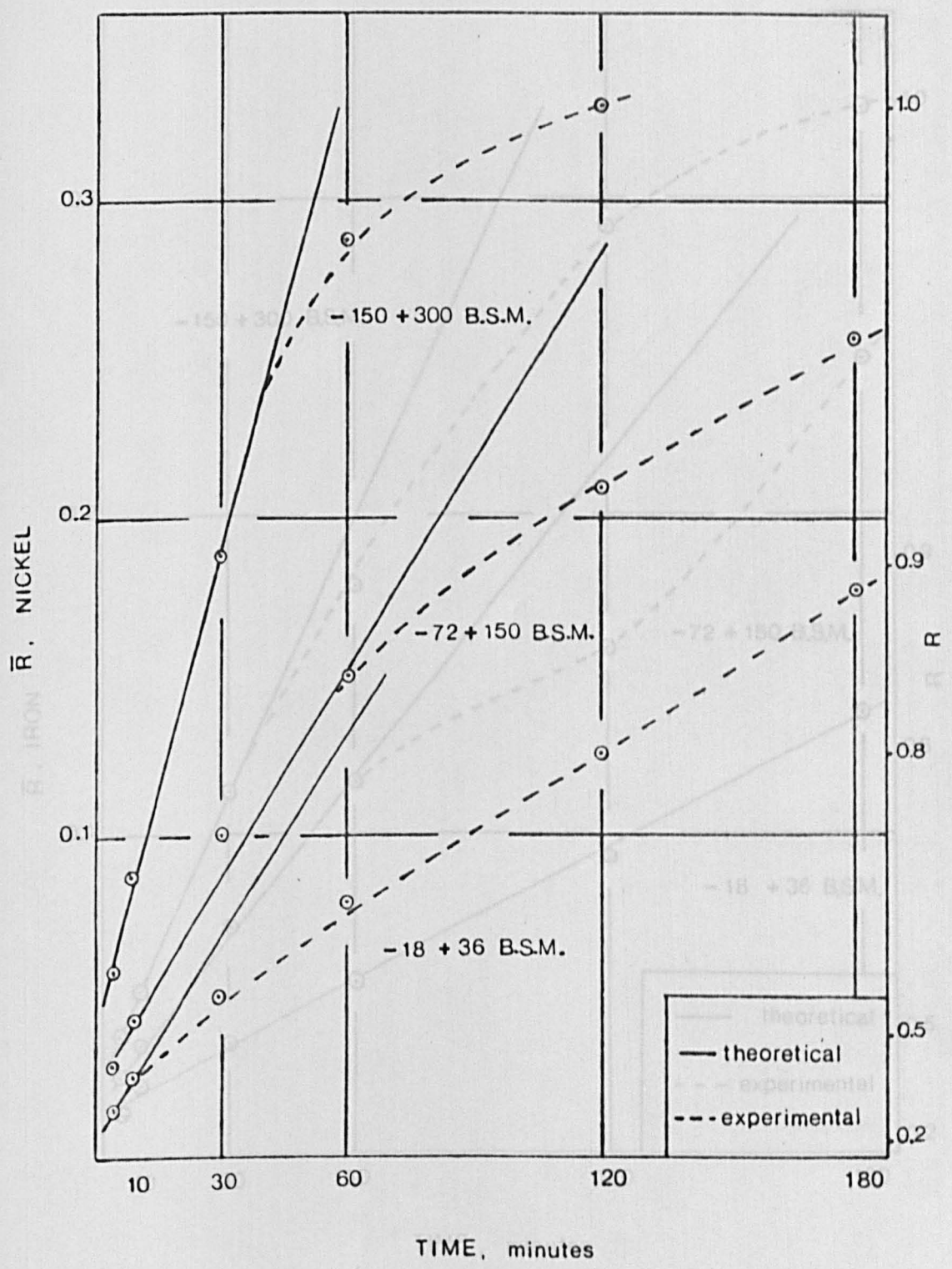


Fig. 5. 21. Plot of  $\bar{R}$  v/s  $T$  for nickel dissolved at  $70^{\circ}\text{C}$  in  $4 \text{ mol/dm}^3$  pure HCl for different specific size fractions.

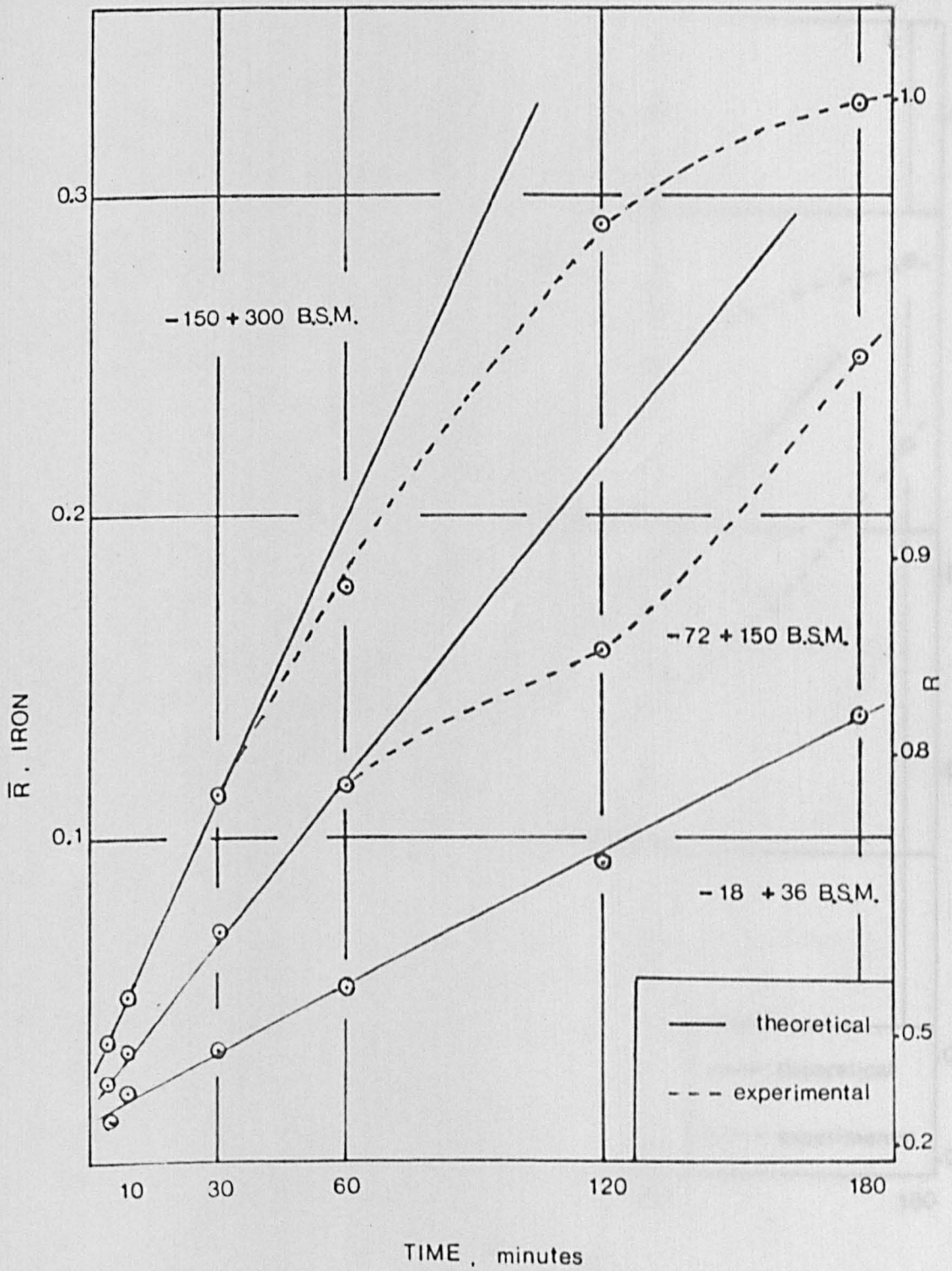


Fig. 5.22. Plot of  $\bar{R}$  v/s  $T$  for iron dissolved at  $70^{\circ}\text{C}$  in  $4 \text{ mol/dm}^3$  pure HCl for different specific size fractions.

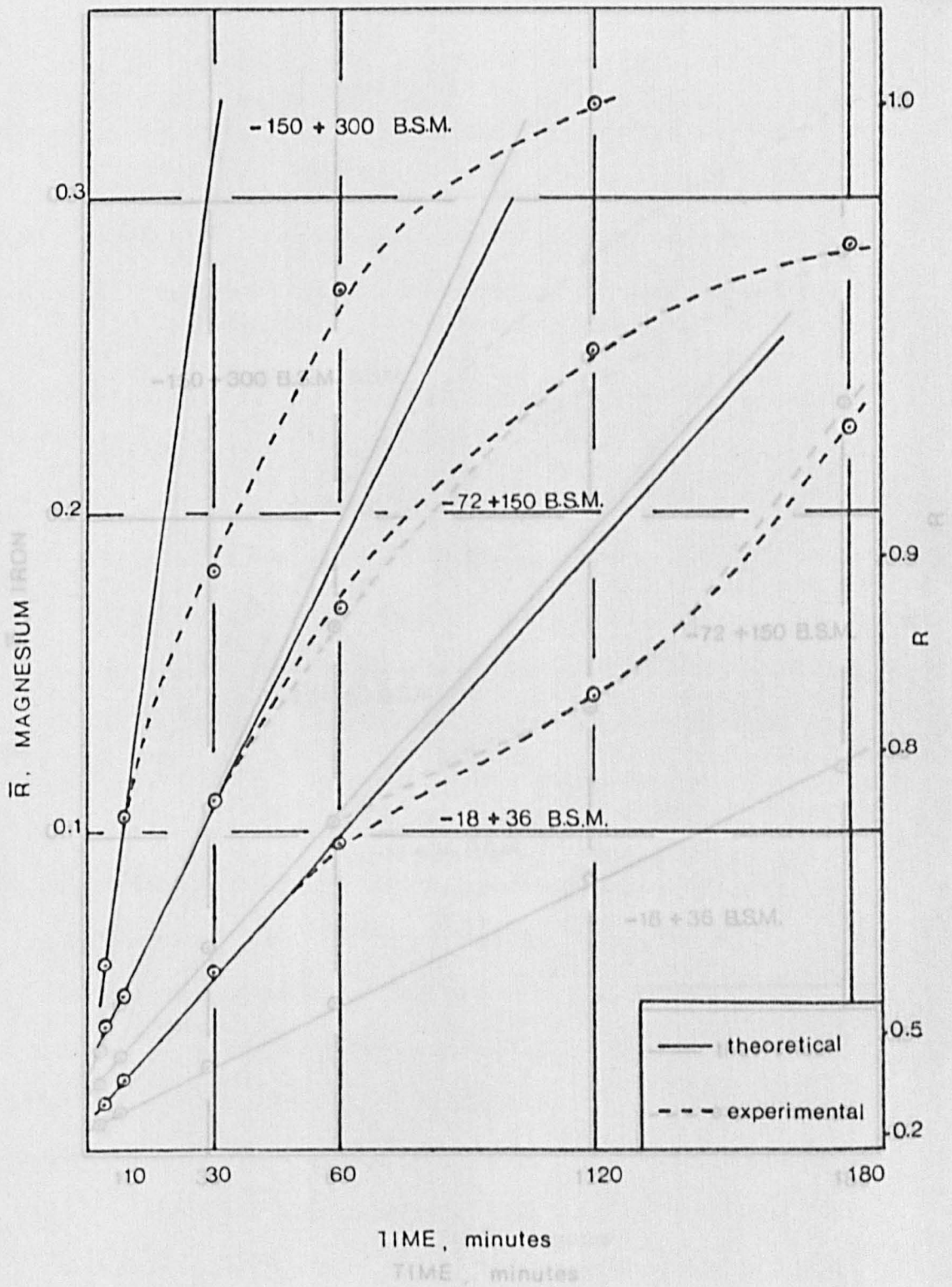


Fig. 5. 23. Plot of  $\bar{R}$  v/s T for magnesium dissolved at 70°C in  $4 \text{ mol/dm}^3$  pure HCl for different specific size fractions.



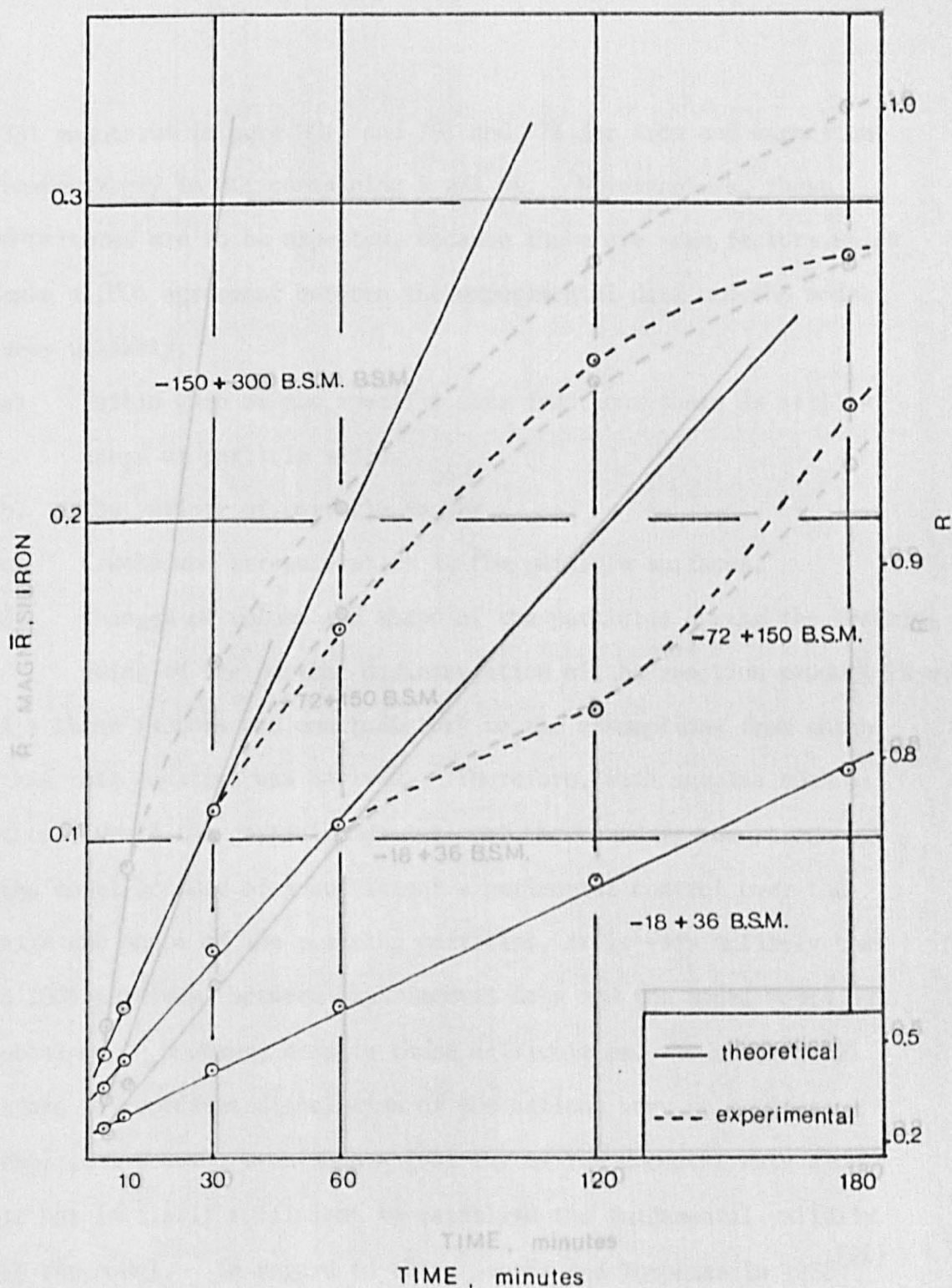


Fig. 5.25. Plot of  $\bar{R}$  v/s  $T$  for magnesium dissolved at  $70^{\circ}\text{C}$  in  $4 \text{ mol/dm}^3$  HCl (containing  $5 \text{ g/l Ni}$ ) for different specific size fractions.  
 Fig. 5.24. Plot of  $\bar{R}$  v/s  $T$  for iron dissolved at  $70^{\circ}\text{C}$  in  $4 \text{ mol/dm}^3$  HCl (containing  $5 \text{ g/l Ni}$ ) for different specific size fractions.

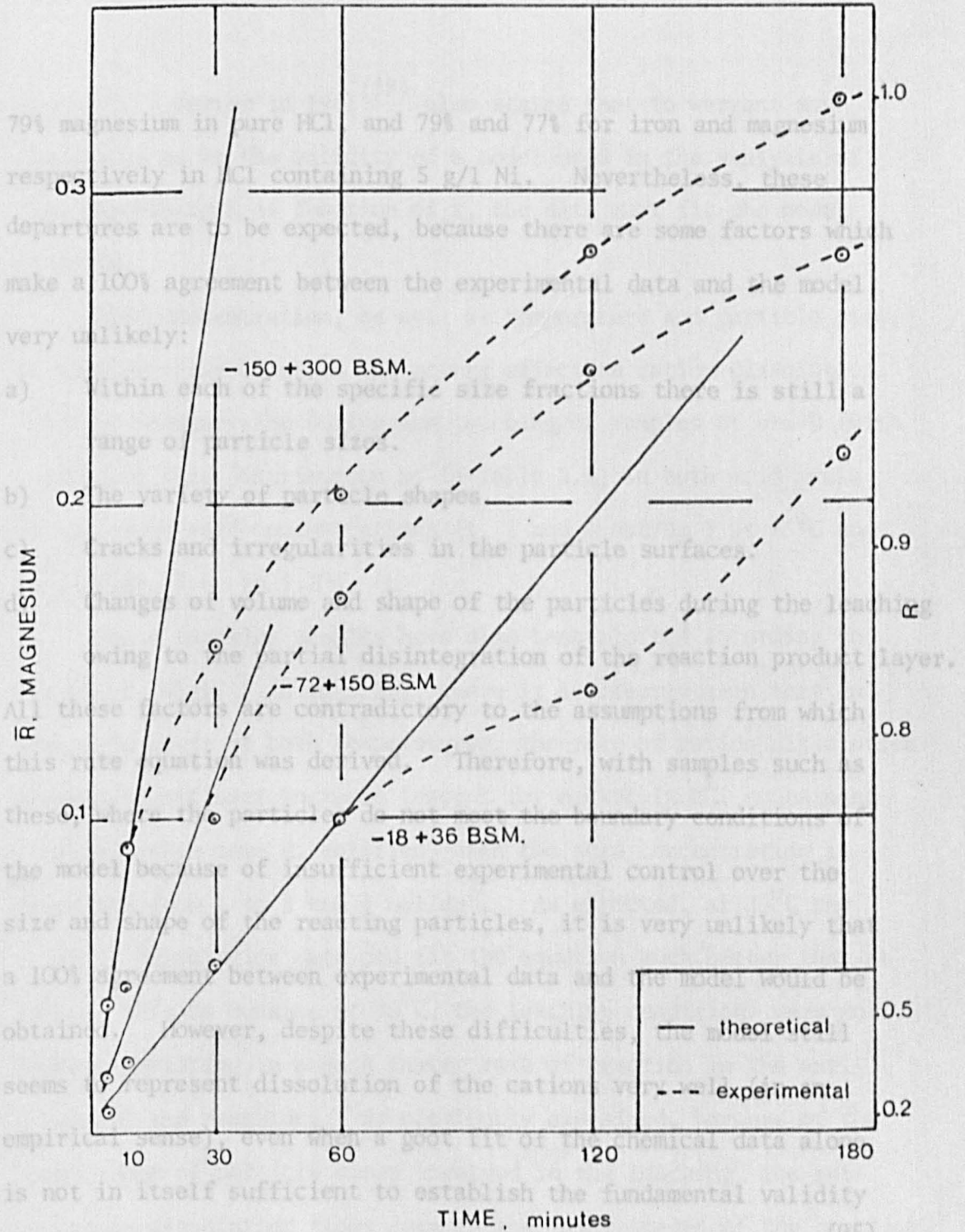


Fig. 5.25. Plot of  $\bar{R}$  v/s  $T$  for magnesium dissolved at  $70^{\circ}\text{C}$  in  $4 \text{ mol/dm}^3 \text{ HCl}$  (containing  $5 \text{ g/l Ni}$ ) for different specific size fractions.

79% magnesium in pure HCl, and 79% and 77% for iron and magnesium respectively in HCl containing 5 g/l Ni. Nevertheless, these departures are to be expected, because there are some factors which make a 100% agreement between the experimental data and the model very unlikely:

- a) Within each of the specific size fractions there is still a range of particle sizes.
- b) The variety of particle shapes.
- c) Cracks and irregularities in the particle surfaces.
- d) Changes of volume and shape of the particles during the leaching owing to the partial disintegration of the reaction product layer.

All these factors are contradictory to the assumptions from which this rate equation was derived. Therefore, with samples such as these, where the particles do not meet the boundary conditions of the model because of insufficient experimental control over the size and shape of the reacting particles, it is very unlikely that a 100% agreement between experimental data and the model would be obtained. However, despite these difficulties, the model still seems to represent dissolution of the cations very well (in an empirical sense), even when a good fit of the chemical data alone is not in itself sufficient to establish the fundamental validity of the model. In regard to this, Jacobs and Tompkins in 1955<sup>(95)</sup> have pointed out that agreement between experimental results and rate equations (expressing  $R$  as a function of  $t$  and deduced theoretically) does not necessarily establish the validity of the model from which the equations are derived, and that other information about the reactions in addition to  $R$  versus  $t$  data may sometimes be

required. Carter in 1961<sup>(88)</sup> also states that to warrant any conclusion as to the validity of a model used in the analysis of data expressing R as function of t, the data must fit the model to 100%R.

Acid concentration, as well as temperature and particle size, is another variable which has strong effect on cation dissolution. This was demonstrated during the leaching of samples of ore-B (with a particle size distribution as in Table 5.1) in both acid media at different acid concentrations (1, 2 and 4 mol/dm<sup>3</sup>) at 25°C and 70°C (Figs. 5.6 to 5.10).

These leaching results have also been plotted according to the model (Figs. 5.26 to 5.35), where it is clearly seen that in both acid media at both temperatures, the rate of cation dissolution shows a significant increase (except for nickel in HCl containing 5 g/l Ni, with zero dissolution) when the acid concentration is increased from 1 to 2 and 4 mol/dm<sup>3</sup>. As expected, at 25°C the chemical dissolution data did fit the equation much better than at 70°C. This is because at 70°C, the leaching conditions were more severe, resulting in a much faster rate of reaction in the early stages of the reaction; as previously explained, because of the large range of particle sizes involved in the leaching, the rate of cation dissolution slows down in the later stages of the reaction, causing the departure from the model. Further discussion of the fitting of these chemical dissolution data to the model will not be attempted in order to avoid undue repetition, but once again the model holds only at lower R values, and any factor speeding up the reaction rate leads to a departure from linearity which is earlier



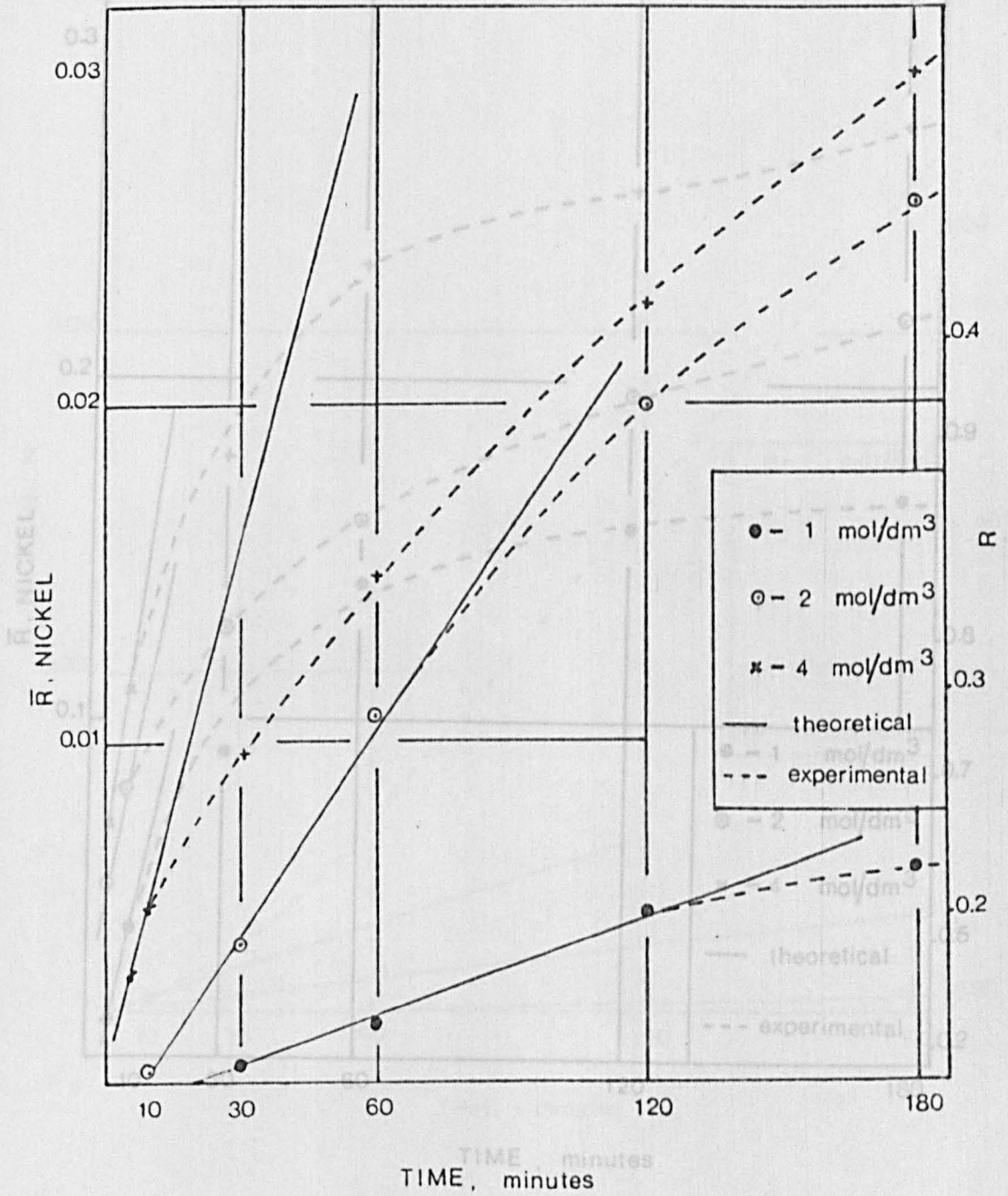


Fig. 5. 26. Plot of  $\bar{R}$  v/s T for nickel dissolved at 25°C at different

acid concentrations (pure HCl).

Fig. 5. 27. Plot of  $\bar{R}$  v/s T for nickel dissolved at 70°C at different

acid concentrations (pure HCl).

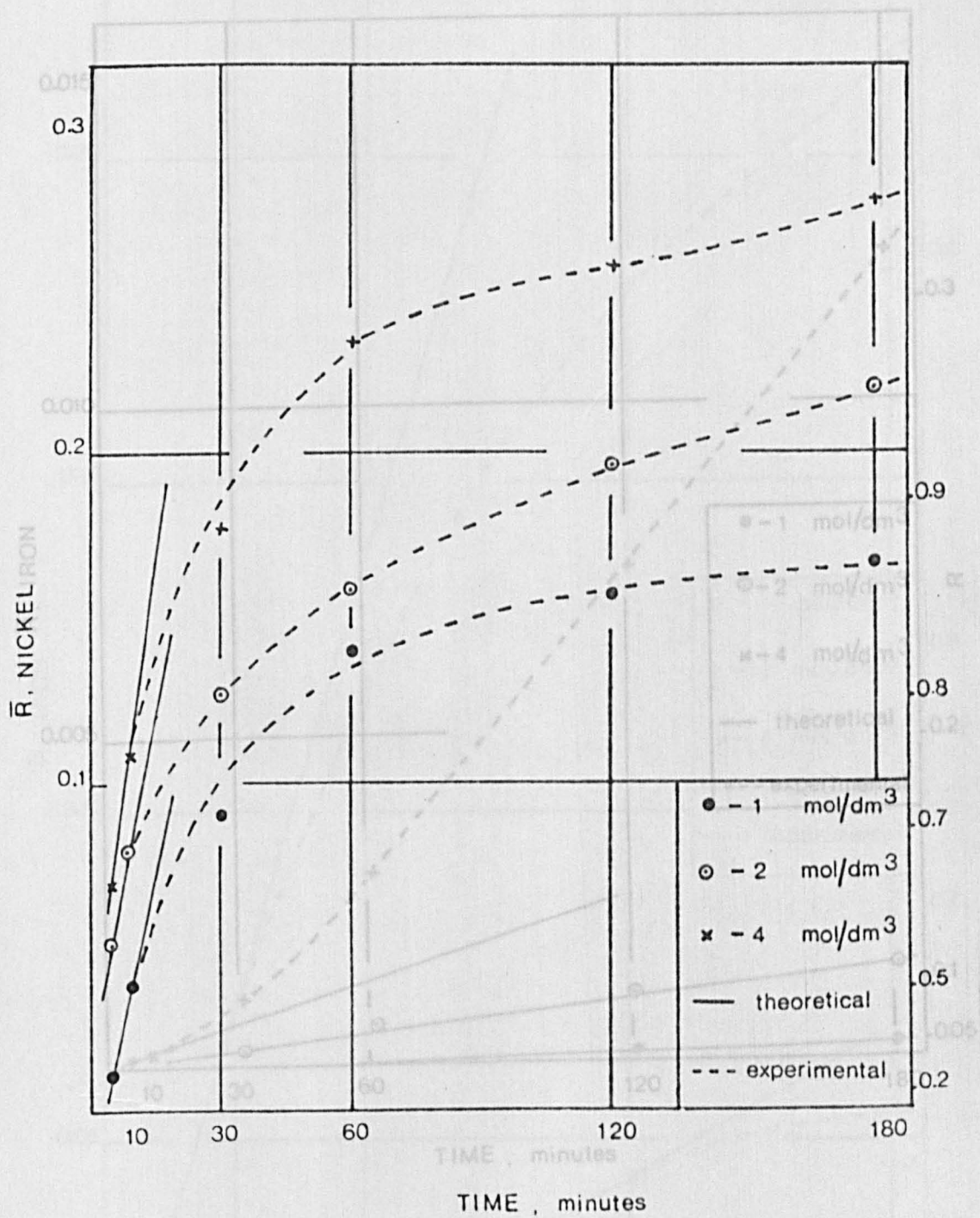


Fig. 5.27. Plot of  $\bar{R}$  v/s  $T$  for nickel dissolved at 70°C at different acid concentrations (pure HCl).

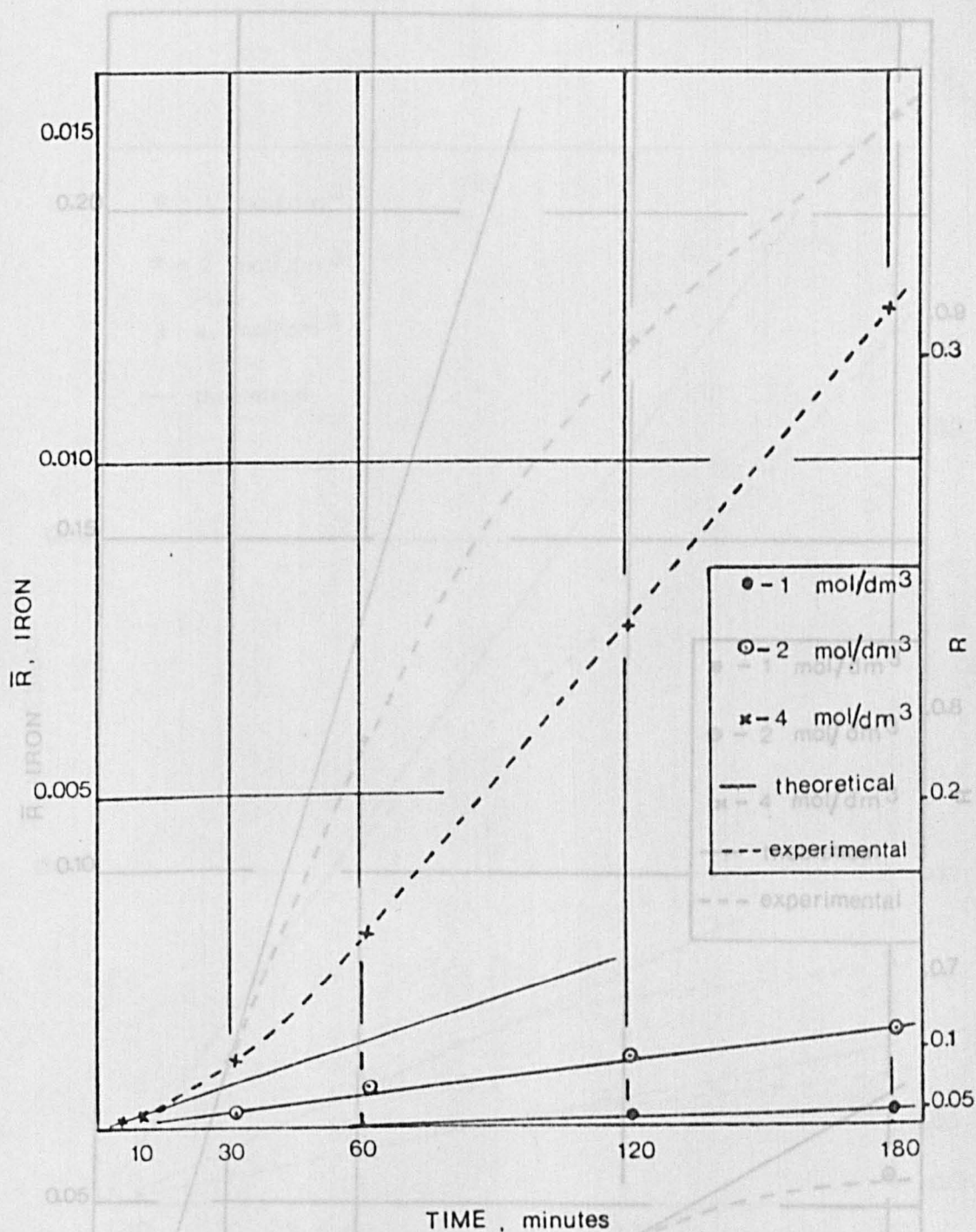


Fig. 5.28. Plot of  $\bar{R}$  v/s T for iron dissolved at  $25^\circ\text{C}$  at different acid concentrations (pure HCl).

Fig. 5.29. Plot of  $\bar{R}$  v/s T for iron dissolved at  $70^\circ\text{C}$  at different acid concentrations (pure HCl).



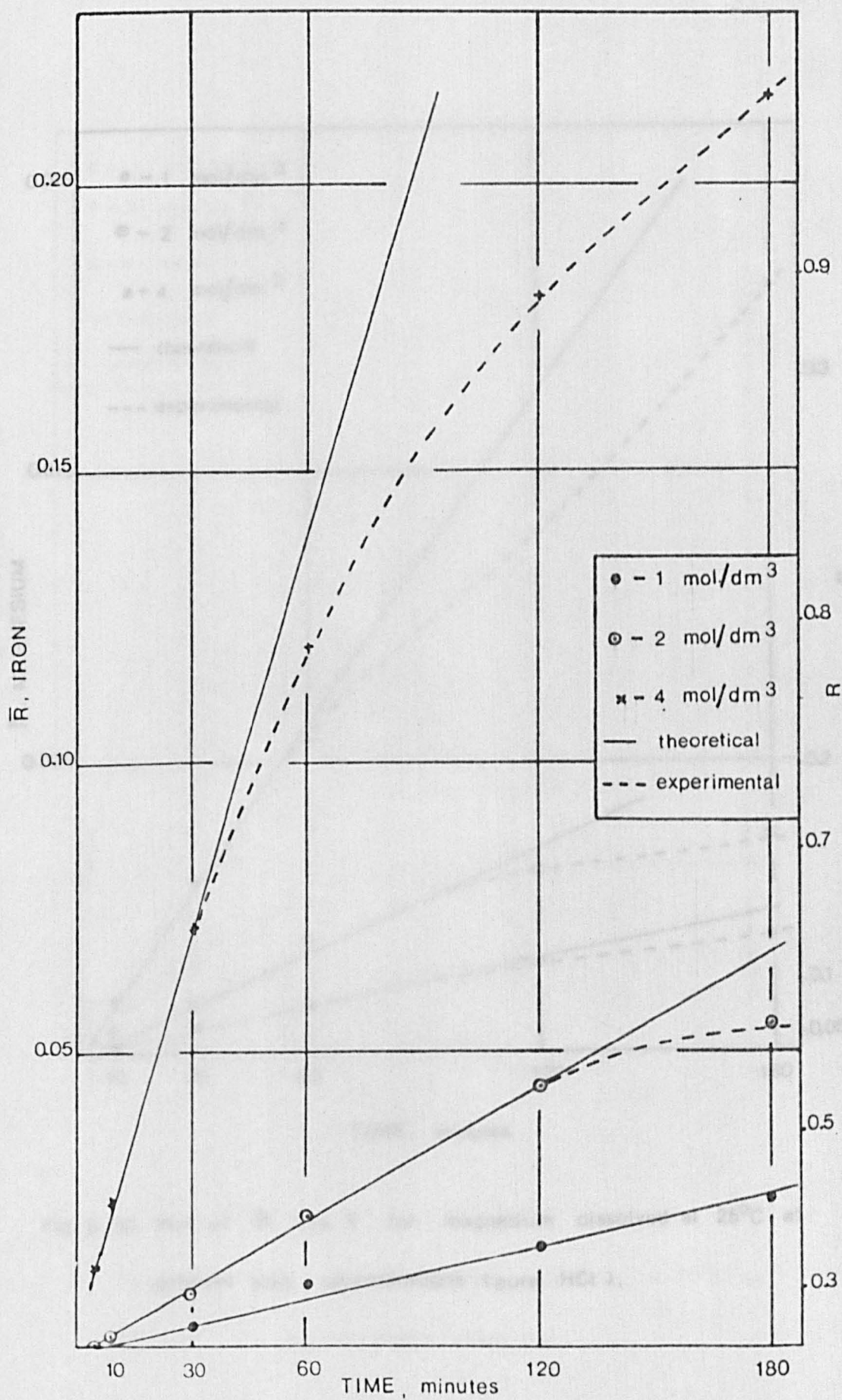


Fig. 5.29. Plot of  $\bar{R}$  v/s T for iron dissolved at 70°C at different acid concentrations (pure HCl).

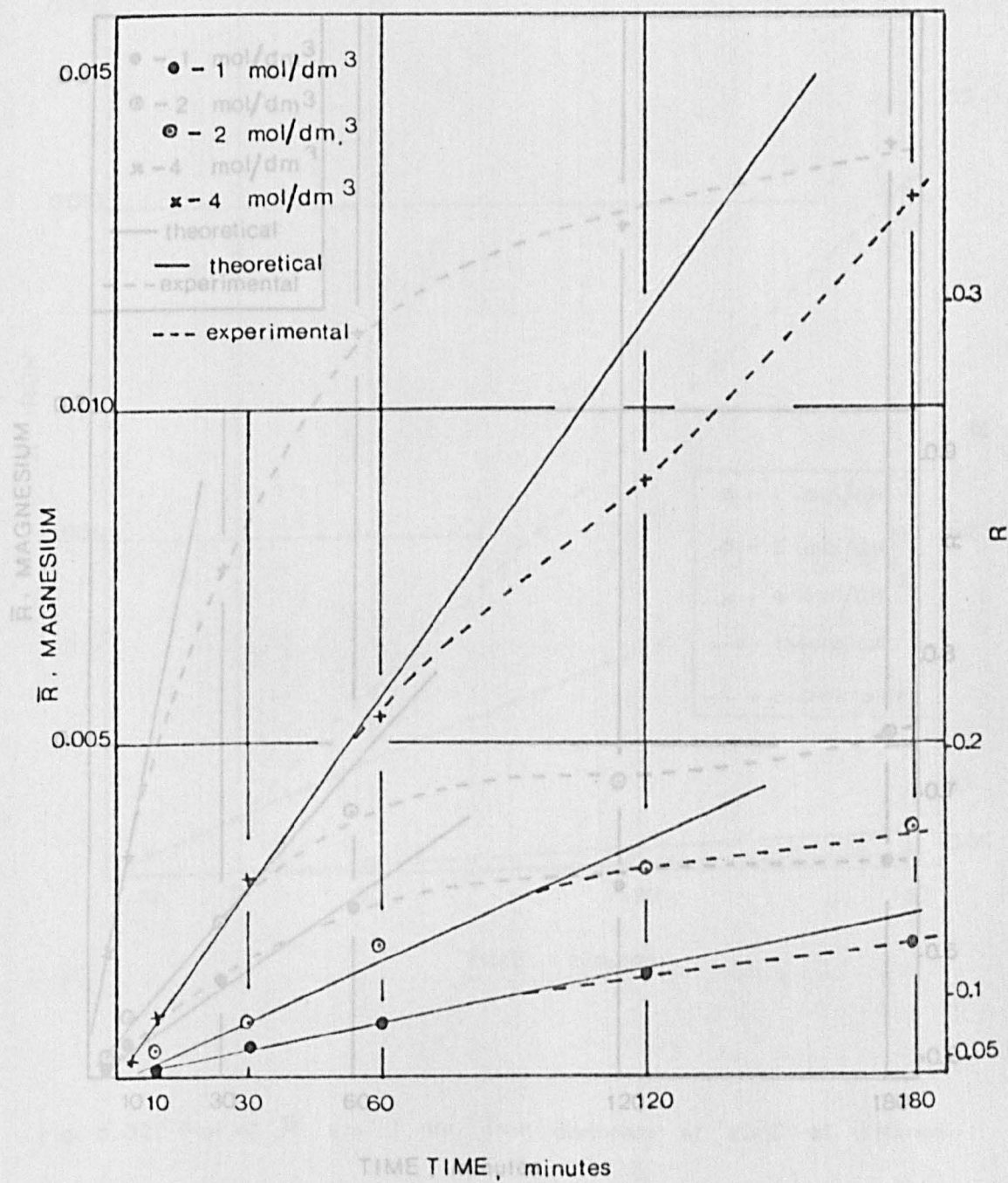


Fig. 5. 30. Plot of  $\bar{R}$  v/s  $T$  for magnesium dissolved at  $25^\circ\text{C}$  at

different acid concentrations (pure HCl).

Fig. 5. 31. Plot of  $\bar{R}$  v/s  $T$  for magnesium dissolved at  $70^\circ\text{C}$  at

different acid concentrations (pure HCl).

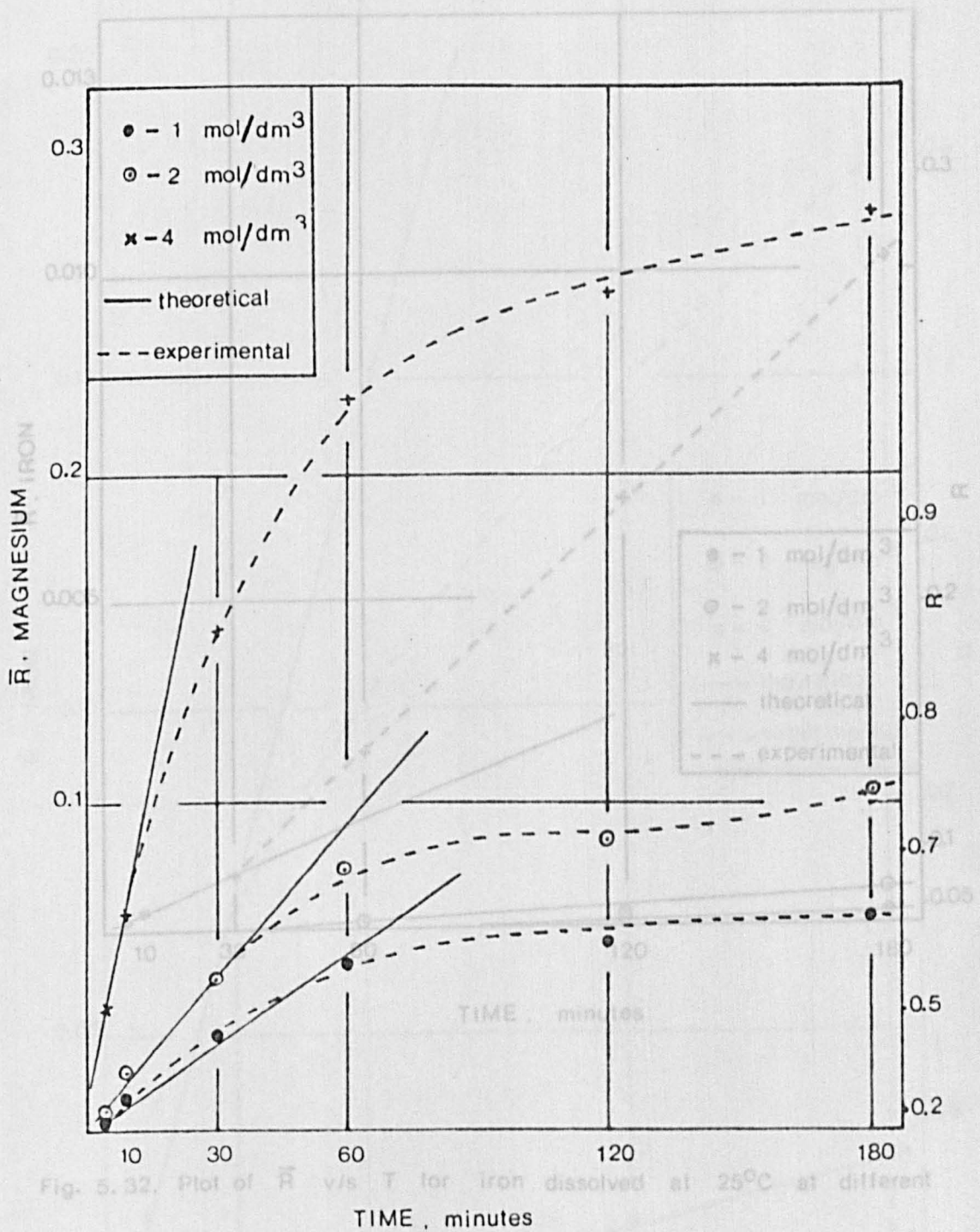


Fig. 5.32. Plot of  $\bar{R}$  v/s  $T$  for iron dissolved at 25°C at different acid concentrations (HCl containing 5 g/l Ni).

Fig. 5.31. Plot of  $\bar{R}$  v/s  $T$  for magnesium dissolved at 70°C at different acid concentrations (pure HCl).



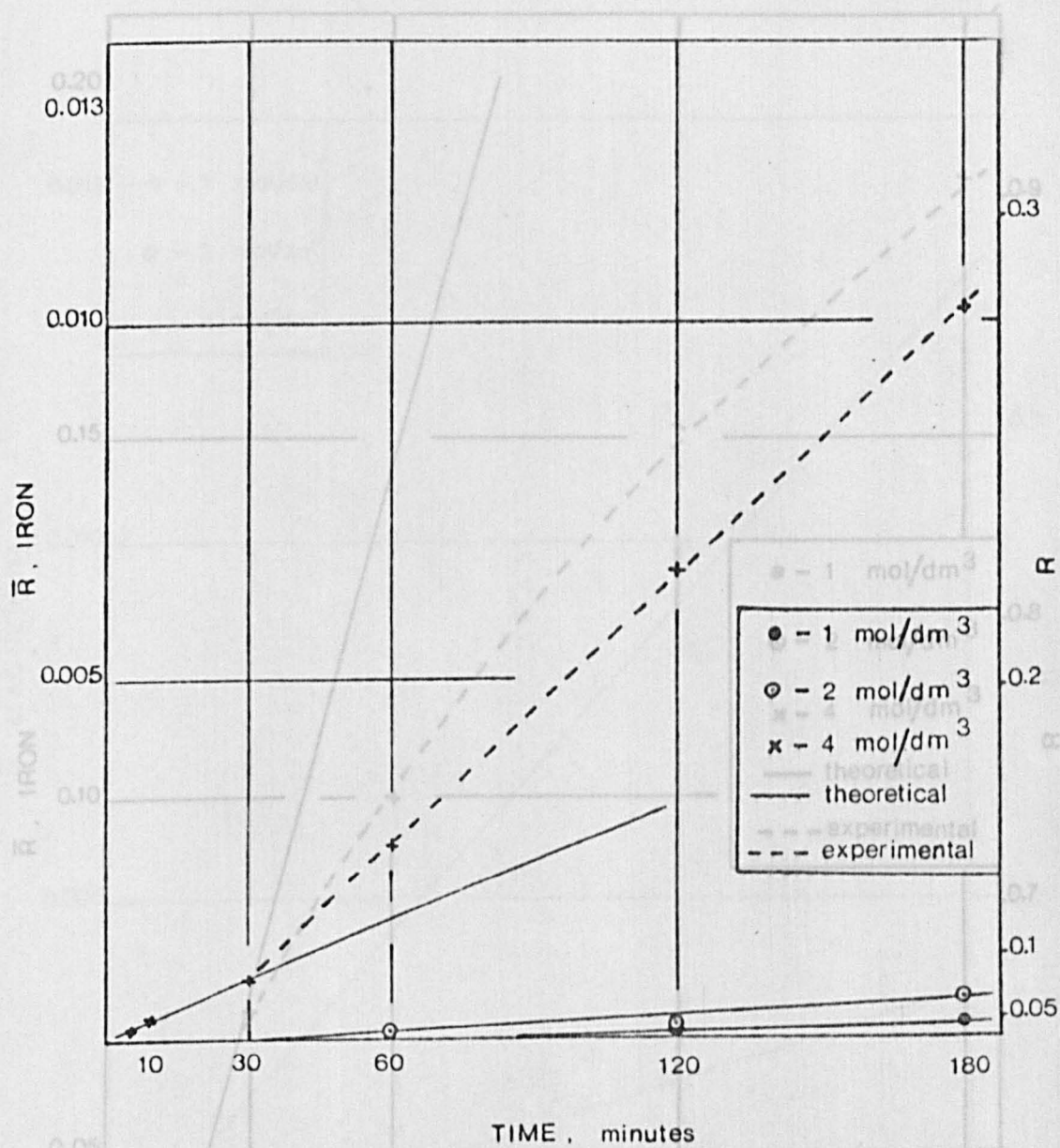


Fig. 5.32. Plot of  $\bar{R}$  v/s  $T$  for iron dissolved at  $25^{\circ}\text{C}$  at different acid concentrations (HCl containing 5 g/l Ni).

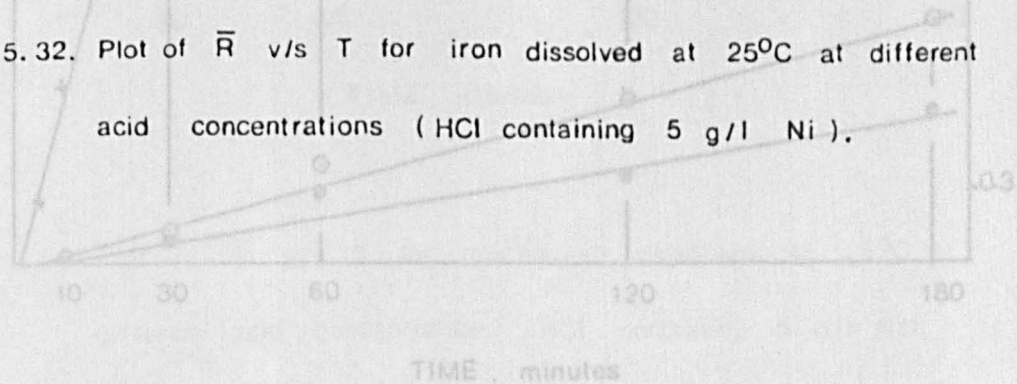


Fig. 5.33. Plot of  $\bar{R}$  v/s  $T$  for iron dissolved at  $70^{\circ}\text{C}$  at different acid concentrations (HCl containing 5 g/l Ni).



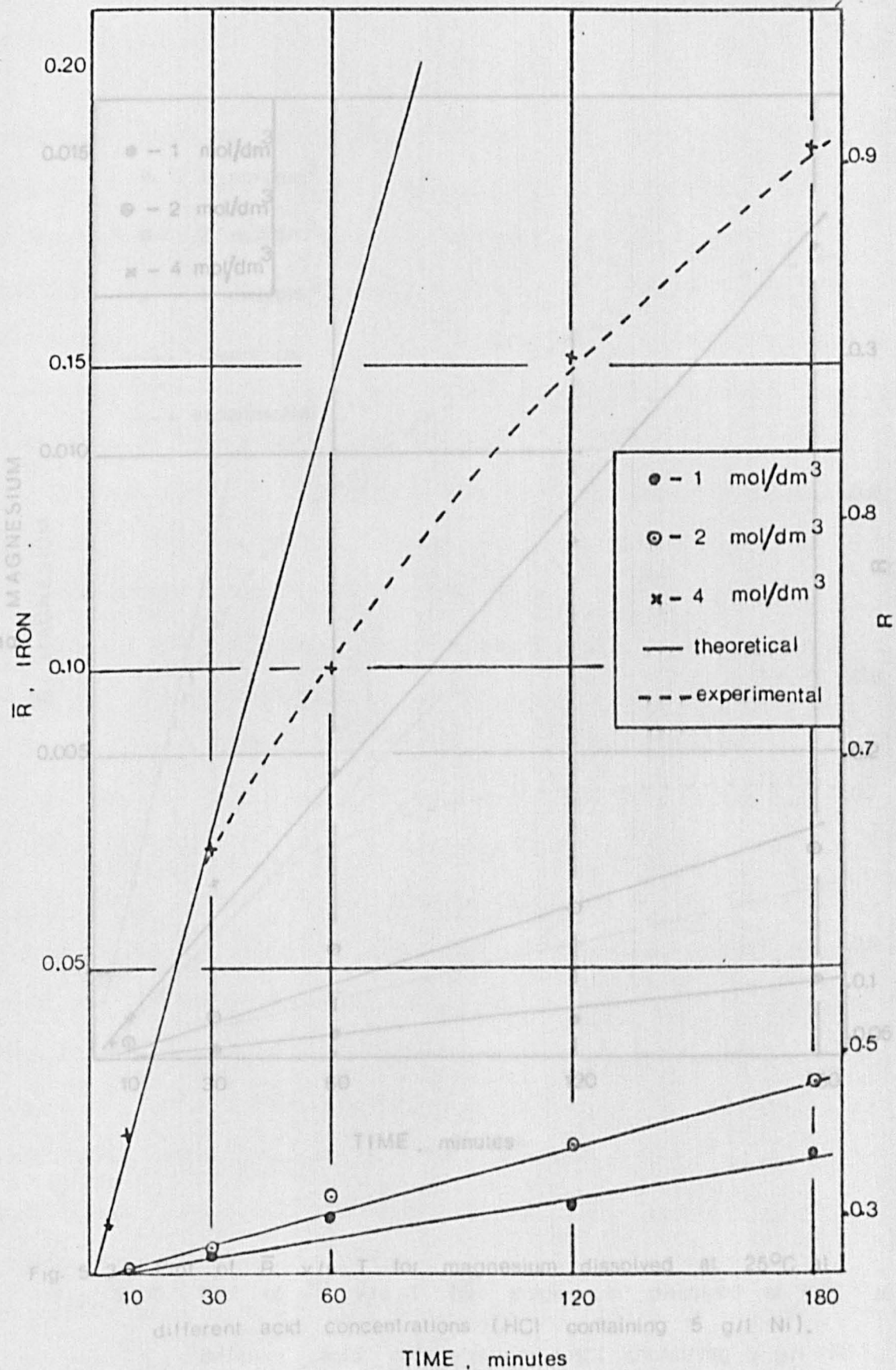


Fig. 5.33. Plot of  $\bar{R}$  v/s T for iron dissolved at 70°C at different acid concentrations (HCl containing 5 g/l Ni).

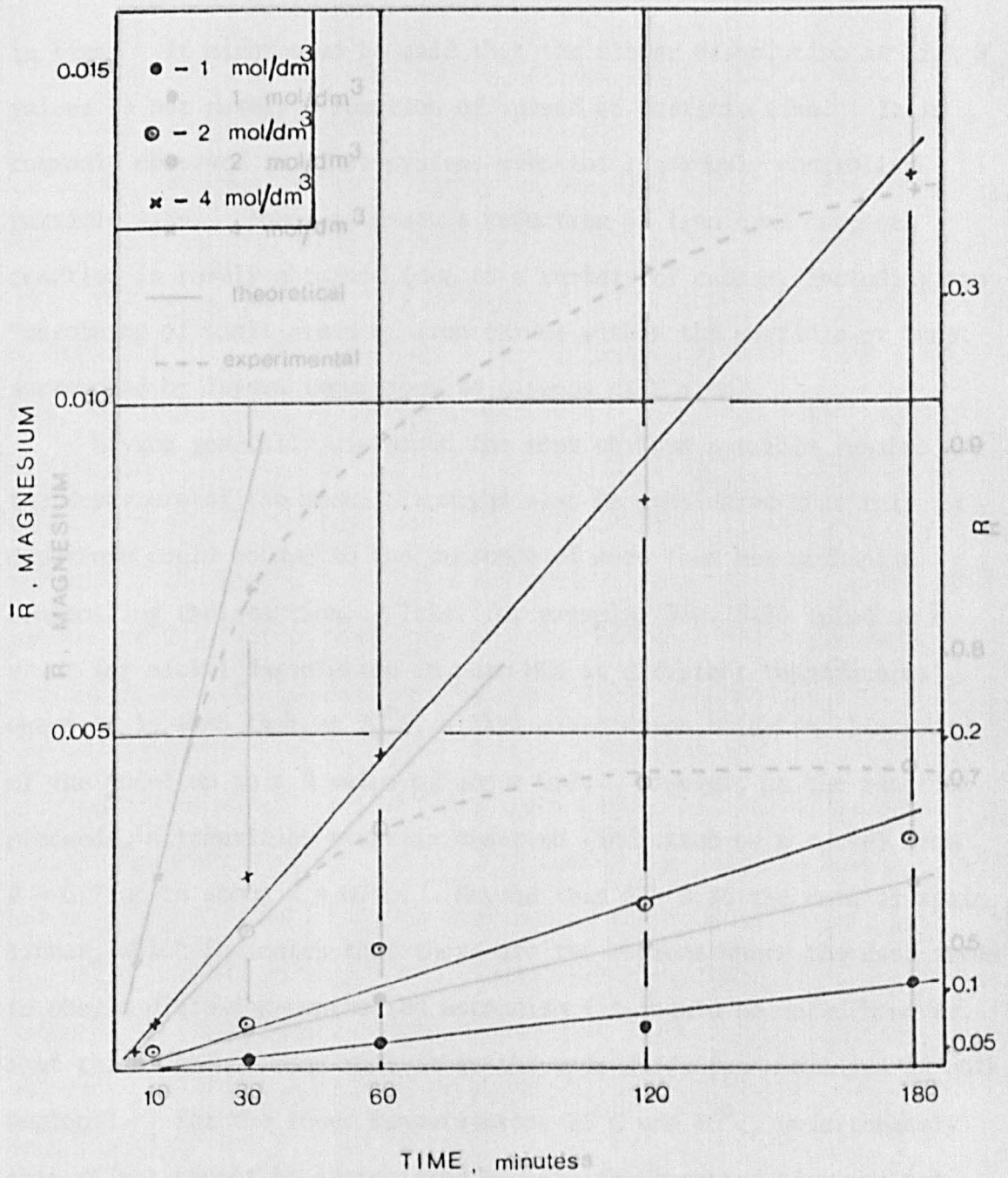


Fig. 5.34. Plot of  $\bar{R}$  v/s T for magnesium dissolved at 25°C at

Fig. 5.35. Plot of  $\bar{R}$  v/s T for magnesium dissolved at 70°C at

different acid concentrations (HCl containing 5 g/l Ni).

different acid concentrations (HCl containing 5 g/l Ni).

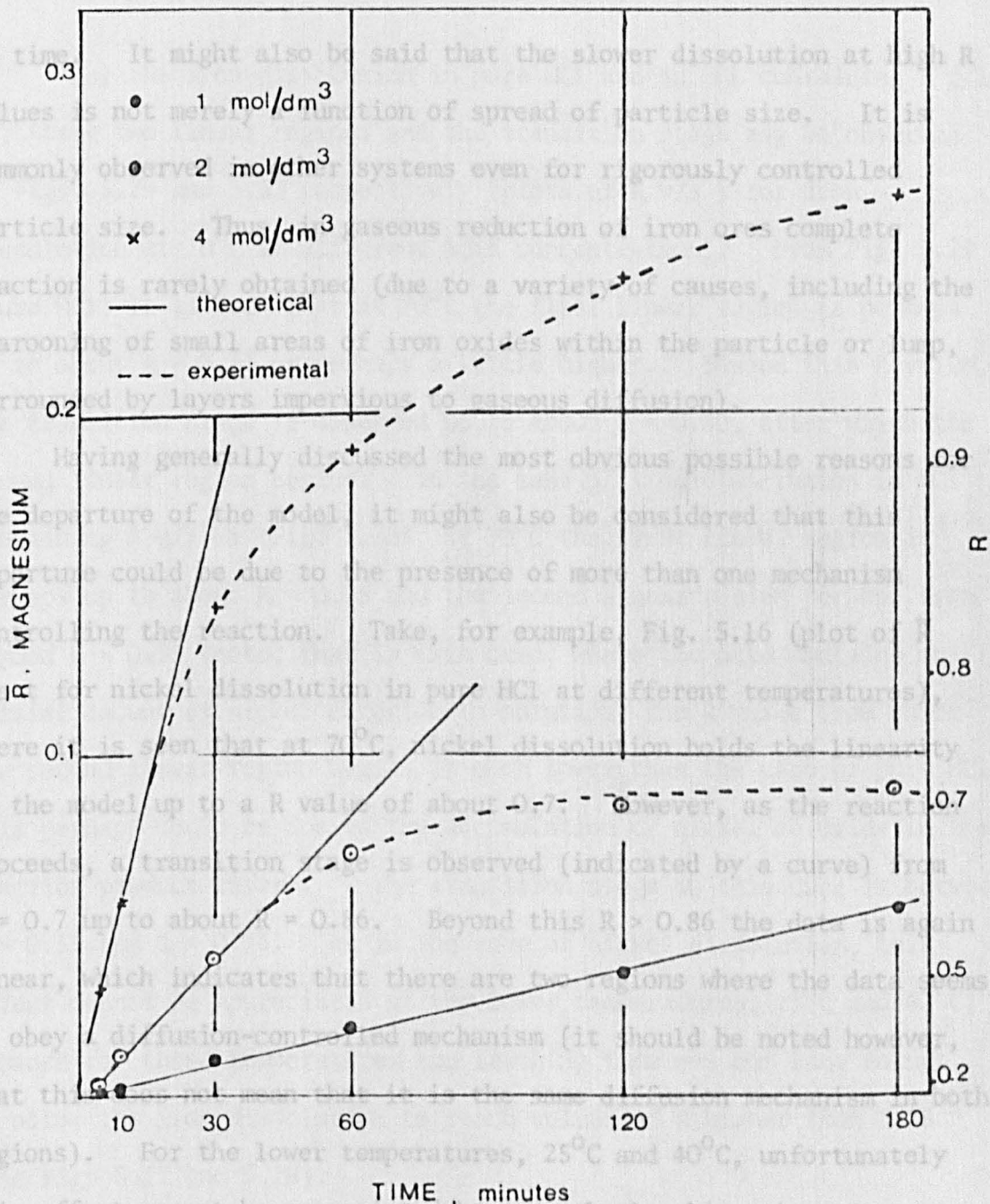


Fig. 5.35. Plot of  $\bar{R}$  v/s T for magnesium dissolved at 70°C at different acid concentrations (HCl containing 5. g/l Ni).

in time. It might also be said that the slower dissolution at high  $R$  values is not merely a function of spread of particle size. It is commonly observed in other systems even for rigorously controlled particle size. Thus, in gaseous reduction of iron ores complete reaction is rarely obtained (due to a variety of causes, including the "marooning of small areas of iron oxides within the particle or lump, surrounded by layers impervious to gaseous diffusion).

Having generally discussed the most obvious possible reasons for the departure of the model, it might also be considered that this departure could be due to the presence of more than one mechanism controlling the reaction. Take, for example, Fig. 5.16 (plot of  $\bar{R}$  v/s  $t$  for nickel dissolution in pure HCl at different temperatures), where it is seen that at  $70^{\circ}\text{C}$ , nickel dissolution holds the linearity of the model up to a  $R$  value of about 0.7. However, as the reaction proceeds, a transition stage is observed (indicated by a curve) from  $R = 0.7$  up to about  $R = 0.86$ . Beyond this  $R > 0.86$  the data is again linear, which indicates that there are two regions where the data seems to obey a diffusion-controlled mechanism (it should be noted however, that this does not mean that it is the same diffusion mechanism in both regions). For the lower temperatures,  $25^{\circ}\text{C}$  and  $40^{\circ}\text{C}$ , unfortunately this effect cannot be appreciated because the leaching time was not long enough to achieve  $R$  values higher than 0.7. Another figure, perhaps showing a better picture of these two linear regions and the transition stage in the nickel dissolution is Fig. 5.27 (plot  $\bar{R}$  v/s  $t$  for nickel dissolution at  $70^{\circ}\text{C}$  at different acid concentrations).



For the iron dissolution in pure HCl and in HCl containing 5 g/l Ni, these two linear regions and the transition stage may be observed in Figs. 5.29 and 5.33 respectively (plots of  $\bar{R} v/s t$  for iron dissolution at 70°C at different acid concentration). From Fig. 5.29 (pure HCl) it is seen that at 70°C the first linear region is perhaps up to about  $R = 0.55$  or perhaps a little higher. Beyond this  $R$  value, the transition stage is observed up to about  $R = 0.89$ , after which the second linear region begins. In the case of iron dissolution in HCl containing 5 g/l Ni (Fig. 5.33), at 70°C the first linear region is perhaps up to about  $R = 0.55$  and the second linear region perhaps from beyond  $R = 0.75$  (note, that in this case, where the acid contains an initial amount of nickel chloride in solution, the  $R$  value from which the second linear region begins is much lower than the case of pure HCl, this perhaps could be due to the accumulation of nickel chloride in the reaction product layer). The transition stage in this case is between  $R = 0.55$  and  $R = 0.75$ . As in the case of nickel dissolution, this effect cannot be appreciated at the lower temperatures, 25°C and 40°C, because for these temperatures the leaching time was not long enough to allow the iron dissolution to reach values of  $R$  higher than 0.55 (see Figs 5.17 and 5.19).

For magnesium dissolution, these two linear regions and the transition stage, may be observed at 40°C and 70°C in both acid media from Figs. 5.18 and 5.20 (plots of  $\bar{R} v/s t$  for magnesium dissolution at different temperatures). From these, it is seen that in both acid media at 40°C and 70°C, the first linear region occurs up to about  $R = 0.36$ . Beyond this point however, the transition stage and the second linear region are completely different for both temperatures. At 40°C

the transition stage (both acid media) seems to be from  $R = 0.36$  up to about  $R = 0.38$ , whilst at  $70^{\circ}\text{C}$  it seems to be from  $R = 0.36$  up to about  $R = 0.7$ . Thus, the second linear region seems to begin at  $R = 0.38$  for  $40^{\circ}\text{C}$  and  $R = 0.7$  for  $70^{\circ}\text{C}$ . The reason for this, unfortunately, is not understood. A similar behaviour can be observed for the magnesium dissolution at  $70^{\circ}\text{C}$  at different acid concentrations (see Figs. 5.31 and 5.35).

Although the evidence of the presence of these two diffusion mechanism during the cation dissolution is still not very clear, it should be mentioned that L.W. Strong<sup>(13)</sup> reported a similar conclusion during the kinetic study of acid dissolution (pure HCl) of a lateritic nickel ore (a silicate ore from Salomon Island). Luce<sup>(96)</sup> also reached similar conclusions using diluted acid to leach silica and magnesium from hydrated magnesium silicates. Because of the similarity in the leaching conditions and type of silicate ore used by Strong in his study with those leaching conditions and type of silicate ore used in this research, it was considered worthwhile to give some details of Strong's approach for the determination of the mechanism controlling the reaction and also to replot his data (included in appendix I) according to the model discussed here.

In order to determine the mechanism controlling the reaction, Strong quoted that the reaction mechanism can often be determined by plotting the fraction of reaction completed (defined by Strong as  $\alpha$ , which corresponds to  $R$  in this research) against some function of time and that for diffusion controlled reactions the data is normally plotted against the square root of time (in other words by using the well known parabolic law generally applied for one-dimensional diffusion process



with constant diffusion coefficient<sup>(89)</sup>). According to this, Strong plotted his kinetic data (from leaching experiments dealing with specific size fraction, -85 + 170 mesh) in terms of  $\alpha$  versus  $(T^{1/2})$ , illustrated in Figs. 5.36 and 5.37. From these plots Strong commented and concluded:

- a) "For nickel at low temperatures, where  $\alpha < 0.3$  all the points lie on a single straight line. The lines become steeper (i.e. the reaction rate increases) as the temperature and acid concentration of acid increases. As the reaction proceeds a transition stage is reached. Beyond this,  $\alpha > 0.86$ , the data is again linear".
- b) "There are two distinct regions where the data obeys a diffusion mechanism. The initial reaction rate is much faster than that in the later stages of extraction. The transition between these two stages varies for each cation,  $\alpha$  values for nickel are 0.6 - 0.8, and for magnesium, 0.5 - 0.6. The transition stage is much less distinct for iron, but is about an  $\alpha$  value of 0.3"
- c) "Differentiation between alternative diffusion mechanism is impossible since there are difficulties in assigning the cation to either specific lattice position or to impurities".

Strong also provides an Arrhenius plot, illustrated in Fig. 5.38, from which the activation energies for these cation could be obtained. These were:

Nickel	6.38	Kilojoule/mole
Iron	1.43	Kilojoule/mole
Magnesium	3.92	Kilojoule/mole

which certainly agree with the activation energy which characterizes

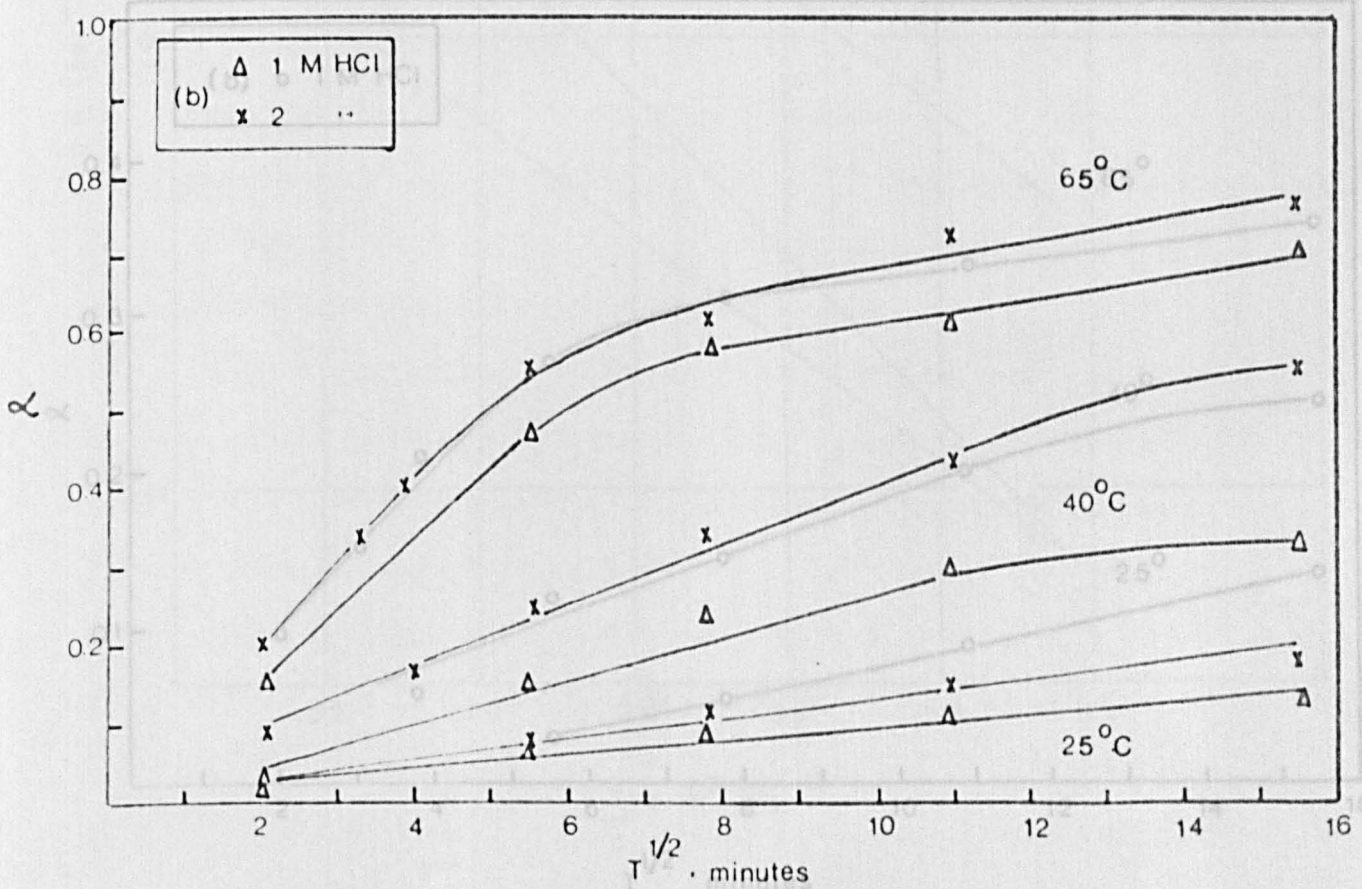
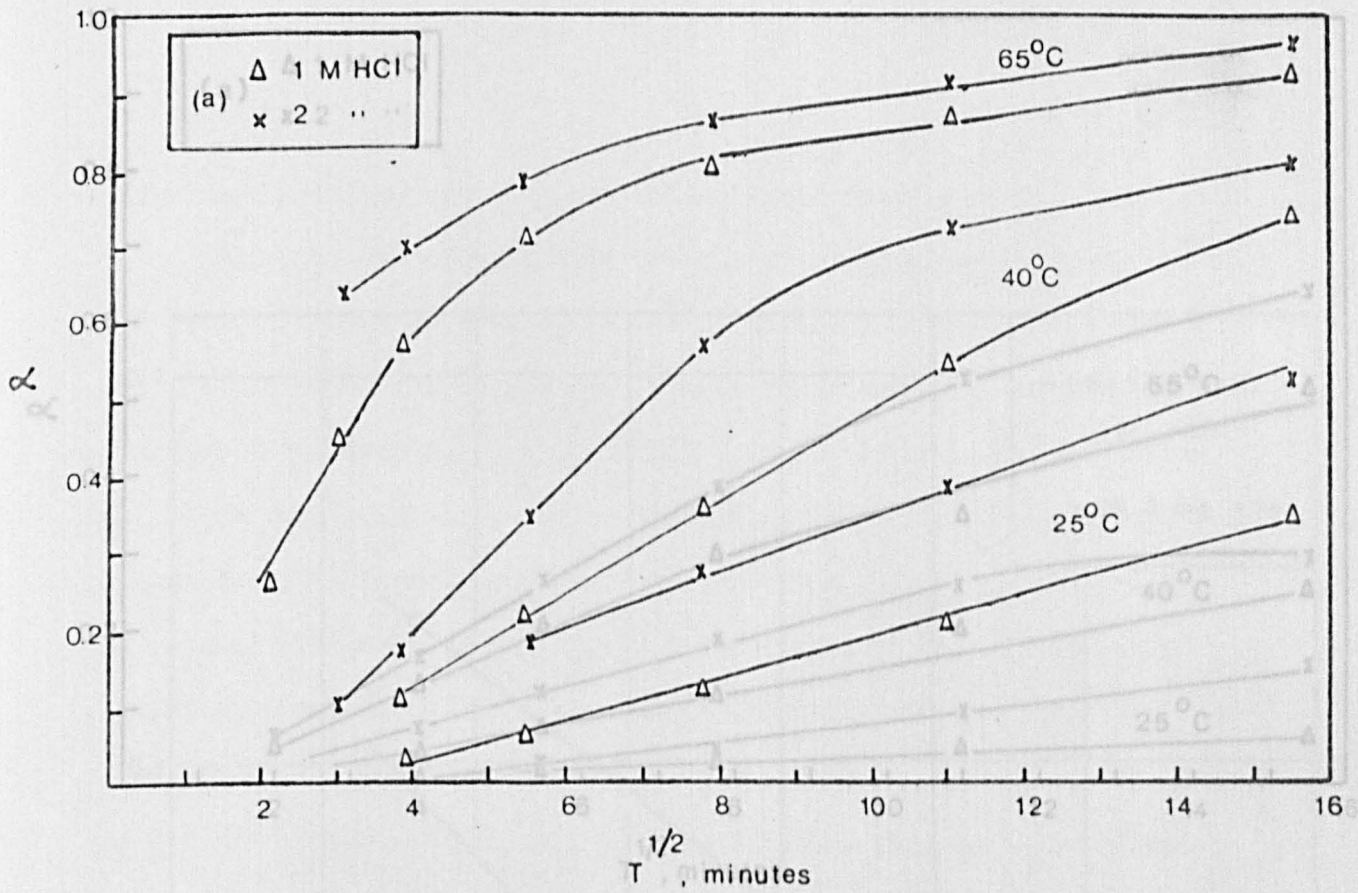


Fig. 5.36 (Strong's Fig. 6.9) Plots of  $\alpha$  vs.  $T^{1/2}$  for (a) Nickel (b) Magnesium. (-85+170 mesh)

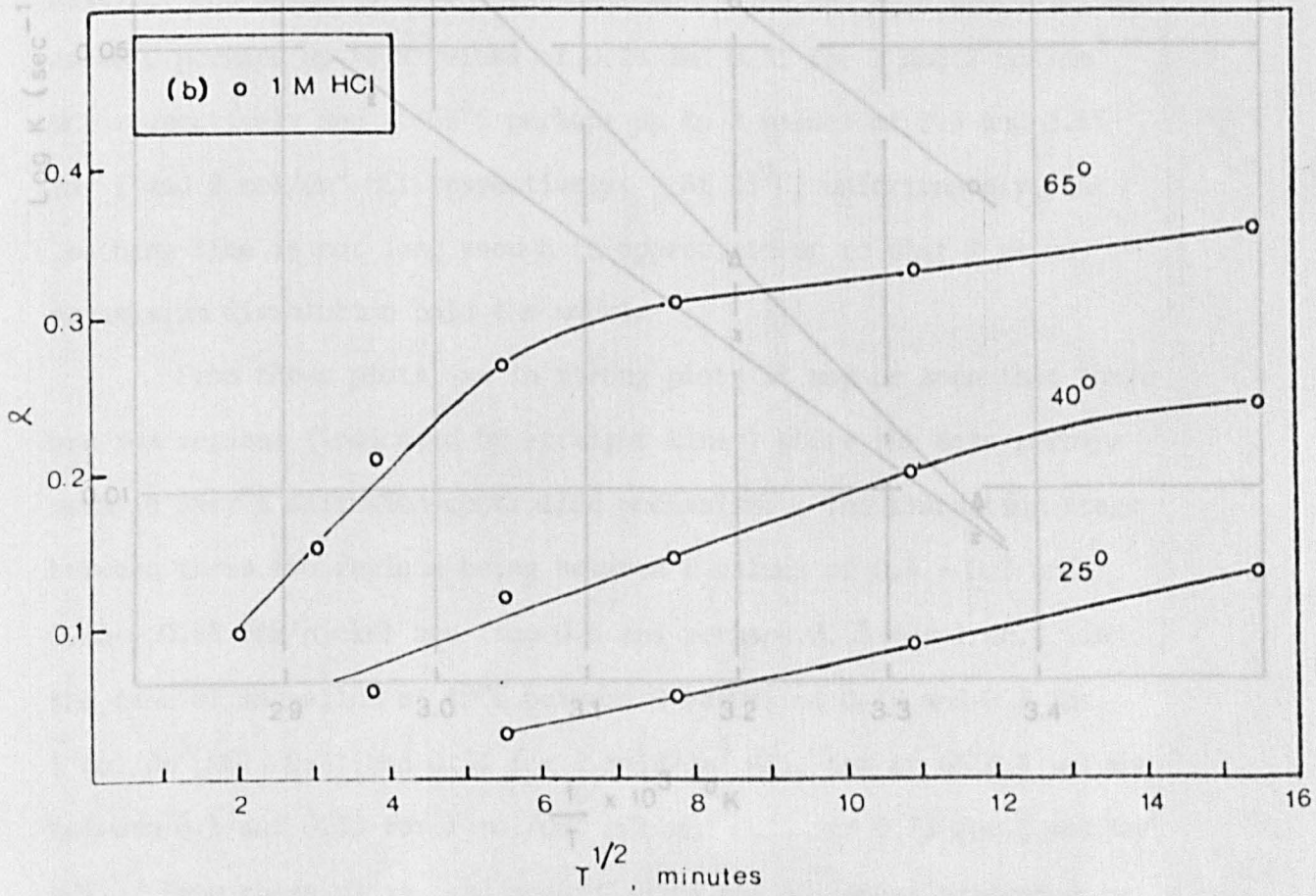
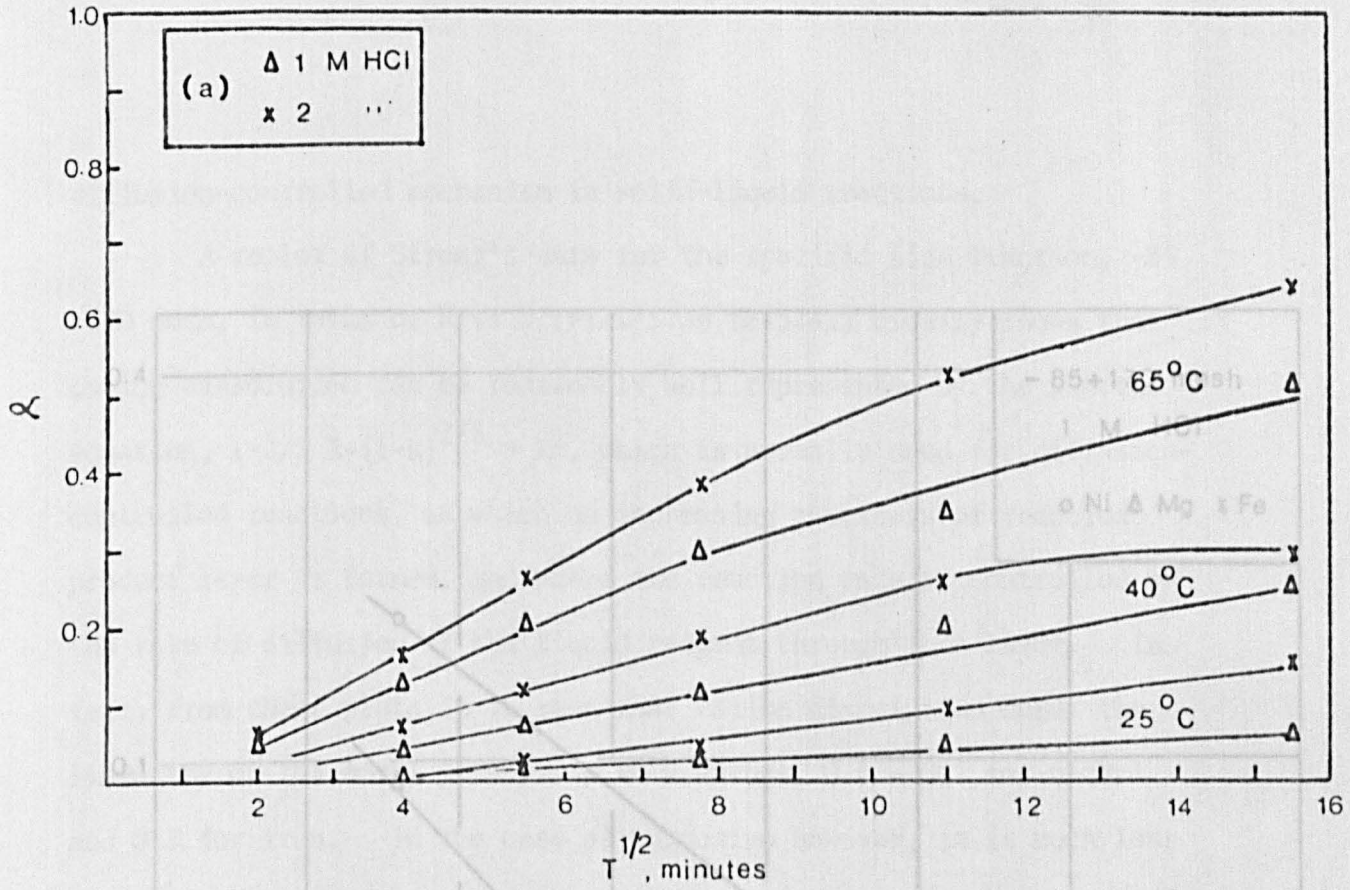


Fig. 5.37 (Strong's Fig. 6.10) Plots of  $\alpha$  vs.  $T^{1/2}$  for (a) iron (b) weight of laterite dissolved (-85 + 170 mesh)

diffusion-controlled mechanism in solid-liquid reactions.

A replot of Strong's data for the specific size fraction, -85

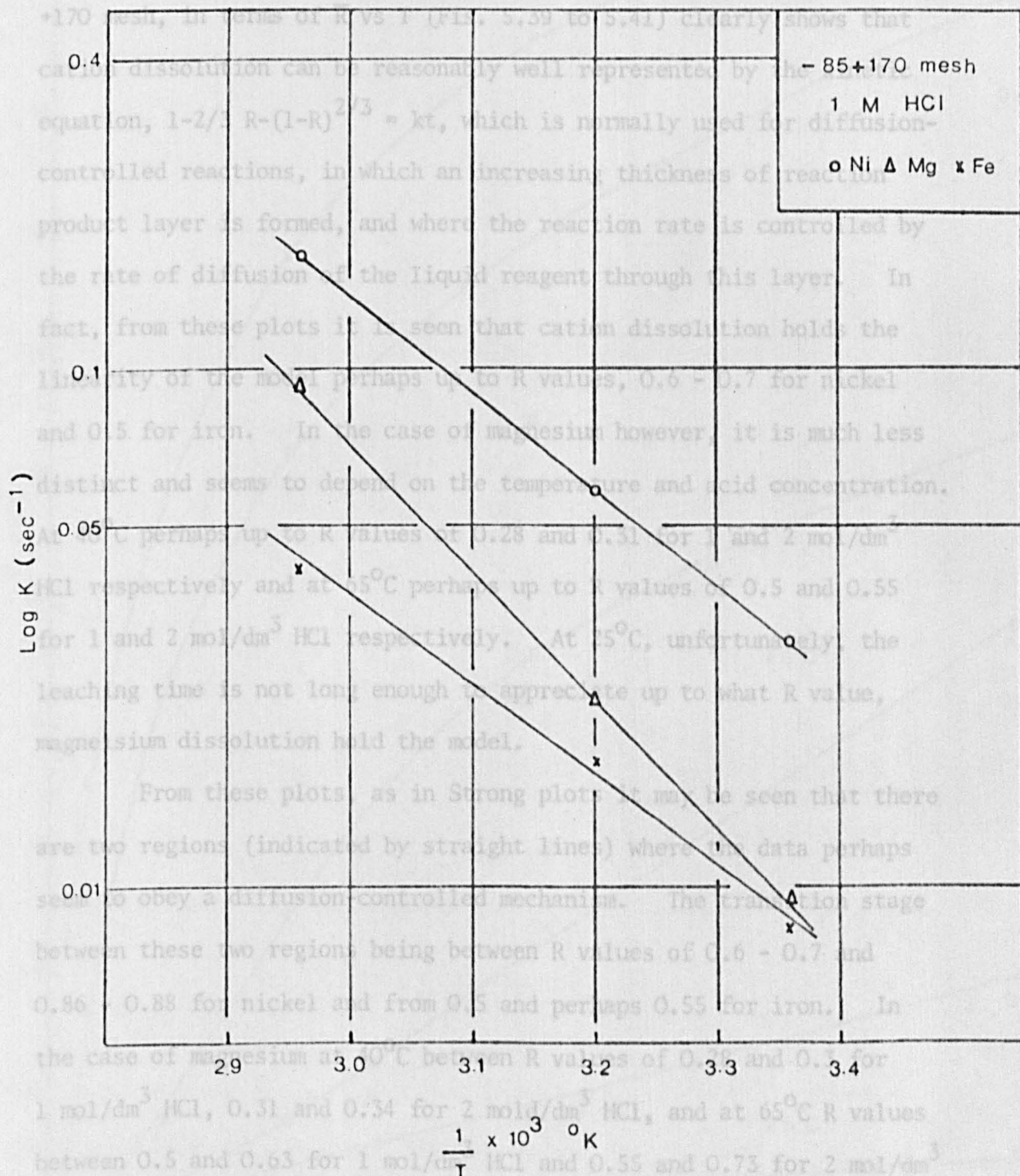


Fig. 5.38 (Strong's Fig. 6.11) Arrhenius plots for cation extraction



diffusion-controlled mechanism in solid-liquid reactions.

A replot of Strong's data for the specific size fraction, -85 +170 mesh, in terms of  $\bar{R}$  vs  $T$  (Figs. 5.39 to 5.41) clearly shows that cation dissolution can be reasonably well represented by the kinetic equation,  $1 - \frac{2}{3} R - (1-R)^{2/3} = kt$ , which is normally used for diffusion-controlled reactions, in which an increasing thickness of reaction product layer is formed, and where the reaction rate is controlled by the rate of diffusion of the liquid reagent through this layer. In fact, from these plots it is seen that cation dissolution holds the linearity of the model perhaps up to  $R$  values, 0.6 - 0.7 for nickel and 0.5 for iron. In the case of magnesium however, it is much less distinct and seems to depend on the temperature and acid concentration. At 40°C perhaps up to  $R$  values of 0.28 and 0.31 for 1 and 2 mol/dm<sup>3</sup> HCl respectively and at 65°C perhaps up to  $R$  values of 0.5 and 0.55 for 1 and 2 mol/dm<sup>3</sup> HCl respectively. At 25°C, unfortunately, the leaching time is not long enough to appreciate up to what  $R$  value, magnesium dissolution hold the model.

From these plots, as in Strong plots it may be seen that there are two regions (indicated by straight lines) where the data perhaps seem to obey a diffusion-controlled mechanism. The transition stage between these two regions being between  $R$  values of 0.6 - 0.7 and 0.86 - 0.88 for nickel and from 0.5 and perhaps 0.55 for iron. In the case of magnesium at 40°C between  $R$  values of 0.28 and 0.3 for 1 mol/dm<sup>3</sup> HCl, 0.31 and 0.34 for 2 mol/dm<sup>3</sup> HCl, and at 65°C  $R$  values between 0.5 and 0.63 for 1 mol/dm<sup>3</sup> HCl and 0.55 and 0.73 for 2 mol/dm<sup>3</sup> HCl. From these plots, and according to the evidences presented in this research (Chapter 4, lump leaching, and in this chapter) it is

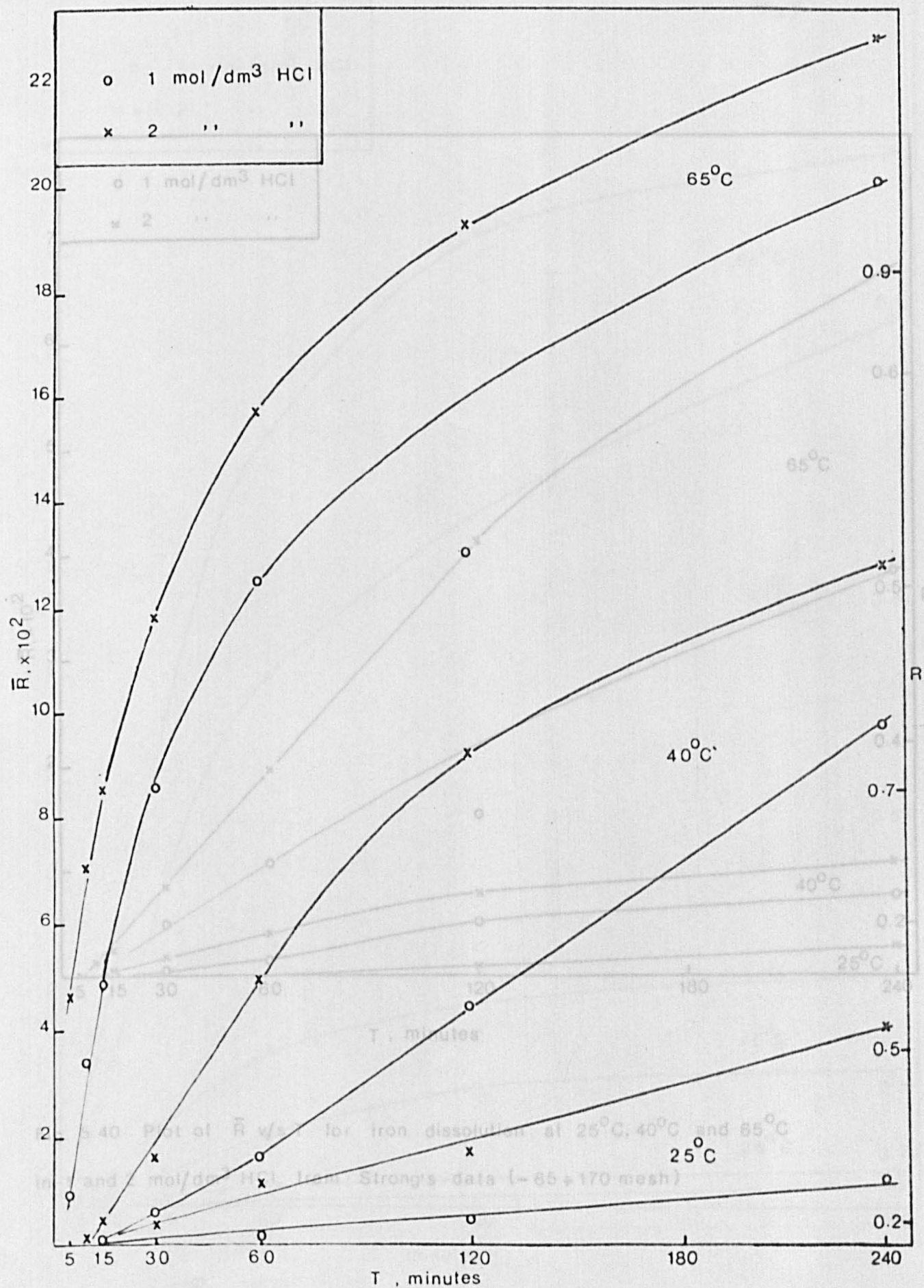


Fig 5-39 Plot of  $\bar{R}$  v/s  $T$  for nickel dissolution at 25°C, 40°C and 65°C in 1 and 2 mol/dm<sup>3</sup> HCl from Strong's data (-85 + 170 mesh)



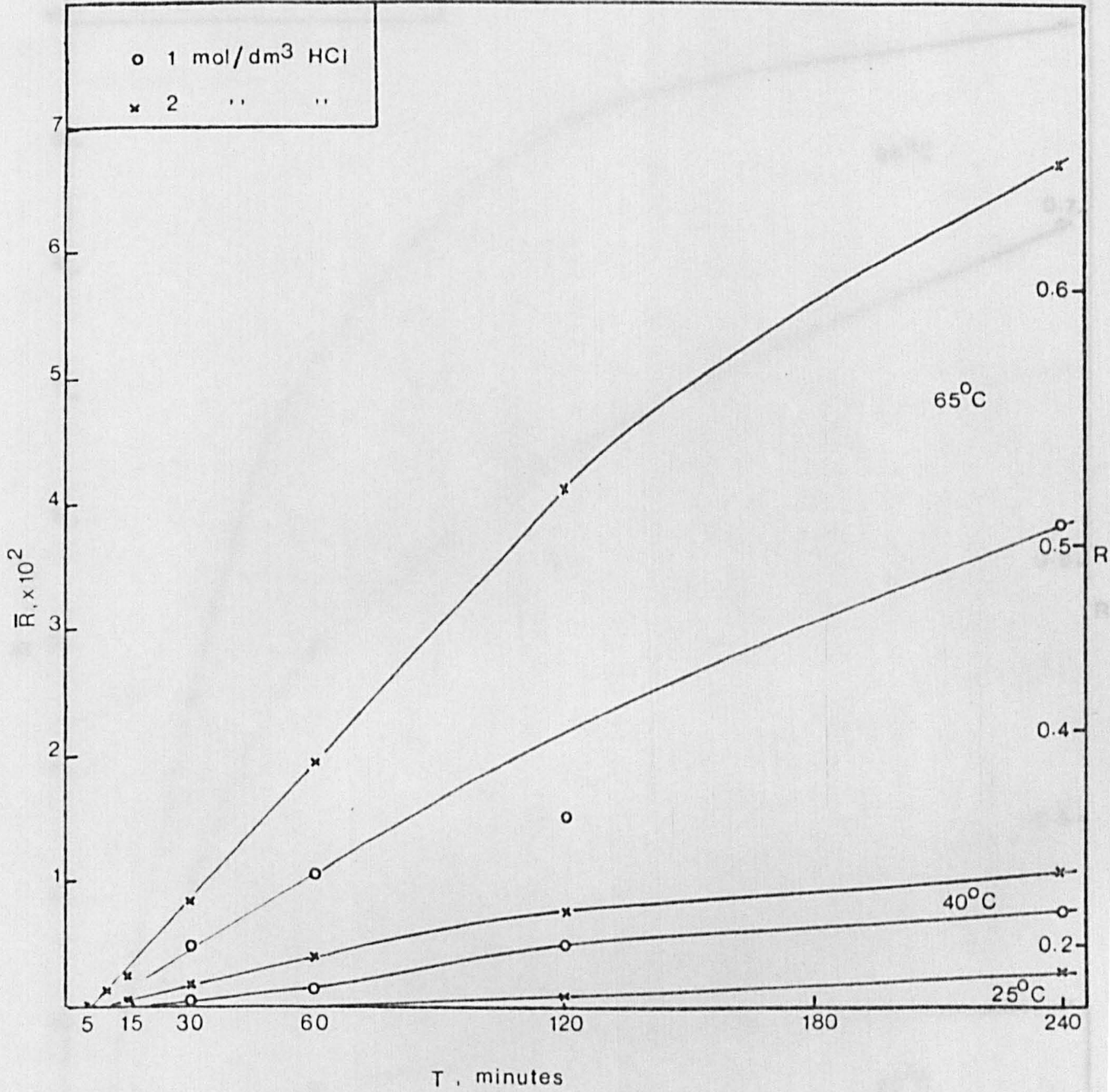


Fig. 5.40 Plot of  $\bar{R}$  v/s T for iron dissolution at 25°C, 40°C and 65°C in 1 and 2 mol/dm<sup>3</sup> HCl from Strong's data (-85+170 mesh)

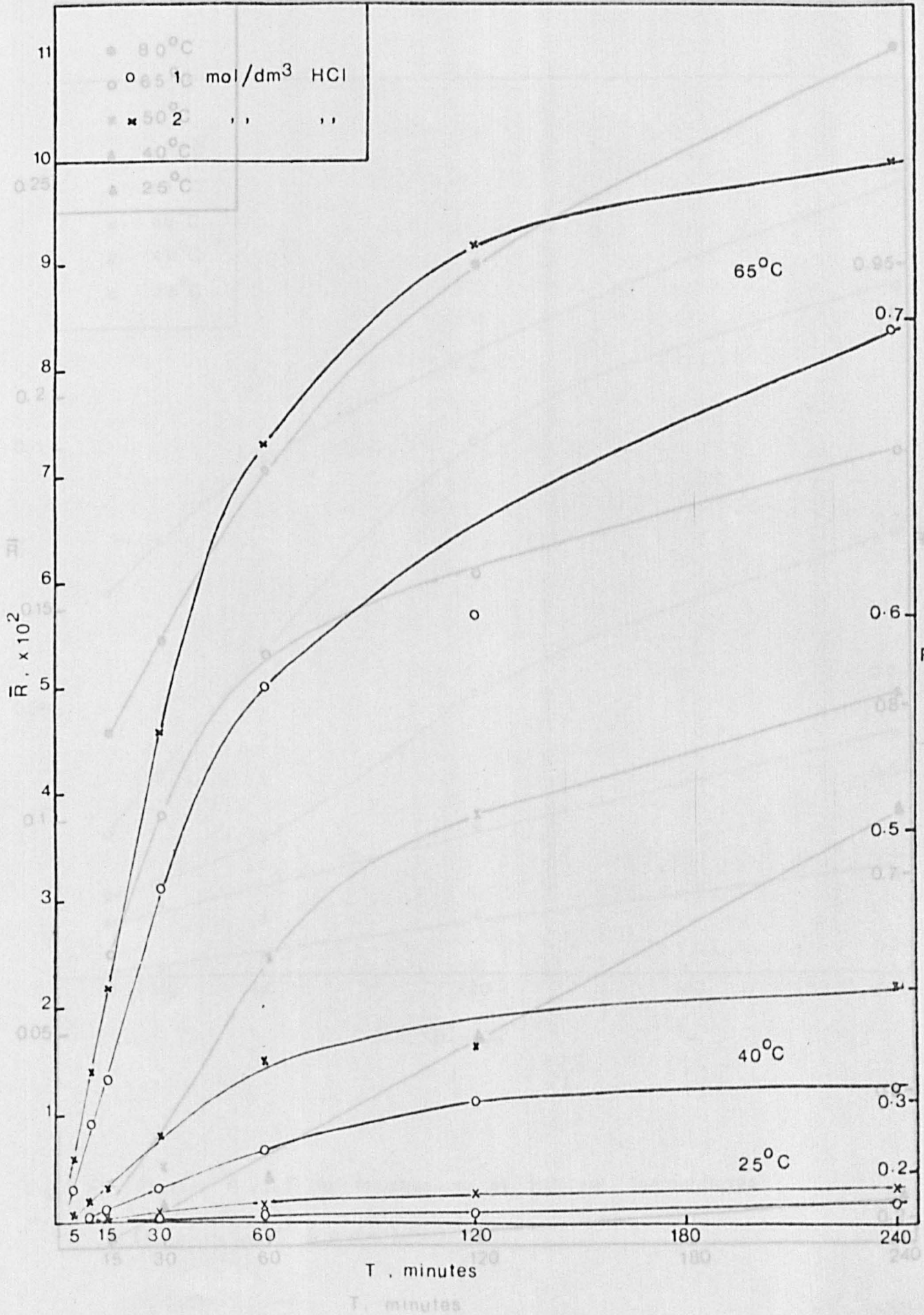


Fig 5.41 Plot of  $\bar{R}$  v/s T for magnesium dissolution at 25°C, 40°C and 65°C in 1 and 2 mol/dm<sup>3</sup> HCl from Strong's data (- 85+170 mesh)

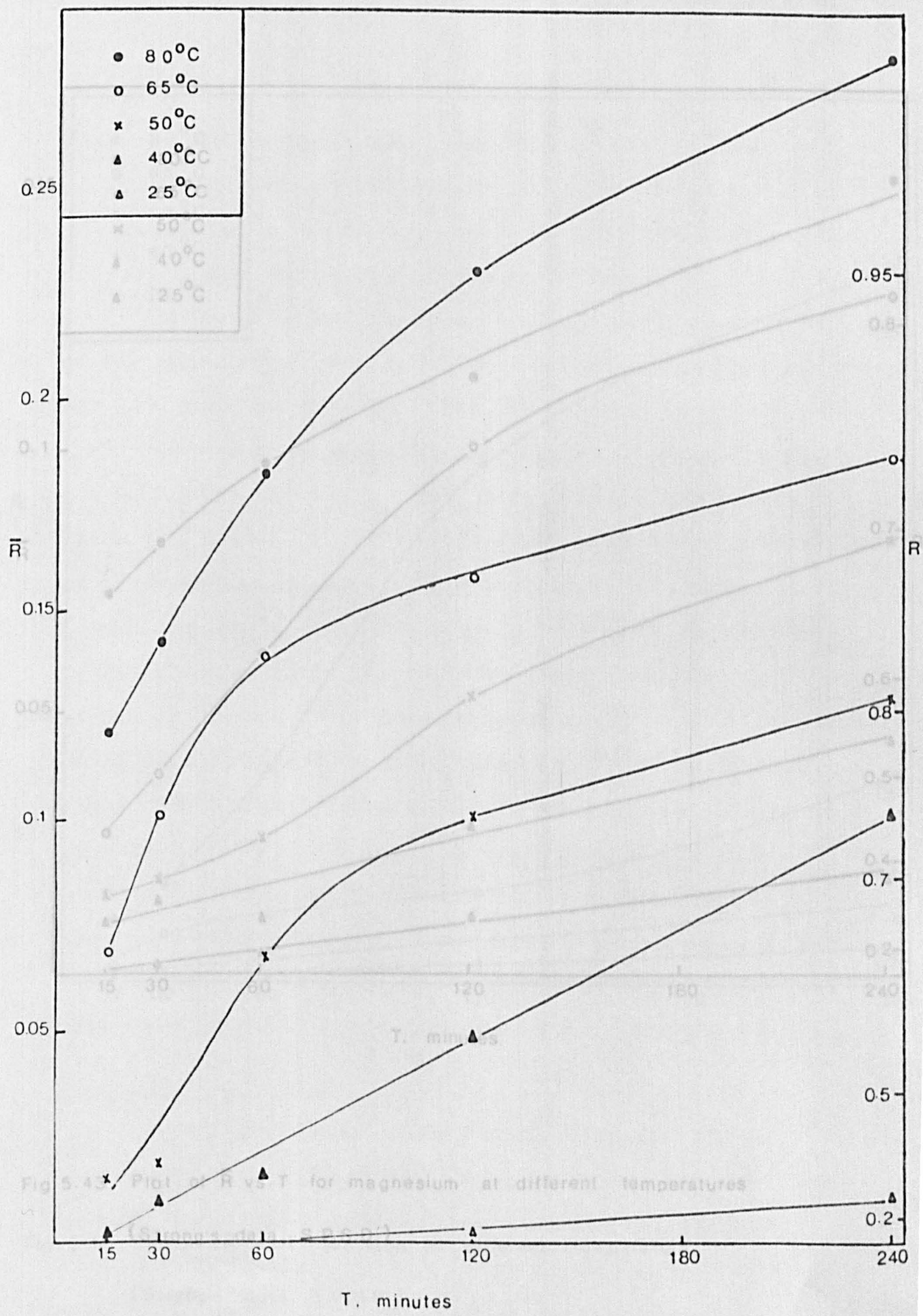


Fig. 5.42 Plot of  $\bar{R}$  vs. T for nickel dissolution at different temperatures (Strong's data, S.P.S.D.)



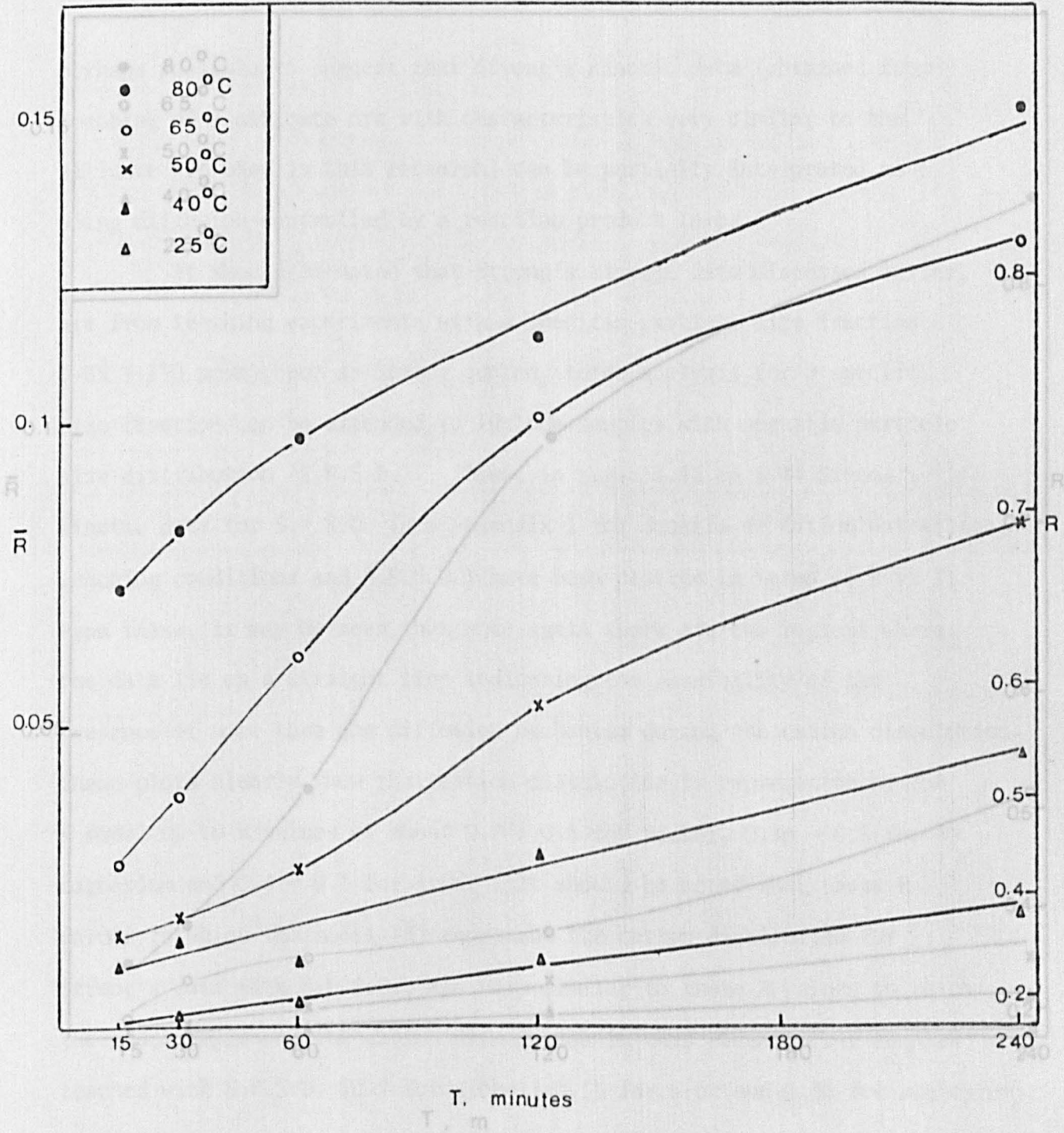


Fig. 5.43 Plot of  $\bar{R}$  vs.  $T$  for magnesium at different temperatures

(Strong's data, S.P.S.D.)

Fig. 5.44 Plot of  $\bar{R}$  vs.  $T$  for iron at different temperatures

(Strong's data, S.P.S.D.)

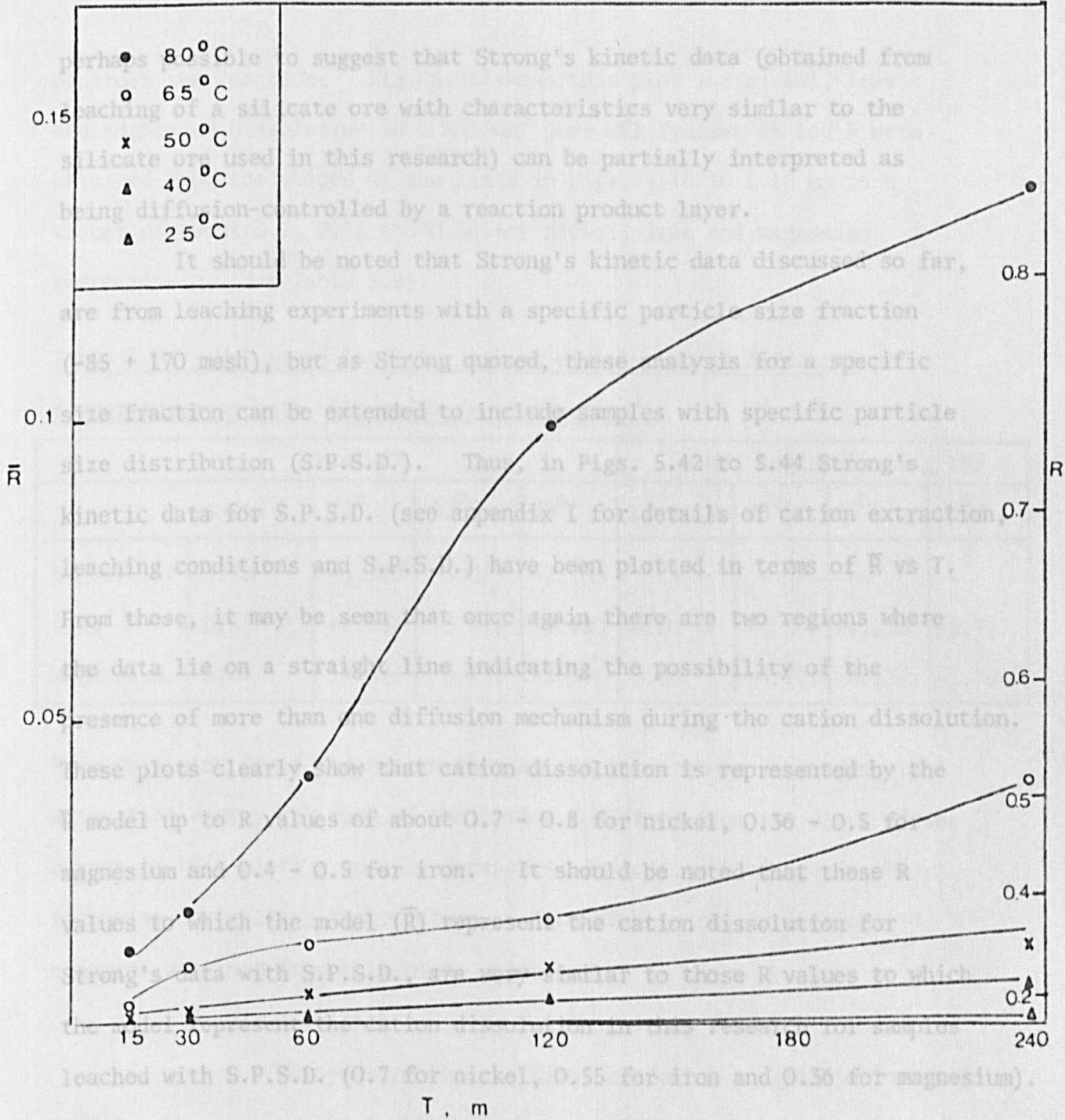


Fig. 5.44 Plot of  $\bar{R}$  vs.  $T$  for iron at different temperatures (Strong's data, S.P.S.D.)

5.6 Reaction Mechanism

According to the fit of the chemical dissolution data to the kinetic equation  $1 - \frac{2}{3} R - (1-R)^{2/3} = kt$ , the cation dissolution can be partially interpreted as being diffusion-controlled by a reaction product layer. However, a plot of the log of the rate constant  $k$  versus  $1/T$  (Arrhenius plot) indicates that more than one mechanism

perhaps possible to suggest that Strong's kinetic data (obtained from leaching of a silicate ore with characteristics very similar to the silicate ore used in this research) can be partially interpreted as being diffusion-controlled by a reaction product layer.

It should be noted that Strong's kinetic data discussed so far, are from leaching experiments with a specific particle size fraction (-85 + 170 mesh), but as Strong quoted, these analysis for a specific size fraction can be extended to include samples with specific particle size distribution (S.P.S.D.). Thus, in Figs. 5.42 to 5.44 Strong's kinetic data for S.P.S.D. (see appendix I for details of cation extraction, leaching conditions and S.P.S.D.) have been plotted in terms of  $\bar{R}$  vs T. From these, it may be seen that once again there are two regions where the data lie on a straight line indicating the possibility of the presence of more than one diffusion mechanism during the cation dissolution. These plots clearly show that cation dissolution is represented by the  $\bar{R}$  model up to R values of about 0.7 - 0.8 for nickel, 0.36 - 0.5 for magnesium and 0.4 - 0.5 for iron. It should be noted that these R values to which the model ( $\bar{R}$ ) represent the cation dissolution for Strong's data with S.P.S.D., are very similar to those R values to which the model represent the cation dissolution in this research for samples leached with S.P.S.D. (0.7 for nickel, 0.55 for iron and 0.36 for magnesium).

#### 5.6 Reaction Mechanism

According to the fit of the chemical dissolution data to the kinetic equation  $1 - \frac{2}{3} R - (1-R)^{2/3} = kt$ , the cation dissolution can be partially interpreted as being diffusion-controlled by a reaction product layer. However, a plot of the log of the rate constant k versus 1/T (Arrhenius plot) indicates that more than one mechanism



controls the reaction. Fig. 5.45 shows this plot for nickel, iron and magnesium dissolution in  $2 \text{ mol/dm}^3$  pure HCl (values of  $\log k$  were obtained from the slopes of the lines in Figs. 5.16 to 5.18 up to R values of about 0.7, 0.55 and 0.36 for nickel, iron and magnesium respectively. See Table 5.9).

Table 5.9. Values of  $\log k$  for cation dissolution at different temperatures in both acid media ( $k$  in minutes<sup>-1</sup>)

	Pure HCl				HCl containing 5 g/lNi			
	up to R	25°C	40°C	70°C	up to R	25°C	40°C	70°C
Nickel	0.70	-3.747	-3.033	-2.203	-	-	-	-
Iron	0.55	-5.064	-3.985	-3.420	0.50	-5.380	-4.210	-3.717
Magnesium	0.36	-4.574	-3.471	-2.676	0.36	-4.703	-3.530	-2.764

From this plot it is clear seen that as the temperature increases, the activation energy for each of the cation (obtained from the slope of the curves in this plot) gradually decreases, indicating a change in the mechanism controlling the reaction. According to the activation energies obtained from this plot, which are:

	Nickel (Kilojoule/mole)	Magnesium (Kilojoule/mole)	Iron (Kilojoule/mole)
25°C	94.4	139.9	148.5
30°C	88.1	133.2	136.5
40°C	77.2	95.7	86.2
45°C	65.8	66.4	59.1
50°C	64.1	53.4	46.1
60°C	48.8	44.3	24.8
65°C	42.5	41.1	18.0
70°C	38.3	38.8	15.6

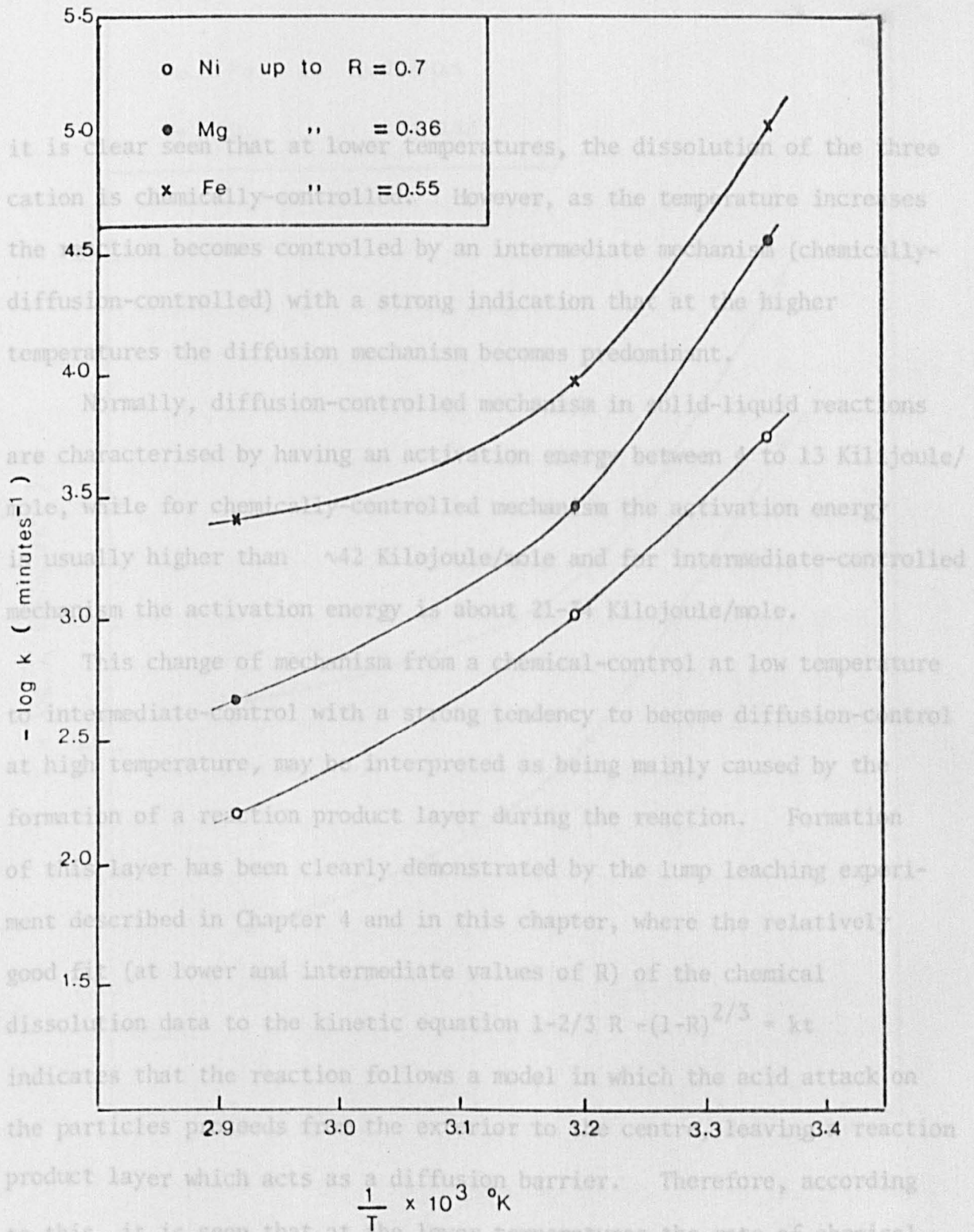


Fig. 5.45 Arrhenius plot for cation dissolution in pure HCl

it is clear seen that at lower temperatures, the dissolution of the three cation is chemically-controlled. However, as the temperature increases the reaction becomes controlled by an intermediate mechanism (chemically-diffusion-controlled) with a strong indication that at the higher temperatures the diffusion mechanism becomes predominant.

Normally, diffusion-controlled mechanism in solid-liquid reactions are characterised by having an activation energy between 4 to 13 Kilojoule/mole, while for chemically-controlled mechanism the activation energy is usually higher than  $\sim 42$  Kilojoule/mole and for intermediate-controlled mechanism the activation energy is about 21-34 Kilojoule/mole.

This change of mechanism from a chemical-control at low temperature to intermediate-control with a strong tendency to become diffusion-control at high temperature, may be interpreted as being mainly caused by the formation of a reaction product layer during the reaction. Formation of this layer has been clearly demonstrated by the lump leaching experiment described in Chapter 4 and in this chapter, where the relatively good fit (at lower and intermediate values of  $R$ ) of the chemical dissolution data to the kinetic equation  $1 - \frac{2}{3} R - (1-R)^{2/3} = kt$  indicates that the reaction follows a model in which the acid attack on the particles proceeds from the exterior to the centre, leaving a reaction product layer which acts as a diffusion barrier. Therefore, according to this, it is seen that at the lower temperatures the rate of chemical reaction is much slower than the rate of diffusion through the layer, i.e. the rate is chemically-controlled. However, with the rise of temperature, the rate of chemical reaction is accelerated, becoming more and more competitive with the rate of diffusion, i.e. the rate is intermediate-controlled, and at the higher temperatures it seems

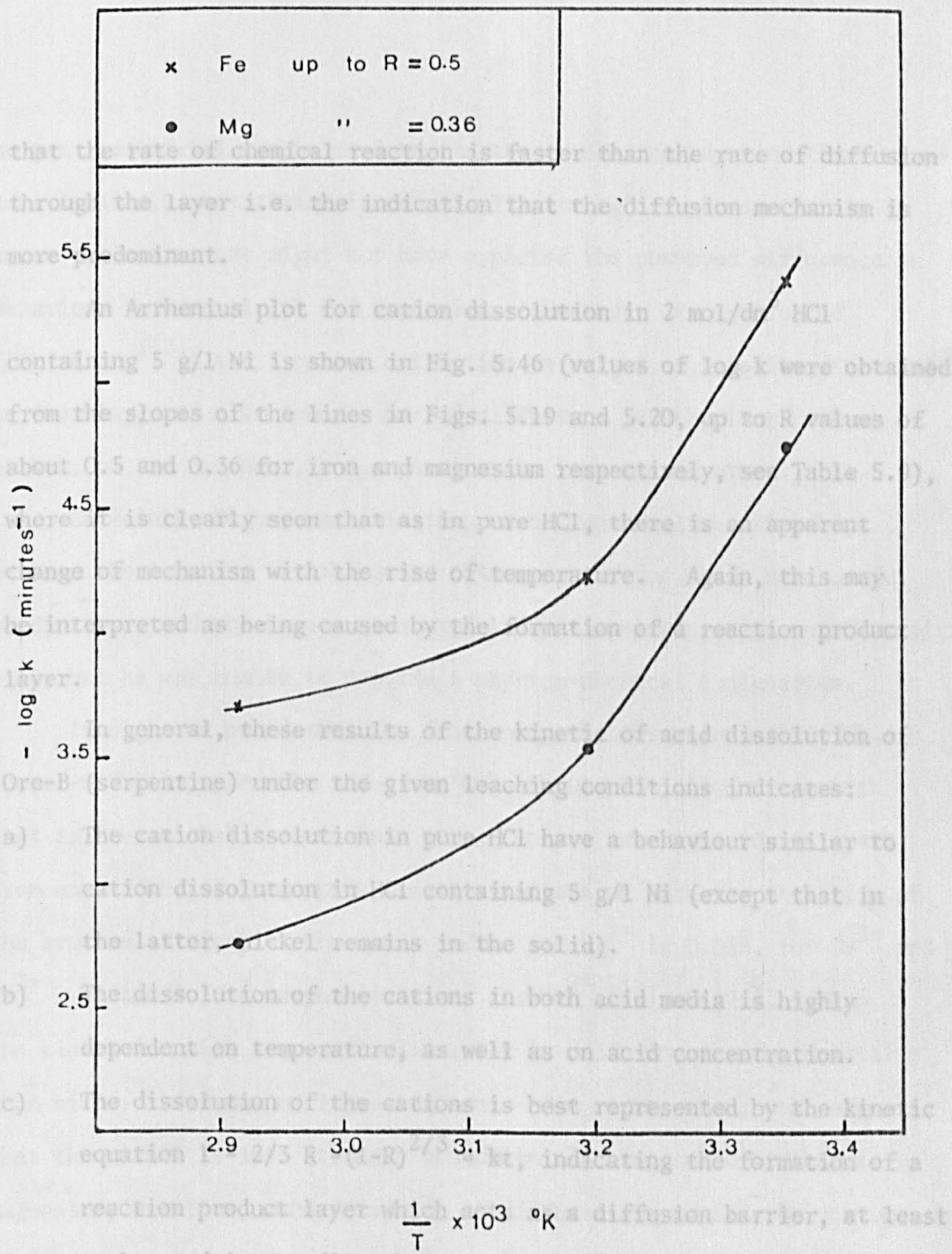


Fig. 5.46 Arrhenius plot for cation dissolution in HCl containing 5 g/l Ni the largest range of R values.

Thus, it must be mentioned that Strong (13) has reported that there is a distinction between "lattice" and "no-lattice" ions. In

that the rate of chemical reaction is faster than the rate of diffusion through the layer i.e. the indication that the diffusion mechanism is more predominant.

An Arrhenius plot for cation dissolution in 2 mol/dm<sup>3</sup> HCl containing 5 g/l Ni is shown in Fig. 5.46 (values of log k were obtained from the slopes of the lines in Figs. 5.19 and 5.20, up to R values of about 0.5 and 0.36 for iron and magnesium respectively, see Table 5.9), where it is clearly seen that as in pure HCl, there is an apparent change of mechanism with the rise of temperature. Again, this may be interpreted as being caused by the formation of a reaction product layer.

In general, these results of the kinetic of acid dissolution of Ore-B (serpentine) under the given leaching conditions indicates:

- a) The cation dissolution in pure HCl have a behaviour similar to cation dissolution in HCl containing 5 g/l Ni (except that in the latter, nickel remains in the solid).
- b) The dissolution of the cations in both acid media is highly dependent on temperature, as well as on acid concentration.
- c) The dissolution of the cations is best represented by the kinetic equation  $1 - \frac{2}{3} R - (1-R)^{2/3} = kt$ , indicating the formation of a reaction product layer which acts as a diffusion barrier, at least at low and intermediate values of R (0.7, 0.5 and 0.36 for nickel, iron and magnesium respectively). In regard to this, one might note that it is for nickel that the diffusion model hold over the largest range of R values.

Thus, it must be mentioned that Strong<sup>(13)</sup> has reported that there is a distinction between "lattice" and "no-lattice" ions. In

serpentines nickel can be assigned to the octahedral layer of the serpentine lattice, substituting isomorphically for  $Mg^{2+}$ . Hence, purely in terms of lattice one might not have expected the observed difference in behaviour between nickel and magnesium. However, Strong plotted (Fig. 6.23 <sup>(13)</sup>) the % cation extraction vs weight of laterite dissolved in leaching, and also found a marked difference in behaviour between nickel, on the one hand, and magnesium and iron on the other.

Certainly, Strong was able to present empirical relationships between the leaching variables and cation extraction which were useful predictions, and which were also useful for classifying types of "lateritic" ores, but he was unable to provide a physico-chemical explanation.

It might be noted that the free energy of formation of  $Ni(OH)_2$  is about -542 Kilojoule/mole and of  $Mg(OH)_2$  about -834 Kilojoule/mole; that is, the nickel form is less stable in its own right (quite apart from any effect of isomorphous nickel substitution upon the stability of the brucite lattice). The ionic radius for  $Mg^{2+}$  is  $0.65\text{\AA}$ , for  $Fe^{2+}$  and  $Fe^{3+}$   $0.64$  and  $0.76\text{\AA}$  respectively and for  $Ni^{2+}$  it is  $0.72\text{\AA}$ . Thus the nickel ion will have more difficulty in diffusing through a lattice than either a ferrous or magnesium ion. One might, then, make a guess that the nickel is less strongly bonded in the brucite layer than is magnesium, but that, once detached, it diffuses less rapidly by virtue of its ionic size. This view agrees qualitatively with the observations made from the experimental results.

d) According to the Arrhenius plots, at low temperature, cation dissolution is chemically-controlled. However, with the rise of temperature cation dissolution becomes intermediate-controlled with strong indication that at the higher temperatures diffusion control is predominant.



## CHAPTER 6

### WASHING

#### 6.1. Introduction

The work in Chapter 4 has established that during the leaching of the seven laterite samples with HCl containing different concentrations of  $\text{NiCl}_2$  in solution, the extraction of nickel from all dropped off rapidly as the aqueous nickel chloride concentration in the leach acid increased. However, it was found that upon contacting or washing the leach residues with pure HCl, extraction of nickel occurred to a degree similar to that when the laterites were leached in pure HCl solution.

Therefore, the work described in this chapter involves a systematic study of the washing of the residues of laterites leached in HCl which contained high concentrations of nickel chloride in solution.

#### 6.2. Single Batch Washing

It was first necessary to determine the effect of leaching variables upon cation extraction during the washing, and then to determine the effect of washing variables upon the cation extraction during the washing of leach residues (washing efficiency). To do so, washing of the residues were performed using single batch tests. For details of washing technique, see Chapter 3.

##### 6.2.1. Effect of leaching variables upon the cation extraction during the washing of leaching residues

In Chapter 5, it was shown that during the leaching of Ore-B samples (2% solid W/V) in HCl containing 5 g/l Ni in solution, leaching variables such as temperature, contact time, acid concentration

and particle size did not affect at all nickel extraction (0%), according to the determination of cation extraction by the analysis of leaching solutions. This was not so for the extraction of iron and magnesium, which was as significantly affected by those variables as when leaching took place in pure HCl, where the extraction of the three cations is highly dependent on the above variables.

However, as previously established in Chapter 4, washing the leaching residues of laterites for which, whatever the leaching conditions, nickel extraction was zero, because of the presence of nickel in the leach acid, resulted in a degree of extraction of nickel similar to when the laterites were leached in pure HCl. This indicated that despite the fact that the effect of the leaching variables upon nickel extraction cannot be appreciated during the leaching stage, leaching variables still do affect the extraction of nickel, but their influence can only be observed and determined after washing with pure HCl.

#### 6.2.1.1. Temperature, Acid Concentration and Particle Size

To determine the effect of these variables, residues from the leaching of Ore-B (2% solid W/V) in HCl containing 5 g/l Ni from the kinetic study in Chapter 5 (where the ore samples were leached at different temperatures, acid concentrations and particles size), were selected and washed with pure HCl ( $2 \text{ mol/dm}^3$ ). After washing the final cation extractions were compared with cation extraction from Ore-B samples leached (under the same leaching conditions) in pure HCl (before washing).

Tables 6.1 and 6.2 show the effect of the aforementioned variables upon the cation extraction in both acid media. It should be noted

Table 6.1. Effect of temperature and acid concentration upon the cation extraction from Ore-B leached in pure HCl and in HCl with 5 g/l Ni in solution.

Temperature °C	Acid Conc. (mol/dm <sup>3</sup> )	%	Pure * HCl	HCl with 5 g/l Ni	
				B.W.	A.W.
25	1	Ni	22.3	0.0	19.7
		Fe	4.5	4.1	5.0
		Mg	13.0	10.5	11.8
	2	Ni	43.3	0.0	43.0
		Fe	10.8	7.0	10.1
		Mg	17.4	16.8	17.6
	4	Ni	46.0	0.0	45.2
		Fe	30.8	28.2	28.5
		Mg	31.8	31.9	32.0
70	1	Ni	87.4	0.0	84.8
		Fe	42.5	37.9	40.3
		Mg	63.2	59.2	61.0
	2	Ni	94.0	0.0	94.2
		Fe	58.6	47.2	59.5
		Mg	75.5	71.0	76.3
	4	Ni	98.3	0.0	98.1
		Fe	93.6	90.4	93.0
		Mg	98.5	97.5	97.9

Leaching conditions: 2% solid (W/V), 70°C, 4 mol/dm<sup>3</sup> HCl and 3 hours contact time

Washing conditions: 2 mol/dm<sup>3</sup> pure HCl, room temperature, 30 minutes contact time and no agitation.

\* Cation extraction data obtained from analysis of leaching solutions  
 B.W. Cation extraction before the washing (analysis of leach solution)  
 A.W. Cation extraction after the washing (analysis of residues and wash solutions)

Table 6.2. Effect of particle size upon the cation extraction from Ore-B leached in pure HCl and in HCl with 5 g/l Ni in solution

Size Fraction B.S. Mesh	%	Pure * HCL	HCl with 5 g/l Ni	
			Before Washing	After washing
-18 + 36	Ni	89.0	0.0	86.9
	Fe	82.6	79.2	80.7
	Mg	94.6	93.5	94.1
-72 + 150	Ni	97.1	0.0	97.5
	Fe	96.5	95.4	96.0
	Mg	98.6	98.3	98.6
-150 + 300	Ni	100.0	0.0	98.9
	Fe	100.0	98.5	99.0
	Mg	100.0	100.0	/

Leaching conditions: 2% solid (W/V), 70°C, 4 mol/dm<sup>3</sup> HCl and 3 hours contact time.

Washing conditions: 2 mol/dm<sup>3</sup> pure HCl, room temperature, 30 minutes contact time and no agitation.

\* : Cation extraction data obtained from analysis of leaching solutions

Cation extraction before washing (analysis of leaching solutions).

Cation extraction after washing (analysis of residues and wash solution).

that the cation extraction data from the leaching in pure HCl are given only for before the washing (by analysis of leaching solutions).

From these tables it may be clearly seen, that in pure HCl, extraction of nickel, iron and magnesium is highly affected by temperature, acid concentration and particle size. The same occurs with the extraction of iron and magnesium in HCl containing 5 g/l Ni before and after the washing of the residues. The nickel extraction however, before the washing remains unaltered at 0%, but as soon as the residues are washing with pure HCl, the effect of the above mentioned leaching variables can be observed.

From the tables it can also be seen that for each of the given set of leaching conditions, the final degree of cation extraction (after leaching and washing have taken place) from samples leached in HCl containing 5 g/l Ni, is very similar to the degree of cation extraction reached during the leaching of ore samples in pure HCl. This demonstrates that despite the retarding effect of 5 g/l Ni upon the extraction of nickel, and also to a smaller degree iron and magnesium, after washing of the residues with pure HCl, the leaching variables affect the extraction of nickel, iron and magnesium in both acid media to the same extent.

#### 6.2.1.2. Pulp Density

To determine the effect of this variable, residues from the leaching of Ore-B (under the following conditions: 80°C, 6 mol/dm<sup>3</sup> HCl, 1 hour contact time), at different pulp densities in pure HCl as well as in HCl containing different concentrations of nickel in solution (Chapter 4, section 4.3.5. ) were washed with pure HCl (6 mol/dm<sup>3</sup>).

The results of cation extraction before and after the washing of residues are given in Table 6.3. From this table, one can see that in pure HCl, before and after the washing, the extraction of nickel, iron and magnesium decreases as the pulp density increases.

It should be noted however, that after the washing of the residues, an improvement in the cation extraction was obtained for each pulp density. This indicates that during the leaching stage, the maximum possible degree of extraction for the three cations, according to the given leaching conditions, were retarded to some extent by the aqueous  $\text{NiCl}_2$ ,  $\text{MgCl}_2$  and  $\text{FeCl}_3$  concentrations that resulted from leaching itself, but as soon as the residues were washed with pure HCl, the maximum degree extraction for each cation was achieved.

In the cases where the leach solution contained 5, 20 or 40 g/l Ni in solution, the results show that before the washing of the residues, the extraction of nickel increases as the pulp density increases, reaching a maximum after which the extraction starts to drop off. This was not the case for the extraction of iron and magnesium, which decreased as the pulp density increased (see effect of pulp density, Chapter 4, Section 4.3.5.). However, after washing of the residues, when the maximum degree of cation extraction has been reached (for a given set of leaching conditions), the extraction of nickel, iron and magnesium decreases with the increase of pulp density, as in the case of leaching in pure HCl. It should be noted that after the washing of the residues, the final cation extractions (for each of the pulp densities) from samples leached in pure HCl and in HCl with 5, 20 and 40 g/l Ni were very similar. This demonstrates once again that the presence



Table 6.3. Effect of pulp density upon cation extraction from Ore-B leached in HCl containing different nickel concentrations in solution (before and after the washing of residues)

Nickel concentration Leach acid (g/l Ni)	Pulp density % solid (W/W)	CATION EXTRACTION %					
		Nickel		Iron		Magnesium	
		B.W.	A.W.	B.W.	A.W.	B.W.	A.W.
0	5	95.34	98.86	97.03	98.54	95.10	98.10
	10	89.83	98.76	94.70	98.95	94.39	98.03
	30	78.53	93.19	71.35	86.55	63.04	83.50
5	5	61.50	97.48	96.86	97.36	93.72	98.54
	10	78.26	98.05	94.62	98.10	93.54	98.10
	30	76.22	94.17	69.31	83.28	63.11	86.28
20	5	0.00	99.05	94.81	98.18	89.02	98.21
	10	0.00	98.89	90.73	98.77	87.25	97.70
	30	52.18	92.87	68.49	82.95	60.51	87.59
	40	46.36	87.21	41.63	74.90	30.14	82.95
40	5	0.00	98.66	93.41	98.65	86.45	96.51
	10	0.00	98.60	89.47	98.04	83.97	97.64
	30	17.32	91.93	66.05	86.49	56.69	85.49
	40	34.40	83.14	41.51	80.56	29.76	81.53

B.W. = Before washing. A.W. = After washing

of nickel in the leach solution has only a retarding effect, and once the residues have been washed with the appropriate volume of pure HCl, the final cation extraction from any of the samples leached in any of the above mentioned acid media, is determined only by the original leaching conditions.

Although leaching variables such as contact time and agitation were not studied, the results shown in Tables 6.1 to 6.3 indicate that:

- a) Provided that the leaching residues are washed with pure HCl the final extraction of nickel, iron and magnesium from Ore-B is dependent only on the leaching conditions and not on the initial nickel concentration. The more severe the leaching conditions, the higher the degree of cation extraction.
- b) Leaching samples of Ore-B in pure HCl under a given set of conditions and determination of the cation extraction allows the prediction with reasonable accuracy, of the extraction after the washing of the residues from leaching under the same conditions, in HCl containing nickel in solution. However, it must be remembered that even during leaching in pure HCl, cation extraction is retarded to some extent, because of the formation of  $\text{NiCl}_2$ ,  $\text{MgCl}_2$  and  $\text{FeCl}_3$  in the leach acid, due to the cation extraction. This effect was observed to be stronger at high pulp densities. Table 6.4 shows the improvement of cation extraction for each of the pulp densities after the washing of residues from pure HCl leaching, which indicates the extent of the retardation of the cation extraction during leaching.

Table 6.4 Increase of cation extraction by the washing of residues from samples of Ore-B previously leached in pure HCl at different pulp densities.

Pulp Density % solid W/W	Increase %		
	Nickel	Iron	Magnesium
5	3.52	1.51	3.00
10	8.93	4.25	3.64
30	14.66	15.20	20.46

Leaching conditions: 80°C, 6 mol/dm<sup>3</sup> HCl, 1 hour contact time

Washing conditions: Room temperature, 6 mol/dm<sup>3</sup> HCl, 30 minutes contact time, no agitation and a solid/liquid ratio of about 0.01

6.2.2. Effect of washing variables upon cation extraction during the washing of leach residues.

In order to determine the optimum washing conditions for an efficient nickel extraction during the washing of leach residues, variables such as acid concentration, temperature, agitation, contact time and solid/liquid ratio were studied. To do so, samples of Ore-B with a particle size distribution as shown in appendix II, were previously leached at a pulp density (unless otherwise stated) of 10% solid (W/W) in 6 mol/dm<sup>3</sup> HCl containing 20 g/l Ni at 80°C for 1 hour contact time, and the residues from these leaching submitted to washing under different conditions.

It is obvious that for the purpose of this work, the evaluation of any set of washing conditions is based on their ability to achieve the maximum cation extraction efficiency (especially nickel) from the leaching residues during the washing. Thus, the efficiency of washing for any set of conditions is determined by the percentage of each cation extracted from the total amount of that cation initially present in the solid leaching residues before washing.

#### 6.2.2.1. Acid Concentration, Temperature and Agitation.

To study these variables, leaching residues were washed in large volumes of pure HCl (about 0.01 solid/liquid ratio) in order to avoid any possible retarding effect on the cation extraction by the nickel in the leach solution present with the residues.

Table 6.5 shows the cation extraction from leach residues washed in 0.5, 2, 4 and 6 mol/dm<sup>3</sup> pure HCl at room temperature, 30 minutes contact time and no agitation. From this table, it may be seen that whatever the acid concentration of the washing solution between 0.5 to 6 mol/dm<sup>3</sup>, the percentage of each cation extracted from the total amount initially present in the solid residues, is practically the same i.e. about 98.5% nickel, 81.6% iron and 81.7% magnesium. This indicates that the efficiency of the washing is independent of the acid concentration in the washing solution. Table 6.6 shows the cation extraction from leach residues washed in 2 mol/dm<sup>3</sup> pure HCl at 25°C, 50°C and 70°C with a contact time of 30 minutes and no agitation. These results clearly show that as in the case of acid concentration, whatever the temperature of the washing solution between 25°C to 70°C, the percentage of cation extracted from the

Table 6.5. Effect of acid concentration upon cation extraction during the washing of leach residues.

Acid Conc. (mol/dm <sup>3</sup> )	Cation extraction from residues %		
	Nickel	Iron	Magnesium
0.5	98.72	81.17	82.43
2.0	97.76	80.02	78.66
4.0	98.64	82.27	82.77
6.0	98.70	83.01	82.89

Washing conditions: 0.01 solid/liquid ratio, room temperature, 30 minutes contact time and no agitation.

Table 6.6. Effect of temperature upon cation extraction during the washing of leach residues.

Temperature °C	Cation extraction from residues %		
	Nickel	Iron	Magnesium
25	98.53	82.12	81.72
50	98.57	81.36	81.54
70	98.65	81.68	81.72

Washing conditions: 0.01 solid/liquid ratio, 2 mol/dm<sup>3</sup> HCl, 30 minutes contact time and no agitation.

total amount initially present in the solid residues is very similar. About 98.6% nickel, 81.7% iron and 81.7% magnesium. This again indicates that the efficiency of the washing is not affected by the temperature of the washing solution.

Table 6.7 shows the cation extraction from leach residues washed in  $2 \text{ mol/dm}^3$  pure HCl with and without agitation for 5, 10 and 30 minutes contact time (room temperature). The results presented in this table clearly demonstrate that agitation did not give any improvement in extraction within experimental error. The extraction rate for the three cations was practically the same, reaching about 98.7% nickel, 81.8% iron and 82.0% magnesium after 30 minutes washing. This indicates that agitation (at least for this particular solid/liquid ratio) has little effect on the washing efficiency.

The final cation extractions achieved (after both leaching and washing) for all samples used in these tests are given in Tables 6.8 to 6.10, where the cation extraction from each sample is presented before and after the washing of the residues. From these tables it may be seen that:

- a) After leaching samples of Ore-B (particle size distribution as shown in appendix II ) at a pulp density of 10% solid (W/W) in  $6 \text{ mol/dm}^3$  HCl containing 20 g/l Ni in solution, at  $80^\circ\text{C}$  for a period of 1 hour, the cation extraction that can be expected during the leaching is about zero % nickel, 90.7% iron and 87.1% magnesium.
- b) After washing the residues (from the above mentioned leaching), at a solid /liquid ratio of about 0.01 in pure HCl, whatever the acid concentration (between  $0.5$  to  $6 \text{ mol/dm}^3$ ) and temperature (between  $25^\circ\text{C}$  to  $70^\circ\text{C}$ ), either with or without agitation for 30



Table 6.7. Effect of agitation upon cation extraction during the washing of leach residues.

Agitation	Time Minutes	Cation extraction from residues %		
		Nickel	Iron	Magnesium
without	5	95.39	79.14	78.42
	10	97.46	79.60	80.37
	30	98.73	82.42	82.49
with	5	97.10.	80.35	80.12
	10	97.94	80.72	81.26
	30	98.62	81.10	81.54

Washing conditions: 0.01 solid/liquid ratio, room temperature,  
2 mol/dm<sup>3</sup> HCl and 30 minutes contact time.

minutes contact time, the final degree of cation extraction that can be expected after leaching and washing have taken place is about 98.5% nickel, 98.3% iron and 97.6% magnesium.

Table 6.8. Cation extraction from leached Ore-B samples before and after the washing of residues in pure HCl at different acid concentrations.

Cation extraction before washing %			Acid Conc.	Cation extraction after washing%		
Ni	Fe	Mg	mol/dm <sup>3</sup>	Ni	Fe	Mg
0.00	90.47	87.25	0.5	98.72	98.21	97.76
0.00	89.96	86.10	2.0	97.76	97.99	97.03
0.00	91.39	86.95	4.0	98.64	98.47	97.75
0.00	90.12	87.14	6.0	98.70	98.32	97.80

Leaching conditions: 10% solid (W/W), 80°C, 6 mol/dm<sup>3</sup> HCl containing 20 g/l Ni and 1 hour contact time.

Washing conditions: 0.01 solid/liquid ratio, room temperature, 30 minutes contact time and no agitation.

Table 6.9. Cation extraction from leached Ore-B samples before and after the washing of residues in pure HCl at different temperatures.

Ore-B Samples	Cation extraction before washing %			Temp. °C	Cation extraction after washing %		
	Ni	Fe	Mg		Ni	Fe	Mg
1	0.00	91.63	87.32	25	98.53	98.50	97.68
2	0.00	89.28	86.17	50	98.57	98.00	97.45
3	0.00	92.15	88.23	70	98.65	98.56	97.85

Leaching conditions: 10% solid (W/W), 80°C, 6 mol/dm<sup>3</sup> HCl containing 20 g/l Ni and 1 hour contact time.

Washing conditions: 0.01 solid/liquid ratio, 2 mol/dm<sup>3</sup> HCl, 30 minutes contact time and no agitation.

Table 6.10. Cation extraction from leached Ore-B samples before and after the washing of residues in pure HCl with and without agitation

Ore-B Samples	Cation extraction before washing %			Agita- tion	Cation extraction after washing %		
	Ni	Fe	Mg		Ni	Fe	Mg
1	0.00	90.12	87.14	Without	98.73	98.26	97.74
2	0.00	91.30	87.54	With	98.62	98.36	97.65

Leaching conditions: 10% solid (W/W), 80°C, 6 mol/dm<sup>3</sup> HCl containing 20 g/l Ni and 1 hour contact time.

Washing conditions: 0.01 solid/liquid ratio, room temperature, 2 mol/dm<sup>3</sup> HCl and 30 minutes contact time.

#### 6.2.2.2. Contact Time and Solid/Liquid Ratio

To determine the effect of these two variables, residues from samples of Ore-B leached at a pulp density of 30% solid (W/W) were washed with different volumes of pure  $2 \text{ mol/dm}^3$  HCl at room temperature with no agitation for a total of 60 minutes, during which samples of washing solution were taken at 2, 5, 10, 30 and 60 minutes, in order to determine the nickel extraction for different washing times (iron and magnesium were not determined).

Results of these tests are presented in Table 6.11, from which it is clear that nickel extraction during washing is certainly affected by contact time and solid/liquid ratio. Extraction of nickel increases as the washing time increases, almost reaching the maximum attainable between 10 to 30 minutes washing for most of the solid/liquid ratios. This is illustrated in Fig. 6.1, where nickel extraction from residues washed at different solid/liquid ratios is plotted in function of contact time.

As expected, for an increase in the volume of pure HCl (i.e. decreasing the ratio of solid to liquid), the rate and degree of nickel extraction are both increased. This dependence of nickel extraction on the volume of washing solution (refer to Fig. 6.2, where the nickel extraction is replotted as a function of the volume of washing solution) indicates that during washing of the residues (which are a mixture of soluble and insoluble solids plus leaching solution with a high nickel concentration, in this case about  $23.6 \text{ g/l Ni}$ ), nickel concentration in the washing solution has an effect on the nickel extraction similar to that during leaching i.e. the higher the nickel concentration, the lower the nickel extraction. This is confirmed in

Table 6.11. Effect of contact time and solid/liquid ratio upon nickel extraction during the washing of leach residues.

Vol. of leach. sol. mixed with residues.	Vol. of pure HCl	Total wash. solution	Weight* solid	Solid/liquid ratio	Initial nickel conc.wash.sol.	NICKEL EXTRACTION %				
						contact time (minutes)				
ml	ml	ml	gr	gr/ml	g/l Ni	2	5	10	30	60
25	100	125	12	0.0960	4.6	13.49	36.80	44.45	48.28	48.47
25	300	325	12	0.037	1.769	33.52	43.33	48.08	50.69	56.02
25	700	725	12	0.017	0.793	59.90	67.94	81.40	83.72	83.78
25	1000	1025	12	0.012	0.561	79.77	88.82	94.92	94.98	94.98

Washing conditions: room temperature,  $2 \text{ mol/dm}^3$  pure HCl and no agitation

\* average value (see appendix II)

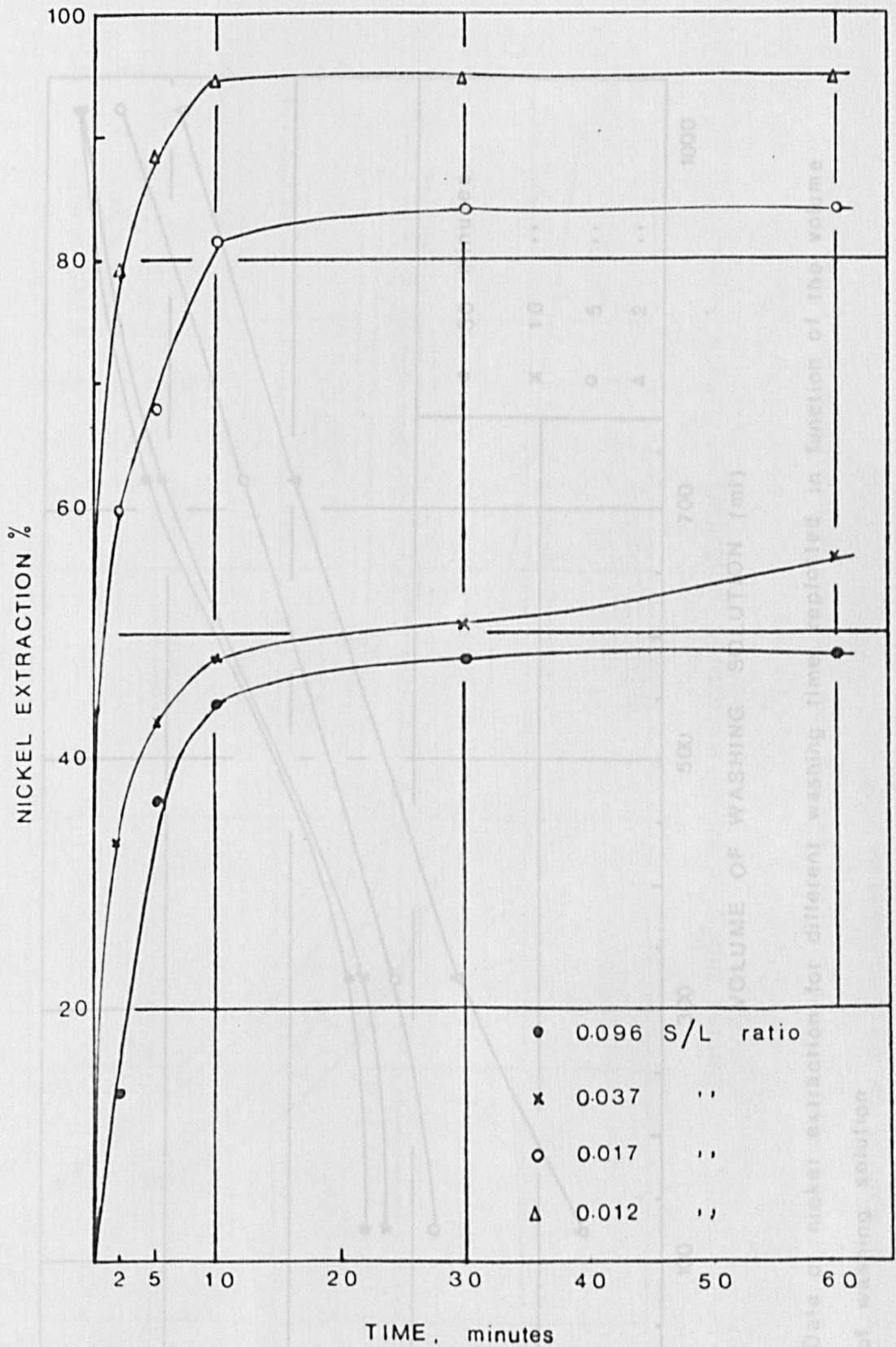


Fig. 6.1 Effect of contact time upon the nickel extraction during the washing of residues at different solid/liquid ratio



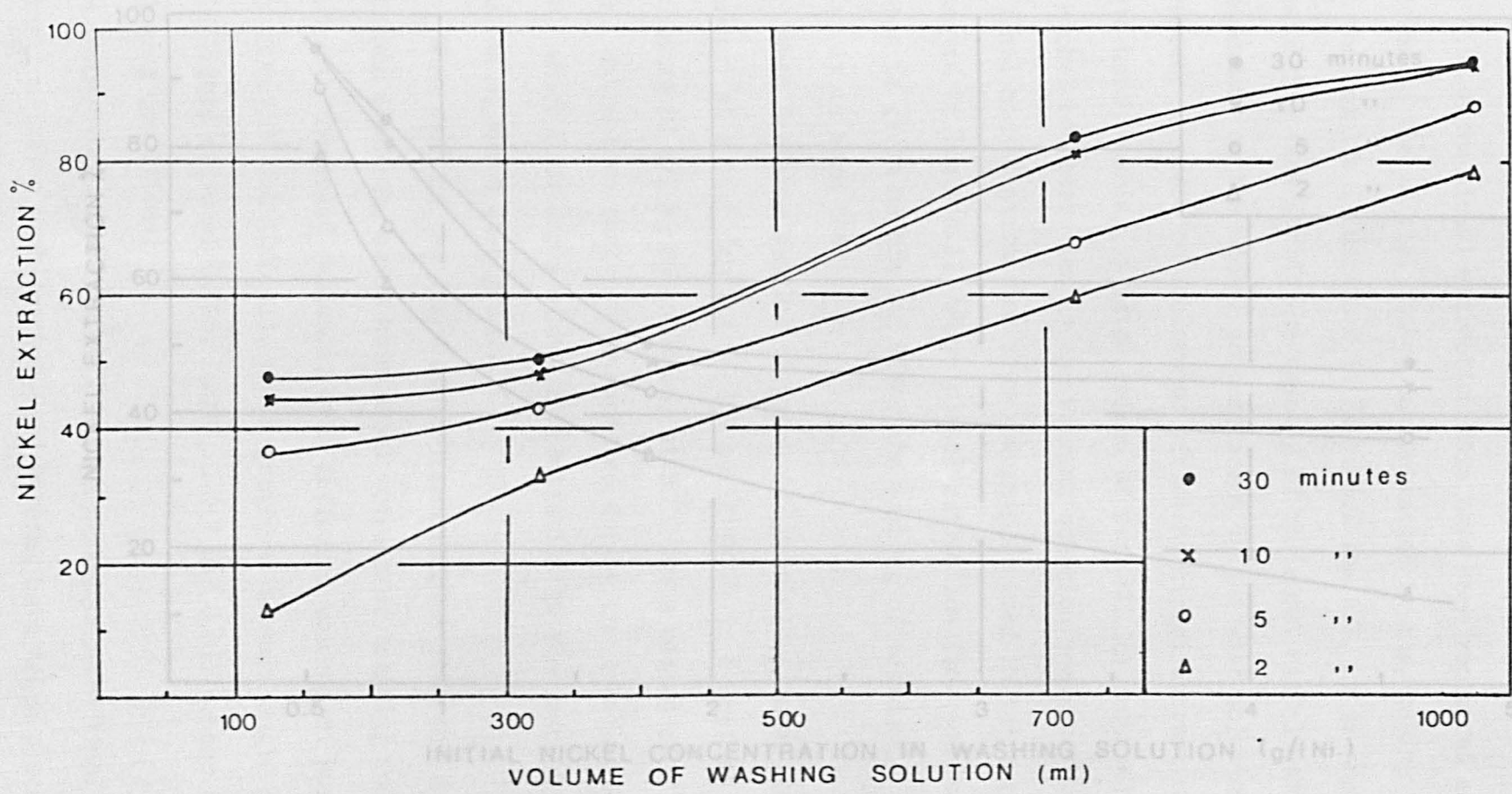


Fig 6.2 Data of nickel extraction for different washing time replotted in function of the volume of washing solution

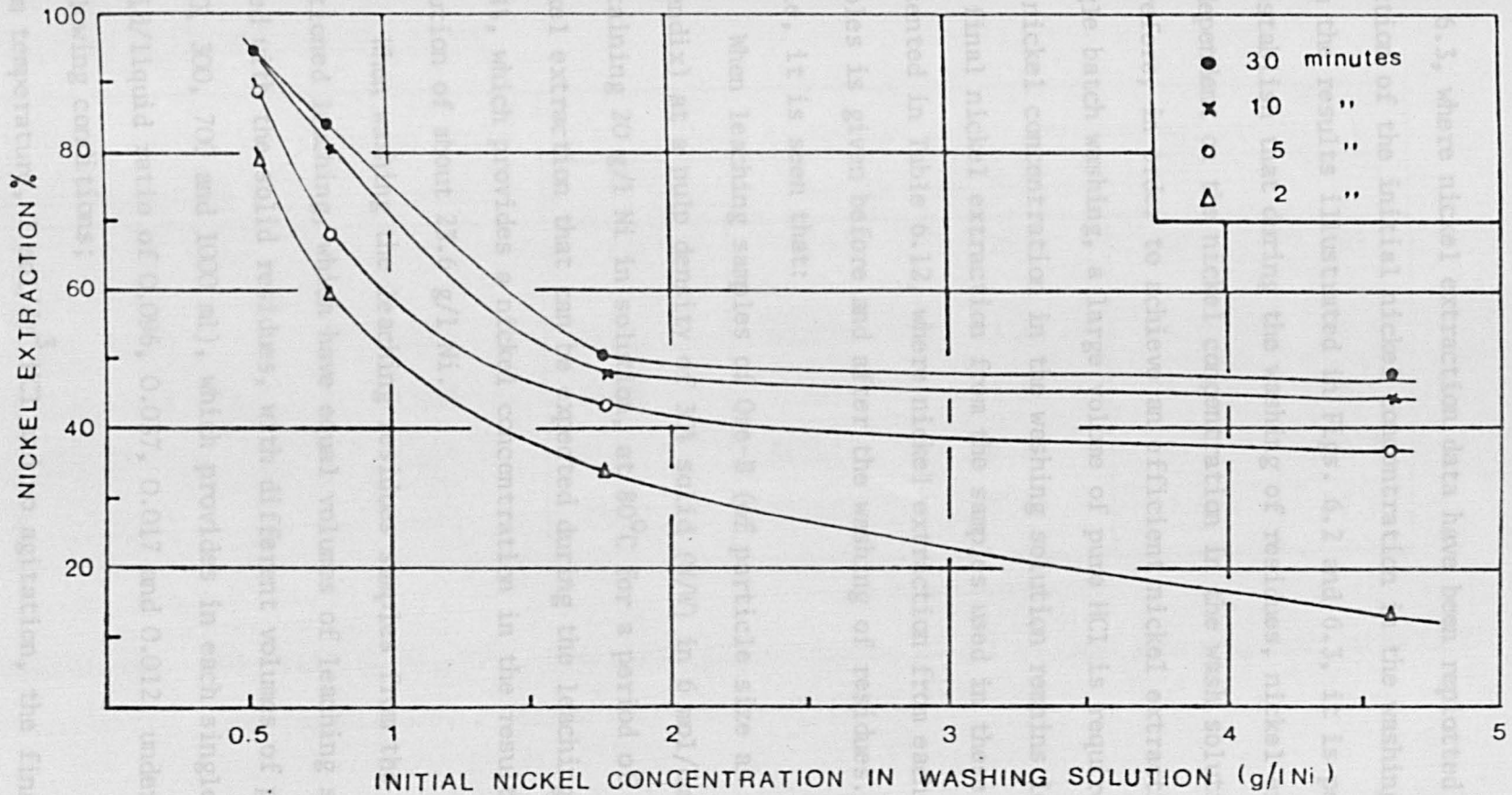


Fig. 6.3 Data of nickel extraction for different washing time replotted in function of the initial nickel concentration in the washing solution

Fig. 6.3, where nickel extraction data have been replotted as a function of the initial nickel concentration in the washing solution. From the results illustrated in Figs. 6.2 and 6.3, it is possible to establish that during the washing of residues, nickel extraction is dependent on the nickel concentration in the wash solution. Therefore, in order to achieve an efficient nickel extraction in a single batch washing, a large volume of pure HCl is required so that the nickel concentration in the washing solution remains low. The final nickel extraction from the samples used in these tests is presented in Table 6.12, where nickel extraction from each of the samples is given before and after the washing of residues. From this table, it is seen that:

- a) When leaching samples of Ore-B (of particle size as shown in appendix) at a pulp density of 30% solid (W/W) in  $6 \text{ mol/dm}^3$  HCl containing 20 g/l Ni in solution, at  $80^\circ\text{C}$  for a period of 1 hour, the nickel extraction that can be expected during the leaching is about 52.4%, which provides a nickel concentration in the resulting leach solution of about 23.6 g/l Ni.
- b) When washing the leaching residues samples from the above mentioned leaching, which have equal volumes of leaching solution mixed with the solid residues, with different volumes of pure HCl (100, 300, 700 and 1000 ml), which provides in each single test a solid/liquid ratio of 0.096, 0.037, 0.017 and 0.012, under the following conditions;  
room temperature,  $2 \text{ mol/dm}^3$  HCl and no agitation, the final nickel extraction (after both leaching and washing have taken place) that can be expected is about 75.3%, 76.4% 92.4% and 97.6% respectively.

Table 6.12. Nickel extraction from leached Ore-B before and after washing of residues at different solid/liquid ratios for different contact times

Ore-B samples	Nickel extraction before washing %	Solid/liquid ratio	Final nickel extraction (after leaching and washing) %				
			contact time (minutes)				
			2	5	10	30	60
1	52.26	0.096	58.70	69.83	73.48	75.31	75.40
2	52.18	0.037	68.21	72.90	75.17	76.42	78.97
3	53.02	0.017	81.16	84.94	91.26	92.35	92.38
4	52.15	0.012	90.32	94.65	97.57	97.60	97.60

Leaching conditions: 30% solid (W/W), 80°C, 6 mol/dm<sup>3</sup> HCl containing 20 g/l Ni, and 1 hour contact time.

Washing conditions: room temperature, 2 mol/dm<sup>3</sup> HCl and no agitation.

It should be noted that extraction data given are those values obtained for 30 minutes washing, because beyond this washing time, the increase on nickel extraction is insignificant.

The results in Tables 6.5 to 5.7 and 6.11 have shown that the contact time and volume of pure HCl are the only variables which affect nickel extraction during washing. Acid concentration, temperature and agitation did not show any influence.

From the results presented in Tables 6.5 to 6.12, it is possible to determine the most favourable washing conditions for an efficient nickel extraction in a single-stage wash. At the same time, these results provide the basis for a study of nickel extraction in multi-stage washing systems.

### 6.3 Multistage Batch Cross-Current Washing

Earlier in this chapter, it was demonstrated that nickel extraction during the washing of residues is dependent on the nickel concentration in the washing solution, the lower the nickel concentration, the higher the nickel extraction. This indicates that the nickel concentration in the leaching solution and the volume of this solution mixed with the solid residue are of great importance when determining the volume of pure HCl in which the residues should be washed. Obviously, a large volume of pure HCl will give a low nickel concentration in the washing solution, allowing efficient nickel extraction to be achieved. This is clearly demonstrated during the washing of residues in a single batch stage. However, it might also be possible that an efficient nickel extraction could be obtained if residues were successively contacted with small volumes of pure HCl in a cross-current washing

system, as shown in Fig. 6.4.

From this figure, it can be seen that to wash the residues in a multistage cross-current system is nothing more than an extension of a single-stage washing, in which the feed to any stage (except the first stage) is the underflow (containing the solid residues plus solution) from the preceding stage. Therefore, if the volume of solution mixed with the solid residues in the feed to each stage is kept constant, by adding pure HCl at each stage, the nickel concentration in the wash solution will decrease as the number of stages increase, which should allow an efficient nickel extraction to be achieved.

Undoubtedly, the degree of nickel extraction that could be achieved will depend on the volume of pure HCl used to contact the slurry residues at each stage, and on the number of washing stages. Thus, the subsequent work described in this chapter is concerned with a study of nickel extraction during the washing of residues in a multistage cross-current system, involving these two variables.

To perform this study, residues from samples of Ore-B, leached in HCl solutions containing 20 g/l Ni (30% solid, 80°C, 6 mol/dm<sup>3</sup> and 1 hour contact time) were used, and the general washing conditions for each experiment were; room temperature, 6 mol/dm<sup>3</sup> (pure HCl), 30 minutes contact time for each stage and no agitation.



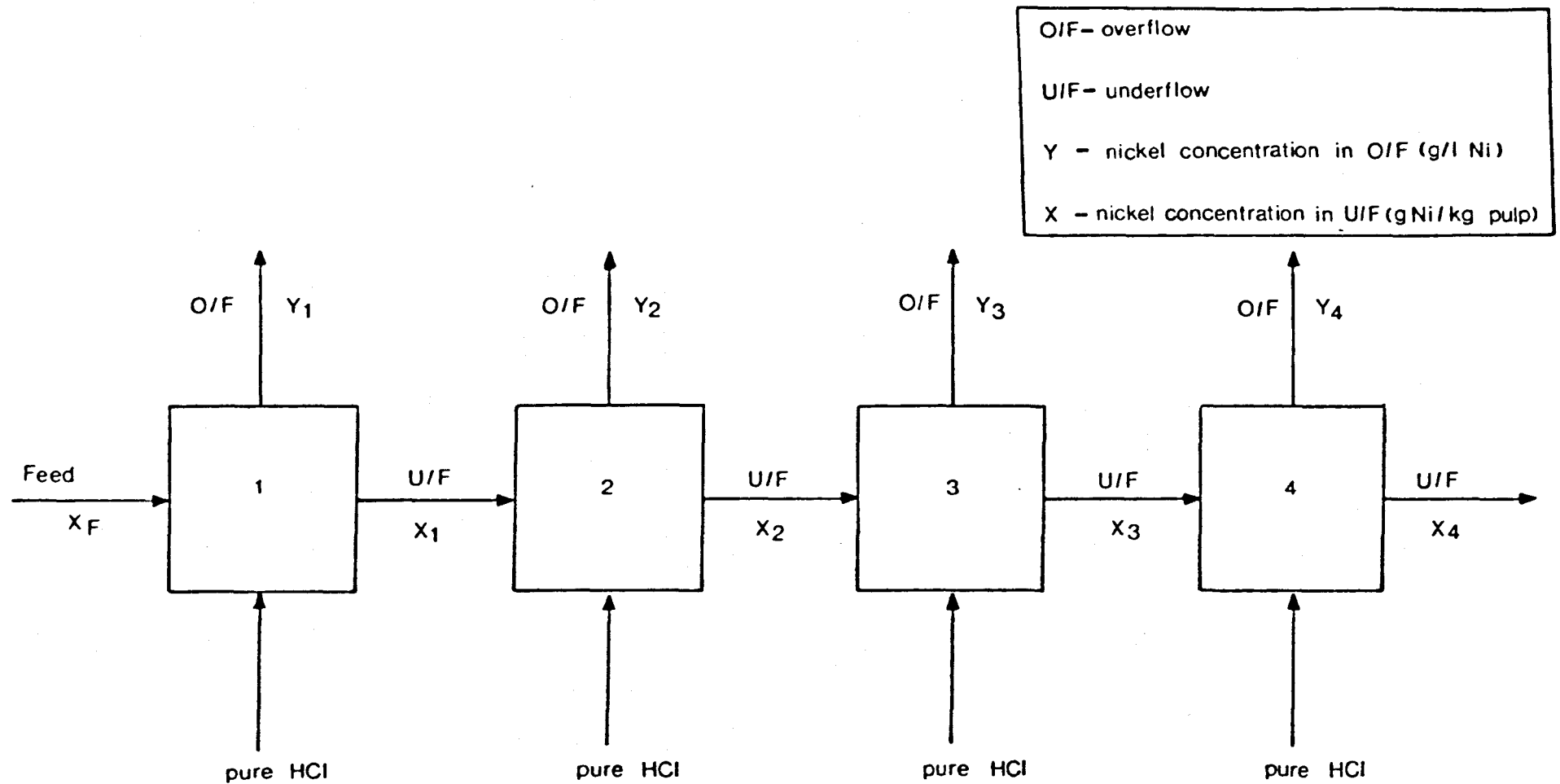


Fig. 6-4. Conceptual representation of a cross-current washing, (4 stages)

### 6.3.1. Washing of Residues in a 4-stage Cross-current System

In four separate experiments, leach residue samples each containing equal volumes of leach liquor (25 ml with a nickel concentration of about 23.6 g/l Ni), were successively washed with equal volumes of pure HCl of 10, 25, 50 and 100 ml respectively for each experiment. Each washing stage involved the introduction and removal of equal volume of solution, so that the ratio of solution in overflow to solution in underflow was constant for each stage in each experiment. See Table 6.13

Table 6.13. Addition and removal of solution in each washing stage.

Test No.	Solution in residues	Addition of pure HCl	Total volume of washing solution	Solution in overflow	Solution in underflow
	ml	ml	ml	ml	ml
1	25	10	35	10	25
2	25	25	50	25	25
3	25	50	75	50	25
4	25	100	125	100	25

The results of these four tests are presented in Tables 6.14 to 6.17, where most of the data were obtained by analysis of the overflow solutions. This was because of the impossibility of performing analysis on the solid residues. In the first place, the amount of solid residue being washed was relatively small (as little ore was available) so that any withdrawal of solid samples (which would also carry some solution) would definitely affect the test as a whole. Secondly, and more important, as an

Table 6.14. Data of Cross-current Washing (4 stages) using 10 ml of Pure HCl to Contact the Slurry Residues in Each Stage (Test 1)

Washing stages No.	Nickel content in feed to each stage		Initial Ni Conc. in wash. sol.	Nickel concentration after washing		NICKEL EXTRACTION (cumulative)
	Solid	Solution		overflow	underflow	
	gm	gm		g/l Ni	g/l Ni	g Ni/kg pulp*
1	0.1646	0.59	16.86	17.38	15.77	11.12
2	0.1463	0.4345	12.41	12.87	12.28	20.78
3	0.1303	0.3218	9.19	9.74	9.64	32.38
4	0.1113	0.2435	6.96	7.32	7.65	40.10
+ 5	0.0986	0.183				

+ Residues

Washing conditions: room temperature,  $6 \text{ mol/dm}^3$  (pure HCl), 30 minutes contact time (each stage) and no agitation.

\*Weight of nickel (dissolved + undissolved) per unit mass of pulp on a nickel-free basis.

Weight of dry solid after washing: about 11.92 gm.

Volume of solution discharged in overflow: 10 ml.

Volume of solution discharged in underflow: 25 ml.

Table 6.15. Data of Cross-current Washing (4-stage) using 25 ml of pure HCl to Contact the Slurry Residues in Each Stage (Test 2).

Washing stages No	Nickel content in feed to each stage		Initial Ni conc. in wash. sol.	Nickel concentration after washing		NICKEL EXTRACTION (cumulative)
	Solid	Solution		overflow	underflow	
	gm	gm	g/l Ni	g/l Ni	g Ni/Kg pulp*	%
1	0.1661	0.5893	11.79	12.59	11.91	24.20
2	0.1259	0.3148	6.30	6.87	7.27	41.48
3	0.0972	0.1718	3.44	3.70	4.77	49.43
4	0.084	0.0925	1.85	2.35	3.18	64.48
+5	0.059	0.0588				

+ Residues

Washing conditions: room temperature,  $6 \text{ mol/dm}^3$  (pure HCl), 30 minutes contact time (each stage) and no agitation.

\*weight of nickel (dissolved + undissolved) per unit mass of pulp on a nickel-free basis.

Weight of dry solid after washing: 12.07 gm

Volume of solution discharged in overflow: 25 m.

Volume of solution discharged in underflow: 25 ml.

Table 6.16. Data of Cross-current Washing (4 stage) using 50 ml of Pure HCl to Contact the Slurry Residues in Each Stage (Test 3).

Washing stages No.	Nickel content in feed to each stage		Initial Ni conc. in wash. sol. g/l Ni	Nickel concentration after washing		NICKEL EXTRACTION (cumulative) %
	Solid	Solution		overflow	underflow	
	gm	gm		g/l Ni	g Ni/kg pulp*	
1	0.1648	0.5898	7.86	8.71	8.66	38.47
2	0.1014	0.2178	2.90	3.20	4.32	51.94
3	0.0792	0.08	1.07	1.58	2.18	75.30
4	0.0407	0.0395	0.53	0.93	0.92	93.63
+ 5	0.0105	0.0233				

+ Residues

Washing conditions: room temperature,  $6 \text{ mol/dm}^3$  (pure HCl), 30 minutes contact time (each stage) and no agitation.

\*Weight of nickel (dissolved + undissolved) per unit mass of pulp on a nickel-free basis.

Weight of dry solid after washing: 11.87 gm.

Volume of solution discharged in overflow: 50 ml.

Volume of solution discharged in underflow: 25 ml.

Table 6.17. Data of Cross-current Washing (4 stage) using 100 ml of Pure HCl to Contact the Slurry Residues in Each Stage (Test 4).

Washing stages No.	Nickel content in feed to each stage		Initial Ni conc. in wash. sol.	Nickel concentration after washing		NICKEL EXTRACTION (cumulative) %
	Solid	Solution		overflow	underflow	
	gm	gm	g/l Ni	g/l Ni	g Ni/kg pulp*	
1.	0.1645	0.59	4.72	5.36	5.93	48.63
2.	0.0845	0.134	1.07	1.41	2.11	74.29
3	0.0423	0.0353	0.28	0.55	0.62	94.59
4	0.0089	0.0138	0.11	0.12	0.29	95.32
+ 5	0.0077	0.003				

+ Residues

Washing conditions: room temperature,  $6 \text{ mol/dm}^3$  (pure HCl), 30 minutes contact time (each stage) and no agitation.

\*Weight of nickel (dissolved + undissolved) per unit mass of pulp on a nickel-free basis.

Weight of dry solid after washing: about 11.85 gm.

Volume of solution discharged in overflow: 100 ml.

Volume of solution discharged in underflow: 25 ml.



analysis of solid samples from the underflow stream of any intermediate washing stage, or even from the last would produce inaccurate results, unless a perfect solid/liquid separation could be achieved or the solution mixed with the solid residues did not contain nickel and no further nickel could be extracted. The reason for this has already been discussed in Chapter 3, Section 3.3.1. and will not be discussed again.

Figs. 6.5 and 6.6 show plots of the experimental "equilibrium" distribution curve for nickel between the overflow and underflow streams for each of these washing tests, from which it is possible to determine the nickel concentration in the overflow solution and in the underflow slurry leaving each washing stage. The values given for the underflow stream include the nickel undissolved in the solid residues plus the nickel dissolved in the washing solution mixed with solid residues. It should be mentioned that in order to plot the distribution curve, it has been assumed that after 30 minutes washing, a practical "equilibrium" has been reached (on the basis of previous results obtained for the washing of residues in a single batch stage, see Table 6.11), so that the washing solution mixed with the solid residues in the underflow has the same nickel concentration to that in the washing solution of the overflow.

From these figures, it may be seen that for tests 1 and 2, during the earlier washing stages, where the nickel concentration in the washing solution is still relatively high, the distribution curve is practically a straight line, but as the washing proceeds and the nickel concentration in the washing solution becomes lower, the curvature of the distribution curve starts to become gradually more pronounced. This indicates that

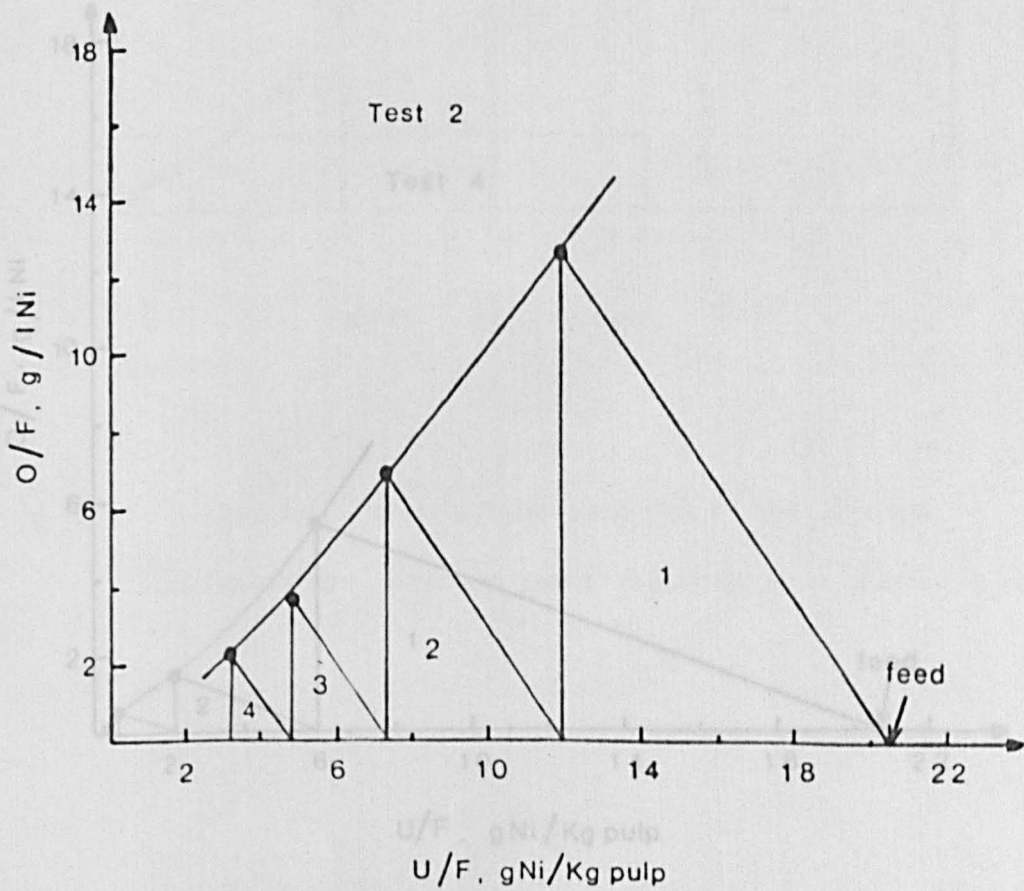
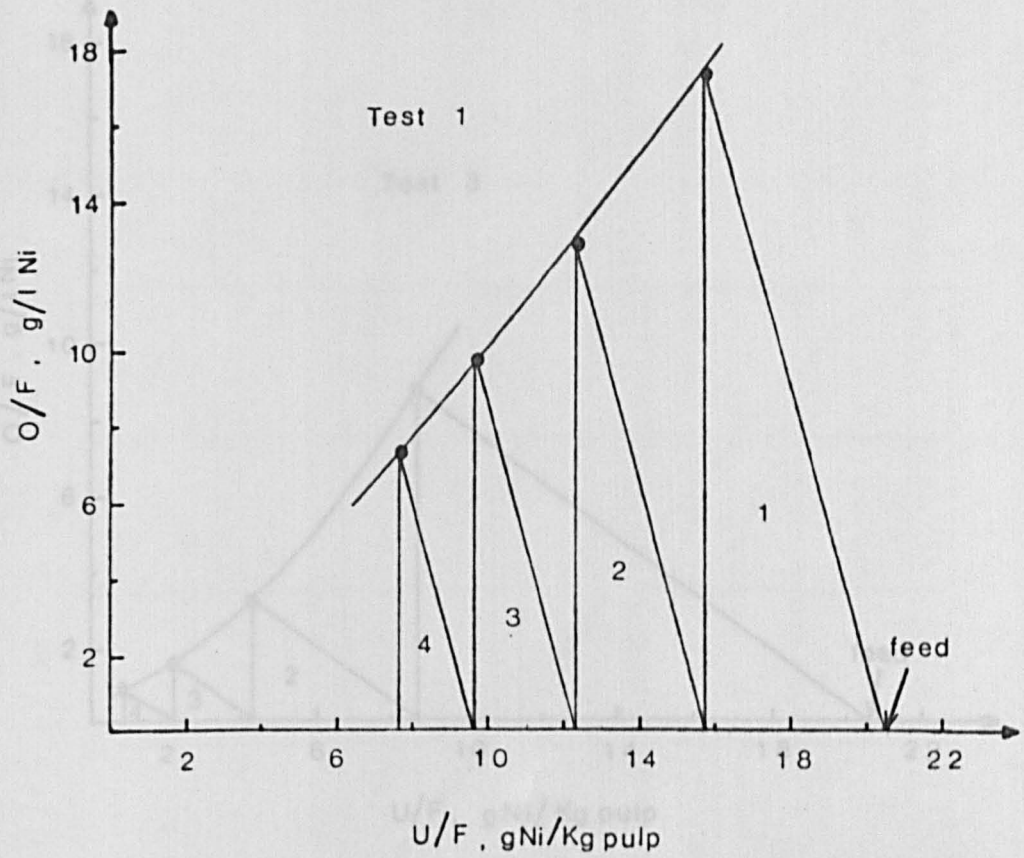


Fig. 6.5 Experimental "equilibrium" distribution curves of the 4-stage cross-current washing tests (1 & 2)

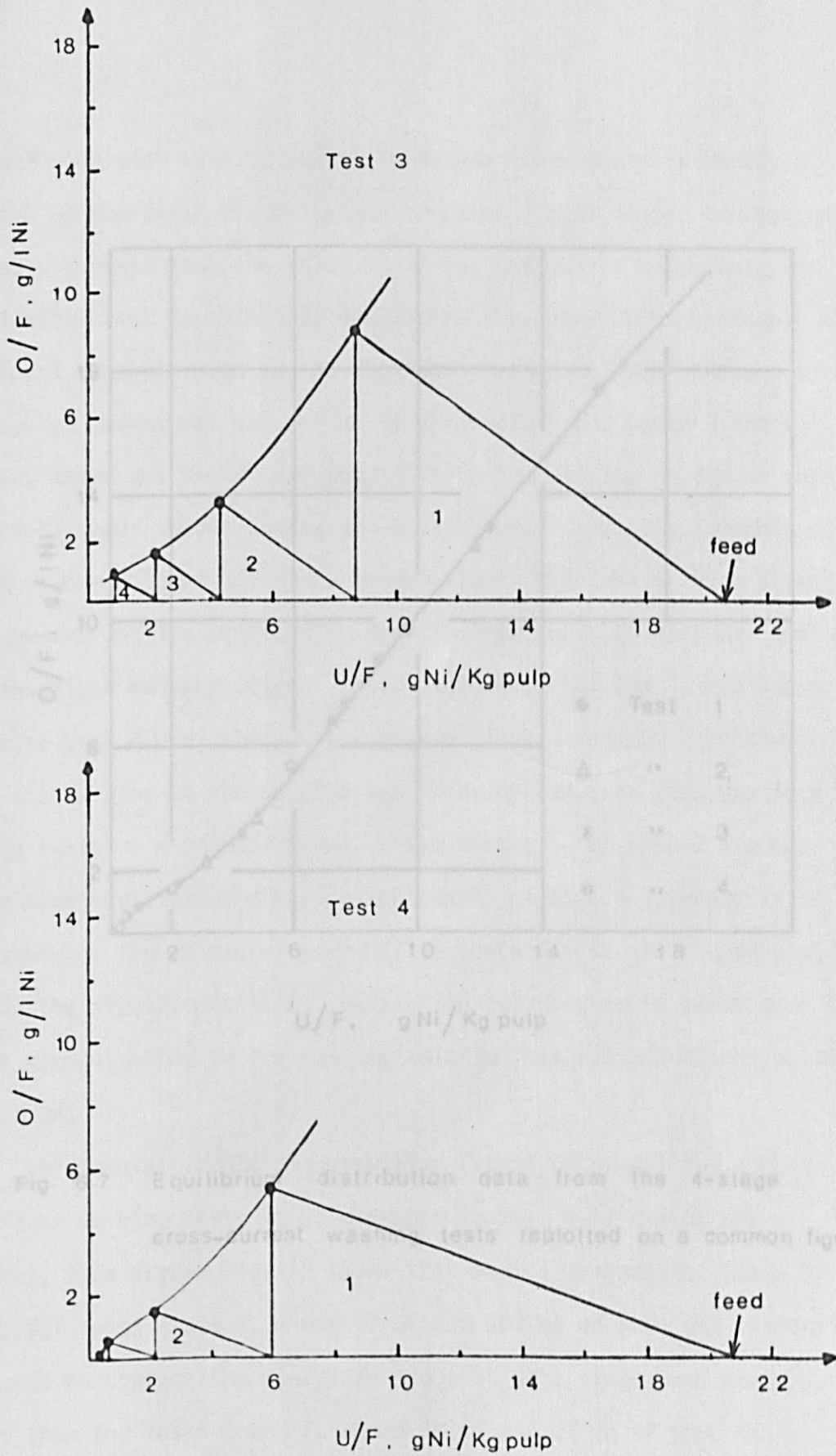
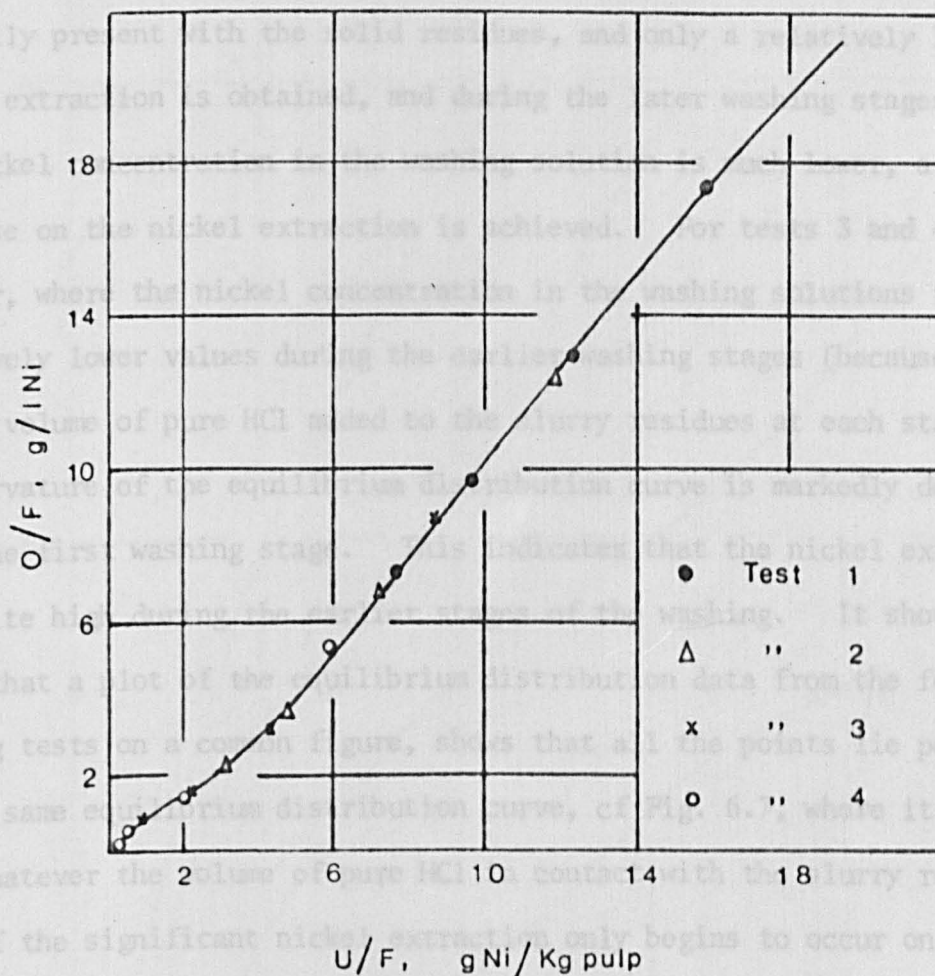


Fig. 6.6 Experimental "equilibrium" distribution curves of the 4-stage cross-current washing tests (3 & 4)

during the earlier washing stages, what has taken place is merely a dilution of the leach liquor (which contains a high nickel concentration) initially present with the solid residues, and only a relatively low nickel extraction is obtained, and during the later washing stages, where the nickel concentration in the washing solutions reached a gradual increase on the nickel extraction is achieved. However, for tests 3 and 4, however, where the nickel concentration in the washing solutions reached relatively lower values during the earlier washing stages (because of the larger volume of pure HCl added to the slurry residues at each stage), the curvature of the equilibrium distribution curve is markedly defined from the first washing stage. This indicates that the nickel extraction was quite high during the earlier washing stages. It should be noted that a plot of the equilibrium distribution data from the four washing tests on a common figure, shows that all the points lie perfectly on the same equilibrium distribution curve, as Fig. 6.7, where it is clear that whatever the volume of pure HCl added to the slurry residues, most of the significant nickel extraction only begins to occur once the nickel concentration in the washing solution has reached values below about 5 g/l Ni.

Fig. 6.7 "Equilibrium" distribution data from the 4-stage cross-current washing tests replotted on a common figure

As expected, this figure clearly shows that nickel extraction, stage by stage, for tests 3 and 4, where 50 ml and 100 ml of pure HCl respectively were used to contact the slurry residues at each stage, was much better than for tests 1 and 2, where 10 ml and 25 ml of pure HCl respectively were used to contact the slurry residues at each stage. After four washing stages, the nickel extraction achieved for tests



during the earlier washing stages, what has taken place is merely a dilution of the leach liquor (which contains a high nickel concentration) initially present with the solid residues, and only a relatively low nickel extraction is obtained, and during the later washing stages, where the nickel concentration in the washing solution is much lower, a gradual increase on the nickel extraction is achieved. For tests 3 and 4 however, where the nickel concentration in the washing solutions reached relatively lower values during the earlier washing stages (because of the larger volume of pure HCl added to the slurry residues at each stage), the curvature of the equilibrium distribution curve is markedly defined from the first washing stage. This indicates that the nickel extraction was quite high during the earlier stages of the washing. It should be noted that a plot of the equilibrium distribution data from the four washing tests on a common figure, shows that all the points lie perfectly on the same equilibrium distribution curve, cf Fig. 6.7, where it is clear that whatever the volume of pure HCl in contact with the slurry residues, most of the significant nickel extraction only begins to occur once the nickel concentration in the washing solution has reached values below about 5 g/l Ni.

The cumulative nickel extraction (stage by stage) for each of these four washing tests is illustrated in Fig. 6.8, and as was expected, this figure clearly shows that nickel extraction, stage by stage, for tests 3 and 4, where 50 ml and 100 ml of pure HCl respectively were used to contact the slurry residues at each stage, was much better than for tests 1 and 2, where 10 ml and 25 ml of pure HCl respectively were used to contact the slurry residues at each stage. After four washing stages, the nickel extraction achieved for tests



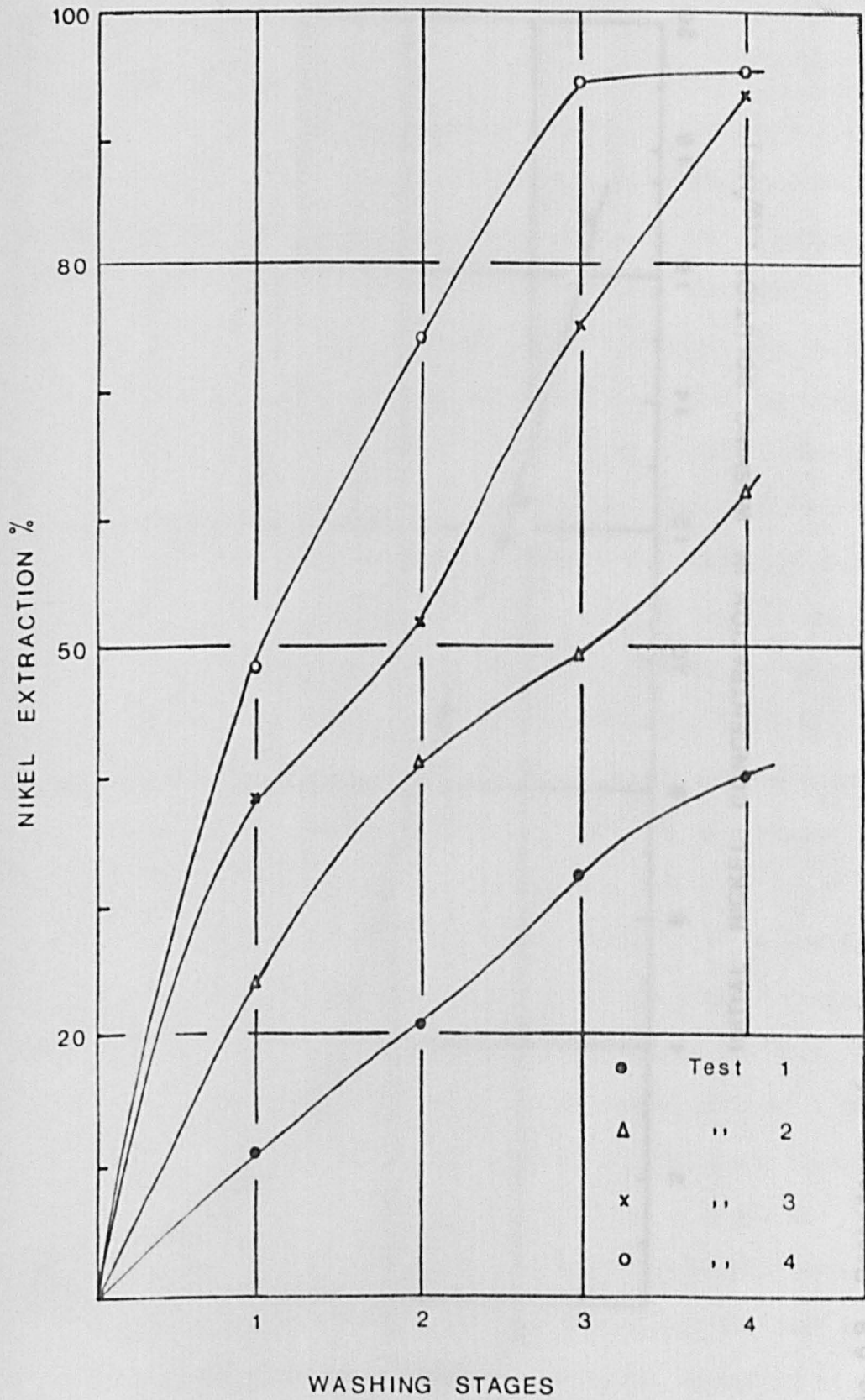


Fig. 6.8 Cumulative nickel extraction for tests 1 to 4



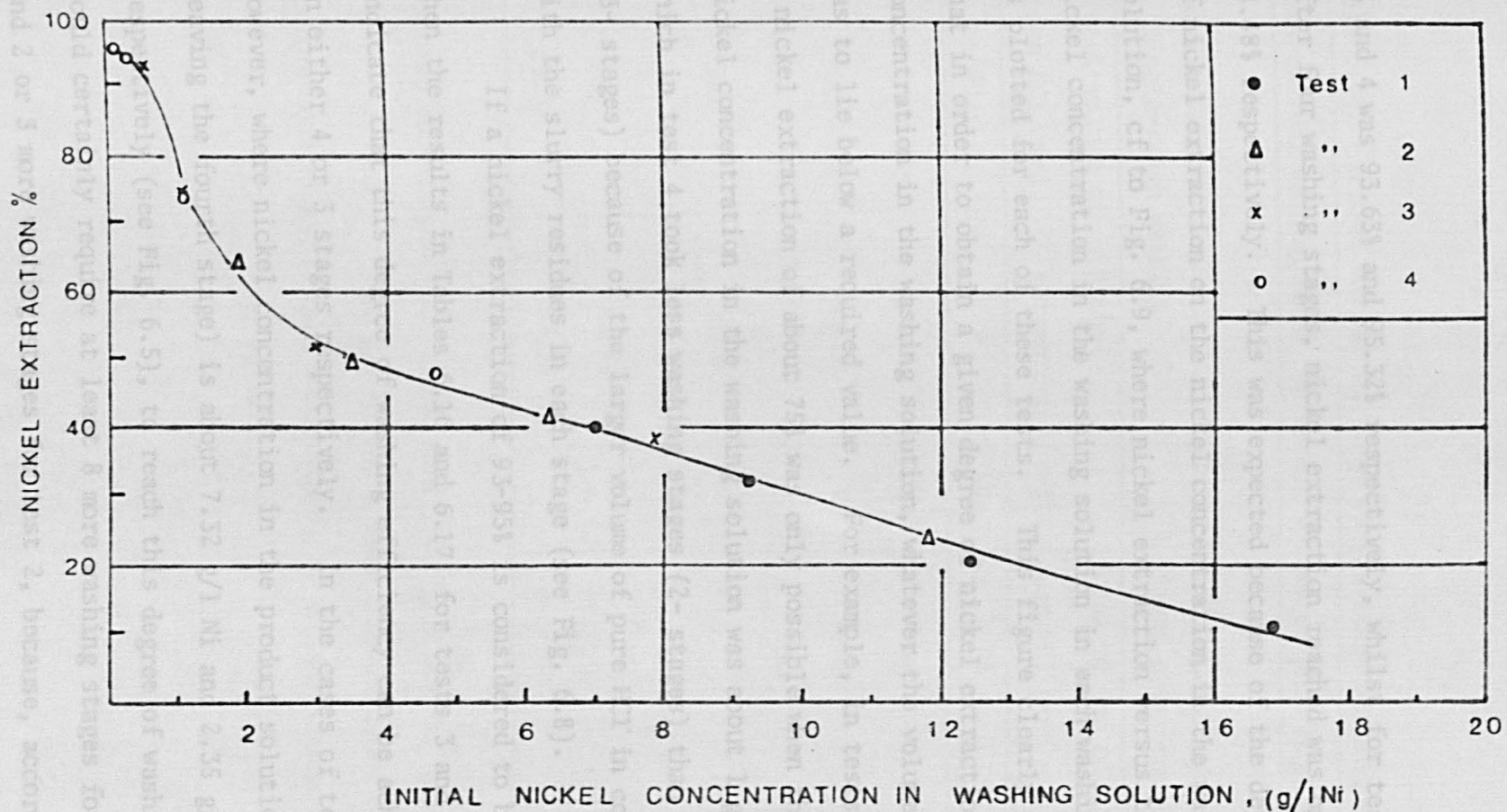


Fig. 6.9 Dependence of nickel extraction on the initial nickel concentration in the washing solution

3 and 4 was 93.63% and 95.32% respectively, whilst for tests 1 and 2, after four washing stages, nickel extraction reached was only 40.1% and 64.48% respectively. This was expected because of the dependence of nickel extraction on the nickel concentration in the washing solution, cf to Fig. 6.9, where nickel extraction versus the initial nickel concentration in the washing solution in each washing stage is plotted for each of these tests. This figure clearly demonstrates that in order to obtain a given degree of nickel extraction, the nickel concentration in the washing solution, whatever the volume of solution, has to lie below a required value. For example, in tests 3 and 4, a nickel extraction of about 75% was only possible when the initial nickel concentration in the washing solution was about 1 g/l Ni., which in test 4 took less washing stages (2- stages) than in test 3 (3- stages) because of the larger volume of pure HCl in contact with the slurry residues in each stage (see Fig. 6.8).

If a nickel extraction of 93-95% is considered to be desirable, then the results in Tables 6.16 and 6.17, for tests 3 and 4 clearly indicate that this degree of washing efficiency can be achieved in either 4 or 3 stages respectively. In the cases of tests 1 and 2, however, where nickel concentration in the product solution (i.e. leaving the fourth stage) is about 7.32 g/l Ni and 2.35 g/l Ni respectively (see Fig. 6.5), to reach this degree of washing efficiency would certainly require at least 8 more washing stages for test 1, and 2 or 3 more washing stages for test 2, because, according to Fig. 6.9, to reach a nickel extraction of 93-95%, nickel concentration in the washing solution has to drop to about 0.5 g/l Ni. Results of

Table 6.18. Nickel extraction from single-stage washing and 4-stages cross-current washing using different volume of pure HCl.

Single-stage washing		4-stages cross-current washing		
total volume of pure HCl used	nickel extraction	test	total volume of pure HCl used	nickel extraction
ml	%	No	ml	%
100	48.28	1	40	40.10
		2	100	64.48
		3	200	93.63
300	50.69	4	400	95.32
700	83.72			
1000	94.98			

Leaching conditions: 30% solid (W/W), 80°C, 6 mol/dm<sup>3</sup> HCl containing 20 g/l Ni and 1 hour contact time.

Washing conditions: room temperature, 30 minutes contact time and no agitation.

a 10-stage cross-current washing test, where the same conditions as test 1 were used, are given in appendix II, and here it is shown that after 10 washing stages (where the nickel concentration in the overflow was 1.6 g/l Ni) a nickel extraction of only 67.02% was reached.

The results of these four tests provide good evidence that in cross-current washing, where the volume of solution mixed with the solid residues in the underflow stream at each stage is constant, the number of washing stages and the volume of pure HCl contacting the slurry residues in each washing stage are the main factors that determine the degree of nickel extraction which can be reached. It is also shown by these tests, that the total volume of pure HCl used in a cross-current washing is much less than that required for a similar degree of nickel extraction in a single stage batch washing, cf to Table 6.18.

The total nickel extractions (after both leaching and washing have taken place) for each of these four tests are given in Table 6.19.

Table 6.19. Total nickel extraction from Ore-B samples after leaching and washing of leaching residues in cross-current (4 stages).

Test	Extraction
No	%
1	71.37
2	82.87
3	96.95
4	97.76

#### 6.4 Multistage Batch Counter-Current Washing.

It has already been shown in this chapter that by washing the leach residues in a single stage batch system or in a multistage batch cross-current system, efficient nickel extraction can be achieved. However, one of the main drawbacks when using either of these two washing systems is the inconveniently low nickel concentration which is provided in the final product solution. Therefore, it was considered that by using a multistage counter-current washing system, the problem might be overcome. The subsequent work in this chapter describes a study of the extent to which the washing of leach residues counter-currently can provide a high nickel concentration in the product solution together with efficient nickel extraction.

##### 6.4.1. Washing System

Before discussing the experimental work, a multistage counter-current washing system will first be defined. Consider a system of "n" washing stages, as shown in Fig. 6.10. The residues entering stage 1 will progress towards the right contra to the washing solution which moves from right to left entering the nth stage. The volume of washing solution (pure HCl) entering stage n is V and the mass of slurry residues (on a nickel-free basis) entering stage 1 is  $W = v + w$ , where v is the mass of leach liquor associated with the solid residues and w is the mass of insoluble solid residues (both v and w are on a nickel-free basis).  $Y_h$  refers to the nickel concentration in the washing solution leaving the hth stage and is expressed as g/l Ni,  $X_h$  refers to the nickel concentration in the slurry residues entering the hth stage and is expressed as g Ni/Kg pulp. Thus,  $X_1$  and  $X_{n+1}$  refer to the nickel concentrations in the slurry residues entering

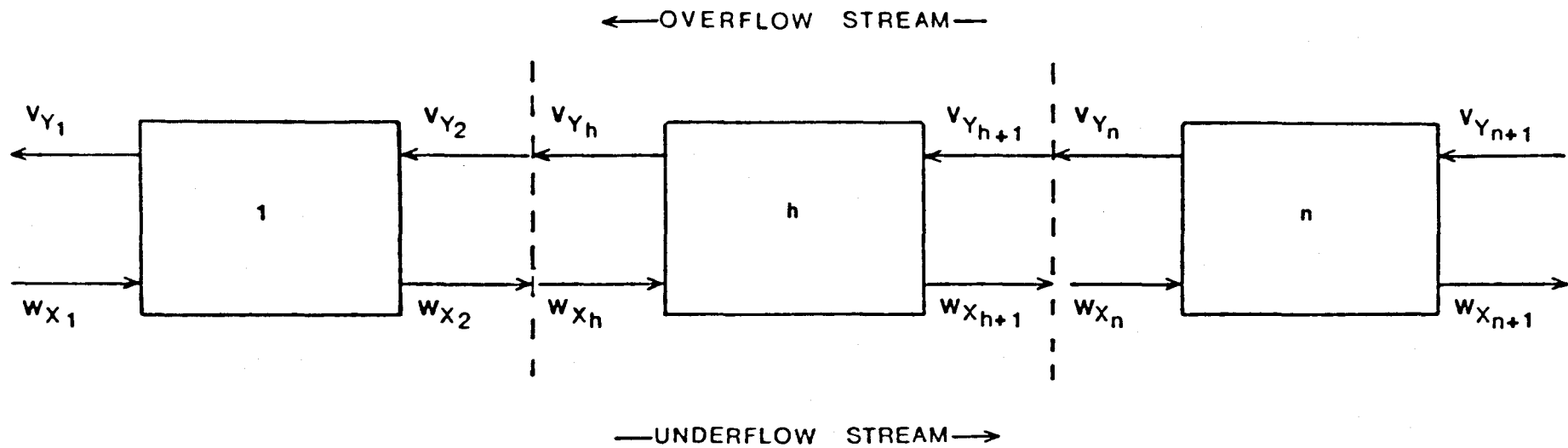


Fig. 6.10 Conceptual representation of a multistage counter-current washing system



and leaving the washing system respectively, and  $Y_{n+1}$  and  $Y_1$  the nickel concentration in the washing solution entering and leaving the washing system respectively. Note, that  $Y_{n+1} = 0$ , because pure HCl is used.

It should be mentioned that although in solid-liquid operations of this kind, it is common use to express the solute concentration in the overflow stream as mass of solute per unit mass of pure solvent and in the underflow stream as mass of solute per unit mass of insoluble solid, or in some cases both streams as mass of solute per unit mass of insoluble solid (97-99), in this, for convenience and in order to keep a continuity with those units used in previous experiments, it was decided to express the nickel concentration in the overflow stream as mass of solute per unit volume of pure wash solution and in the underflow stream as mass of solute per unit mass of pulp.

In each washing stage of this system, the volume of wash solution, referred to as the overflow, and a mixture of solid residue and solution, referred to as the underflow, were brought into contact for a given period of time, allowing a 'practical equilibrium' to be reached, so that the solution leaving in the overflow has the same composition as that associated with the solid residues in the underflow. (This is on the assumption that no adsorption occurs during the washing). Now, if in this washing system, it is established that the volume of solution removed with the solid residues in the underflow from each washing stage is the same, then the volume of solution removed in the overflow from each stage is also the same. Hence,  $R$ , the ratio of solution discharged in the overflow to that in the underflow is constant.

$$R = \frac{\text{Volume of solution discharged in the overflow}}{\text{Volume of solution discharged in the underflow}} \quad 6.1$$

Usually in solid-liquid extraction operations, where a solid material containing a desirable solute is brought into contact with an extracting solvent, it is common practice to assume that the original solid is an inert material and therefore has no influence on the solute; that is, there is no chemical bonding between the two nor any adsorption of solute onto the solid. Because of this simplified situation, the solute will dissolve completely in the solvent and partitioning occurs only by the wetting of the solid by this same solution<sup>(100)</sup>. By using a similar type of approach to this counter-current washing system, it may be possible to say that if the nickel in the solid residues entering the washing system has no chemical bonding with the insoluble solid and no adsorption occurs, the total amount of nickel (in leaching solution plus in solid) entering the system can be assumed to be already dissolved in the leach liquor associated with the solid residues. Therefore, because of this assumption, "the counter-current washing extraction system" is reduced to simple "counter-current washing", where the leach liquor associated with the solid residues feeding the system will be progressively diluted in  $n$  stages by a wash solution flowing in the opposite direction<sup>(97)</sup>.

Now, let a mass balance on nickel over stages  $h$  to  $n$  inclusive be written:

$$V (Y_h - Y_{n+1}) = W (X_h - X_{n+1}) \quad 6.2$$

or

$$Q (Y_h - Y_{n+1}) = (X_h - X_{n+1}) \quad 6.3$$

where  $Q = V/W$ , and is an expression of a control parameter for the system.

Rearranging equation 6.3 gives

$$Y_h = \frac{X_h}{Q} - \frac{X_{h+1}}{Q} + Y_{h+1} \quad 6.4$$

This equation, usually called "the operating solution" show that a linear relation exists between  $Y_h$  and  $X_h$ .

On the basis of the latter stated assumption (the total amount of nickel entering the system is already dissolved in the leach liquor associated with the solid residues), it is obvious that the distribution of nickel between the overflow and underflow streams depends on the volume of solution held by the solid residues in the underflow. Thus the distribution constant  $R$  is given at any stage by:

$$R = \frac{\text{Volume of solution in the overflow}}{\text{Volume of solution in the underflow}} = \frac{\text{Amount of nickel in the overflow}}{\text{Amount of nickel in the underflow}}$$

and since it is assumed that each washing stage in Fig. 6.10 represents an equilibrium stage, the overflow leaving the hth stage is in equilibrium with the underflow leaving the hth stage. Thus;

$$R = V/v' = V(Y_h) / W(X_{h+1}) = Q(Y_h) / (X_{h+1}) \quad 6.5$$

where,  $v'$  is the volume of solution held by the solid residues in the underflow.

Rearranging this equation gives

$$Y_h = \frac{R}{Q} (X_{h+1}) \quad 6.6$$

which is a straight line expression of slope  $R/Q$  and is usually called "the equilibrium equation".

As equation 6.4 and 6.6 are both straight line expressions, and the two lines represent the relation between  $Y_h$  and both  $X_h$  and  $X_{h+1}$ ,

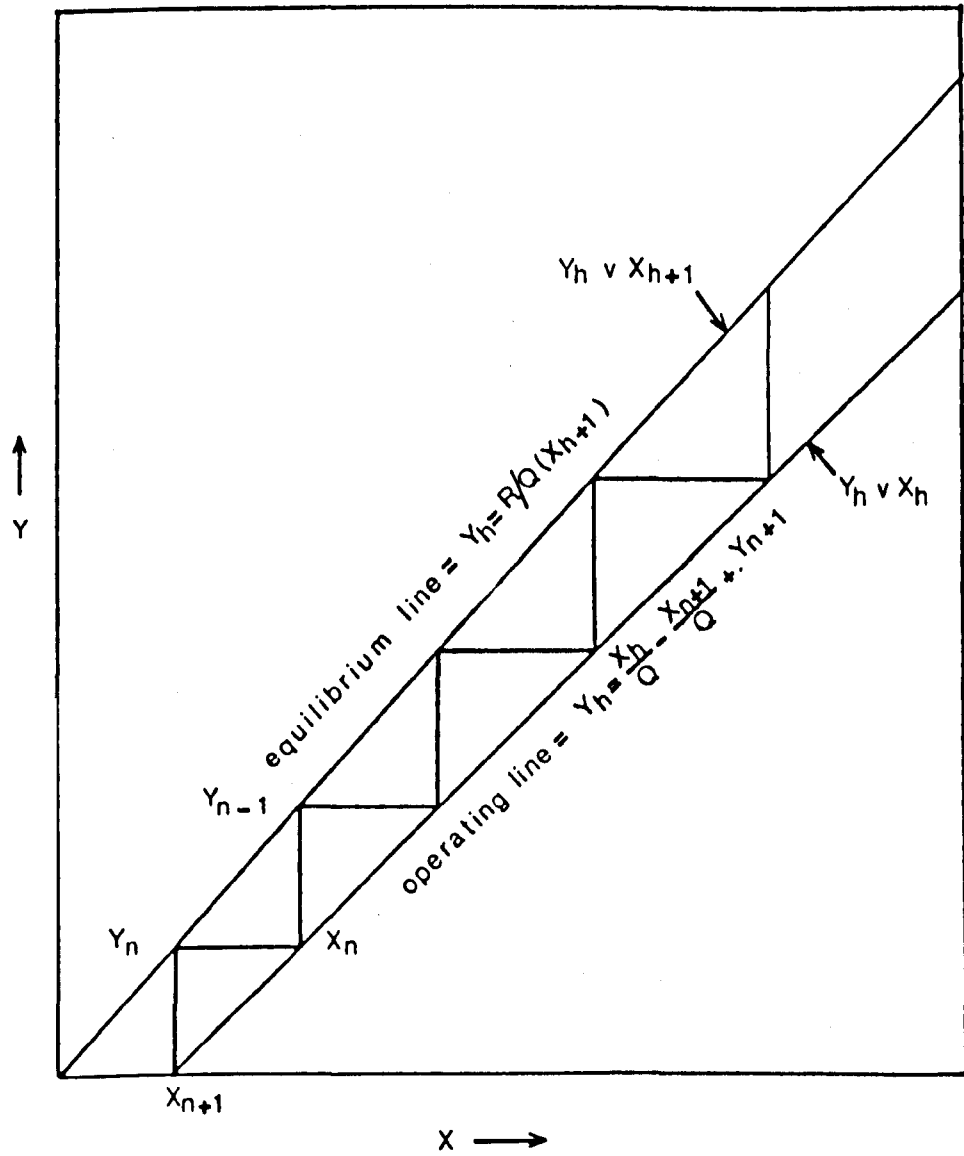


Fig. 6.11 Graphical estimation of equilibrium stages in a counter-current washing system

by graphing these on a Y-X diagram, the change in composition (stage by stage) of the underflow and overflow streams can be easily determined by a simple stepwise construction as shown in Fig. 6.11. Starting at  $X_{n+1}$  (the intercept of equation 6.4 on the X axis) a vertical line intersecting the equilibrium line gives  $Y_n$ . From  $Y_n$ , a horizontal line intersecting the operating line gives  $X_n$  and so on. This graphical method, which is very similar to the McCabe-Thiele method in distillation<sup>(99)</sup> is widely used in counter-current process design (leaching or washing) when determining the number of stages required for the composition of the overflow and underflow streams to meet a given specification. For example, in this washing system, a count of the number of steps required to change the composition of the overflow from  $Y_{n+1}$  to  $Y_1$  or the underflow from  $X_1$  (defined during the experimental work as  $X_f$ ) to  $X_{n+1}$  is the number of washing stages required.

#### 6.4.2. Preliminary Counter-current Washing Tests

As a first attempt to study the nickel extraction during the washing of leach residues in a counter-current system, a 3-stage washing test was set up using residues from Ore-B (particle size distribution as shown in appendix II) leached in HCl solutions containing 20 g/l Ni according to the conditions:

Weight of ore sample = 21 g

Volume of leaching solution = 50 ml.

Acid concentration = 6 mol/dm<sup>3</sup>.

Temperature = 80°C.

Contact time = 1 hour

Agitation = strong stirring.

Leaching of Ore-B samples according to these conditions, gave a nickel extraction of about 52%, and a nickel concentration in the resulting

leach liquor of about 23.6 g/l Ni. The mass of solid residues (approximately 12 g) contained about 0.1645 g of nickel (see appendix II).

The operating conditions for this test are given in Table 6.20 and the experimental technique used to simulate a batch counter-current washing operation are described in Chapter 3 (see 3.3.1. ). As in cross-current washing, the general washing conditions used in this test were; room temperature, 6 mol/dm<sup>3</sup> acid concentration, 30 minutes contact time (for each washing stage) and no agitation.

The results for this test are presented in Table 6.21 and Fig. 6.12, where a graphical representation of the washing at practical equilibrium, showing the nickel concentration in the overflow solution and the underflow slurry entering and leaving each washing stage, is illustrated. From these results, it can be seen that from the total amount of nickel in the solid residues entering the washing system, about 90.1% was extracted, and as expected because of the dependence nickel extraction has on the nickel concentration in the washing solution, this extraction occurred gradually as the solid residues moved towards washing stages in which the solution contained lower nickel concentrations (see Table 6.21).

The data illustrated in Fig. 6.12 show that whilst the nickel concentration of the underflow slurry decreases stage by stage from about 20.48 g Ni/Kg pulp to about 1.02 g Ni/Kg pulp, the nickel concentration of the overflow solution increases stage by stage from zero to about 7.13 g/l Ni when leaving the washing system. This demonstrates that washing the leach residues in a counter-current mode results in efficient nickel extraction, and at the same time in a high nickel concentration in the product solution.



Although a nickel extraction of 90.1% could be considered satisfactory, it has been demonstrated earlier in this chapter that an extraction of about 95% can be achieved from these residues by cross-current washing (see Table 6.17). However, to reach this degree of nickel extraction by cross-current washing, the results (test 4) show that the solid residues in the underflow were associated with solution containing a nickel concentration of about 0.55 g/l for 94.59% extraction and about 0.12 g/l for 95.32% extraction. This suggests that in the counter-current washing system discussed here (where the nickel concentration in the washing solution at practical equilibrium is 0.85 g/l Ni in the last stage), the addition of an extra stage might provide a similar degree of nickel extraction to that obtained in the cross-current washing. This is because the extra washing stage would allow the solid residues to be contacted in a washing solution with a nickel concentration within a suitable range (see Fig. 6.9). To verify this, a 4-stage washing test with the same operating conditions as the 3-stage test (see Table 6.20) was performed, and as suggested, the results of this test (presented in Table 6.22 and Fig. 6.13) showed that the degree of nickel extraction reached was about 95%.

By comparing the results of these two counter-current washing tests, it is possible to appreciate that even though the 4-stage test provides a more efficient nickel extraction than the 3-stage test, the nickel concentrations which were obtained in the product solutions (i.e. overflow solutions leaving stage 1) in both tests were very similar (about 7.13 g/l Ni in the 3-stage test and about 7.37 g/l Ni in the 4-stage test). This indicates that when washing these leach

Table 6.20. Operating conditions for preliminary counter-current washing tests (3-stage and 4-stage)

---

Feed to the washing system:

Wash. solution feed = 100 ml pure hydrochloric acid

Slurry feed = 25 ml leaching solution

= 12 g \* solid residues

Overflow stream:

Volume of solution feeding each stage = 100 ml.

Volume of solution leaving each stage = 100 ml.

Underflow stream:

Volume of solution associated with  
solid residues entering each stage = 25 ml.

Volume of solution associated with  
solid residues leaving each stage = 25 ml.

---

\* average value (see appendix II)

Table 6.21. Data for 3-stage counter-current washing at practical equilibrium.

	Nickel concentration		Weight of nickel left in solid	Nickel extraction cumulative
	overflow	underflow		
	g/l Ni	g Ni/Kg pulp	gm	%
feed		20.48*	0.1645*	
stage-1	7.13	7.52	0.0989	39.9
stage-2	2.36	3.39	0.0658	60.0
stage-3	0.85	1.02	0.0163	90.1

Weight of dry solid after washing = 11.85\*

$$R = 100/25 = 4$$

\* average value

Table 6.22. Data for 4-stage counter-current washing at practical equilibrium

	Nickel concentration		Weight of nickel left in solid	Nickel extraction cumulative
	overflow	underflow		
	g/l Ni	g Ni/Kg pulp	gm	%
feed		20.48*	0.1645*	
stage-1	7.37	7.68	0.0987	40.00
stage-2	2.65	3.76	0.0723	56.05
stage-3	1.21	1.45	0.0231	85.96
stage-4	0.36	0.47	0.0082	95.02

Weight of dry solid after washing = 11.84\*

$$R = 100/25 = 4$$

\*average value

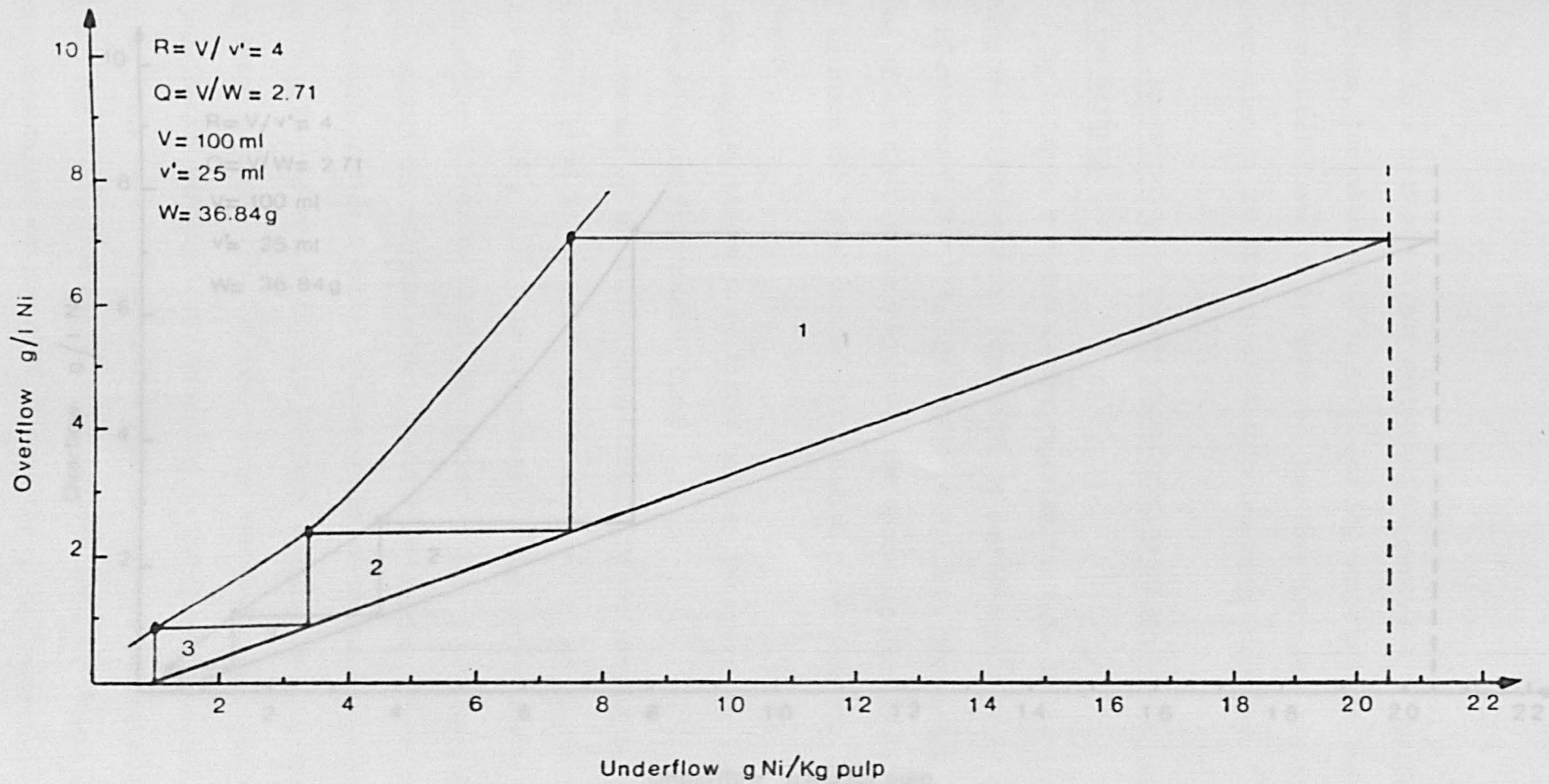


Fig. 6.12 Graphical representation of the 3-stage counter-current washing test at practical "equilibrium"

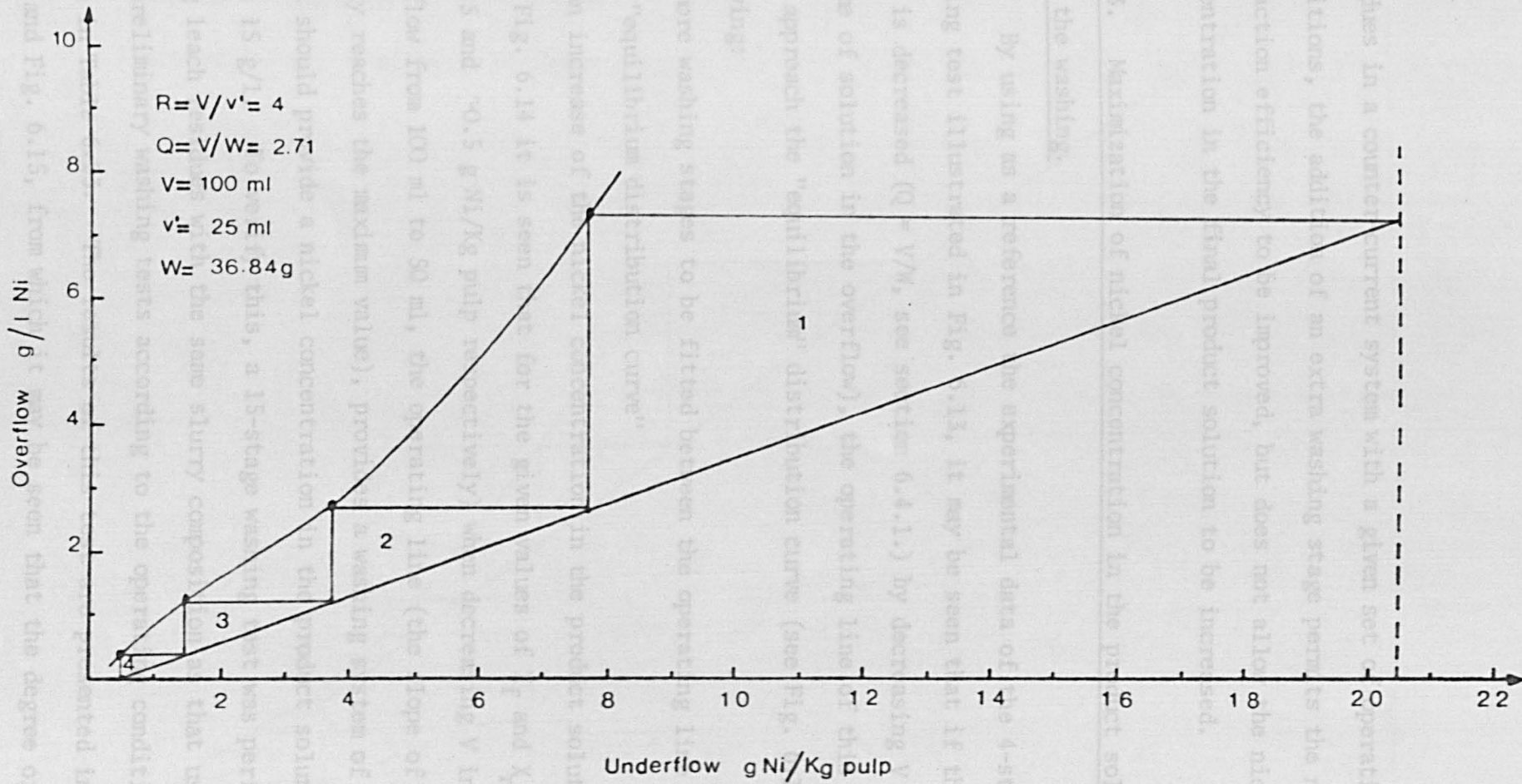


Fig. 6.13 Graphical representation of the 4-stage counter-current washing test at practical "equilibrium"

residues in a counter-current system with a given set of operating conditions, the addition of an extra washing stage permits the nickel extraction efficiency to be improved, but does not allow the nickel concentration in the final product solution to be increased.

#### 6.4.3. Maximization of nickel concentration in the product solution from the washing.

By using as a reference the experimental data of the 4-stage washing test illustrated in Fig. 6.13, it may be seen that if the value of  $Q$  is decreased ( $Q = V/W$ , see section 6.4.1.) by decreasing  $V$  (the volume of solution in the overflow), the operating line of this system will approach the "equilibrium" distribution curve (see Fig. 6.14), allowing:

- a) more washing stages to be fitted between the operating line and the "equilibrium distribution curve"
- b) an increase of the nickel concentration in the product solution ( $Y_1$ ).

From Fig. 6.14 it is seen that for the given values of  $X_F$  and  $X_{n+1}$  ( $\approx 20.5$  and  $\approx 0.5$  g Ni/Kg pulp respectively) when decreasing  $V$  in the overflow from 100 ml to 50 ml, the operating line (the slope of which nearly reaches the maximum value), provides a washing system of 15 stages which should provide a nickel concentration in the product solution of about 15 g/l. To verify this, a 15-stage washing test was performed using leach residues with the same slurry composition as that used in the preliminary washing tests according to the operating conditions given in Table 6.23. The results of this test are presented in Table 6.24 and Fig. 6.15, from which it may be seen that the degree of nickel extraction obtained was about 93.5%, and the nickel concentration obtained in the product solution was about 14.6 g/l. From this, it

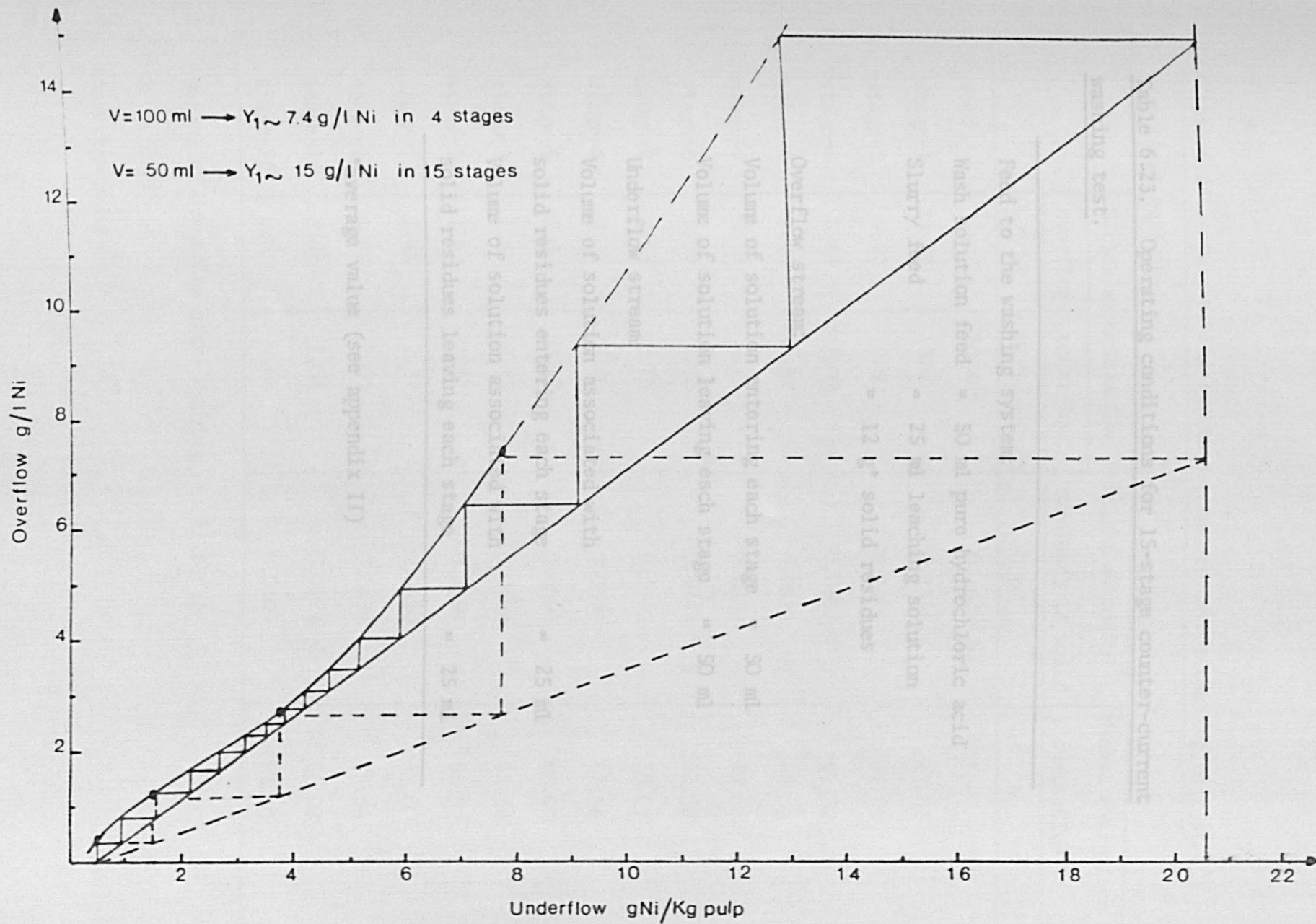


Fig. 6.14 Effect of the volume of wash liquor removed in the overflow upon the nickel conc. in the product solution



Table 6.23. Operating conditions for 15-stage counter-current washing test.

---

Feed to the washing system:

Wash solution feed = 50 ml pure hydrochloric acid

Slurry feed = 25 ml leaching solution

= 12 g\* solid residues

Overflow stream:

Volume of solution entering each stage = 50 ml

Volume of solution leaving each stage = 50 ml

Underflow stream:

Volume of solution associated with  
solid residues entering each stage = 25 ml

Volume of solution associated with  
solid residues leaving each stage = 25 ml

---

\*average value (see appendix II)

Table 6.24. Data of the 15-stage counter-current washing test at practical equilibrium.

	Nickel concentration		Weight of nickel remaining in solid	Nickel extraction cumulative
	overflow	underflow		
	g/l Ni	g Ni/Kg pulp	g	%
feed		20.48*	0.1645*	
stage-1	14.59	13.61	0.1365	17.02
stage-2	9.52	9.50	0.1119	31.98
stage-3	6.49	7.02	0.0962	41.52
stage-4	4.66	5.57	0.0888	46.02
stage-5	3.59	4.71	0.0839	49.0
stage-6	2.96	4.13	0.0781	52.52
stage-7	2.53	3.73	0.0740	55.02
stage-8	2.24	3.40	0.0691	57.99
stage-9	2.0	3.12	0.0650	60.49
stage-10	1.81	2.85	0.0599	63.58
stage-11	1.62	2.62	0.0559	66.02
stage-12	1.45	2.37	0.0510	69.0
stage-13	1.27	2.02	0.0428	73.98
stage-14	1.02	1.31	0.0229	86.08
stage-15	0.5	0.63	0.0107	93.50

Weight of dry solid after washing = 11.82\* g

$$R = 50/25 = 2$$

\*average value.

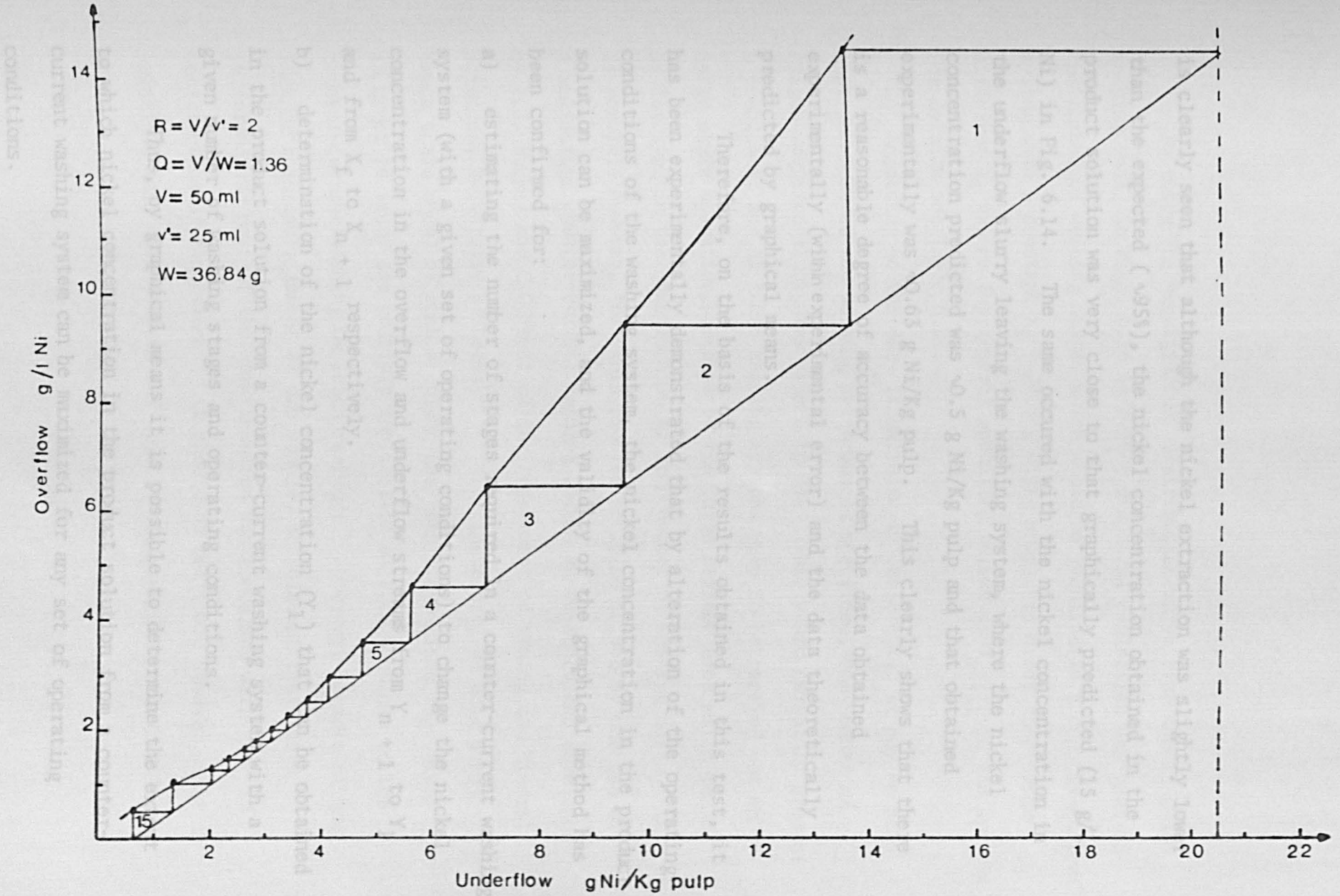


Fig 6.15 Graphical representation of the 15-stage counter-current washing test at practical "equilibrium"

is clearly seen that although the nickel extraction was slightly lower than the expected ( $\sim 95\%$ ), the nickel concentration obtained in the product solution was very close to that graphically predicted (15 g/l Ni) in Fig. 6.14. The same occurred with the nickel concentration in the underflow slurry leaving the washing system, where the nickel concentration predicted was  $\sim 0.5$  g Ni/Kg pulp and that obtained experimentally was  $\sim 0.63$  g Ni/Kg pulp. This clearly shows that there is a reasonable degree of accuracy between the data obtained experimentally (within experimental error) and the data theoretically predicted by graphical means.

Therefore, on the basis of the results obtained in this test, it has been experimentally demonstrated that by alteration of the operating conditions of the washing system, the nickel concentration in the product solution can be maximized, and the validity of the graphical method has been confirmed for:

- a) estimating the number of stages required in a counter-current washing system (with a given set of operating conditions) to change the nickel concentration in the overflow and underflow streams from  $Y_{n+1}$  to  $Y_1$  and from  $X_f$  to  $X_{n+1}$  respectively.
- b) determination of the nickel concentration ( $Y_1$ ) that can be obtained in the product solution from a counter-current washing system with a given number of washing stages and operating conditions.

Thus, by graphical means it is possible to determine the extent to which nickel concentration in the product solution from a counter-current washing system can be maximized for any set of operating conditions.

By using the "equilibrium" distribution curve from the 15-stage washing test, in Figs. 6.16 to 6.23 a graphical estimation was made of the number of washing stages which would be required in a counter-current system with a constant  $X_f$  ( $\sim 20.5$  g Ni/Kg pulp), in order to provide different  $Y_1$  values for several specified values of  $X_{n+1}$  in the system. For details see Table 6.25.

According to the data illustrated in Table 6.25, it may be seen that for most of the washing performances specified, the number of stages required fluctuates from 6 to 31. This would certainly present a problem if any of these washing systems were to be carried out on a large scale operation, because of the large surface area which would be involved in the construction of such number of washing units. It is possible however, that this problem could be solved by the use of a multistage counter-current washing column as designed and developed by D.I. Hughes and C.C. Dell of the Department of Mining and Mineral Sciences, University of Leeds<sup>(101,102)</sup>. Therefore, an acid proof bench scale model of such a column was constructed (see Fig. 6.24) in order to study the possible application of such a column to the counter-current washing of leach residues. However, because of the lack of a suitable amount of ore sample, no relevant tests were performed and most of the work involved was concerned with the construction of the column. It should be mentioned however, that in principle this column works and further study would be worthwhile.

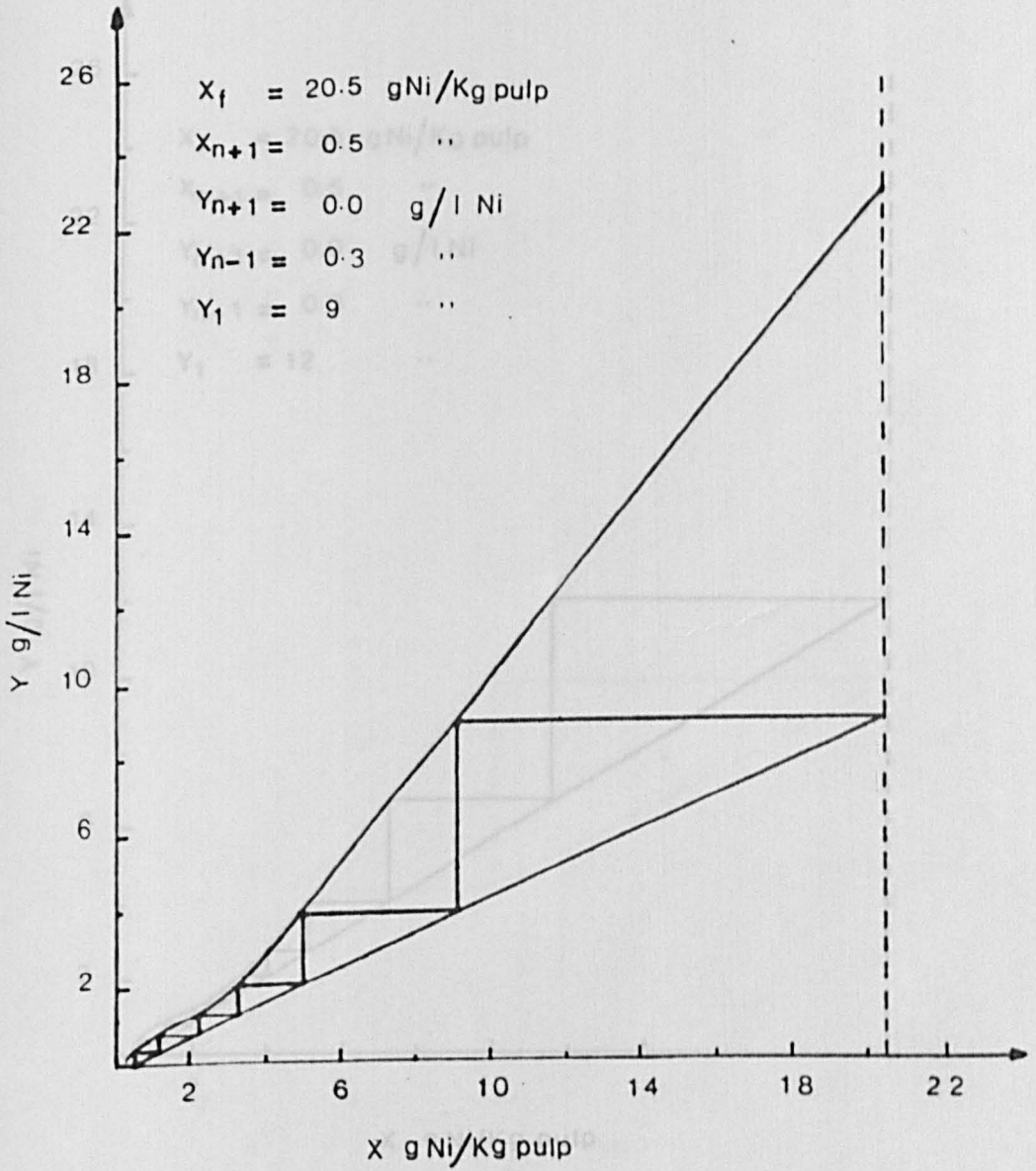


Fig. 6.16 Graphical estimation of the number of stages required to achieve a specified washing performance (6 stages)

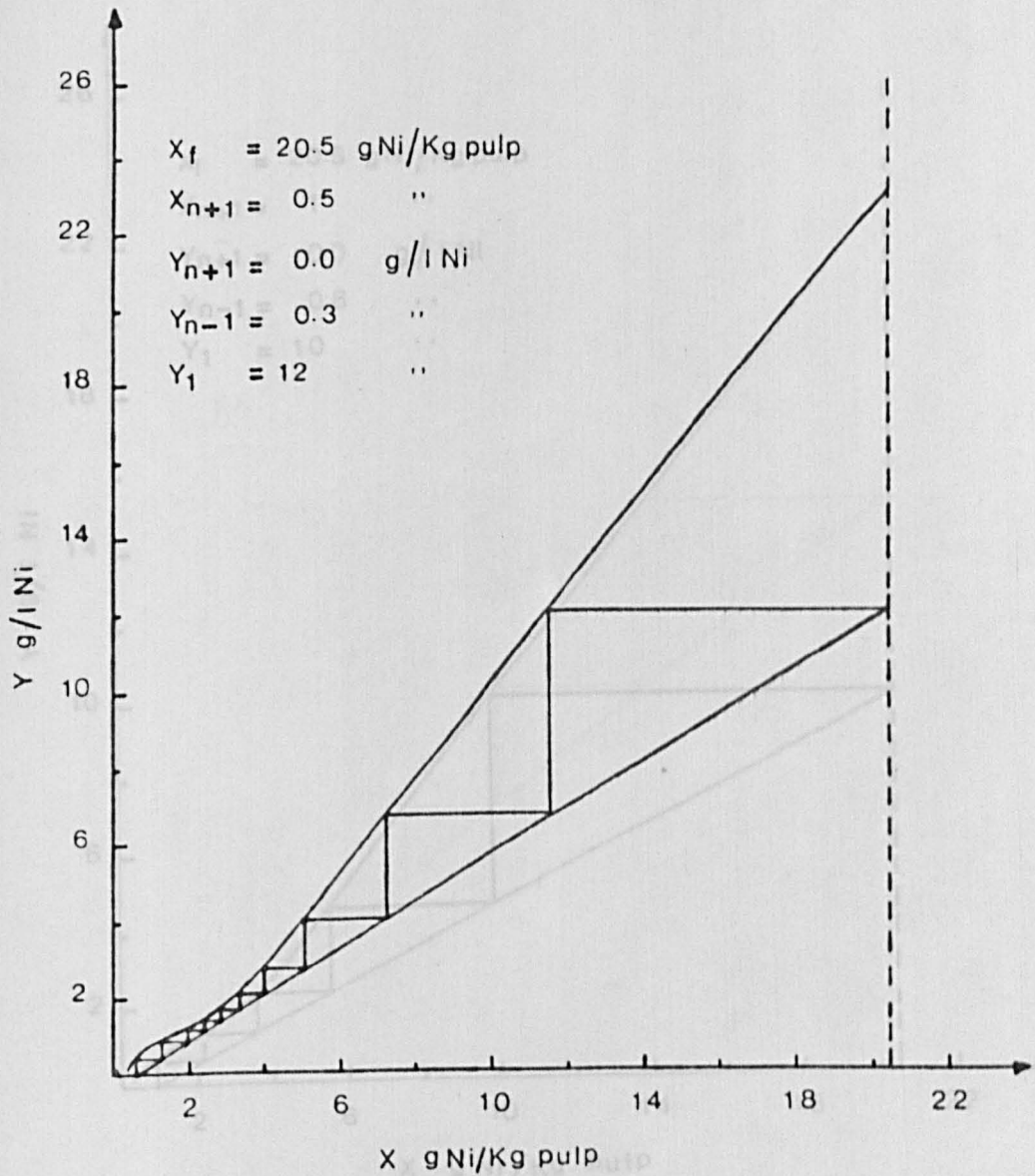


Fig. 6-17 Graphical estimation of the number of stages required to achieve a specified washing performance (10 stages)



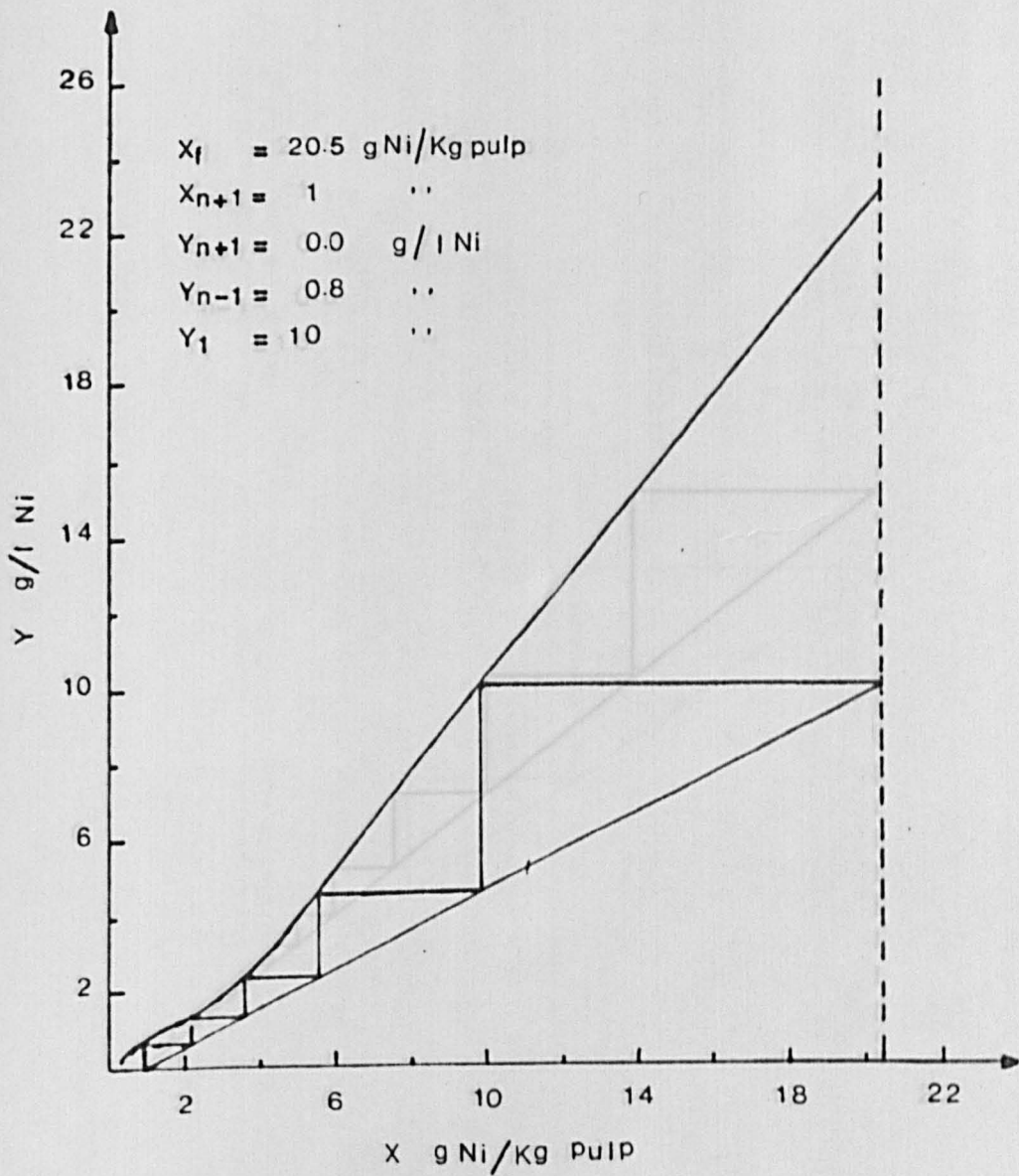


Fig. 6.18 Graphical estimation of the number of stages required to achieve a specified washing performance (5 stages)

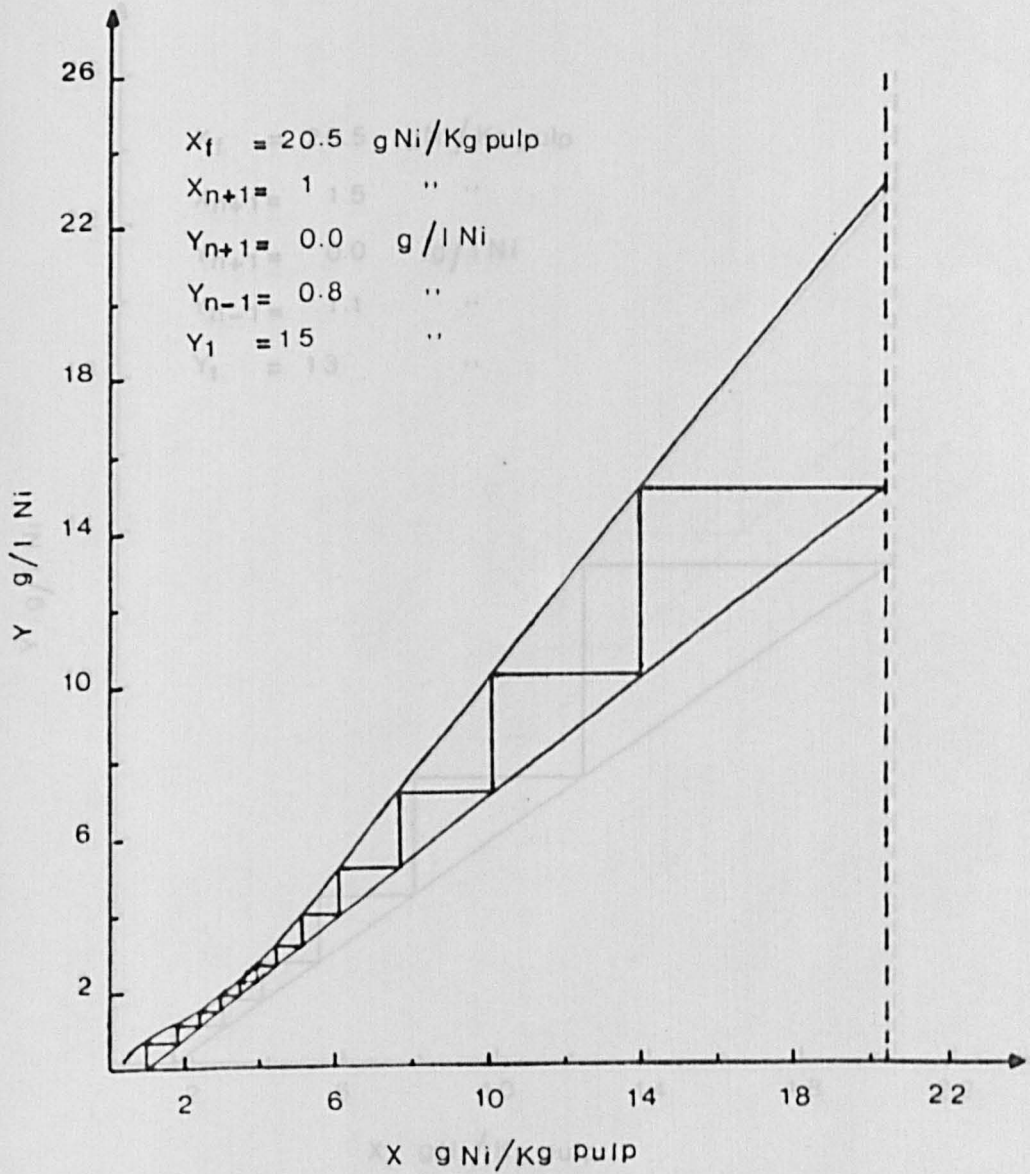


Fig. 6.19 Graphical estimation of the number of stages required to achieve a specified washing performance (12 stages)

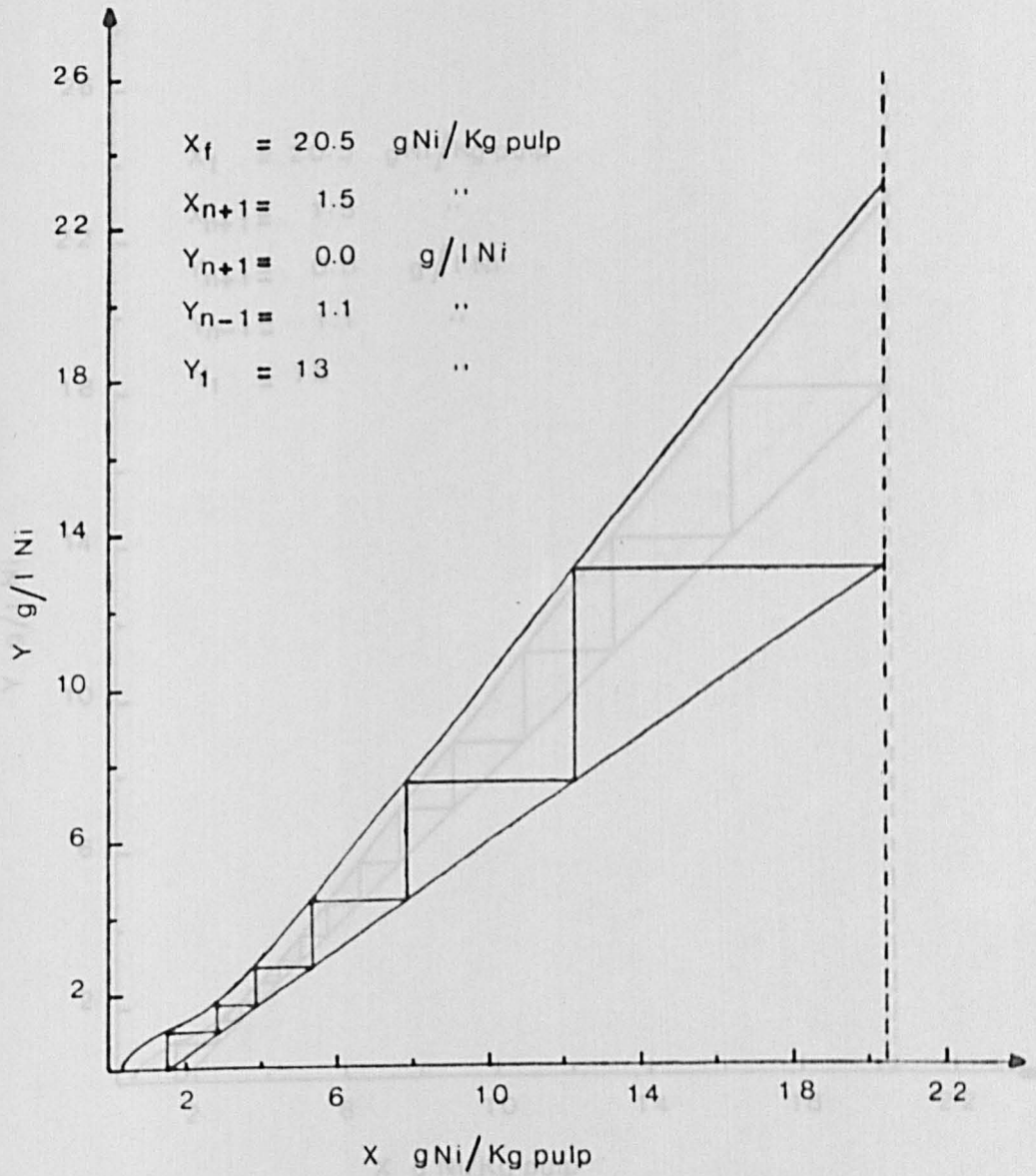


Fig. 6-20 Graphical estimation of the number of stages required to achieve a specified washing performance (6 stages)



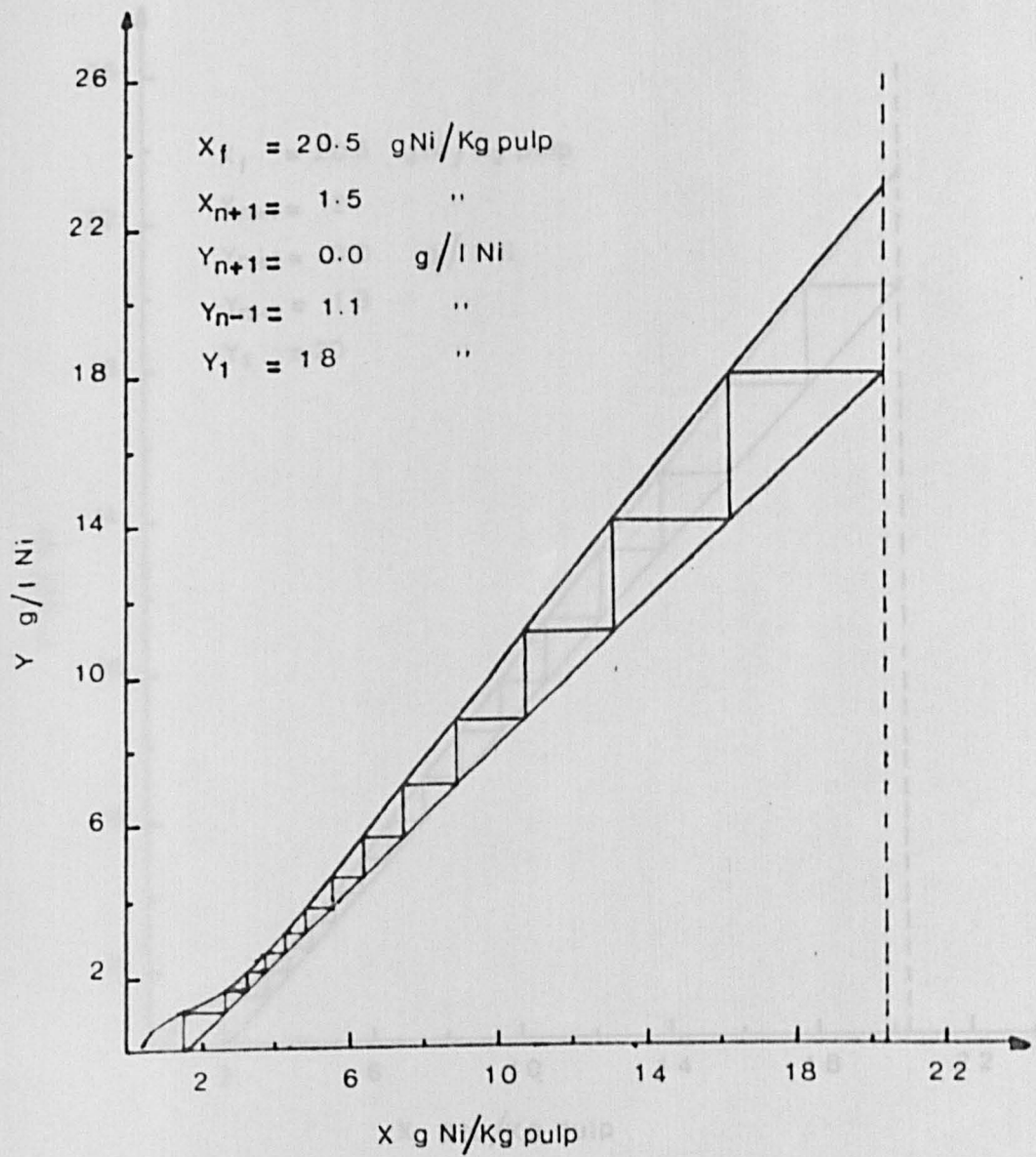


Fig. 6.21 Graphical estimation of the number of stages required to achieve a specified washing performance (13 stages)

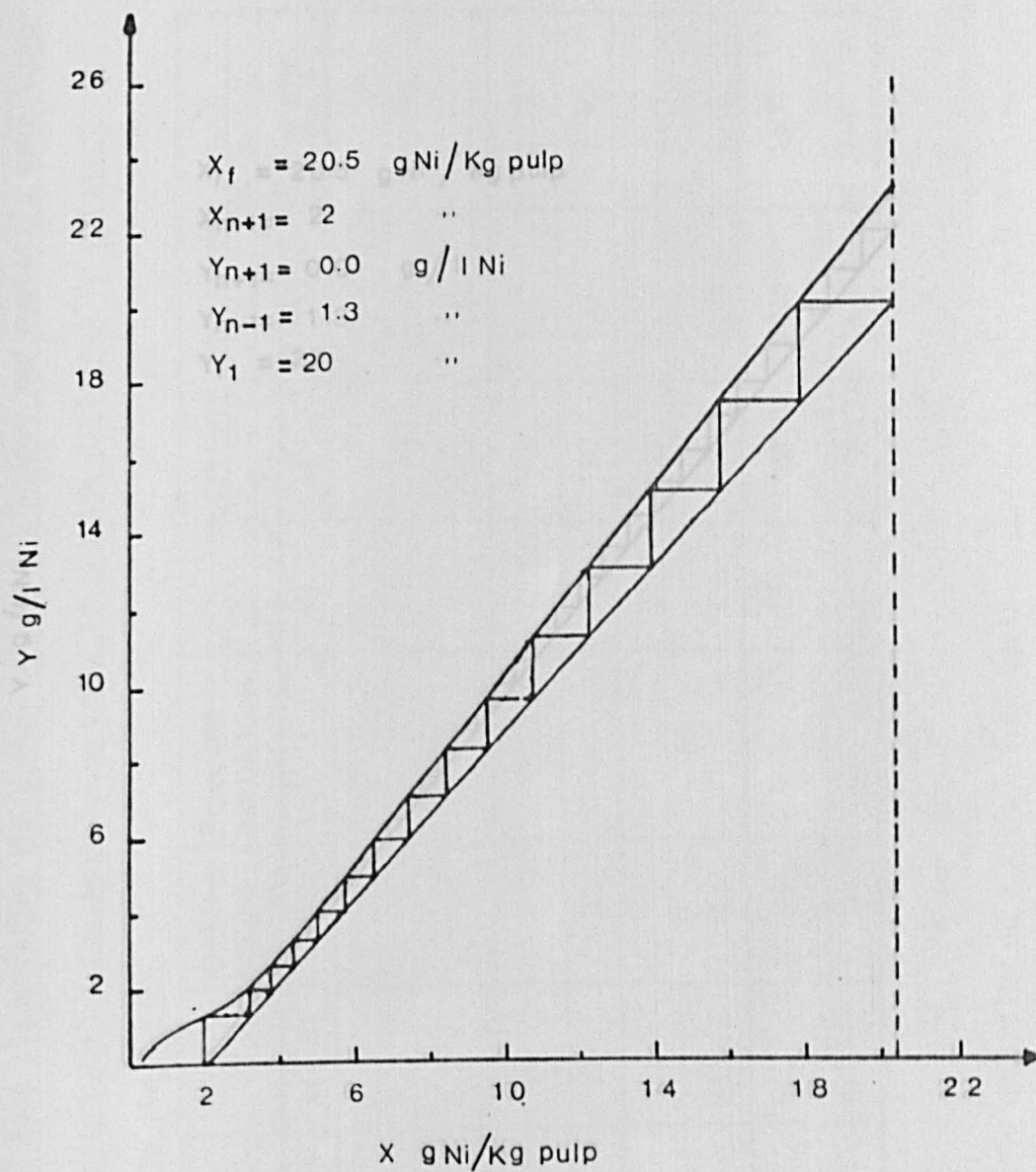


Fig. 6.22 Graphical estimation of the number of stages required to achieve a specified washing performance (15 stages)

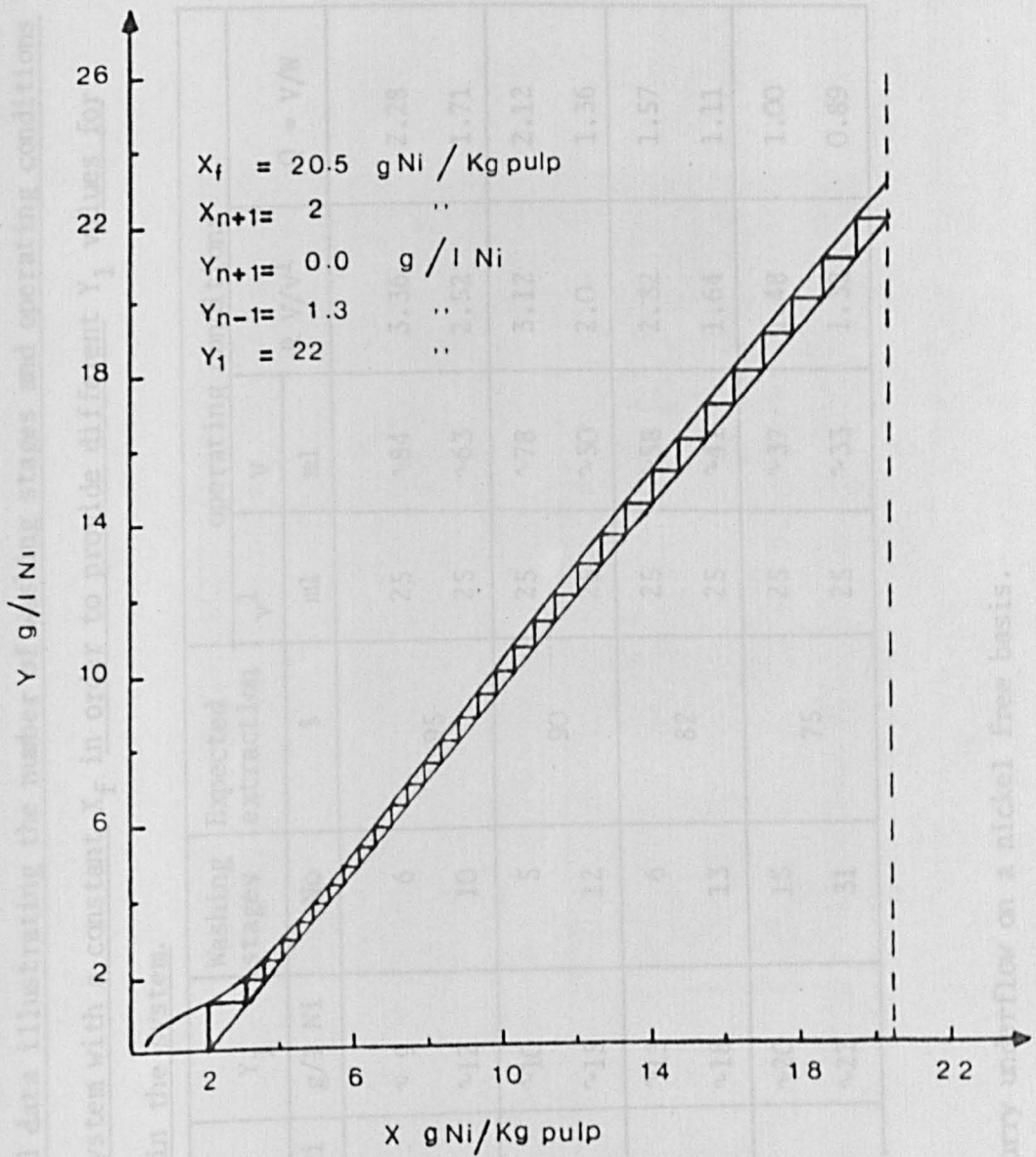


Fig. 6.23 Graphical estimation of the number of stages required to achieve a specified washing performance (31 stages)

Table 6.25. Graphical listed data illustrating the number of stages and operating conditions required for a counter-current system with constant  $V_f$  in order to provide different  $Y_1$  values for several specified  $X_{n+1}$  values in the system.

$X_f$ g Ni/Kg pulp	$X_{n+1}$ Ni/Kg pulp	$Y_{n-1}$ g/l Ni	$Y_1$ g/l Ni	Number of stages
20.5	0.5	0.5	22	31
20.5	1.0	1.0	22	25
20.5	1.5	1.5	22	21
20.5	2.0	2.0	22	18
20.5	2.5	2.5	22	16
20.5	3.0	3.0	22	14
20.5	4.0	4.0	22	11
20.5	5.0	5.0	22	9
20.5	6.0	6.0	22	8
20.5	7.0	7.0	22	7
20.5	8.0	8.0	22	6
20.5	10.0	10.0	22	5
20.5	15.0	15.0	22	3
20.5	20.0	20.0	22	2

$N^* = 35.84$

\* = average weight of the slurry underflow on a nickel free basis.

Table 6.25. Graphical estimated data illustrating the number of washing stages and operating conditions required for a counter-current system with a constant  $X_f$  in order to provide different  $Y_1$  values for several specified  $X_{n+1}$  values in the system.

$X_f$	$X_{n+1}$	$Y_{n-1}$	$Y_1$	Washing stages	Expected extraction	operating conditions			
						$v^1$	V	R $V/v^1$	Q = V/W
g Ni/Kg pulp	Ni/Kg pulp	g/l Ni	g/l Ni	No	%	ml	ml		
20.5	0.5	0.3	~ 9	6	95	25	~84	3.36	2.28
			~12	10		25	~63	2.52	1.71
20.5	1.0	0.8	~10	5	90	25	~78	3.12	2.12
			~15	12		25	~50	2.0	1.36
20.5	1.5	1.1	~13	6	82	25	~58	2.32	1.57
			~18	13		25	~41	1.64	1.11
20.5	2.0	1.3	~20	15	75	25	~37	1.48	1.00
			~22	31		25	~33	1.32	0.89

$W^*$  = 36.84 g

\* = average weight of the slurry underflow on a nickel free basis.



PROPOSED IMPROVED FLOW-SHEET

NICKEL/PURIFICATION

The acid  
have on nickel  
concentration  
disadvantage  
was to be used  
recycling of  
concentration  
solution at  
Chapter 4 level  
solved by the  
the leaching  
Fig. 7.1

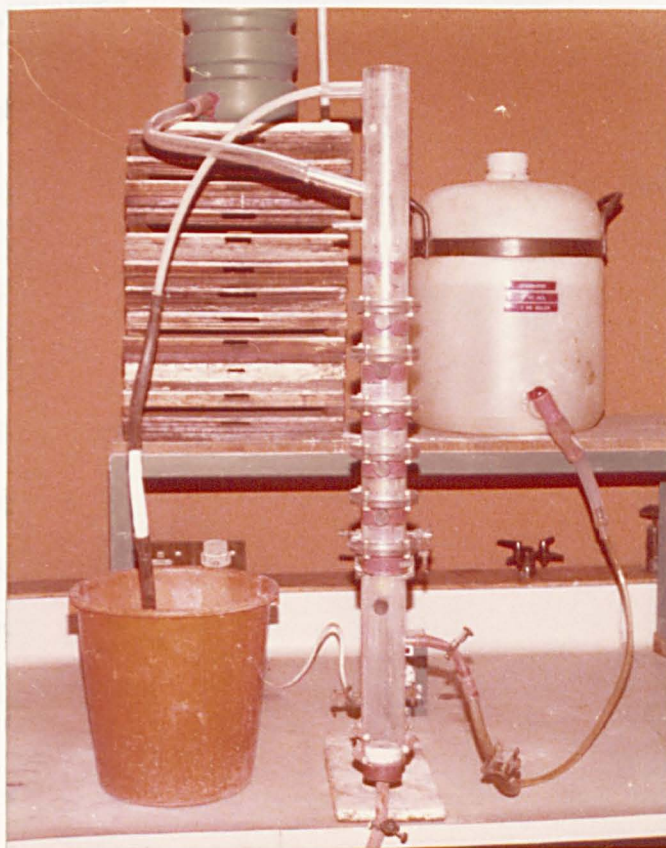


Fig. 6.24 Multistage Counter-Current Washing Column

## CHAPTER 7

### PROPOSED INTEGRATED FLOW-SHEET FOR HYDROCHLORIC ACID LEACHING OF NICKELIFEROUS LATERITES

The marked dependence which nickel extraction has been shown to have on nickel concentration in the leach liquor (i.e. the higher the concentration, the lower the extraction), would certainly present a disadvantage if a process for treating laterites by leaching in HCl was to be developed. This is because, it would severely limit the recycling of leach liquor as a method of increasing the nickel concentration in the liquor to a point where economic recovery from solution is feasible. Based on the washing studies reported in Chapter 6 however, it may be possible that this problem could be solved by the application of multistage counter-current washing following the leaching stage as shown in the conceptual flowsheet illustrated in Fig. 7.1.

Experimental tests have shown that leaching of Ore-B samples (serpentine) in HCl solutions containing 20 g/l Ni ( $80^{\circ}\text{C}$ ,  $6 \text{ mol/dm}^3$  HCl, 1 hour contact time and 30% solid W/W), provide a leach liquor containing about 23.6 g/l Ni, with about 52.2% nickel extraction from the ore. After solid/liquid separation of the leach liquor and residues, a 15-stage counter-current washing test on the slurry has shown that a nickel extraction of 93.5% from the solid residues is obtainable (giving an overall extraction after leaching and washing of about 96.9%), whilst the final product washing solution contains about 15 g/l Ni (see Table 6.23 and 6.24). By using graphical construction however, it was shown that for slurry of the same composition ( $\sim 20 \text{ g Ni/Kg pulp}$ ), by the use

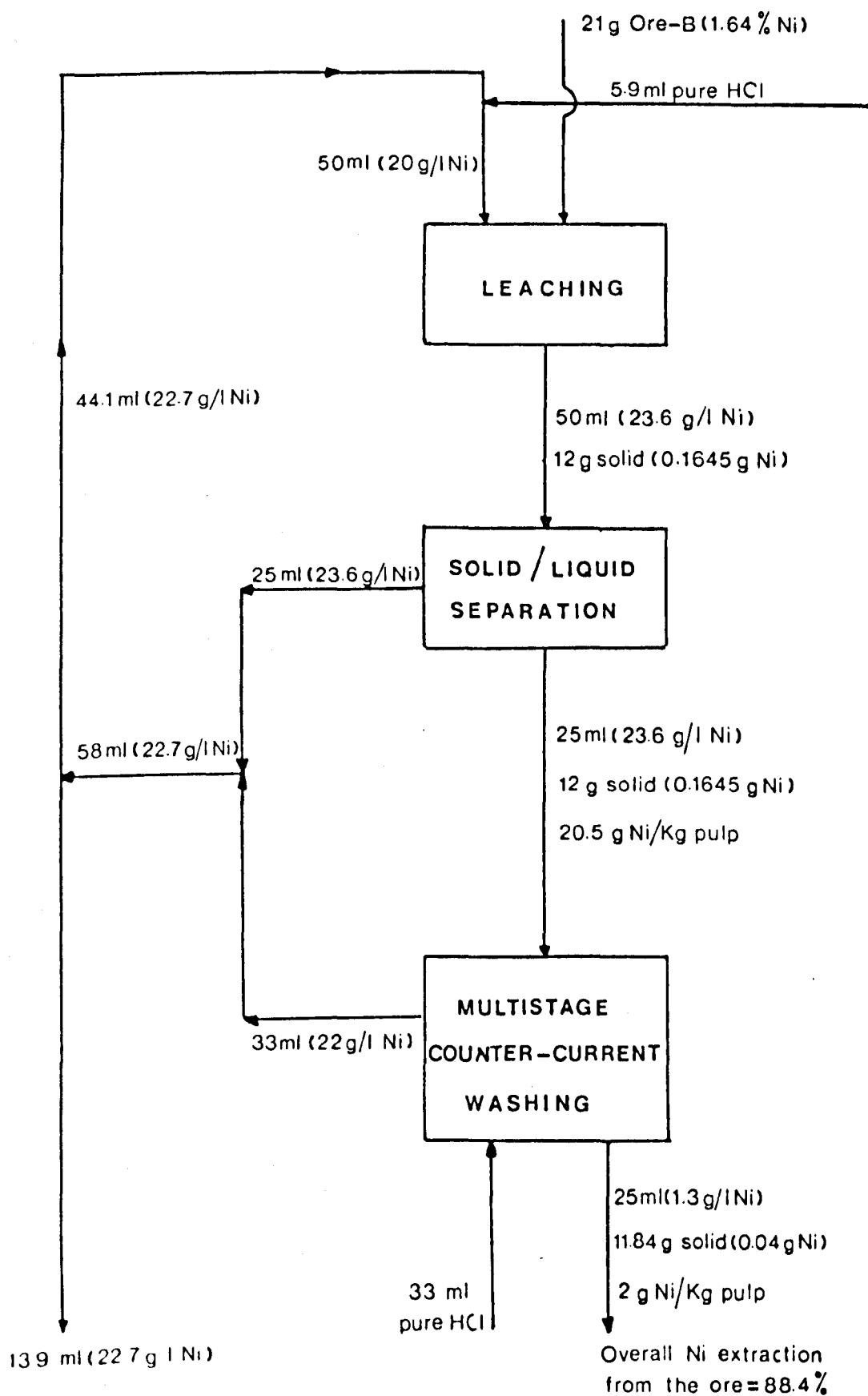


Fig 7.2 Typical example of a leach-washing performance

of more stages and a higher solid liquid ratio, it should be possible to achieve a washing performance in which the final washing solution produced contains a much higher nickel concentration (see Table 6.25).

Based therefore, on these experimental leaching tests and on the assumption that the washing performances predicted graphically could be achieved in practice, it is seen that the proposed leaching-washing flowsheet would permit final leach-wash solutions containing 20-23 g/l Ni to be produced with 92 - 88% overall nickel extraction from the ore respectively. To illustrate this, Fig. 7.2 shows a typical example using experimental leaching data from the above test (see section 6.4.2. in Chapter 6) and from the estimated washing performances given in Table 6.25. The calculation is based on the mass balance in the system.

It should be noted that in this example, the estimated data used from Table 6.25 are those which would provide the highest nickel concentration in the final leach-wash product solution. From Table 6.25 however, it can be seen that there are two other sets of washing parameters which could also satisfy the minimum requirements of the flowsheet (that is to provide a final leach-wash solution containing at least 20 g/l Ni).

These are:

- (1) Counter-current washing in 13 stages providing a product wash solution containing 18 g/l Ni, with 82% nickel extraction from the solid residues.
- (2) Counter-current washing in 15 stages providing a product wash solution containing 20 g/l Ni, with 75% nickel extraction from the solid residues.

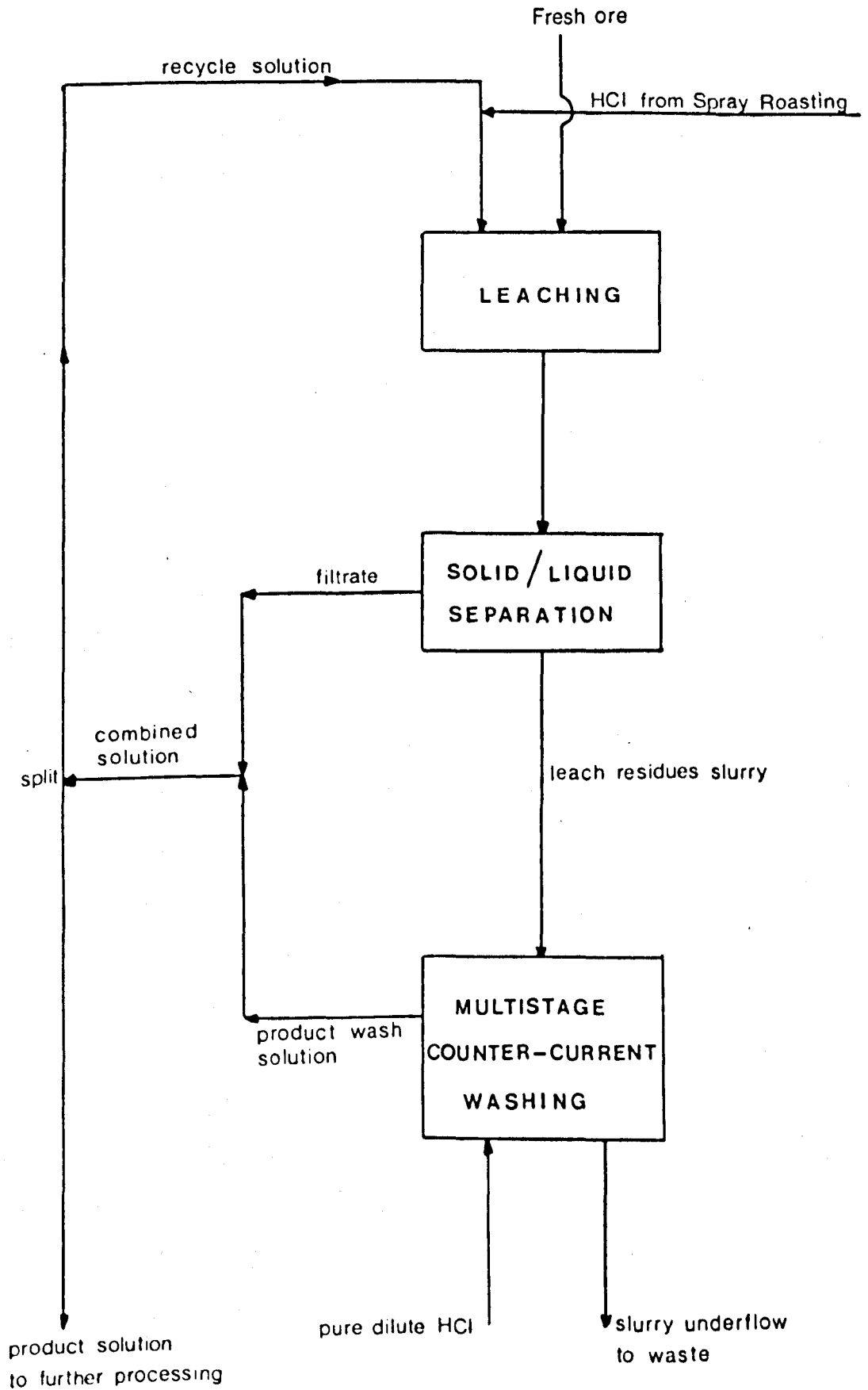


Fig 7.1 Conceptual leaching-washing flowsheet

The application of these two counter-current washing performances to the flowsheet would provide the following final leach-wash product solutions and overall nickel extractions from the ore:

- 1) 20.1 g/l Ni                      91.9% extraction
- 2) 21.5 g/l Ni                      88.4% extraction

From the example given in Fig. 7.2, it is clear that the alteration in the composition on flow of any stream in the flowsheet would affect the system as a whole, and would certainly alter the nickel concentration in the final product solution. Thus, in order to determine the effect which would be produced in the system by any kind of alteration in any of the streams, a mathematical model based on the mass balances in the system and on separate models of each stage (leaching and washing) would be necessary. To do so, however, a study of the interaction of leaching and washing on pilot scale would be needed.

Furthermore, from Table 6.25 it is seen that for the above washing performances, a large number of washing stages are required, which would certainly present a problem if the leach-washing process was to be applied on a large scale operation. This problem however, as mentioned in Chapter 6, could be solved by the use of a multistage counter-current washing column (see Fig. 6.24). Thus, further work on this column would be needed in order to establish technical and economic feasibility of the proposed leach-washing process.

On the assumption that the leach-washing flowsheet discussed above could be technically possible, the data given shows that it should be able to provide solution suitable for subsequent processing for nickel recovery and at the same time achieve an adequate nickel extraction from



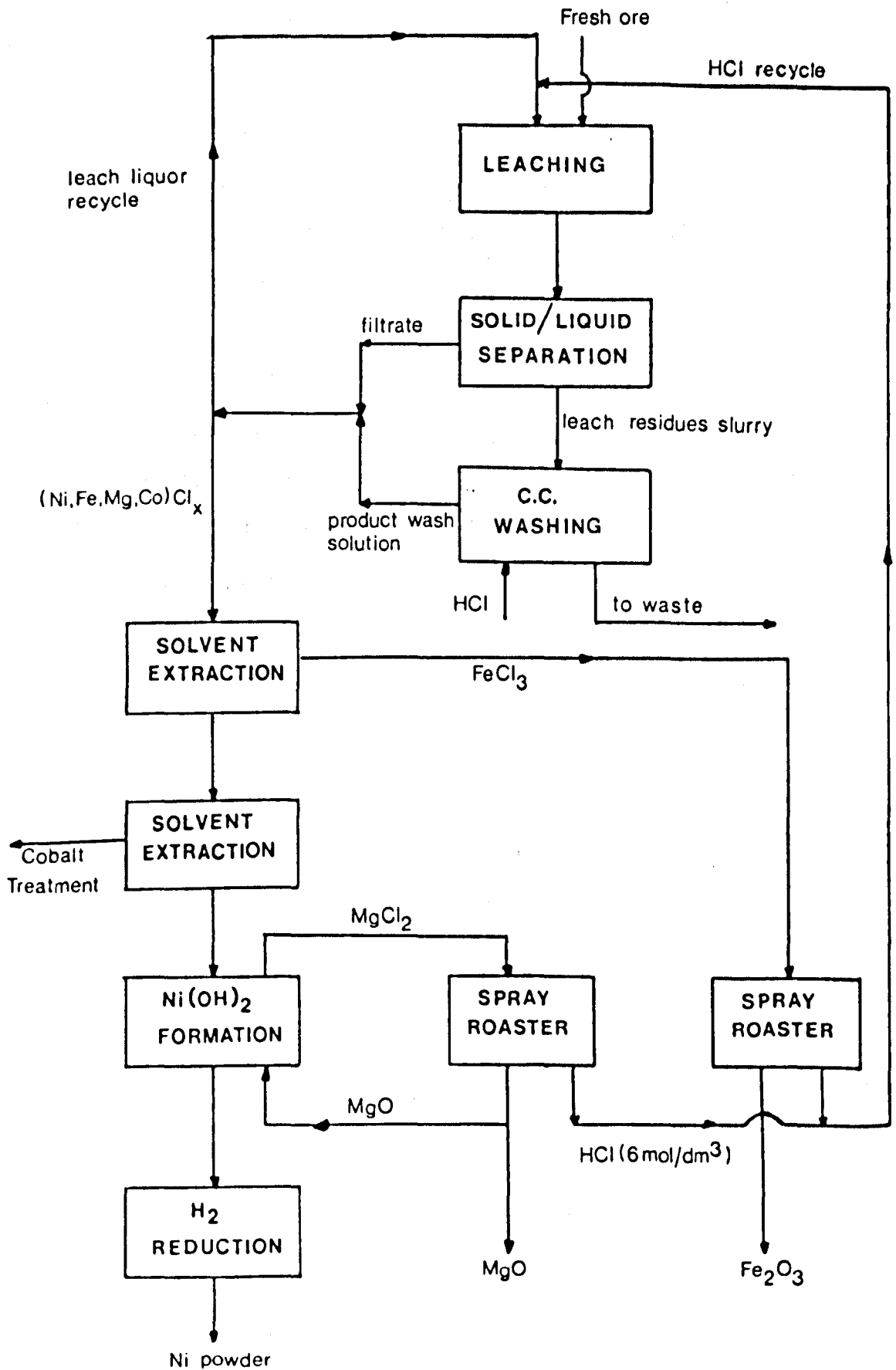


Fig. 7.3 Proposed flowsheet for the treatment of nickeliferous laterites

the ore. On this basis therefore, it may be possible that a promising process might be developed for hydrochloric acid leaching of nickeliferous laterites. Fig. 7.3 shows in a general way the type of flowsheet that could perhaps be appropriate for such a process. Fe and Co could be removed from the leach liquor by solvent extraction (e.g. as in the Falconbridge Matte leach Process<sup>(51,52)</sup>) while nickel could be recovered by hydrogen reduction of the hydroxide as in the Derry Process<sup>(69,70)</sup>, after neutralization of the leach liquor with MgO recycled from spray washing. It should be noted that this general flowsheet for the treatment of laterites has previously been proposed by Rice and Strong<sup>(7)</sup> In this the authors emphasized the necessity to build up the nickel concentration in the leach liquor e.g. by cross-current leaching or using high solid/liquid ratios.

## CHAPTER 8

### CONCLUSION

From the experimental work described above, it has been established that when leaching lateritic nickel ores in dilute hydrochloric acid, the degree of extraction of nickel, as well as iron and magnesium, is considerably decreased in the presence of moderate concentrations of the respective cations in the leach liquor.

For the case of nickel in solution in particular, it has been shown that the effect on nickel extraction is drastic (but is less marked for the extraction of iron and magnesium). Extraction falls from a relatively high value in pure HCl to zero with 20 g/l Ni initially present in the solution. (This effect is reported for leaching with a pulp density of 10% solid. With increasing pulp density initially an increase on nickel extraction is observed due to the effect of attrition, see section 4.3.5 in Chapter 4). It has been demonstrated however, that after leaching laterites with acid solutions containing up to 20 g/l Ni, washing of the leach residues with pure dilute HCl readily increases the extraction of nickel to about 98%. This indicates that during the leaching stage, the presence of nickel in the leach liquor only has a retarding effect on the nickel extraction and does not prevent the reaction between the acid and the ore.

For the cases of magnesium and iron in solution, it was shown that the effect on magnesium and iron extraction respectively was much less drastic than that for nickel extraction with nickel in solution. In fact, extraction of magnesium from a typical nickeliferous serpentine (Ore-A) falls from about 93% in pure HCl to about 43% with 100 g/l Mg initially present in the solution, and extraction of iron from a typical

nickeliferous goethite (Ore-E) falls from about 98% in pure HCl to about 60% with 100 g/l Fe initially present in the solution. As in the case of nickel, it was shown that the washing of leach residues (after extraction in acid solution containing 100 g/l Mg or 100 g/l Fe depending on the ore) with pure dilute HCl, readily increases the extraction of the respective cation. For the case mentioned above, extraction of magnesium increases to about 93% (Ore-A), and extraction of iron increases to about 98% (Ore-E).

The kinetic study of acid dissolution of a nickeliferous serpentine (Ore-B) showed that at low temperatures the rate of cation dissolution is chemically-controlled, but with increasing temperature cation dissolution becomes intermediate-controlled with a strong indication that at higher temperatures diffusion control is predominant. This change of mechanism with the rise of temperature has been interpreted as being caused by the formation of a reaction product layer during the reaction. Formation of this layer has been clearly demonstrated by lump leaching tests. This theory is supported by the relatively good fit of the chemical dissolution data to the kinetic equation  $1 - \frac{2}{3}R - (1-R)^{2/3} = kt$ , which indicates that the reaction follows a model where the acid attack on the particles proceeds from the exterior to the centre, leaving a reaction product layer which acts as a diffusion barrier.

Based on the evidence that a reaction product layer was formed during leaching, it is suggested that the decrease of nickel extraction with increasing nickel concentration in the leach liquor could perhaps be attributed to crystallization of  $\text{NiCl}_2$  in the pores of the layer due to saturation of the solution in the pores. This saturation may be

caused by a faster chemical reaction (rapid rate of aqueous  $\text{NiCl}_2$  formation there) and a slow rate of diffusion (due to the high nickel chloride concentration in the bulk solution). This saturation might also be due to diffusion of nickel from the bulk solution into the layer contributing to the overall increase of nickel concentration in the pores. This theory of  $\text{NiCl}_2$  crystallization in the pores of the layer, has been perhaps supported to some extent by the slight increase in extraction with increasing severity of leaching conditions, especially temperature (see section 4.3.4.3. in Chapter 4).

Extraction of nickel from solidleach residues (after leaching in HCl solutions containing up to 20 g/l Ni) has been demonstrated to occur by washing the wet residues with pure dilute HCl.

The degree of extraction has been shown to depend on:

- a) Severity of conditions during leaching; the more severe the leaching conditions, the higher the degree of extraction during washing (see section 6.2.1. in Chapter 6).
- b) Nickel concentration in the bulk wash solution containing the solids; as in leaching the higher the concentration, the lower the extraction.
- c) Contact time.

Parameters such as temperature, acid concentration and agitation did not show any influence.

All these facts indicate that most of the nickel in the solid residues has already reacted during leaching and been retained in the solid as solid  $\text{NiCl}_2$  (due to the high nickel concentration in the leach acid). Hence, extraction during washing is merely due to the dissolution of this  $\text{NiCl}_2$ .

Washing of the residues in a multistage counter-current system was found to be the most suitable method of recovering this nickel as this provided both efficient nickel extraction and a high nickel concentration on the product washing solution (see section 6.4.2. to 6.4.3. in Chapter 6). Based on experimental tests and from the use of graphical construction it was estimated that counter-current washing could provide final product washing solutions containing about 18-22 g/l Ni with 82-75% nickel extraction from the solid residues respectively (see Table 6.25) which correspond to about 91.9 - 88.4% overall extraction from the ore respectively as calculated from the mass-balances from the proposed leach-washing flowsheet shown in Fig. 7.1.

From this it was concluded that the process should be able to provide a solution suitable for subsequent processing for nickel recovery and at the same time achieve an adequate nickel recovery from the ore.

However, much further development work on the full process flowsheet would be necessary in order to confirm whether such a process for nickeliferous laterites would in fact be either technically or economically feasible.

## ACKNOWLEDGEMENTS

The author's grateful thanks are due to Professor P.A. Young, M.A., Ph.D. (Cantab), F.I.M.M., M.I.Aus. M.M., M.Can.I.M.M., C.Eng., and Dr. N.M. Rice, M.Sc.(Eng.) Rand, D.I.C., Ph.D., M.I.M.M., Head of Department and Senior Lecturer respectively, in the Department of Mining and Mineral Sciences, for their supervision, advice, encouragement and interest during this work.

I also thank those members of staff for their assistance with some of the analytical techniques and the construction of some experimental apparatus.

My thanks also to World University Services for the provision of a grant during the course of this research.



## REFERENCES

1. Sherrit Gordon Mines Ltd. "Recovery of nickel and cobalt values from oxidic ores" Brit. Pat. 1,168,858 (1969)
2. Sherrit Gordon Mines Ltd. "Leaching process for reduced nickel and cobalt bearing lateritic ores". Brit. Pat. 1,182,207 (1970)
3. Wilson F. "The Moa-Bay-Port nickel project" Min. Eng. 10, (1958) 563-565
4. Carlson E.T. and Simons, C.S. "Acid leaching Moa Bay's nickel". J. Metals. N.Y. 12 (1960) 206-213
5. Meddings B. and Evans D.J.I. "The changing role of hydrometallurgy" Can.Inst.Min. Metall. Bull. 64 (706) 1971, 48.57
6. Derry R. "Pressure hydrometallurgy: A review". Min. Sci. Eng. 4(1): 3-24 (1972).
7. Rice N.M. and Strong L.W. "The leaching of lateritic nickel ores in hydrochloric acid". Can. Met. Quart., 13, No.3, (1974) 485-493.
8. Rice N.M. and Strong L.W. "The leaching of nickeliferous laterites with hydrochloric acid. Paper presented at I. Chem. E. Symposium, Series No.42, April 1974.
9. Canterford J.H. "The extractive metallurgy of nickel" Rev. Pure Appl. Chem. Vol. 22 (1972) 13-46.
10. Roorda H.J and Queneau P.E. "Recovery of nickel and cobalt from limonites by aqueous chlorination in sea water". Trans Inst. Min. Metall. Vol.82, (1973) C79-C87.

11. Boldt J. "The winning of nickel". London, Methuen, 1967.
12. Canterford J.H. "The treatment of nickeliferous laterites" Minerals. Sci. Engng. Vol.7, No.1, (1975) 3-17.
13. Strong L.W. "Leaching of lateritic nickel ores" Ph.D. Thesis, Department of Mining & Mineral Sciences, University of Leeds, England, 1978.
14. Canterford J.H. "Mineralogical aspects of the extractive metallurgy of nickeliferous laterites" The Aus. I.M.M. Conference, North Queensland Sept. 1978.
15. Takahashi et al. "A method of dressing laterite iron ores which contain nickel, chromium and cobalt" German Pat. 1,230,371 (1967).
16. Weston D. "Flotation of lateritic nickel ores" Australian Pat. application 71/26573 (1971)
17. Power L.F. and Geiger G.H. "The application of the reduction roast-ammoniacal ammonium carbonate leach to nickel laterites" Minerals Sci. Engng. Vol. 9, No. 1 (1977) 32-51.
18. Limerick J.M. "Correlation of extraction process with properties of laterites". Ph.D. Thesis, School of Metallurgy, University of New South Wales, Australia, 1978.
19. Queneau P.E. "Cobalt and the nickeliferous limonites" Ph.D. Thesis, University of Delft, Holland 1971.

20. Anonymous "Inco Inaugurates laterite nickel project on Indonesia's Sulawesi Island". Eng. Min. J. Vol. 178, No. 5 (1977) 23-24.
21. Anonymous 'Exmibal tunes up to produce 28 million lb per year of Ni' Eng. Min. J. Vol. 178, No.11 (1977) 162-165.  
ibid, 'Eximal's Guatemala nickel laterite project enters Producer Rank'. No. 8, p.27-30.
22. Mackey P.J. and Balfour G.C. "Metallurgical processer" Pyrometallurgy J. Metals. April 1978, 30 (4) 36-43.
23. Dowsing R.J. "Nickel, Part 2. Refining, Marketing and Use" Metals and Materials, May (1977) 20-26.
24. Moussoulos L. "Process for enrichment of a ferronickel alloy to 90% Ni." Metall. Trans. B. Dec. 1976, 7B(4) 631-637.
25. Moussoulos L. "Advances in extractive metallurgy" I.M.M. (1963) 264-286.
26. Kell K.K. "Contribution to data on theoretical metallurgy" United States Bureau of Mines, Bulletin 584 (1960).
27. Kellogg H.H. and Henderson J.M. Energy use in sulphide smelting of copper-extractive metallurgy of copper, Vol. 1 ed. J.C. Yannopoulos and J.C. Agarwal. The A.I.M.E., New York (1976), 373-415.
28. Kay H. U.S. Pat. 3,466,144 (1969).
29. Sobol S.I. Rev. Technol. Vol. 4, No.5, (1966) 3-19.
30. Sobol S.I. Rev. Technol. Vol. 6, Nos. 5-6 (1968) 3-24.
31. Sobol S.I. Rev. Technol. Vol. 7, No. 1 (1969) 3-23.

32. Chavez R.A., Tsvet. Metal. Vol.9, No.4 (1968) 66-70  
Karelin V.V. and  
Sobolev B.P.
33. Chou, E.C., Queneau "Sulphuric acid pressure leaching of  
P.B. & Rickard R.S. nickeliferous limonites". Metall. Trans.  
B. Dec. 1977, 8B(4) 547-554.
34. Caron M.H. "Fundamental and practical factor in ammonia  
leach of nickel and cobalt ores". Trans.  
TMS-AIME, 188 (1950) 67-90.
35. Stevens L.G, "Hydrometallurgical recovery of nickel values  
Geoller L.A. and from laterites" U.S. Pat. 3,903,241 Sept.  
Miller M. 1975.
36. O'Neill C.E. "Acid extraction of nickel from lateritic  
ores". U.S. Pat. 3,773,891 Oct. 1972.
37. Clarkson C.J. and "Leaching of reduction-roasted garnierite  
Distin P.A. in aerated sulphuric acid solutions".  
Canadian Metallurgical Quarterly Vol.15,  
No. 1 (1976) 91-95.
38. Matsuzuka K. "A method of treating nickel-chromium-  
containing iron ores". Brit. Pat. 951,063,  
March (1964).
39. Hedley N and "Treatment of Garnierite Ores". U.S. Pat.  
Kness J.J. 2,349,223, May 1944.
40. Queneau P.E. and "Impressive new process uses chlorine and  
Roorda H.J. seawater for improved recovered of cobalt  
from nickeliferous limonites". Mining  
Eng. 23(8) (1971) 70-73.

41. Roorda H.J. "Chloride hydrometallurgy Proceeding"  
Bemelux metallurgie. Brussels, Sept.  
(1977) 182-201.
42. Distin P.A. "Nickel extraction from reduction-roasted  
laterite ores by copper sulphate leaching"  
J. Metals. Nov. 1978, 30 (11) 30-35.
43. De Graff J.E. "The treatment of lateritic nickel ores -  
further study of the Caron process and other  
possible improvements" Part I Effect of  
reduction conditions. Part II Leaching  
studies. Hydrometallurgy (in press)  
J. Metals, 5 (1971) 31.
44. Bauer D.J. and  
Lindstrom R.E.
45. Bryson J.P and  
Distin P.A. "The recovery of nickel from laterites by  
chelate formation and reduction with hydrogen"  
Hydrometallurgy. Oct. 1978, 3(4) 343-354.
46. Barber S.P. and  
Wilson H.A. "Investigation into the treatment of a nickel  
laterite". Final year project. Department  
of Mining & Mineral Sciences, University of  
Leeds 1971.
47. Lupton J. and  
Perry G.L. "Extraction of nickel from an oxidised copper  
ore" Final year project. Department of  
Mining and Mineral Sciences, University of  
Leeds, 1972.
48. Scott T.A. "Unit processes in hydrometallurgy". New York  
Gordon and Breach (1964) 169-182.
49. Woodhall-Duckham "Regeneration Process". Brit. Chem. Eng.  
Vol. 15, 1970.

50. Brooks P.T., Potter. "Chemical reduction of superalloy scrap"  
G.M. and Martini Rep. invest. U.S. Bureau Mines. No. 7316  
D.A. (1969).
51. Thornhill P.G. "The Falconbridge Matte leach process".  
Wigstol E. and Paper presented at Annual meeting AIME,  
van Weert G. New York, 1971.
52. Wigstol E. and "Solvent extraction in nickel metallurgy -  
Fryland K. The Falconbridge matte leach process".  
Proc. Int. Symp. Solvent extraction in metal  
processing. Antwerp (1972) 62-72.
53. van Weert G. Can. Pat. 830,905 (1969).
54. van Weert G. and U.S. Pat. 3,466,021 (1969).  
Walen J.
55. van Eyk L.A. "Chlorination of laterite ores"  
Chem. Tech. Rev. 20(3), 1965, 77-8, 80-81.
56. Shindo H, Nagoya, "Preparation of nickel oxide ore". Suiyokwai  
and Ishii K. Shi, 13 (1958) 689-93.
57. Bogatskii D.P. "Complex chlorination treatment of silicate  
and Urazov G.G. ores of the iron group metals". Zhur.  
Priklad. Khim. 31 (1958) 325-32.
58. Westcott E.W. U.S. Pat. 2,036,664 (1936).
59. Graham M.E. et al. U.S. Pat. 2,766,115 (1956).
60. Heertjes P.M. and Recl. Trav. Chem. pays-Bar, Belg., T79  
van Nes C.L. (1960) 595.
61. Daubenspeck J.M. "Recovery of nickel and cobalt from low-grade  
nickeliferous ores". U.S. Pat. 2,733,983  
(1956).
- 62 Aman J. Israel Pat. B722 (1956).

63. Aman J. Brit. Pat. 793,700 (1958).
64. Conners A. "Hydrochloric acid regeneration as applied to the steel and mineral processing industries" CIM Bulletin. February (1975) 75-81.
65. Gravenor C.P. et al. "A hydrometallurgical process to produce iron powder from scrap iron". CIM Bulletin January (1970) Vol. 63. No. 693 pp.59-64.
66. Gravenor C.P. et al. "A hydrometallurgical process for the extraction of iron from low-grade ores". CIM Bulletin, April (1964) Vo.. 57, No.634, pp.421-428.
67. Chakraborty J. et al. "New method of leaching: electrolytic leaching of low grade lateritic iron ores". Trans. Inst. Metall. (ref. 44).
68. Meixner M. et al. "Leaching of manganese nodules". German Pat. 2,240,586.
69. Derry R and Whittemore R.G. "The recovery of nickel by pressure reduction of nickel hydroxide". Chemica '70 (University of N.S. Wales, Sydney, Australia) 1970, pp. 107-121.
70. Derry R and Whittemore R.G. Proc. Second Int. Symp. Hydrometallurgy Chicago, 1973, AIME pp. 42-62.
71. Walsh A and Willis J. Standard methods of chemical analysis., 6th ed. Vol. 3, Van Nostrand. N.Y. 1966.
72. Walsh A. Spectrochim. Acta. 7, 108, (1955).
73. Elwell and Gidley Atomic absorption spectroscopy. Pergamon Press 1966.



74. Slavin W. Atomic absorption spectroscopy, Wiley Interscience 1970.
75. Young R.S. Chemical analysis in extractive metallurgy, Griffin and Co. Ltd., 1971.
76. Easton A.J. Chemical analysis of silicate rocks, Elsevier Publishing Co., 1972.
77. Nesbitt R.W. Anal. Chim. Acta, 35, 413-420 (1966).
78. Kinson K. and Belcher Nickel in steel by atomic absorption spectroscopy, Anal. Chim. Acta, 30, 64 (1964).
79. Long J.V.P. "Electron probe microanalysis", Chapter 5 in "Physical methods in determinative mineralogy" J. Zussman (ed.), Academic Press, Lond., 1967.
80. Keil K. "Application of the electron microprobe in geology", Chapter 5 in "Microprobe analysis" C.A. Andersen (ed.) Wiley, N.Y. 1973.
81. Stephens J.D. Microprobe application in mineral exploration and development programmes. Miner. Sci. Eng. 3 (1). 26-37, 1971.
82. Melford, D.A. The use of electron-probe microanalysis in physical metallurgy, J.Inst. Metals. 90, 217 (1962).
83. Heinrich K.F.J. Electron-probe analysis in metallurgical research. A.S.T.M. Publication STP 349 (1964).
84. Heinrich K.F.J. Bibliography on electron-probe microanalysis and related subjects (second revision) in "The electron microprobe", Wiley N.Y. (1966a).

85. Moore W.J. Physical chemistry (fourth edition). Longmans, 1965.
86. Peters E. The electrochemistry of sulphide minerals. Paper reprinted from: Trends in electrochemistry, pp. 285 (1977).
87. Etienne A. Electrochemical aspects of the aqueous oxidation of copper sulphides. Ph.D. thesis, Department of Metallurgy, University of British Columbia, Canada (1967) pp. 71-81.
88. Carter R.E. "Kinetic model for solid-state reactions" Journal of Chemical Physics, Vol. 34, (1961) 2010-2015.
89. Sharp J.H. et al. "Numerical data for some commonly used solid state reaction equations". Journal American Ceramic Soc. Vol. 49, (1966), 379-382.
90. Valensi G. "Kinetics of the oxidation of metallic spherules and powders". Compt. Rend. 202 (1936) 309-312
91. Ginstling A.M. "The diffusion kinetics of reactions in spherical particles". Zh. Prikl. Khim. 23 (1950) 1249  
and Brounshtein English Trans. in J. Appl. Chem. USSR, 23 (1950) B.I. 1327-38.
92. Appostohidis C.I. "The kinetics of the sulphuric acid leaching of  
and Distin P.A. nickel and magnesium from reduction roasted serpentine". Hydrometallurgy Vol. 3, No.2 (1978) 181-196.
93. Gastuche M.A. and Fripiat J.J. Sci. Ceram. 1, 121 (1962).

94. Ross G.J. "Kinetics of acid dissolution of an orthochlorite mineral". Can. J. Chem. Vol. 45 (1967) 3031-34.
95. Jacobs P.W.M. "Classification and theory of solid reactions".  
and Tompkins F.C. Chemistry of the solid state (edited by Garner, W.E.) pp. 184-212, Butterworths, London.
96. Luce R.W. Ph.D. thesis, Stanford University U.S.A. 1969 (ref. 13).
97. Sawistowski H. "Mass transfer process calculation" (1963)  
and Smith W. Interscience library of chemical engineering and processing.
98. Treybal R.E. "Mass transfer operations" (1968). (second edition) McGraw-Hill Chemical Engineering Series.
99. Coulson J.M. and Chemical engineering. Vol. 2 (2nd Edition)  
Richardson J.F. Pergamon Press (1976).
100. Heald C. and "Applied physical chemistry". Macmillan  
Smith A.C.K. chemistry text (pp.134-142)
101. Hughes D.I. "Design and development of a multistage  
sedimentation counter current washing column".  
M.Phil. Thesis. Department of Mining and  
Mineral Sciences, University of Leeds 1977.
102. Dell C.C. "The multistage counter current washing column".  
Inst. of Chem. Engineers. Yorkshire branch.  
Symposium solid/liquid separation practice  
March (1979) 70-77.

APPENDIX I

Chemical analyses of the seven laterites (dried at 110°C) from  
L.W. Strong's data<sup>(13)</sup>

	Ore-A	Ore-B	Ore-C	Ore-D	Ore-E	Ore-F	Ore-G
	%	%	%	%	%	%	%
*SiO <sub>2</sub>	34.40	36.90	76.85	32.80	2.20	2.10	18.30
+Al <sub>2</sub> O <sub>3</sub>	1.60	0.69	0.34	7.20	4.23	3.10	7.50
NiO	1.73	1.95	4.85	4.28	1.60	1.72	1.45
Fe <sub>2</sub> O <sub>3</sub>	20.00	10.00	3.50	23.00	77.00	77.10	52.20
MgO	26.60	34.00	11.50	13.00	0.60	0.80	2.32
L.O.I.	15.08	14.17	5.69	11.12	12.78	15.96	12.15
Total	99.41	97.71	102.73	91.40	98.41	100.78	93.92
+HCl ins	32.79	37.40	44.42	42.49	2.17	2.15	19.96
‡Di sol	17.01	7.97	-	20.65	55.87	56.62'	46.00

\* Weight fraction insoluble in boiling conc. HCl

‡ Weight fraction soluble in sodium dithionite

' Taylors (44) value for Goethite -58.8%

\* Determined by X-ray fluorescence

L.O.I. Determined from T.G. curves.

Determination of nickel, iron and magnesium content in selected laterite ores by atomic absorption analysis.

Ore	Ni	Fe	Mg
	%	%	%
A	1.79	14.05	15.58
B	1.64	7.31	21.04
C	3.78	1.85	6.55
D	3.47	15.72	7.74
E	1.36	51.00	n.d.
F	1.38	50.12	n.d.
G	1.24	35.74	n.d.

n.d. Not determined

Size distribution of ore samples used for leaching tests

B.S. Mesh	Aperture (microns)	Cumulative % Passing			
		A	B	C	D
				99.54	98.35
5	3.353	-	-	99.08	97.99
10	1.676	99.79	100.00	97.72	97.44
18	853	98.99	99.86	89.27	96.12
36	420	94.36	89.63	68.56	87.66
72	210	81.87	69.52	44.23	69.97
150	105	64.62	52.94	29.49	48.83
300	53	36.45	37.41	17.10	29.35

Aperture (microns)	Cumulative % Passing		
	E	F	G
	100.0	100.0	100.0
45	90.2	89.7	87.0
30	81.6	83.1	72.4
20	74.2	76.7	61.9
15	57.0	68.3	57.2
10	52.5	64.7	48.8

Strong's<sup>(13)</sup> kinetic data illustrating "The effect of acid concentration and temperature on cation extraction from Ore BS-1" (-85 + 170 mesh, 2% solid, 1100 r.p.m.)

Temp °C	Acid Molar	%	Contact time, minutes						
			5	10	15	30	60	120	240
25	1.0	W <sub>D</sub>	0.5	1.0	1.2	3.1	5.2	8.6	12.9
		Ni	1.0	2.4	3.5	6.3	11.4	19.6	30.0
		Fe	<1.0	<1.0	<1.0	1.0	1.6	4.2	4.5
		Mg	1.6	2.9	4.0	5.8	8.5	10.5	12.4
	2.0	W <sub>D</sub>	1.1	1.9	3.6	6.0	9.2	12.8	18.0
		Ni	2.0	4.7	9.0	16.6	30.0	36.0	52.0
40	1.0	W <sub>D</sub>	1.6	3.9	4.9	8.2	14.2	19.9	23.7
		Ni	4.5	7.2	10.5	21.0	35.3	54.0	73.5
		Fe	1.5	2.6	3.5	6.0	11.0	20.0	24.5
		Mg	3.6	6.8	8.9	15.0	23.0	29.5	31.6
	2.0	W <sub>D</sub>	1.8	3.7	5.9	10.6	16.4	23.6	28.0
		Ni	5.5	11.4	17.5	35.2	56.6	72.0	80.5
65	1.0	W <sub>D</sub>	11.0	15.8	20.0	27.1	30.7	32.9	35.0
		Ni	27.0	48.5	56.0	70.0	80.2	81.0	92.0
		Fe	3.5	5.4	7.2	20.0	28.7	34.0	51.0
		Mg	15.9	27.0	32.0	46.5	56.8	59.8	69.6
	2.0	W <sub>D</sub>	20.0	25.1	27.0	30.8	33.7	35.8	38.5
		Ni	55.0	65.0	70.0	78.5	86.0	91.0	94.8
		Fe	5.8	12.0	14.4	26.0	38.1	52.3	63.9
		Mg	22.1	32.8	40.0	55.0	66.0	71.8	75.0

W<sub>D</sub> Weight of laterite dissolved



Strong's<sup>(13)</sup> extraction kinetic data for samples with specific size distribution (Ore BS-1, 1.0 m HCl, 2% solids)

Temp °C	%	CONTACT TIME, minutes				
		15	30	60	120	240
25	W <sub>D</sub>	1.8	3.2	5.3	6.2	11.6
	Ni	1.0	1.8	5.0	13.5	29.2
	Fe	< 1.0	1.0	6.2	5.0	12.2
	Mg	8.0	14.2	18.6	29.4	37.0
40	W <sub>D</sub>	5.5	8.0	12.8	16.5	25.5
	Ni	13.6	30.0	35.5	56.0	74.5
	Fe	3.5	10.3	11.2	17.5	23.2
	Mg	28.0	33.1	29.2	45.0	54.2
50	W <sub>D</sub>	9.5	13.5	21.0	26.5	32.0
	Ni	34.0	37.0	64.1	74.4	80.0
	Fe	11.4	13.0	20.0	26.5	31.4
	Mg	34.0	36.8	43.0	58.2	69.4
65	W <sub>D</sub>	21.0	25.5	31.0	32.0	35.0
	Ni	64.5	74.4	82.6	86.0	90.3
	Fe	16.3	27.3	31.5	36.0	52.2
	Mg	43.5	50.6	61.5	76.0	81.0
80	W <sub>D</sub>	30.3	33.8	35.7	40.0	41.0
	Ni	79.4	83.5	89.7	95.0	98.5
	Fe	30.0	37.0	52.2	74.0	83.0
	Mg	66.0	69.2	73.6	77.6	85.4

W<sub>D</sub> Weight of laterite dissolved

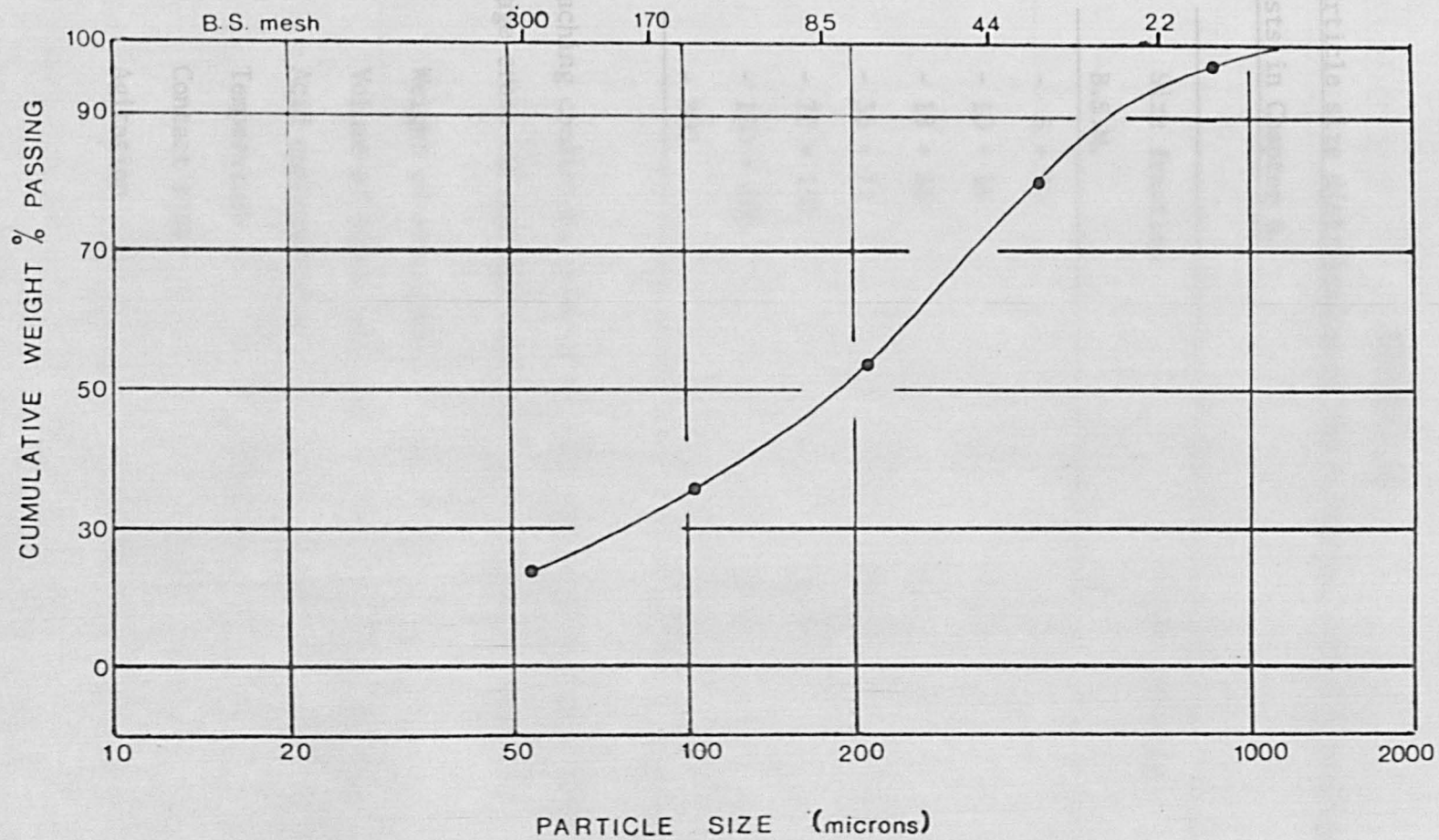


FIG. I. STRONG'S SIZE ANALYSIS FOR SIZE DISTRIBUTION OF ORE BS-1 USED IN THE KINETIC STUDY (13)

APPENDIX II

Particle size distribution of Ore-B samples used for leach-washing tests in Chapter 6.

Size fraction	Weight retained
B.S.M.	%
- 5 + 10	-
- 10 + 18	0.14
- 18 + 36	10.23
- 36 + 72	20.11
- 72 + 150	16.58
- 150 + 300	15.53
- 300	37.41

Leaching conditions used to provide the leach residues for the multi-stage cross-current and counter-current washing tests

Weight of ore samples = 21 g  
Volume of leach solution = 50 ml (20 g/l Ni)  
Acid concentration = 6 mol/dm<sup>3</sup>  
Temperature = 80°C  
Contact time = 1 hour  
Agitation = Strong stirring

Data of cross-current washing (10 stages) using 10 ml of pure HCl to contact the slurry residues in each stage.

Washing stages No.	Nickel content in feed to each stage		Initial Ni conc. in was solu.	Nickel concentration after washing		Nickel extraction (cumulative)
	Solid	Solution		Overflow	Underflow	
	g	g	g/l Ni	g/l Ni	g Ni/Kg pulp*	%
1	0.1689	0.5878	16.79	17.20	15.80	8.41
2	0.1547	0.43	12.29	12.93	12.30	21.73
3	0.1322	0.3232	9.24	9.67	9.70	30.67
4	0.1171	0.2418	6.91	7.33	7.72	39.37
5	0.1024	0.1833	5.24	5.54	6.22	45.65
6	0.0918	0.1385	3.96	4.12	5.11	49.02
7	0.0861	0.103	2.94	3.15	4.26	53.29
8	0.0789	0.0788	2.25	2.47	3.60	57.79
9	0.0713	0.0618	1.76	2.14	3.02	65.54
10	0.0582	0.0535	1.53	1.60	2.59	67.02
+11	0.0557	0.04				

+ Residues

Washing condition: room temperature,  $6 \text{ mol/dm}^3$  (pure HCl), 30 minutes contact time (each stage) and no agitation

\* Weight of nickel (dissolved and undissolved) per unit mass of pulp on a nickel free basis

Weight of dry solid after washing = 12.07

Volume of solution discharged in overflow = 10 ml.

Volume of solution discharged in underflow = 25 ml.

The average weight of dry solid leach residues (before washing) for cross-current and counter-current washing tests was determined by performing 10 leach tests according to the leaching conditions specified in this appendix. Leach residues were filtered, dried (110°C) and weighed. The average weight was 12 g, where the highest was 12.32 g and the lowest 11.82 g.

The approximate nickel content in the solid leach residues used for the counter-current washing tests was determined by the analyses of the leach liquors (from 76 leaching tests). From these analyses it was found that the average amount of nickel in the solid leach residues was 0.1645 g. The highest value was 0.1664 g and the lowest 0.1627 g.